IDENTIFICATION OF INTELLIGENT BIOMARKERS OF EXPOSURE IN THE RESPIRATORY EPITHELIA TO TOBACCO SMOKE COMPONENTS

Keith Sexton

CARDIFF UNIVERSITY

PRIFYSGOL CAERDYD

A thesis presented for the degree of Doctor of Philosophy

Cardiff University

December 2008

Cardiff School of Biosciences
Cardiff University
Museum Avenue
CARDIFF
CF10 3AX

UMI Number: U585193

UMI

Dissertation Publishing

ProQuest

To Krista, Ioan and Efa

CONTENTS

CONTENTS

7.0 REFERENCES   174

ACKNOWLEDGEMENTS

I would like to say a huge thank you to Dr. Kelly BéruBé and Dr Tim Jones for giving me this opportunity to write up my research as a PhD. Your continuous support and encouragement has no limits (just like the ink in your red pen). Thank you both for all the time and energy you have spent on me, I hope you are pleased with the end product. I am also grateful for the opportunities to visit Beijing, China; it was an experience I will always look back upon with fond memories and a fantastic photograph album.

Thanks to everyone in W2.01 in particular the previous members of the RJR group and the present members of the KAB group who all made my time in the LPRG so enjoyable. I would like to especially thank Dominique, my personal thesaurus and conference buddy; I really appreciated your support on a day to day basis, without you, it would have been so difficult. Lata, I'm still waiting for the samosas, Zoe, it's not too late to change your allegiance to the Blues and Tracy for cell culture challenges and American political debates, thank you all for listening when I needed to get out of the windowless office. Special thanks to the DPR group, especially James without his knowledge of westerns and the patience of the DPR group especially Nishi, I would be still trying to get the technique to work.

Finally I would like to thank my family for all their support, Mum and Dad for the school runs, and last but by no means least Krista for her continuous encouragement and support without which would have made it all too much! I'm forever grateful.

DECLARATION

This work has not previously been accepted for any degree and is not concurrently submitted in candidature for any degree.

Signed .... *R. Sexton* .... (candidate)

Date .... 28th April 2009 ....

STATEMENT 1

This thesis is the result of my own investigations, except where otherwise stated. Other sources are acknowledged by footnotes giving explicit references. A bibliography is appended.

Signed .... *R. Sexton* .... (candidate)

Date .... 28th April 2009 ....

STATEMENT 2

I hereby give consent for my thesis, if accepted, to be made available for photocopying and for inter-library loan, and for the title and summary to be made available to outside organisations.

Signed .... *R. Sexton* .... (candidate)

Date .... 28th April 2009 ....

PUBLICATIONS

Sexton, K., Balharry, D. and BéruBé, K.A. (2008). Genomic biomarkers of pulmonary exposure to tobacco smoke components. *Pharmacogenetics and Genomics* **18**(10):853-60

Balharry, D., Sexton, K. and BéruBé, K.A. (2008). An *In vitro* Approach to Assess the Toxicity of Inhaled Tobacco Smoke Components: Nicotine, Cadmium, Formaldehyde and Urethane. *Toxicology* **244**(1):66-76

BéruBé KA, Jones TP, Moreno T, Sexton K, Balharry D, Hicks M, Merolla L, Mossman BT. (2006) "Characterisation of airborne particulate matter and related mechanisms of toxicity." In: *Air Pollution Reviews*, Vol. 3. Ayres J, Maynard R, Richards R (Editors). Imperial College Press, London, *in press.*

PUBLICATIONS (IN PREPARATION)

Sexton, K., Balharry, D. and BéruBé, K.A. (2008). Proteomic biomarkers of pulmonary exposure to tobacco smoke components. *Molecular and Cellular Proteomics*

Sexton, K., Balharry, D. and BéruBé, K.A. (2008). Morphological Changes in the EpiAirway model when exposed to tobacco smoke components. *Histopatholgy*

PUBLISHED ABSTRACTS

Sexton, K., Balharry, D., BéruBé, K.A. (2007). Using Toxicogenomics to Search for Biomarkers of Exposure and Harm in Respiratory Epithelium. Institute for Science and Health, *Symposium on Tobacco Science and Health,* Louisville, USA. (Poster): Web Publication: http://www.ifsh.org

Sexton, K., Balharry, D., BéruBé, K.A. (2006). The Use of Toxicogenomics to Identify Biomarkers of Exposure in an Airway Epithelium Model Exposed to Tobacco Smoke Components, Abstracts of the 16th ERS European Respiratory Society Annual Congress, 2006, Munich, Germany (poster). *European Respiratory Journal* **28** Suppl 50, 825

Balharry, D., Sexton, K., BéruBé, K.A. (2006).Characterisation of the Dose Response of a Human Airway Epithelium Model to Tobacco Smoke Components, Abstracts of the 16th ERS European Respiratory Society Annual Congress, 2006, Munich, Germany (poster). *European Respiratory Journal* 28 Suppl 50, 824

Balharry, D., Sexton, K., Jones, T.P., BéruBé, K.A. (2006). Identification of Intelligent Biomarkers for Exposure and Harm in a Human Airway Epithelium Model. Institute for Science and Health, Research Symposium on Tobacco Science and Health, Vienna, Austria. Web Publication: http://www.ifsh.org

Sexton K., Balharry D., Jones T.P., BéruBé K.A. (2005). Intelligent Biomarkers of Exposure and Harm in the Respiratory Epithelial to Tobacco Smoke Components. Nanoparticles and the lung, British association of lung research (BALR), September 2005, Edinburgh, UK (Poster) *Exp. Lung Res.*, **32**(3-4), pg.119.

COMMUNICATIONS

Sexton K., Balharry D., BéruBé K.A. (2008). (Oral): Using Toxicogenomics to Search for Biomarkers of Exposure and Harm in Respiratory Epithelium. Symposium on Tobacco Science and Health, Cardiff UK. *Biomarkers*

Sexton K., Balharry D., Jones T.P., BéruBé K.A. (2006). (Oral): In for the Long Drag: The Search for Biomarkers when Exposed to Tobacco Smoke Components. MCB meeting, Cardiff University, UK

Abbreviations

AB/HRP	Streptavidin Horseradish Peroxidase Complex
ABCC1	ATP-Binding Cassette, sub-family C (CFTR/MRP), member 1
ABCC2	ATP-Binding Cassette, sub-family C (CFTR/MRP), member 2
ADP	Adenosine Diphosphate
ALDH-2	Aldehyde Dehydrogenase
ANXA1	Annexin A1
AOX	Aldehyde Oxidase
AS	Alignment Spots
ATP	Adenosine Triphosphate
ATSDR	Agency for Toxic Substances and Disease Registry
B	Blastoid Changes
BAX	BCL2-Associated X protein
BC	Basal Cell
BCH	Basal Cell Hyperplasia
BCL2	B-cell Leukemia / Lymphoma 2
C	Cytolysis
Ca	Calcium
CASP10	Caspase 10, Apoptosis-Related Cysteine Peptidase
CB	Cytoplasmic Blebbing
CC	Ciliated Cell
CCND1	Cyclin D1
Cd	Cadmium
CdCl$_2$	Cadmium Chloride
CDKN2A	Cyclin-Dependent Kinase Inhibitor 2A
cDNA	Complementary Deoxyribonucleic Acid
CdO	Cadmium Oxide
CdSO$_4$	Cadmium Sulphate
CHEK2	CHK2 Checkpoint Homolog
CI	Cilia
CK 5/6	Cytokeratin 5/6
CO	CO: Carbon Monoxide

COX1	Mitochondrially Encoded Cytochrome C Oxidase I
COX2	Mitochondrially Encoded Cytochrome C Oxidase II
CT	Cycle Threshold
CTPS	CTP Synthase
CXCL10	Chemokine (C-X-C motif) ligand 10
CYP1A1	Cytochrome P450, family 1, subfamily A, polypeptide 1
CYP20A1	Cytochrome P450, family 20, subfamily A, polypeptide 1
CYP2E1	Cytochrome P450, family 2, subfamily E, polypeptide 1
CYP4B1	Cytochrome P450, family 4, subfamily B, polypeptide 1
CYP7A1	Cytochrome P450, family 7, subfamily A, polypeptide 1
CYS	Cysteine
dA	Deoxyadenosine
DAB	Diaminobenzidine
dC	Deoxycytidine
dG	Deoxyguanosine
DIGE	Differential In Gel Electrophoresis
DNA	Deoxyribonucleic Acid
DPX	Cross Linkages between Protein and Single Stranded DNA
dR	Deoxyribose
DTT	1,4-Dithiothreitol
E2F1	E2F Transcription Factor 1
EC	Ethyl Carbamate
ECM	Extracellular Matrix
EGFR	Epidermal Growth Factor Receptor
ELK1	ELK1, member of ETS oncogene family
EPA	US Environmental Protection Agency
ET	Extrathoracic
ETM	EpiAirway Tissue Model
ETS	Environmental Tobacco Smoke
FA	Formaldehyde
FAD	Flavin Adenine Dinucleotide
FB	Foreign Body
FDH	Formaldehyde Dehydrogenase
FN	Focal Necrosis

GC	Goblet Cell
GMCSF	Granulocyte Macrophage Colony Stimulating Factor
GSH	Glutathione
HGFR	Hepatocyte Growth Factor
HIF1A	Hypoxia-Inducible Factor 1, Alpha subunit
HMOX1	Heme Oxygenase
Homocys	Homocysteine
HPLC	High Pressure Liquid Chromatography
IARC	International Agency for Research on Cancer
IC	Intermediate Cell
IC10	10% Reduction in Cell Viability
IC50	50% Reduction in Cell Viability
ICAT	Isotope Coded Affinity Tags
IFN-g	Interferon-Gamma
IHC	Immuno-histochemistry
IL	Interleukin
LC	Liquid Chromatography
LM	Light Microscopy
LV	Lipid Vacuolation
M	Membrane
MALDI	Matrix Assisted Laser Desorption Ionization
MARCKS	Myristoylated Alanine-Rich Protein Kinase C Substrate
MET	Met Proto-Oncogene
Mg	Magnesium
MMTS	Methylmethanethiosulfonate
MN	Mean Nuclei Number per Unit Length
mRNA	Messenger Ribonucleic Acid
MS	MainStream
MS TOF/TOF	Tandem Mass Spectrometry
MT	Metallothionein
MT2A	Metallothionein 2A
MT3	Metallothionein 3
MTT	[3-(4,5-dimethylthiazol-2-yl)-2,5-diphenyl tetrazolium bromide]
MU	Mucin

MVP	Major Vault Protein
N-Acetyl-Cys	Acetylcysteine
NaCl	Sodium Chloride
NAD	Nicotinomide Adenosine Dinucleotide
Nano-LC	Nano-Liquid Chromatography
NBF	Neutral Buffered Formalin
NGAL	Neutrophil Gelatinase-Associated Lipocalin
NHBE	Normal Human Bronchial Epithelium
NIH	National Institutes of Health
NNO	Nicotine N'-Oxide
NSAIDs	Nonsteroidal Anti-Inflammatory Drugs
P	Parenchyma
p63	Protein 63
PBS	Phosphate Buffered Saline
PBST	Phosphate Buffered Saline -Tween
PCL	Periciliary Liquid
PCR	Polymerase Chain Reaction
PG1-2	Prostaglandin 1-2
PGE2	Prostaglandin E2
pI	Isoelectric Point
PMN	Polymorphonuclear
PMSF	Phenylmethylsulfonyl Fluoride
PPARD	Peroxisome Proliferator-Activated Receptor Delta
PR	End Stage Plaque Reaction
PTGS1	Prostaglandin-Endoperoxide Synthase 1
PVDF	Polyvinylidenedifluoride
qPCR	Quantitative Polymerase Chain Reaction
RH	Regional Hypertrophy
RNA	Ribonucleic Acid
ROI	Reactive Oxygen Intermediates
ROS	Reactive Oxygen Species
RP	Reverse Phase
RS	Respiratory System
RT	Room Temperature

RT-PCR	Quantitative Reverse Transcriptase-Polymerase Chain Reaction
S/N	Signal to Noise Ratio
SAM	Significance Analysis of Microarrays
SCX	Strong Cation Exchange
SD	Standard Deviation
SDS	Sodium Dodecyl Sulfate
SDS-PAGE	Sodium Dodecyl Sulfate Polyacrylamide Gel Electrophoresis
SFGH	S-Formyl Glutathione
SHS	Second Hand Smoke
SOC	Super Optimal Broth with Catabolite Repression (Glucose)
SS	Sidestream
SULT2A1	Sulfotransferase family, Cytosolic, 2A
TB	Tracheo-Bronchial
TBM	Tracheo-Bronchial Model
TD_{20}	Toxic Dose 20% (Dose required to Kill 20% of cells)
TEER	Trans-Epithelial Electrical Resistance
TGF-ß	Transforming Growth Factor Beta
TH4	Tetrahydrofolic Acid
TMPT	Thiopurine S-Methyl Transferase
TNF-α	Tumor Necrosis Factor-Alpha
TOF	Time Of Flight
TS	Tobacco Smoke
TSC	Tobacco Smoke Components
TXA-2	Thromboxane 2
VC	Vinyl Carbamate
VCO	Vinyl Carbamate Epoxide
VOC	Volatile Organic Compound
VSMC	Vascular Smooth Muscle Cells
WHO	World Health Organisation

ABSTRACT

A novel toxicological tool, which consisted of a differentiated, 3-D, *in vitro* model of human respiratory epithelia, i.e. EpiAirway-100 cells (MatTek Corp., USA), was utilised to identify intelligent biomarkers in human respiratory epithelia following exposure to selected particle and vapour phase tobacco smoke components (TSC); thus providing a holistic approach towards the identification of biomarkers in the pulmonary epithelium. A range of TSC doses were used to elicit a classic dose response which was characterised by conventional toxicology techniques (transepithelial electrical resistance [TEER], cell viability [MTT] and protein assay). All four TSC appeared to induce similar stress responses (e.g. protective mechanisms) within the model. Histological (LM level) examination was utilised to investigate the morphological changes in cellular-tissue organisation in the ETM, following exposure challenges with the TSC. In conjunction with this, targeted immuno-histochemistry assays were performed in order to better characterise the tissue response at the cellular level, i.e. basal, ciliated, intermediate and Goblet cells. Three discrete zones of tissue injury and repair were delineated: (1) the apical region, (2) the suprabasal region and (3) the basal zone (i.e. where basal cells acted as progenitors or stem cells).

Toxicogenomics was carried out to identify early molecular markers for events in pulmonary injury. This study identified nine genes, with the potential of being genomic biomarkers, for specific disease mechanisms known to be associated with tobacco smoke. Another potential genomic biomarker was identified which was not previously related to tobacco smoke, *PTGS1*. Its induction could result in a disruption of tissue homeostasis that may lead to the onset of a number of human inflammatory diseases (e.g. chronic obstructive pulmonary disorder). The proteomic analysis identified two proteins (cystatin-A and ubiquitin) that were significantly induced for all TSC exposures and could be described as 'defence proteins'. Consequently, they represented potential biomarkers of general lung injury. This study also identified three proteins (complement C3, calmodulin and CD9) that could be used as biomarkers for specific disease mechanisms (e.g. atherosclerosis).

CHAPTER 1:

INTRODUCTION

1.1 STUDY INTRODUCTION

The respiratory tract is the primary site of exposure to airborne compounds, resulting in a growing need for high throughput in vitro models. This project utilised a differentiated, 3-D, *in vitro* model of human respiratory epithelia to identify intelligent biomarkers in human respiratory epithelia following exposure to selected particle and vapour phase tobacco smoke components (TSC); thus providing a holistic approach towards the identification of biomarkers in the pulmonary epithelium.

1.2 THE RESPIRATORY SYSTEM

The mammalian respiratory system (RS) is a structurally complex arrangement of tissues designed primarily for the intake of oxygen and the removal of carbon dioxide, but also performs a variety of other functions (i.e. clearance of inhaled foreign materials, hormonal regulation and metabolism of xenobiotics). The RS is separated into 4 major regions: (1) the extrathoracic (ET) region or upper respiratory tract comprises of the nasal and oral cavities, pharynx, larynx, and trachea; (2) the tracheo-bronchial region (TB) consists of the trachea, bronchi and bronchioles; (3) the parenchyma region (P) incorporates the alveoli, pulmonary vasculature, mesothelium and connective tissue and; (4) pleura, which is a thin layer (one cell in diameter) of mesothelial tissue (Figure 1.1). Each region has a specific function in gaseous exchange and protection from inhaled xenobiotics.

1.3 THE EXTRATHORACIC REGION

The ET region has the role of conditioning the temperature and humidity of inhaled air, which takes place in the air passages in the head and neck. Air enters via the nasal cavity and/or oral cavities and passes in to the pharynx, and then enters into the first structure in the respiratory tract, i.e. the larynx.
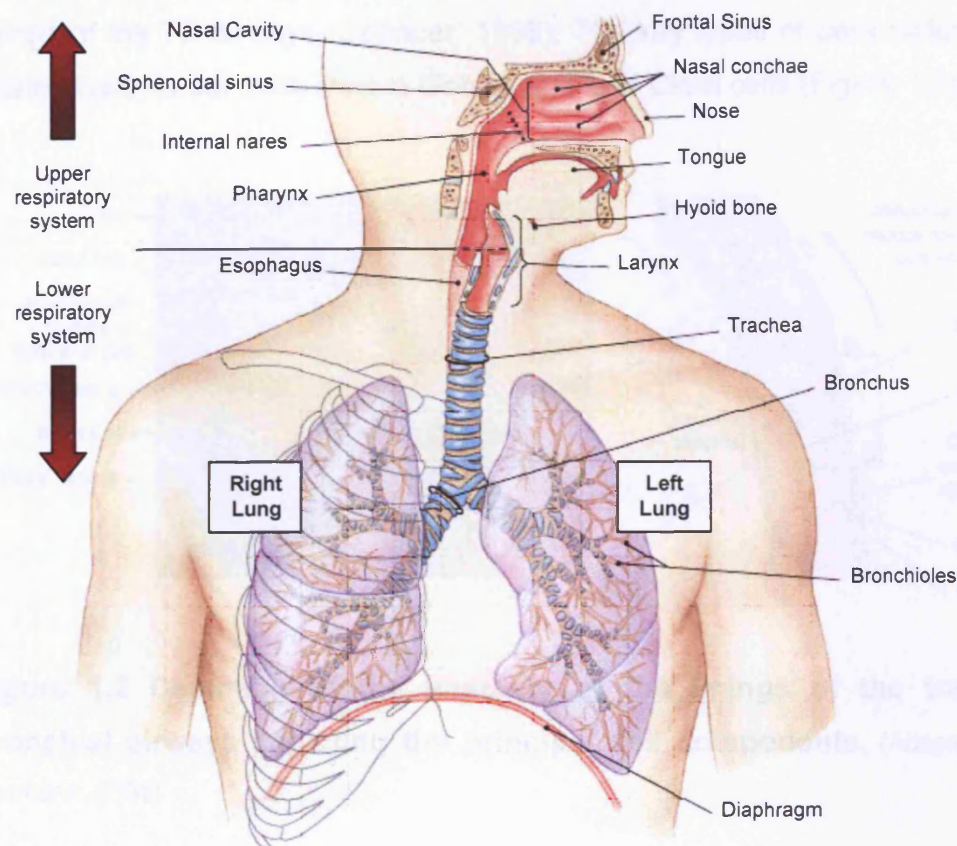
Figure 1.1 Depiction of the anatomy of the respiratory system. (Adapted from Germann, 2004)

1.4 THE TRACHEO-BRONCHIAL REGION

The TB region is responsible for adjusting flow dynamics to ensure optimal oxygen and carbon dioxide exchange at the P region. Excluding the oropharynx and laryngopharynx, the lower two thirds of the nasal cavity down to the terminal bronchioles are lined with pseudo-stratified, ciliated, columnar epithelia. The TB region changes slightly as it progresses through the respiratory tract, although the main cellular components remain the same (e.g. ciliated and columnar cell populations). With further progression towards the respiratory bronchioles, the numbers of Goblet cells diminishes and are replaced by Clara cells.

There are at least eight principal types of epithelial cells identified in the linings of the TB airways (Spencer, 1985). The key types of cells include the ciliated cells, basal cells, mucus Goblet cells and Clara cells (Figure 1.2).

Cilia
Goblet cell
Nucleus of columnar epithelial cell
Lamina propria
Stem Cell
Basal lamina

Sectional view

Movement of mucus towards pharynx
Stem Cell
Goblet cell
Lamina propria
Ciliated columnar epithelial cell
Cilia
Mucus layer
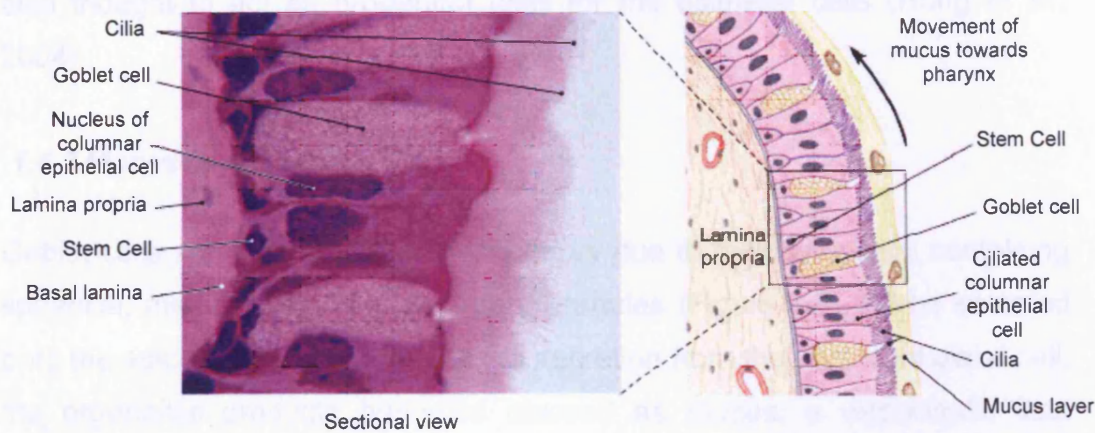
Figure 1.2 Depiction of the anatomy of the linings of the tracheo-bronchial airways depicting the principal cell components. (Adapted from Germann, 2004)

1.4.1 CILIATED CELLS

The ciliated cell is attached to the basal lamina and extends towards the luminal surface (Figure 1.3). Ciliated epithelial cells have many finger-like projections of the plasma membrane (cilia) on their apical surfaces. Epithelial cells are commonly arranged in layers that are one cell thick. The "sides" of the cells join together to form a sheet, while the remaining two surfaces are exposed to either the environment on the top (or apical surface) and the bottom (or basolateral surface). Cells can coordinate the motions of the cilia to create a wave-like motion which moves the overlying mucus and trapped foreign bodies for removal from the RS towards the upper respiratory tract (Sleigh *et al.*, 1988).

1.4.2 BASAL CELLS

Basal cells are flattened in appearance and have a small cytoplasm to nucleus ratio (Figure 1.3). They are closely attached to the basal lamina but

do not extend into the airway lumen. It is the existence of these cells that accounts for the pseudo-stratified classification of the airway epithelium. Studies have demonstrated the primary role of basal cells is to attach columnar cells to the basal lamina (Evans *et al.*, 1989). In addition, they are also thought to act as progenitor cells for the epithelial cells (Hong *et al.*, 2004).
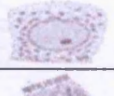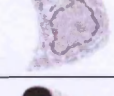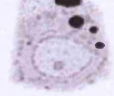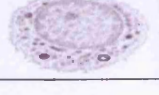
1.4.3 MUCUS GOBLET CELLS

Goblet cells are considered to be secretory due to their cytoplasm containing spherical, membrane bound secretory granules (Figure 1.3). When secreted onto the apical surface, along with the secretion from the muscosal gland cell, the organelles products becomes classed as mucus; a viscoelastic fluid composed primarily of highly glycosylated proteins. The mucus serves many functions that include protection against chemical damage, moistens inspired air, prevents drying of the respiratory epithelia, and traps particulate matter. The number of secretory products that extend into the bronchial lumen increase in number dramatically (mucus hypersecretion) following acute bronchial exposure to a xenobiotic (e.g. tobacco smoke [Coles *et al.*, 1979] and chemical irritants [Clark *et al.*, 1980]). The mucus blanket, along with the ciliated cells, constitutes the muco-ciliary escalator (see Section 1.5).

1.4.4 CLARA CELLS

Clara cells are unique to the bronchioles. The respiratory bronchioles represent the transition from the conducting portion to the respiratory portion of the RS. These narrow channels are usually less than 2 mm in diameter and they are lined by a simple cuboidal epithelium, consisting of ciliated and non-ciliated Clara cells. This region is denoted by the absence of Goblet cells. In addition to being structurally diverse, Clara cells are also functionally variable. One major function they carry out is the synthesis and secretion of the material lining the bronchiolar lumen. This material includes some of the protein components of surfactant, antibodies and lysozymes and play an important defensive role.

Page 9 margin: INTRODUCTION

Particle size			Structure	Cilia	Goblet cells
2.5 – 10µm	Coarse (URT)	Inhalable	Larynx	+++	+++
0.1 – 2.5µm	Fine	Thoracic	Trachea	+++	+++
			Primary bronchi	+++	++
			Secondary bronchi	+++	++
			Tertiary Bronchi	+++	++
			Smaller bronchi	+++	+
			Bronchioles	++	+
<0.1µm	UltraFine	Respirable	Terminal bronchioles	++	0
			Respiratory bronchioles	+	0
			Alveolar sacs	0	0

Cell Type	Diagram of cell	Cell Description
Ciliated Epithelium		▪ Constitute ~50% of cell population ▪ Roughly 20-60µm tall ▪ Main function is the propulsion of mucous
Basal cell		▪ Reside near the basement membrane interspersed between ciliated and secretory cells ▪ Flattened or spindle shaped with scant cytoplasmic regions
Goblet Cell		▪ Characterised by an electron dense cytoplasmic region due to the secretory granules ▪ Mucous produced is designed to trap inhaled particles
Clara Cell		▪ Actively divide and differentiate to form ciliated cells ▪ Produce glycoaminoglycans ▪ Metabolise airborne toxins
Serous Cell		▪ They have microvilli and contain mucin granules that produce mucous to trap inhaled particles
Brush Cell		▪ Small mucous granule cells ▪ Known as brush cells due to their microvilli ▪ Also secrete mucous to trap inhaled particles
Alveolar Type I Cell		▪ Thin and spread over a relatively large area ▪ Make up approximately 95% of the alveoli ▪ Form a thin blood-gas barrier through which gas exchange occurs
Alveolar Type II Cell		▪ Large and cuboidal in shape ▪ Secrete a pulmonary surfactant which decreases the surface tension of the alveolar surface
Macrophage		▪ Specialised defence cells that move freely over the surface of the alveolus ▪ Macrophages ingest foreign particles by a process known as phagocytosis

Figure 1.3 Overview of the cell types through the RS. For continuity but the research will focus on the TB region (e.g. basal, ciliated and Goblet cells; adapted from Germann, 2004)

The heterogeneous nature of the dense granules within the Clara cell's cytoplasm suggests that they may not all have a secretory function. Some of them may contain lysosomal enzymes, which carry out a digestive role, either in defense: Clara cells engulf airborne toxins and degrade them down via cytochrome P-450 enzymes present in their smooth endoplasmic reticulum (Baron et al., 1988 and Serabjit-Singh et al., 1988); or in the recycling of secretory products (Widdicombe and Park, 1982). Clara cells are continuously dividing and differentiating to form both ciliated and non-ciliated epithelial cells (Evans et al., 1976).

1.5 DEFENCE MECHANISMS IN THE LUNG

Defence mechanisms are essential to prevent damage and infection (Figure 1.4). The lung utilises a vast array of biological responses which includes coughs and sneezes to clear debris/excess secretions in the ET region, to specific cell responses in the P region. Defence mechanisms of the lung can be categorised as cellular, immunological and non-cellular responses.

1.5.1 NASAL CAVITY

The initial defence mechanism of the RS is the nasal vibrissae (prominent intranasal hairs). If a foreign body (FB) by-passes these protrubances it will gain access into the nasal cavity. The nasal cavity consists of a transitional epithelium and an olfactory epithelium. The transitional epithelium is characterised by microvilli and the olfactory by the capacity to biotransform xenobiotics. The stimulation of nerves or nerve endings by an inhaled xenobiotic can produce a cough or sneeze reflex (non-cellular response) to propel the FB from the ET region. Moreover, a FB could be swallowed down the gastro-intestinal tract (Hlastala and Berger, 2001).

1.5.2 BUCCAL CAVITY

Moving further into the RS, the buccal (oral) cavity and pharynx have mucus and saliva lined walls, which act by trapping particles and allowing toxic gases to dissolve.

8

Structure	Cilia	Goblet cells
Larynx	+++	+++
Trachea	+++	+++
Primary bronchi	+++	++
Secondary bronchi	+++	++
Tertiary Bronchi	+++	++
Smaller bronchi	+++	+
Bronchioles	++	+
Terminal bronchioles	++	0
Respiratory bronchioles	+	0
Alveolar sacs	0	0

Location	Defence Mechanisms
Buccal cavity and pharynx	• Saliva and mucus line the walls and act to warm the air, trap particles and dissolve toxic gases
Trachea	• Absorption of ions and liquids across the epithelium is needed to maintain the correct level of periciliary liquid (PCL) necessary for the active movement of the cilia • 'Mucociliary escalator' – the cilia beat in a coordinated manner to transport the mucus layer above the cilia and PCL to be removed by swallowing, spitting, sneezing or lymphatic circulation • Stimulation of receptors in the trachea by certain xenobiotics may result in a cough to expel these materials
Bronchi and Bronchioles	• Migratory macrophages roam the epithelial and act to engulf and digest xenobitoic particles • Cellular secretions contain enzymes which act to modify and detoxify toxic materials • Recruitment of PMN or polymorphonuclear cells – white blood cells which include neutrophils and eisinophils. These act like macrophages to break down invaders. The PMN also release cytokines (e.g. IL-6) which act to induce inflammation
Alveoli	• Alveolar macrophages act to engulf and digest xenobiotics • Type II cells secrete GSH, surfactant • Type II cells are able to transform into type I cells in the event of damage

Figure 1.4 Overview of the different mechanisms involved in lung defence. (Adapted from Germann, 2004)

1.5.3 TRACHEO-BRONHCIAL REGION

Increased branching of the tracheo-bronchial region continues to filter out FB's which is enhanced by the mucociliary escalator. The cilia are extensions of plasma membrane from specialised epithelial cells (ciliated cells) and beat unilaterally towards upper respiratory tract by utilising energy in the form of ATP (Wanner et al., 1996). In order to minimise energy use and increase efficiency, cilia flex so the motility is in the serous peri-epithelial layer. Once fully re-coiled the cilia extend into the mucus layer thus propelling it forward. This cycle, repeated by countless cilia, is responsible for transport of xenobiotics up the mucociliary escalator (Satir and Sleigh, 1990).

1.5.4 IMMUNOLOGICAL RESPONSE

The recruitment of polymorphonuclear cells (PMN) further increases the defences, these white cells, which include neutrophils and eosinophils, circulate in the blood and are attracted to a site of injury. The cells are associated with a more persistent inflammation (Lam et al., 2002), and have the ability to release cytokines (e.g. IL-6). The net effect of an inflammatory response is determined by the balance between pro-inflammatory cytokine and anti-inflammatory cytokines. Cytokines such as IL-4, IL-10 (inhibit pro-inflammatory cytokine release) and transforming growth factor (TGF)-ß (growth inhibitor) play a role in anti-inflammatory responses (Fiorentino et al., 1991). It is clear that protective responses are necessary in combating damage caused by xenobiotics. As a result, in many in vivo studies, it is often indeterminate whether cellular injury is due to either initial toxicologic insult or the subsequent immunologic responses (Bhalla et al., 2009).

1.6 TOBACCO

1.6.1 TOBACCO HISTORY

The western hemisphere has used the common tobacco plant for millennia. The plants were cultivated often for religious uses, as depicted in the Mayan

temple carvings dating back to 650-800 A.D. (Slade, 1997). It was in 1492, when Christopher Columbus was offered a dried tobacco leaf at the house of the Arawaks that initiated the spread of tobacco to Europe (IARC 1986a). It is thought the tobacco plant was named 'nicotiana' after the French ambassador to Portugal, Jean Nicot, who presented it to the French court in 1556.

There were two main varieties of tobacco grown in Europe. France and Spain used the Nicotiana tobacum that originated from Brazil and Mexico, whilst England and Portugal used the Nicotiana rustica that originated from Florida and Virginia (IARC 1986a). The trade of tobacco since 1492 to present day has remained an important source of commercial income.

The late nineteenth century witnessed a dramatic change in the history of tobacco with the design and patent of the cigarette machine by James Bonsack (Bonsack, 1881). The spread of Tuberculosis increased concern over spitting with the use of smokeless tobacco and moved users towards cigarette smoking (Glover & Glover, 1992). Post-1920's tobacco use has been dominated by smoking cigarettes, cigars and pipes, although there are small numbers of chewing tobacco users globally. The trends over the last two decades in the 20th century have changed with fashion and health concerns but were heavily influenced by marketing drives by the cigarette industry (Glover & Glover, 1992; Gerlach et al., 1998).

1.6.2 CIGARETTE TOBACCO

Currently, the most common use of tobacco in the developed countries is the manufactured cigarette. A cigarette is defined as 'any role of tobacco wrapped in paper or any other non-tobacco material, which when lit the burning process produces smoke that is inhaled through the unlit end' (IARC, 2004). Cigarettes vary in length (70-120mm) and are usually 8mm in diameter (Borgerding et al., 1998). When they are lit they produce three categories of smoke; mainstream, sidestream and second hand smoke.

1.6.2.1 MAINSTREAM CIGARETTE SMOKE

Mainstream smoke (MS) is defined as cigarette (tobacco) smoke which is emerging from the mouth end of the cigarette during puffing (Borgerding and Klus, 2005; Figure 1.5). It is produced at a high temperature from the cigarette's burning tip. The composition of MS is affected by how the smoker inhales and exhales, and thus, it varies from person-to-person. The frequency of puffs, duration and volume all contribute to the composition of exhaled MS (Dunn-Rankin, 2006). The four main components of MS are tar, carbon monoxide, nicotine and acetaldehyde. The data from the Massachusetts benchmark study (1999) suggests the median yields per cigarette are 25.8mg (tar), 22.5mg (CO), 1.7mg (nicotine) and 1.6mg (acetaldehyde; Brown and Williamson, 2000). This dynamic aerosol also contains particles with an aerodynamic diameter range of 0.3-0.5µm at a concentration of 5×10^9 particles per cm^3 (Anderson et $al.$, 1989).

1.6.2.2 SIDESTREAM CIGARETTE SMOKE

Sidestream smoke (SS) is primarily the smoke emerging into the environment created from the emissions of a smoldering cigarette (Figure 1.5). The same substances present in MS are also found in SS; however, the relative yields per cigarette are totally dependant on the temperature of the glowing cone. An example of this is nicotine, with 50-80% existing in the gaseous form (Johnson et $al.$, 1973; Brown et $al.$, 1980); in MS it is in the particle form. This type of smoke will suspend in the air longer because its aerosolised particles are smaller than those in MS (0.1-0.2µm; Schick and Glantz, 2005). The combination of smaller size of the particles with the toxic chemical properties of this smoke makes it more of a respiratory hazard to breathe in than its MS counterpart (Schick and Glantz, 2005).

1.6.2.3 SECOND HAND CIGARETTE SMOKE

Second hand smoke (SHS) is also known as environmental tobacco smoke (ETS). A toxic cocktail is produced when a cigarette is smoked, approximately

11

half of the smoke is inhaled/exhaled (MS) by the smoker and the other half is suspended in the ambient air (SS).
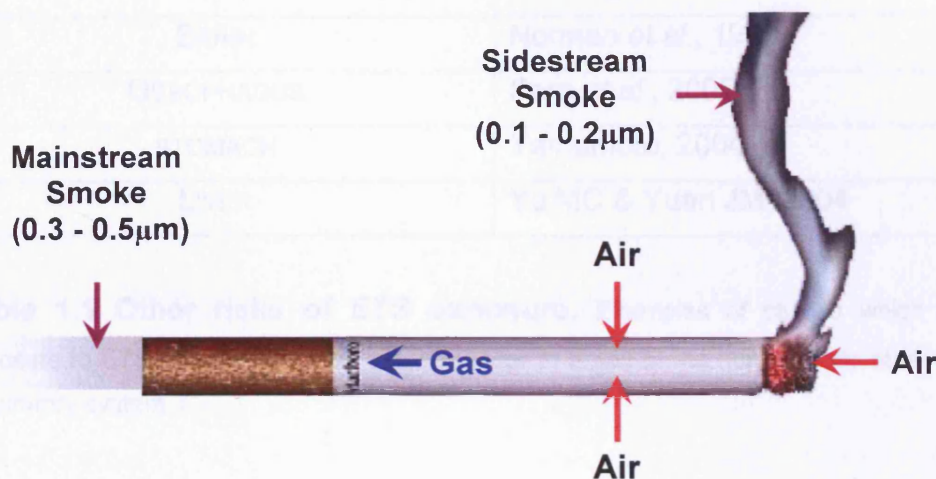
Figure 1.5 Cigarette smoke productions. Diagrammatic overview of the production of mainstream, sidestream smoke and relevant particle sizes from a lit tobacco cigarette

Once released into the environment of the smoker, components are diluted by the ambient air, diffusing in and being transported through it. These smoke constituents may also aggregate with other components in the air, and further age and change its physico-chemical character. SHS is classified as a known human carcinogen by the National Institutes of Health (NIH, 2000) and the International Agency for Research on Cancer (IARC, 2004).

1.6.3 TOBACCO SMOKE AND HUMAN HEALTH

Exposure to ETS is prevalent worldwide despite the growing awareness of the adverse health effects on the users and non-smokers. Traditionally, studies have concentrated on the effects of ETS within the respiratory system. However, studies have demonstrated associations with cancers such as cervical, bladder, nasal-sinus and the brain (Table 1.1).

AREA OF CANCER	REFERENCE
CERVICAL	Hellberg & Stendahl, 2005
BLADDER	Zeegers *et al.*, 2004
NASAL-SINUS	Benninger M, 1999
BRAIN	Norman *et al.*, 1996
OESOPHAGUS	Pera *et al.*, 2005
STOMACH	Yamamoto, 2004
LIVER	Yu MC & Yuan JM, 2004

Table 1.1 Other risks of ETS exposure. Examples of studies which suggest exposure to ETS may increase the risk of cancer to areas of the human body other than the respiratory system

Cancer is not the only adverse health effect associated with tobacco smoke. Studies have shown associations between smoking and heart disease, with increased risk of myocardinal infarction (Rastogi *et al.*, 2005) and ischemic heart disease (inadequate blood supply to the heart; Tonstad & Svendsen, 2005). These conditions can be further exaggerated with components of ETS having damaging effects on blood platelets (Section 1.6.6.3; Benowitz *et al.*, 1993; Folts and Bonebrake, 1982).

A limited number of studies have shown the effects on the fetus when the mother is exposed to cigarette smoke. Cigarette smoking and ETS exposure of non-smokers during pregnancy appeared to be the main cause of lower birth weight of newborns (Adamek *et al.*, 2005). Young children are particularly vunerable to ETS due to their higher ventilation rates. Their exposure to ETS mainly arises from adults smoking in their local vicinity, with maternal smoking being the largest source of children's exposure *in utero* and in early life (Chan-Yeung & Dimich-Ward, 2003).

1.6.4 TOBACCO SMOKE AND RESPIRATORY HEALTH

There are other effects of ETS exposure such as the non-cancer respiratory effects which are predominantly observed in sensitive groups (e.g. asthmatics

the elderly and young children; Reed, 1999; Olivieri *et al.*, 2006; Raherison *et al.*, 2007). These respiratory effects include reduced lung function, lower respiratory tract illness, asthma and non-allergic bronchial hyper-responsiveness (Wang and Pinkerton, 2008).

1.6.4.1 LUNG FUNCTION

Most of the studies investigating lung function of children are based on health effects and air pollution. The Boston cohort (March 1986 to October 1992) study found reductions in lung functions with exposure to ETS. The projected reductions in lung function growth were 28, 51 and 101ml for children of 1, 2 and 5 years of age, respectively (Chan-Yeung & Dimich-Ward, 2003; Wang and Pinkerton, 2008). Another study by Cook *et al.*, (1998), carried out meta-analysis and documented a decrease in lung function of 1.4% when compared to children with no exposure.

1.6.4.2 LOWER RESPIRATORY TRACT ILLNESS

Epidemiology studies in the 1980's (Fergusson and Horwood, 1985; Chen *et al.*, 1986 and Taylor and Wadsworth, 1987), demonstrated links with maternal smoking and the increased chance of contracting lower respiratory tract illness, e.g. bronchitis and pneumonia. Taylor and Wadsworth (1987) also showed an increase in respiratory syncytial virus (RSV) bronchiolitis with maternal smoking, which is a common cause of hospitalisations in children. There is increasing evidence that RSV has been identified as a risk factor in the development of asthma (Bradley *et al.*, 2005; Puthothu *et al.*, 2008).

1.6.4.3 ASTHMA AND NON-ALLERGIC BRONCHIAL HYPER-RESPONSIVENESS

Smoking or ETS exposure is considered as a risk factor for asthma and it is suggested that smoking or ETS-exposed asthmatics exhibit a different phenotype when compared to non-smoking asthmatics (Gusbin *et al.*, 2006). Clinically, the asthma of smokers has an increased severity than in a non-smoker, both at the symptomatic and the functional level. The asthma severity

in smokers is partly linked to a resistance to inhaled corticoids; the cornerstone of maintenance treatment in asthma (Gusbin et al., 2006).

Cook and Strachen (1997) investigated the prevalence of asthma, wheezing and chronic cough with parental smoking. They found an increase of 21% in childhood asthma, a 24% increase in children with a wheeze and an increase of 40% in children with a chronic cough whose parents smoke. This study also found that maternal smoking had a greater effect than paternal smoking. A year later Cook and Strachen (1998) used meta-analysis and found an increase in bronchial hyper-responsiveness in children with smoking mothers.

1.6.5 TOBACCO SMOKE COMPONENTS

Tobacco and tobacco smoke are complex chemical matrices consisting of thousands of compounds. A total of 3044 constituents (vapour phase [95% by weight] and particle phase [5% by weight]) have been identified/isolated from tobacco, and in excess of 4000 from the MS (exhaled) of cigarettes (Green and Rodgman 1996; Roberts, 1998; Jenkins et al., 2000).

Qualitatively, there are minimal compositional (by weight) differences between MS, SS and SHS. However, quantitatively their compositions can differ considerably. For example, approximately 1.5mg of formaldehyde can be found in the total smoke from one cigarette, and this was distributed between the MS and SS smoke in the ratio of 1:50, (i.e., 30µg in the MS and 1526µg in the SS) [Jermini et al., 1976; IARC, 2004].

The vapour phase components dominate the constituents of tobacco and tobacco smoke, and being soluble, will likely be reactive metabolites (formaldehyde; de Serres and Brockman, (1999) and urethane; Gupta and Dani (1989)). The solid or particle phase of tobacco and tobacco smoke constitutes only a small fraction (5%) of the bi-products but these can be cytotoxic (e.g. cadmium; Zalups and Ahmad, 2003) or thrombogenic (nicotine; Pfueller et al., 1988).

1.6.6 NICOTINE

Nicotine is a naturally occurring alkaloid found in members of the Solanoceous plant family that includes potatoes, green peppers and tobacco; within these plants nicotine acts as a botanical insecticide (Soloway, 1976; Tomizawa and Casida, 2003). The structure of nicotine is [1-methyl-2-(3-pyridyl-pyrrolidine), $C_{10}H_{14}N_2$] (Figure 1.6).

Nicotine was first isolated from the leaves of *Nicotiana tobacum* (the tobacco plant), in 1828 by Possett and Reiman (Schevelbein, 1982). This extraction instigated the interest of nicotine and its actions on the body. Experiments carried out by Orfila in 1843, initiated the first pharmacological studies involving nicotine. Following these primary experiments work continued with Lanley and Dickinson (1889) identifying the prime site of interaction between nicotine and the nervous system of animals. This work demonstrated the ability of nicotine to interact with the body and possible involvement in the etiology of a number of disease processes (e.g. inhibition of cell proliferation; Wonnacott, 1999).

Nicotine is one of the few naturally occurring liquid alkaloids, which means that it has some unique chemical properties. Pure nicotine is clear and turns brown when exposed to air (Schevelbein, 1962), it is also soluble in water and readily forms aqueous salts, and the free nicotine is also soluble in organic media with a boiling point of 274.5°C. These properties are pH dependant and explain nicotine's biological properties within the body; these can include increased pulse and blood pressure, mobilisation of blood sugar and an increase in plasma free fatty acids (Benowitz, 1988; Dani and Heinemann, 1996; Waldum *et al.*, 1996; Ashakumary and Vijayammal, 1991).

1.6.6.1 ABSORPTION OF NICOTINE

There are many routes of nicotine absorption in the human body which include the oral cavity, skin, lungs and gastrointestinal tract (Schevelbein *et al.*, 1973).
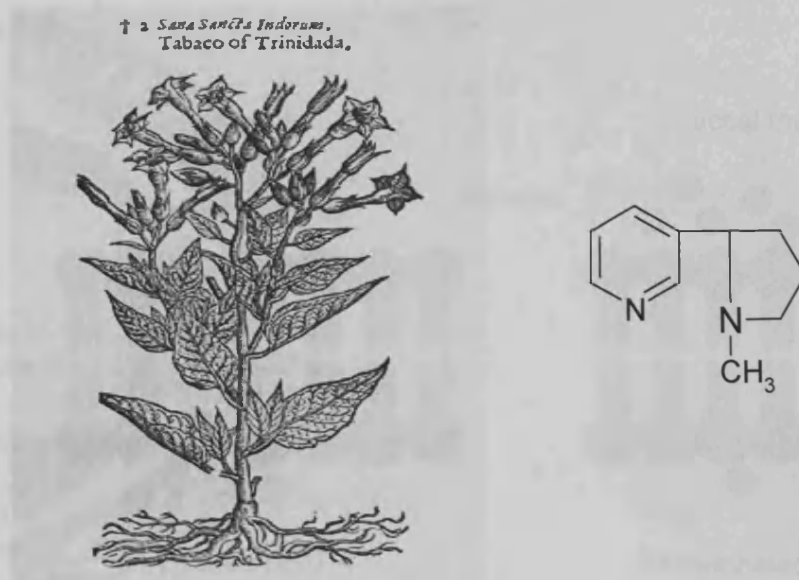
Figure 1.6 A tobacco plant. Drawing made by John Gerard (1545-1612) and the chemical structure of nicotine

Absorption of nicotine across a biological membrane is a pH dependent process (Fowler, 1954; Schevelbein *et al.*, 1973). Due to the presence of pyridine and pyrrolidine nitrogen, nicotine can be classed as dibasic with a pKa of 7.84 and 3.04 at 25°C. The proportion of uncharged nicotine increases as the pH of a solution increases. The uncharged organic bases are lipophilic (readily permeable to membranes), whereas charged organic bases are hydrophilic (not permeable to membranes) and consequently, the rate of absorption of nicotine increases as the pH increases (Yildiz, 2004).

This is demonstrated by the differences between smokers that inhale and smokers that do not inhale. The pH of cigarette smoke is generally in the range of 5.5, where the nicotine fraction at this pH is largely positively charged. Smokers that inhale have the primary route of absorption through the alveoli; this site has a pH of 7.4 and 31% of nicotine will be uncharged and able to pass through the membranes into the blood circulation. Very little nicotine will be absorbed at the buccal mucosa (primary route of absorption for smokers that do not inhale). The lipophilic nature of nicotine at a pH of 7.4 results in nicotine plasma levels reaching 40ηg/ml compared to nicotine

plasma levels of 2.5-8ŋg/ml for non inhaling-smokers (Russel *et al.*, 1980; Figure 1.7).
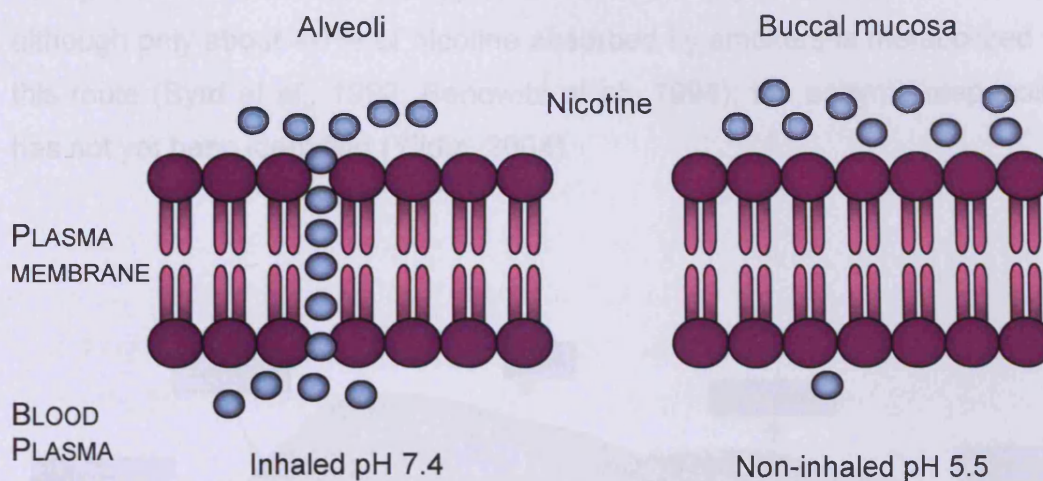
Figure 1.7 Principle sites of nicotine exposure. Schematic overview of the pH dependent absorption of nicotine at two of the principle sites of absorption

1.6.6.2 METABOLISM OF NICOTINE

Studies of nicotine metabolism have been conducted over several decades but problems have occurred due to investigators using different names for the same metabolite (e.g. *Trans*-3'-hydroxycotinine has been called Hydroxycotinine, 3'-Hydroxycotinine and 3-hydroxy-1-methyl-5-(3-pyridinyl) (Hukkanen *et al.*, 2005). The liver extensively metabolises nicotine into a number of metabolites (Figure 1.8). The metabolic pathways elucidated have identified the participation of cytochrome P450 and flavin adenine dinucleotide (FAD) containing monooxygenases (Peyton *et al.*, 1988) in nicotine metabolism. Present day studies, (Lee *et al.*, 2005) have made advancements in understanding nicotine metabolism with improved enzyme purification combined with a number of immunochemical and biochemical techniques.

Quantitatively, the most important metabolite of nicotine in most mammalian species is cotinine. In man, 70-80% of nicotine is converted to cotinine (McKennis *et al.*, 1963). This transformation involves two steps. The first is mediated by a cytochrome P450 system (mainly CYP2A6 and CYP2B6) to

produce nicotine iminium ion (Nakajimi *et al.*, 1996; Messina *et al.*, 1997). The second step is catalyzed by aldehyde oxidase (AOX; Brandage and Lindblom, 1979). Nicotine N'-oxide (NNO) is another primary metabolite of nicotine, although only about 4-7% of nicotine absorbed by smokers is metabolized via this route (Byrd *et al.*, 1992; Benowitz *et al.*, 1994); the enzyme responsible has not yet been identified (Yildiz, 2004).
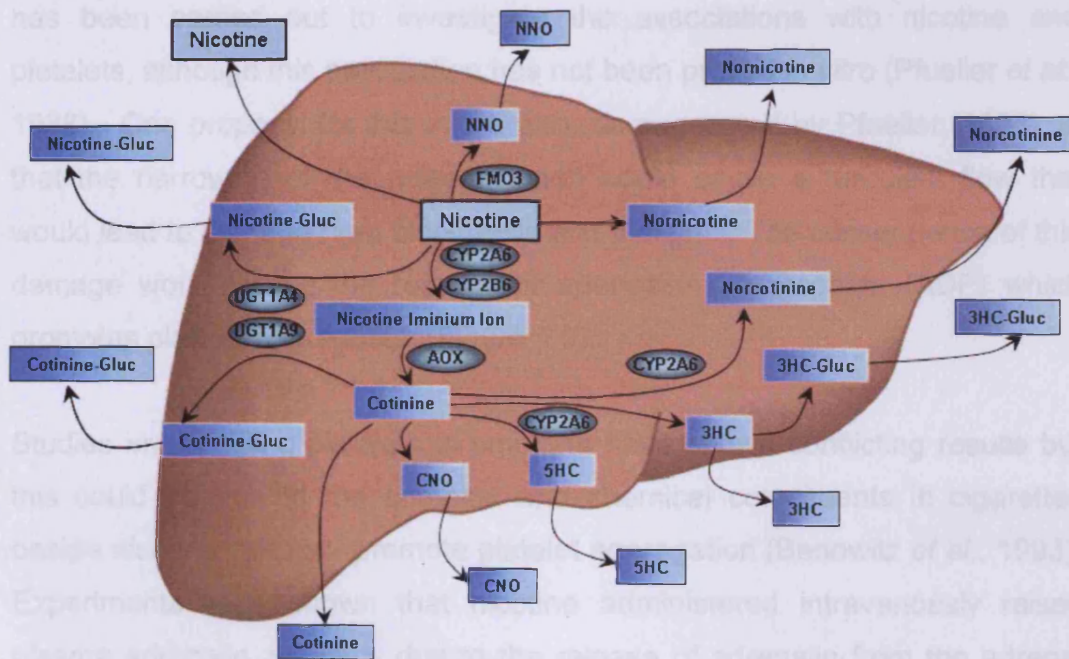
Figure 1.8 Pathway showing metabolism of nicotine in human liver.
Adapted from Ring *et al.* (2005)

The conversion of nicotine to NNO involves a flavin-containing monooxygenase 3 (FMO3; Cashman *et al.*, 1992; Park *et al.*, 1993). It appears that NNO is not further metabolized to any significant extent, except by reduction back to nicotine, which may lead to recycling of nicotine in the body (Duan *et al.*, 1991).

1.6.6.3 BIOLOGICAL EFFECTS OF NICOTINE

The effect of nicotine in the animal and cell system has been comprehensively researched (e.g. Yildiz, 2004; Hukkanen *et al.*, 2005). Nicotine has been shown to elict a variety of physiological effects (i.e. cardiac contractility, mobilisation of blood sugars and increased free fatty acids) but for the purpose of this study only the thrombogenic mechanisms of nicotine will be documented. The thrombogenic effects of nicotine can be attributed to interactions with platelets and prostaglandins. To date, extensive research has been carried out to investigate the associations with nicotine and platelets, although this association has not been proved *in vitro* (Pfueller *et al.*, 1988). One proposal for this interaction, as suggested by Pfueller (1988), is that the narrowing of the arterial lumen could cause a turbulent flow that would lead to damaged red blood cells and platelets. The consequence of this damage would cause the release of adenosine diphosphate (ADP) which promotes platelet aggregation (Figure 1.9).

Studies investigating platelets in smokers have shown conflicting results but this could be due to the complex and chemical constituents in cigarettes beside nicotine that may promote platelet aggregation (Benowitz *et al.*, 1993). Experiments have shown that nicotine administered intravenously raises plasma adrenalin, which is due to the release of adrenalin from the adrenal medulla. The presence of epinephrine stimulates platelet aggregation and thrombus formation by alpha-adrenergic mechanisms (Kershbaum and Bellet, 1964). These conditions are likely to be exacerbated by cigarette smoking, leading to sudden coronary death (Folts and Bonebrake, 1982).

The numerous experiments investigating nicotine and the effects on the cardiovascular system only elucidate its possible mechanisms, but the effects of nicotine combined with components of cigarette smoke have the potential to produce a hypercoagulable state via platelet aggregation that may well accelerate atherosclerosis and acute cardiovascular events (Benowitz *et al.*, 1993; Figure 1.10).

- Nicotine

+ Nicotine

Release of ADP

Narrowing of lumen
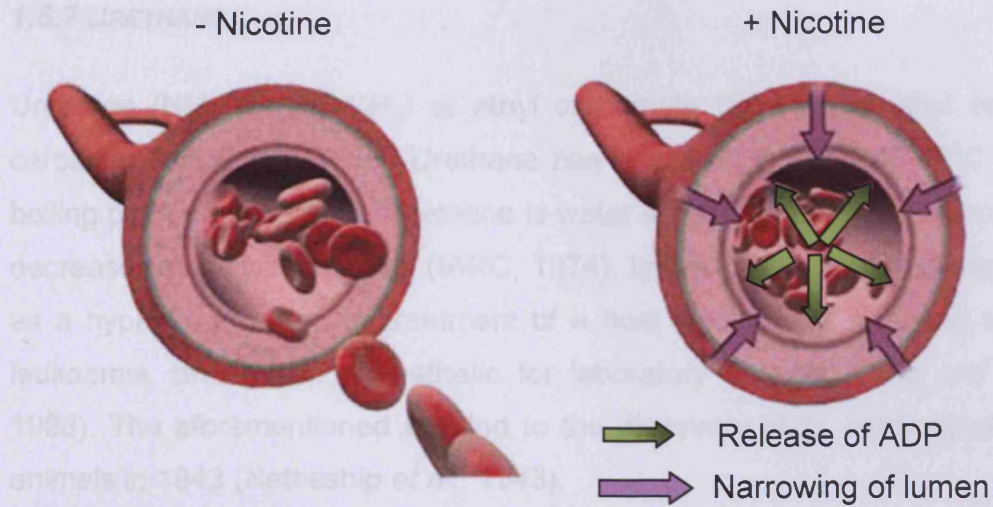
Figure 1.9 Proposed interaction of nicotine and platelets by Pfuller (1988). (Adapted from Lotrel Pharmaceutical 2005)
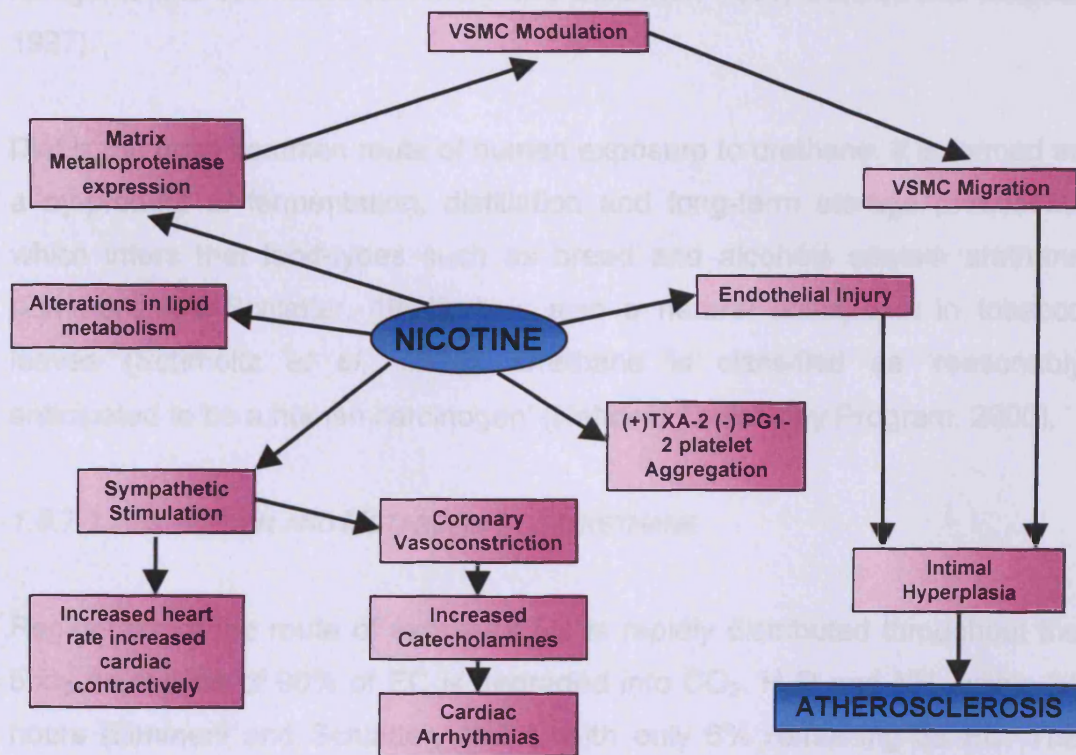
Figure 1.10 Role of nicotine in atherosclerosis. (Adapted from Kilaru *et al.*, 2001). Key: PG1-2, prostaglandin 1-2; TXA-2, thromboxane 2; VSMC, vascular smooth muscle cells

21

1.6.7 URETHANE

Urethane ($NH_2COOCH_2CH_3$) or ethyl carbamate (EC) is the ethyl ester of carbamic acid (NH_2COOH). Urethane has a melting point of 48-50°C and a boiling point of 182-184°C. Urethane is water soluble ($2gml^{-1}$) and its solubility decreases slightly in solvents (IARC, 1974). In the 1940's urethane was used as a hypnotic in man, for treatment of a host of diseases including chronic leukaemia, and as an anaesthetic for laboratory animals (Field and Lang, 1988). The aforementioned use led to the discovery of its carcinogenicity in animals in 1943 (Nettleship *et al.*, 1943).

Three more years passed before the activity of urethane within humans was described by Zimmerli and Schlatter (1991), and since 1948, urethane was known to be mutagenic in *Drosophila melanogaster* (Zimmerli and Schlatter, 1991). Exposure may also occur from the production of textiles, pesticides, fumigants and cosmetics (Zimmerli and Schlatter, 1991; Benson and Beland, 1997).

Diet is the most common route of human exposure to urethane. It is formed as a by-product of fermentation, distillation and long-term storage processes, which infers that food-types such as bread and alcohols contain urethane (Zimmerli and Schlatter, 1991). It is also a natural constituent in tobacco leaves (Schmeltz *et al.*, 1978). Urethane is classified as 'reasonably anticipated to be a human carcinogen' (National Toxicology Program, 2000).

1.6.7.1 ABSORPTION AND METABOLISM OF URETHANE

Regardless of the route of exposure EC is rapidly distributed throughout the body. In excess of 90% of EC is degraded into CO_2, H_2O and NH_3 within 24 hours (Zimmerli and Schlatter, 1991), with only 6% remaining as EC. The remaining EC is then excreted. Rates of EC metabolism have been researched; Yamamoto *et al.* (1988) showed that radio-labelled EC almost disappeared from the blood within 4 hours. However, a single dose of ethanol (5g/kg b.w.) leads to a high consistent blood level of EC that exists in excess

of 8 hours (Waddell *et al.*, 1987; Yamamoto *et al.*, 1988). This data implies that high doses of ethanol may postpone the metabolism of EC by blocking the metabolising enzymes including the group of cytochrome P450's (Schlatter and Lutz, 1990).

Gupta and Dani (1989) investigated the generation of vinyl carbamate (VC) and an epoxy derivative (Figure 1.11). These electrophilic metabolites are thought to be responsible for genetoxicity and carcinogenicity. This research indicated the existence of oxidation reactions at the ethyl group and was carried out *in vitro* using microsomes from rat lung.

This area of research has been further enhanced by the ability to study the bioactivation and/or detoxification of a xenobiotic by a single enzyme with the advent of genetically engineered mice (Gonzales, 1998; Gonzales and Kimura, 1999). Present day research on urethane focuses on the assessment of the role of CYP2E1 in urethane metabolism utilising the availability of CYP2E1-null and wild type mice.

1.6.7.2 BIOLOGICAL EFFECTS OF URETHANE

Extensive research has been prompted into the potential biological effects of urethane given its tumourigenesis in humans. The principle target/site being the liver (Siemiatycki *et al.*, 2004) in animals has prompted extensive research into EC's mechanisms of action. As mentioned in Section 1.6.7.1, the current accepted hypothesis is the chemical activation from EC to VC and subsequently vinyl carbamate epoxide (VCO); a prerequisite for tumour development (Hoffler *et al.*, 2003). Epoxide intermediates are highly reactive electrophiles that easily bind to macromolecules such as DNA, RNA and proteins leading to the production of adducts (Figure 1.11; Melnick, 2002). This led to the hypothesis that CYP2E1-mediated metabolism is a requirement for urethane induced cell proliferation, genotoxicity and carcinogenicity.

Urethane (Ethyl carbamate)

Vinyl carbamate

Vinyl carbamate epoxide

N^2,3-Etheno-dG   1,N^6-Etheno-dA   3,N^4-Etheno-dC   7-(2-Oxoethyl)-dG
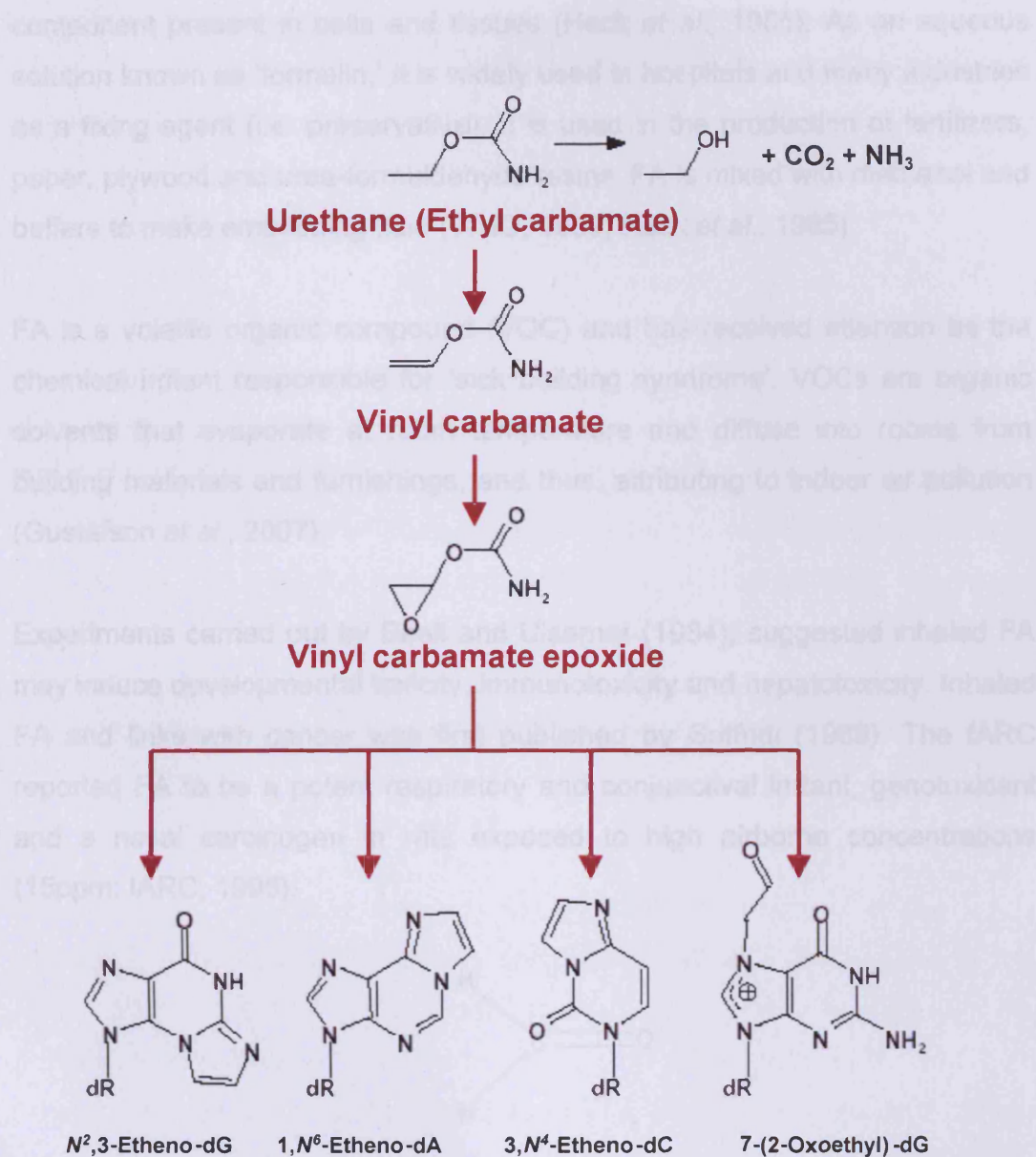
Figure 1.11 Metabolic pathways and DNA adducts derived from urethane (ethyl carbamate). (Adapted from Beland *et al.*, 2005) Key: dG,deoxyguanosine; dA,deoxyadenosine; dC, deoxycytidine; dR, deoxyribose.

1.6.8 FORMALDEHYDE

Formaldehyde (FA) is a colourless, flammable gas at room temperature, with a chemical structure of CH_2O (Figure 1.12). It has a pungent, distinct odour and can cause a burning sensation to the eyes, nose and lungs at high concentration (Cassanova *et al.*, 1988). FA is a naturally occurring biological

component present in cells and tissues (Heck *et al.*, 1985). As an aqueous solution known as 'formalin,' it is widely used in hospitals and many industries as a fixing agent (i.e. preservative). It is used in the production of fertilizers, paper, plywood and urea-formaldehyde resins. FA is mixed with methanol and buffers to make embalming fluid (WHO, 1989; Heck *et al.*, 1985).

FA is a volatile organic compound (VOC) and has received attention as the chemical irritant responsible for 'sick building syndrome'. VOCs are organic solvents that evaporate at room temperature and diffuse into rooms from building materials and furnishings, and thus, attributing to indoor air pollution (Gustafson *et al.*, 2007).

Experiments carried out by Beall and Ulsamer (1984), suggested inhaled FA may induce developmental toxicity, immunotoxicity and hepatotoxicity. Inhaled FA and links with cancer was first published by Soffritti (1989). The IARC reported FA to be a potent respiratory and conjunctival irritant, genotoxicant and a nasal carcinogen in rats exposed to high airborne concentrations (15ppm; IARC, 1995).
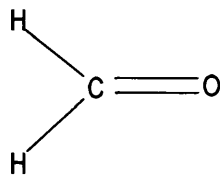
Figure 1.12 Chemical structure of Formaldehyde.

A recent large scale epidemiology study has shown a significant excess of deaths from nasopharyngeal cancer in industrial workers. These workers were exposed to acute high level and lower cumulative levels of FA (Hauptmann *et al.*, 2004). This work supports data from previous studies of U.S. embalmers (Hayes *et al.*, 1990), and an excess of nasopharyngeal cancer observed in a Danish study amongst workers involved in companies that manufactured or used FA (Hansen and Olsen 1995). Although there have been other studies that have reported fewer cases of nasopharyngeal cancer

than expected (Pinkerton *et al.*, 2004; Coggon *et al.*, 2003), these variations in nasopharyngeal cancer were deemed to be small by the IARC who have in turn re-classified FA to carcinogenic to humans (group 1), based on evidence from the Hauptmann *et al.* studies. This classification, in 2005, is higher than those previously issued by the IARC (IARC 1982, 1987 and 1995).

FA can be emitted from incomplete combustion processes and is emitted in the smoke from cigarettes. Approximately 1.5mg of formaldehyde was found in the total smoke from one cigarette, which was distributed between the MS and SS in the ratio of 1:50 (i.e. 30µg in the MS and 1526µg in the SS) [Jermini *et al.*, 1976]. Other investigators measured FA MS concentrations of 60-130µg/m^3. For an individual smoking 20 cigarettes per day, this would lead to an exposure in excess of 1mg/day (WHO 1989), compared with an occupational exposure of 2-6µg/m^3 for persons living in a suburban area (Agency for Toxic Substances and Disease Registry [ATSDR], 2006).

1.6.8.1 ABSORPTION OF FORMALDEHYDE

Formaldehyde vapours are easily absorbed; more than 90% of inhaled FA is absorbed in the upper respiratory tract (Heck *et al.*, 1985). Due to the hydrophilic nature of FA, the nasal mucosa and proximal trachea are the primary targets of inhaled FA (Kerns *et al.*, 1983; Woutersen *et al.*, 1987). At these locations FA is swiftly metabolised (oxidised) to formate and carbon dioxide or can be incorporated into biological macromolecules (IARC, 2005). Therefore, a very small change in FA (2.77±0.28µg/g) can be detected in human and animal blood post-exposure, compared to a FA concentration (2.61±0.41µg/g) pre-exposure (Casanova *et al.*, 1988; Heck *et al.*, 1985). FA concentrations at the primary target (nasal mucosa) and liver are found at 2 to 4-fold higher than that found in the blood (Heck *et al.*, 1982). All remaining FA is excreted in urine and faeces (Heck *et al.*, 1983).

1.6.8.2 METABOLISM OF FORMALDEHYDE

The metabolism of FA to formate (Figure 1.13) takes place in all tissues of the body, as an effect of its endogenous formation via formaldehyde

dehydrogenase (FDH). FDH is a metabolic enzyme distributed throughout animal tissues (particularly in the nasal mucosa of the rat), specifically for the glutathione adduct of FA (ATSDR, 1999a). The FA not metabolised by FDH has a number of fates (Figure 1.13):

- Formation of cross linkages between protein and single stranded DNA (DPX)
- Enter the one-carbon metabolic pool by initially binding to tetrahydrofolate (Bolt, 1987)
- Non-enzymatic reaction to form urea hydroxylmethyl adducts in urine.

Although FDH is the primary enzyme, there are at least 7 enzymes that catalyze the oxidation of FA in animal tissues, namely, aldehyde dehydrogenase, xanthinoxidase, catalase, peroxidase, glycerinaldehyde-3-phosphate dehydrogenase, aldehyde oxidase, and a specific DPN-dependent formaldehyde dehydrogen-ase (Cooper & Kini, 1962). The activity of FDH is not induced when exposed to FA (Casanova-Schmitz *et al.*, 1984).

1.6.8.3 BIOLOGICAL EFFECTS OF FORMALDEHYDE

Formaldehyde is mutagenic and genotoxic (de Serres and Brockman, 1999). The mutagenic and genotoxic potential of FA is consistent with its ability to form DPX. The presence of DPX has been shown in the nasal mucosa of monkeys exposed to FA (Casanova *et al.*, 1991). The existence of DPX has not been associated to pro-mutagenic tendencies but DPX has been associated with clastogenicity, i.e. chromosomal aberrations, deletions and sister chromatid exchanges (Merk and Speit, 1998; Speit and Merk, 2002). Numerous studies have demonstrated that FA does not cause point mutations *in vivo* (Craft *et al.*, 1987; Merk and Speit, 1998; Speit and Merk, 2002). Several studies have shown evidence of point mutations *in vitro* and a limited number of p53 mutations in some rat nasal mucosa tumours post-FA-exposure (Crosby *et al.*, 1988; Recio *et al.*, 1992). These results are consistent with a mechanism in which DPX acts as a replication block (Heck and Casanova, 2004; Merk and Speit, 1998; Permana and Snapka, 1994);

this mechanism could lead to numerous deleterious effects. FA inhibition of DNA replication has previously been reported *in vivo* (Casonova *et al.*, 1989; Casonova-Schmitz *et al.*, 1984) and *in vitro* (Permana and Snapka, 1994; Snyder and Van Houten, 1986).
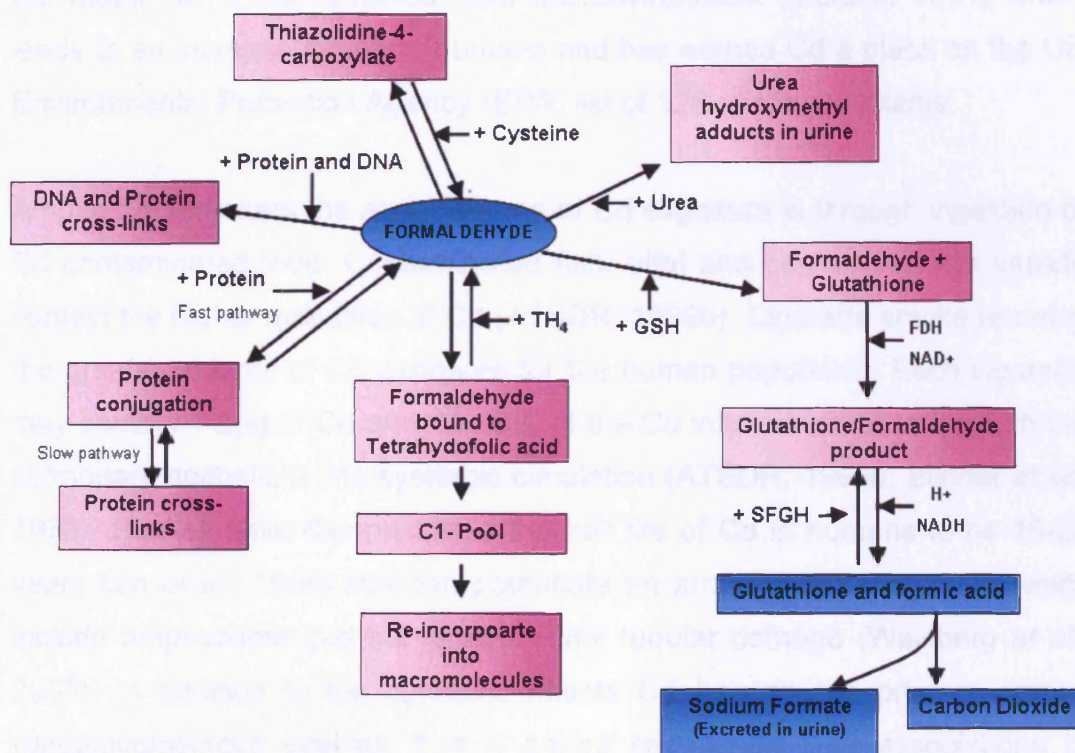
Figure 1.13 Biological reactions and metabolism of formaldehyde.
(Adapted from Bolt, 1987) Key: TH_4 = Tetrahydrofolic acid, SFGH = S-Formyl Glutathione, NAD+ = Nicotinomide adenosine dinucleotide, DNA = Deoxyribonucleic acid, FDH = Formaldehyde Dehydrogenase

1.6.9 CADMIUM

Cadmium (Cd) is a widespread heavy metal and exists in the 0 or 2^+ oxidation state. Large-scale use of Cd began in the 1940's (Stoeppler, 1991) and recent uses of Cd include nickel-cadmium batteries, pigments and plastic stabilisers (Waisberg *et al.*, 2003). Other sources of concern are phosphate fertilizers which often contain high levels of Cd depending on the origin of the rock (Thornton, 1992). Estimates of 25,000 to 30,000 tonnes of Cd are released

into the environment each year; human activities play a huge part of this by contributing 4000 to 13,000 tonnes per year with mining and burning fossil fuels (ATSDR, 1999b). Cd in the environment naturally exists as an inorganic salt such as cadmium oxide (CdO), cadmium chloride ($CdCl_2$) or cadmium sulphate ($CdSO_4$; ATSDR, 1999b). Although Cd may change chemical forms, the metal ion is not removed from the environment (Morselt, 1991) which leads to an increase in risk to humans and has earned Cd a place on the US Environmental Protection Agency (EPA) list of 126 priority pollutants.

Among non-smokers the major source of Cd exposure is through ingestion of Cd contaminated food. Contaminated fish, offal and cereal products usually contain the higher quantities of Cd (ATSDR, 1999b). Cigarette smoke remains the greatest source of Cd exposure for the human population. Each cigarette may contain 1-2μg of Cd and 40-60% of the Cd inhaled will pass through the pulmonary epithelium into systemic circulation (ATSDR, 1999b; Elinder *et al.*, 1976). Studies have demonstrated the half life of Cd in humans to be 15-20 years (Jin *et al.*, 1998) this can potentiate an array of disease states which include emphysema and irreversible renal tubular damage (Waisberg *et al.*, 2003). In addition to the cytotoxic effects Cd has on the primary organs (apoptotic/necrotic events), it is a potent carcinogen with associations to cancers of the lung, prostate, pancreas and kidney, earning Cd a category 1 human carcinogen status (IARC, 1993; National Toxicology Program, 2000).

1.6.9.1 ABSORPTION OF CADMIUM

As mentioned in Section 1.6.9 there are two main routes of Cd exposure, inhalation and ingestion. There is a possible third route, absorption via the skin but this has been shown to be relatively insignificant and the exposure would have to be over a prolonged period of time (Wester *et al.*, 1992). Cadmium exposure from ingestion is generally due to contaminated food or drinking water with $CdCl_2$ in particular, due to it being highly soluble in water when compared with CdO, which is mainly associated with inhalation (ATSDR, 1999b; Oberdorster, 1992).

When comparing absorption Moore *et al.* (1973), demonstrated up to 60% of Cd from the inhaled dose (Cd carbonate) was translocated to the gastrointestinal tract in rats. This is thought to be due to the mucociliary clearance and subsequent ingestion. Absorption of Cd via ingestion is greatly reduced with peak absorption at 16% in ovine (Miller *et al.*, 1969) and a 1-2% absorption in rodents (Ragan *et al.*, 1977).

1.6.9.2 METABOLISM OF CADMIUM

A number of factors contribute to the cellular toxicity of Cd and include dose, route and duration of exposure. The mode of Cd transport into target cells is not fully understood but several hypotheses exist. The first hypothesis, and most scientifically favoured, suggests Cd interacts and competes for binding sites on the membrane proteins involved in the transport of vital elements (e.g. Calcium, Zinc and Iron) into epithelial cells of the route of exposure e.g. lung or gut via ionic mimicry (Zalups and Ahmad, 2003). A second hypothesis suggests endocytosis of proteins containing Cd could be the mechanism by which it enters epithelial cells (e.g. Cd ions bind to metallothionein, albumin or other proteins; these conjugates act as substrates for endocytotic transport) [Zalups and Ahmad, 2003]. Both hypotheses imply the use of mimicry, this can be described as the process by which the Cd ion binds to an essential homeostatic molecule and the function of this molecule remains unchanged, i.e. mimicking the endogenous molecule (Cannon *et al.*, 2000, 2001). This is depicted in Figure 1.14, illustrating the intricate pathways for handling Cd in the body post-oral/pulmonary exposure. Also shown are the potential species of Cd that may be utilised in its transport and elimination.

1.6.9.3 BIOLOGICAL EFFECTS OF CADMIUM

There are many biological effects exerted by Cd on membranes, mitochondrial structure and function, DNA and gene expression (Pinot *et al.*, 2000). Oxidative stress is initiated by Cd in many cell types, this has been determined by decreased activity of antioxidants (Manca *et al.*, 1994; Yang *et al.*, 1997). The toxic effects of reactive oxygen species (ROS) are further

enhanced by the depletion of glutathione and protein bound sulfhydryl groups (Skoczynska, 1997).

This is highlighted at the mitochondrial level, with the inhibition of cellular respiration by Cd, which binds to the sulfhydryl groups, particularly those found within the hydrophobic region of the mitochondrial membrane (Rikans et al., 2000; Figure 1.15). This initiates a cascade effect with the thiol group inactivation leading to oxidative stress, with mitochondrial depolarisation and permeability transition contributing to mitochondrial dysfunction.

Following the opening of the permeability transition pores, ROS and cytochrome c are released from the mitochondria into the cytosol where they activate caspases, the final effectors of apoptosis (Pinot et al., 2000). The severe depletion of ATP leads to cell necrosis, modest depletion leads to protein degradation by ROS. This in turn, reduces the free heat shock protein-70 (Hsp70) pool, and results in activation and induction of the Hsp70 gene (Pinot et al., 2000; Figure 1.15). These Hsp are molecular chaperones essential for 'normal' cells and survival during injury especially oxidative stress (Polla et al., 1988; Polla et al., 1996). Heat shock proteins bind polypeptides, stabilise emerging polypeptides and facilitate their transport (Gething et al., 1995). The Hsp response attenuates oxidative and inflammatory injuries in pulmonary cells and whole lung (Villar et al., 1993; Wong et al., 1996).

1.7 EpiAirway™ Tissue Model

Traditionally, in vivo studies are used to investigate toxicant effects in the lung, however, public opinion and government legislation is leading to a decrease in the popularity of animal testing. A growing number of scientists are now working towards the Three R's principles of Russell and Burch (1959), which refers to the "reduction, refinement and replacement" of animal experiments. Consequently, viable alternatives need to be developed which can reproduce in vitro, toxic events that may occur in the human lung.
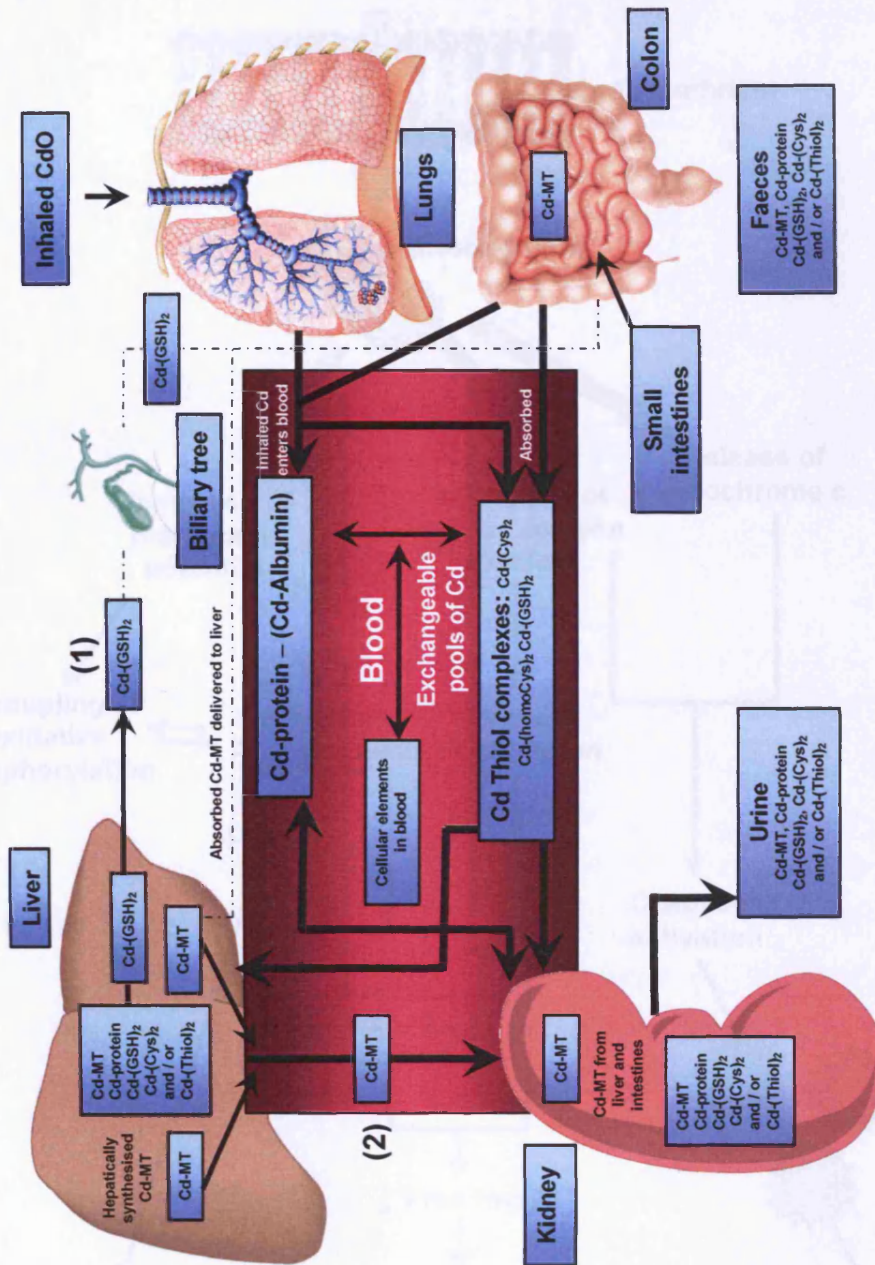
Figure 1.14 The interactions of Cd in the body after oral/gastrointestinal and pulmonary exposure to Cd. Potential pathways are highlighted with the handling and excretion of the different forms of Cd that maybe present in the relevant organs of the body adapted from Zalpus and Ahmad (2003); (1) GSH S conjugates Cd are degraded along the biliary tree to Cd-(Cys)$_2$; (2) Cd-MT released into sinusoidal blood from hepatocytes after induction of necrosis or apoptosis by Cd. Key to figure: MT = Metallothionein, CYS= Cysteine, GSH = Glutathione, *N*-Acetyl-Cys = N-acetylcysteine, homocys = Homocysteine
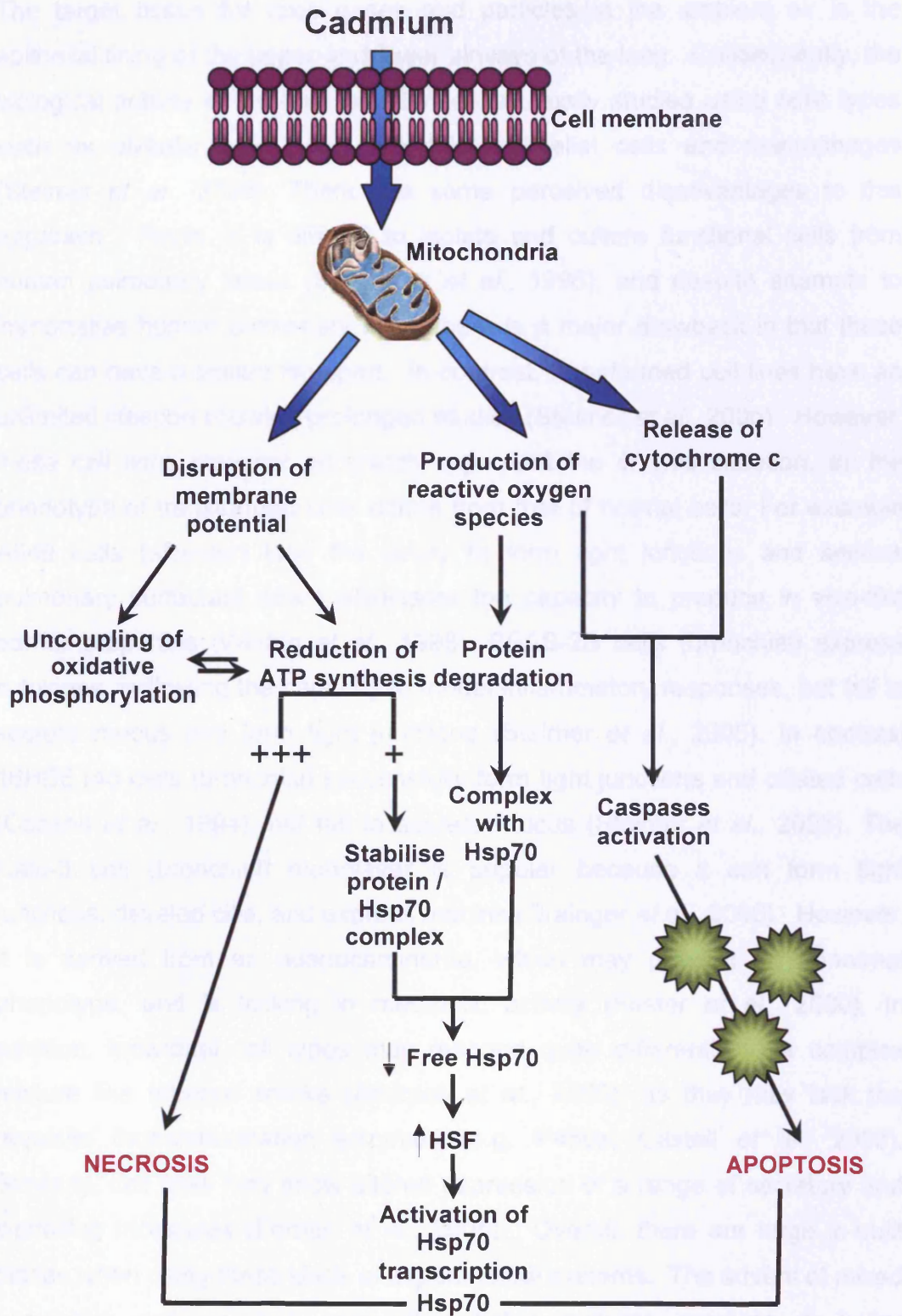
Figure 1.15 Interactions of Cd on mitochondria. The events lead to necrosis, apoptosis and/or activation of Hsp70 (adapted from Pinot *et al.*, 2000)

The target tissue for toxic gases and particles in the ambient air is the epithelial lining of the upper and lower airways of the lung. Consequently, the biological activity of airborne substances is usually studied using cells types such as alveolar type II or, bronchial epithelial cells and macrophages (Steimer et al., 2005). There are some perceived disadvantages to this approach. Firstly, it is difficult to isolate and culture functional cells from human pulmonary tissue (Schwarze et al., 1996), and despite attempts to immortalise human pulmonary cells, there is a major drawback in that these cells can have a limited life-span. In contrast, transformed cell lines have an unlimited lifespan allowing prolonged studies (Steimer et al., 2005). However, these cell lines may not accurately represent the in vivo situation, as the phenotype of transformed cells differs from that of normal cells. For example A549 cells (alveolar) lose the ability to form tight junctions and secrete pulmonary surfactant which eliminates the capacity to produce in vivo-like barrier properties (Winton et al., 1998). BEAS-2B cells (bronchial) express cytokines, indicating the capacity to model inflammatory responses, but fail to secrete mucus and form tight junctions (Steimer et al., 2005). In contrast 16HBE14o cells (bronchial) successfully form tight junctions and ciliated cells (Cozens et al., 1994), but fail to secrete mucus (Steimer et al., 2005). The Calu-3 cell (bronchial) monolayer is popular because it can form tight junctions, develop cilia, and express mucins (Grainger et al., 2006). However, it is derived from an adenocarcinoma, which may present an abnormal phenotype, and is lacking in metabolic activity (Foster et al., 2000). In addition, individual cell types may respond quite differently to a complex mixture like tobacco smoke (Andreoli et al., 2003), as they may lack the requisite biotransformation enzymes (e.g. P450s; Castell et al., 2005). Similarly, cell lines may show altered expression of a range of secretory and signalling molecules (Forbes et al., 2005). Overall, there are large in-built biases when using these kinds of experimental systems. The advent of mixed population cultures and multi-differentiated cultures provides a better indication of cell-cell interactions to generate more in vivo-like characteristics (Gruenert et al., 1995). A highly differentiated, 3-dimensional system is desirable because it models not only the different effects of toxins on specific cell types, but also the interaction between the cells. Moreover, epithelium

cultured at the air-liquid interface would facilitate *in vivo*-like chemical exposures. These requisites are met by a human derived, primary, upper airway, culture known as the EpiAirway™ Tissue Model (Figure 1.16: MatTek Corporation; BéruBé *et al.*, 2006).
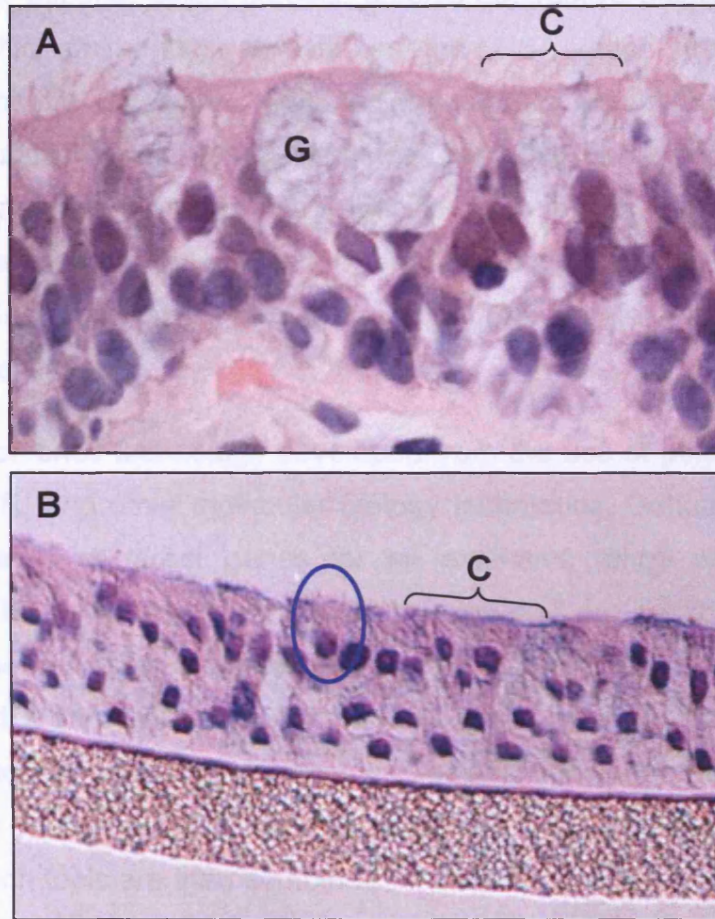
Figure 1.16 LM Comparison of a human epithelium and an EpiAirway™ Tissue model. (A) LM image of a human biopsy section (20X objective: provided by K. BéruBé), fully-differentiated epithelium, cilia present on apical surface (C) and Goblet cell (G). (B) H&E stained cross-sections of EpiAirway™ tissue (10X objective: MatTek Corporation), cilia present on apical surface (C) and Goblet cell (blue oval)

1.8 BIOMARKERS

Lung toxicology is demonstrated by functional assessment and pathology. The development of successful biomarkers requires the combination of a number of disciplines and skills, such as models of different types of toxicity to

generate regiospecific biomarkers, analytical/bioinformatic capability to identify and characterise them, and ability to develop and validate appropriate assays to confirm "fit for purpose".

Respiratory disease has huge healthcare cost. Over £12 billion is spent on medicines for asthma, cystic fibrosis, chronic obstructive pulmonary disease and idiopathic pulmonary fibrosis in the USA each year (Personal communcation Dr P. Bach). Validated biomarkers are needed to replace insensitive functional and labour intensive pathological methods, which only reflect advanced toxicity. Robust (specific and selective) biomarkers will include those used to assess disease, but never validated for toxicology, and novel peptides from proteomics will help improve safety assesment and reduce animal usage.

The advent of 'omic technology developed from the use of polymerase chain reaction (PCR) and other molecular biology techniques. Genomics facilitated the identification of target genes for an extensive range of toxicological endpoints. The development of transcriptomics and proteomics then further identified whether observed gene changes were effectual on a cellular level (Pandey and Mann, 2000). Genomics and proteomics can be useful tools when monitoring interactions between genes, gene products and the environment (Afshari, 2002; Waters et al., 2003). Loosely termed the 'omics', these research tools are then combined in Systems Biology in order to gain a broader understanding of the mechanistics of the test system. These new technologies are being adapted rapidly throughout industry and academia to investigate a range of endpoints and the identification of 'intelligent biomarkers' (Aardema and MacGregor, 2002).

1.8.1 TOXICOGENOMICS

Exposures of chemical and xenobiotics to biological systems and the mechanistics involved in the effects these toxins play are the basis of toxicological investigations. Closer scrutiny of the exposure, harm and repair pathways at the molecular level is essential in the understanding of mechanistic behaviour. Toxicogenomics can broadly be defined as "the study

of the relationship between the structure and activity of the genome (the cellular complement of genes) and the adverse biological effects of exogenous agents" (Aardema and MacGregor, 2002).

1.8.2 GENE EXPRESSION STUDIES

Toxicant exposure, including inhalation of xenobiotics, can alter gene expression either directly or indirectly and the majority of toxicological effects are achieved under molecular control. Gene profiles can be constructed and the toxicological profiles of uncharacterised xenobiotics can be compared to established patterns, minimising testing costs and time compared to conventional toxicological methods (Figure 1.17). Application of this technology could benefit end-users in many other ways, including making improvements to public health policy (Henry, 2002) and risk analyses (Pennie and Kimber, 2002; Olden, 2004).

Mechanisms of toxicity can be also elucidated by analysing patterns of gene expression initially used as a 'fishing' tool. This can lead to identification of molecular targets of toxicants, biomarkers (important for effect and exposure) and improved mechanistic understanding (Pennie, 2000; Pennie et al., 2000). The use of this technology can also enhance toxicological understanding through identification of dose-response relationships from induction of toxicity. Utilisation of these data can provide the basis for chemical screening tools and predictive toxicology. Toxicogenomics has already been successfully applied to evaluating human bronchial epithelial cell response following exposure to cigarette smoke in vivo (Spira et al., 2004) and in vitro (Fields et al., 2005; Maunders et al., 2007).

There are limitations with this technology; this technique generates a vast amount of data and during the data mining stages small/subtle genes can be ignored and could lead to misinterpretation and error. Without concurrent data regarding the relative up- or down-regulation of the functional proteins, significant findings can be overlooked and false positives followed. An

example of this is the lack of separation between downstream (secondary) transcriptional changes in gene expression and causative (primary) changes.
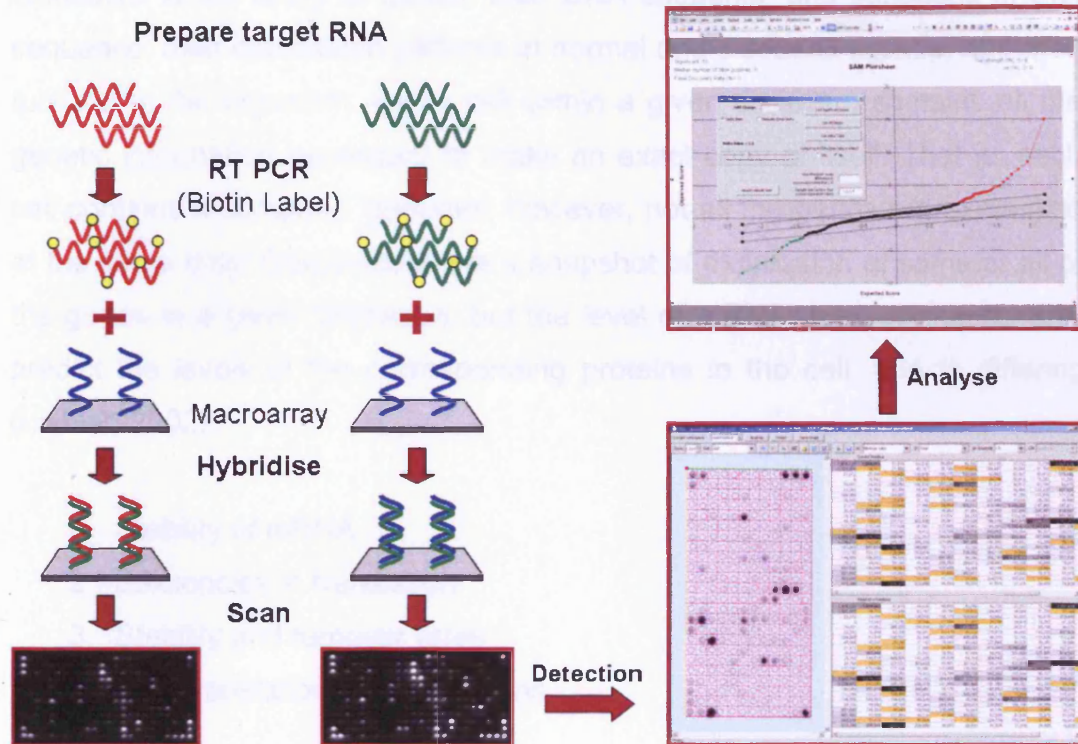
Figure 1.17 An overview of the array process. The RNA is biotin labelled during a reverse transcription reaction and the labelled cDNA copy is then hybridised to the DNA sequences bound to the array. Detection and quantification of the array information is achieved using software specific to the type of array used (SuperArray). Finally, global normalisation and robust statistical analyses are applied (SAM; Stanford University). This enables the relative abundance of each of the gene sequences in two or more biological samples to be compared

1.8.3 PROTEOMICS

Proteomics is used to separate and identify proteins in a complex mixture for the purpose of quantitative and functional analyses of all the proteins present (Abbott, 1999, Hunter *et al.,* 2002). It has proven to be a powerful tool for identifying early changes at the protein level in a variety of disease states (Kvasnicka, 2003). It can also provide a non-invasive technique for evaluating

body fluids in the search for pertinent or specific biomarkers of toxicity (Kennedy, 2001).

Genomics is the study of genes, their DNA sequence and variations of that sequence, their expression patterns in normal and diseased tissues, and their function in the organism. Every cell within a given organism contains all the genetic information necessary to make an exact copy of itself. That is, each cell contains a complete 'genome', however, not all the genes are expressed at the same time. Genomics offers a snapshot of expression of some or all of the genes in a given cell/tissue, but the level of mRNA does not necessarily predict the levels of the corresponding proteins in the cell, due to differing (Liebler, 2002):

1. Stability of mRNA
2. Efficiencies in translation
3. Stability and turnover rates
4. Post-translational modifications

The relative abundance of thousands of different proteins along with their cleaved/modified forms is a reflection of the ongoing physiological and pathological events (e.g. cells will leave a different protein signature depending on their condition such as health, disease, growth rate and drug treatment; Liotta *et al.*, 2003). The Human Proteome Organisation has a goal to catalogue every distinct human protein, all protein-protein interactions and levels of proteins in different cells and tissues (www.hupo.org).

1.8.4 NANO LIQUID CHROMATOGRAPHY

The major development of microcolumns using fused silica capillaries with 20-250µm inner diameters transformed high pressure liquid chromatography (HPLC) in the 1980's. This radical change gave HPLC greater sensitivity and greater separation efficiency (Takeuchi and Ishii, 1980, 1981; Kennedy *et al.*, 1989). The recent development of nano liquid chromatography (nano-LC) separation was coupled to a Nobel Prize technique, matrix-assisted laser

absorption/ionisation (MALDI; Karas and Hillenkamp, 1988), by continuous spotting of the eluate from the nano-LC onto the MALDI plates (Lee *et al.*, 2002; Figure 1.18).
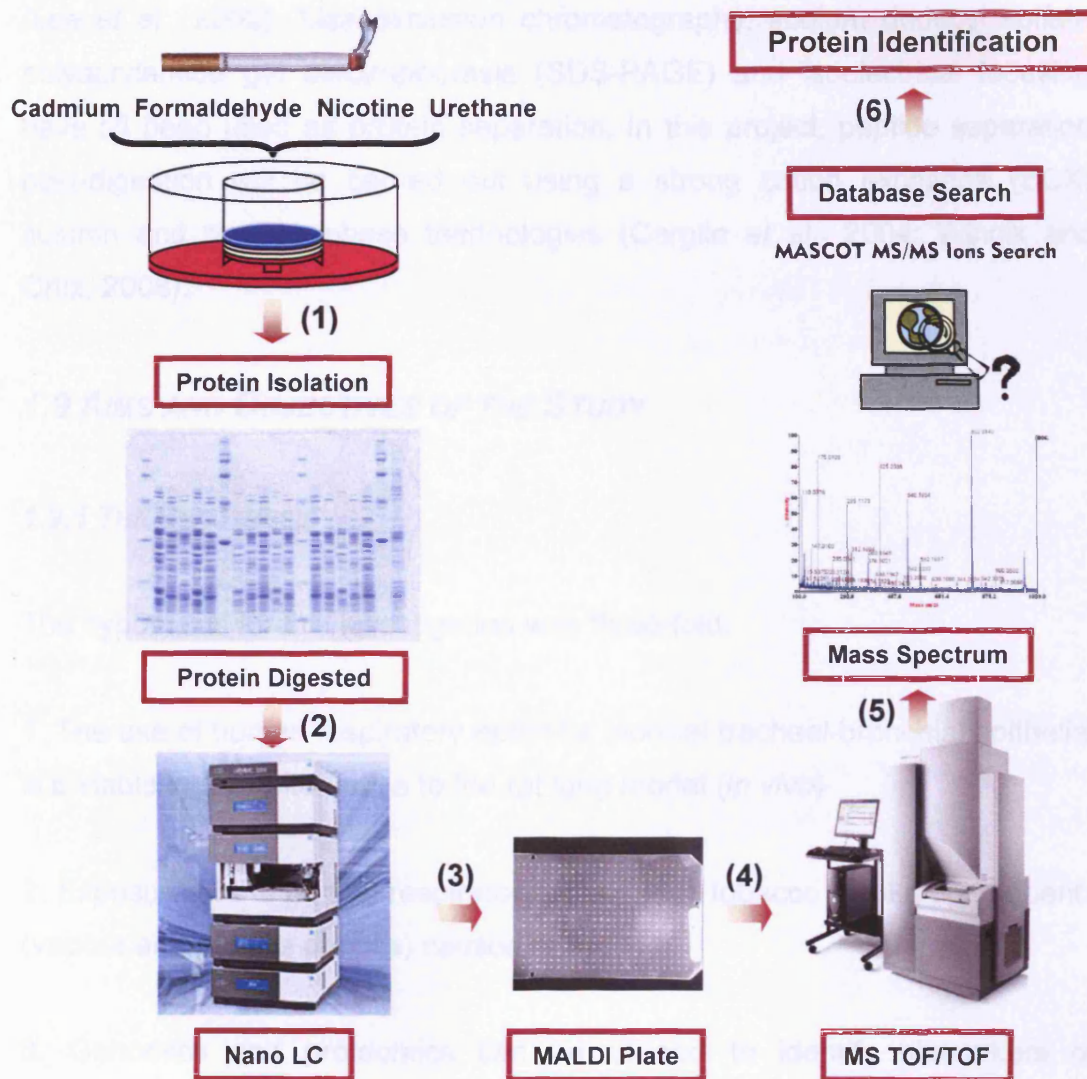
Figure 1.18 Proteomic analysis. A flowchart of the proteomic process involved in identification of proteins and potential biomarkers: (1) exposed cells harvested and lysed, (2) proteins denatured and labelled, (3) fractionation of labelled peptides, (4) fractionated protein spotted on a LC-MALDI sample plate, (5) MS was performed using a MALDI TOF/TOF (6) MS/MS queries were performed using the MASCOT Database search engine, embedded into Global Proteome Server (GPS) Explorer software on the Swiss-Prot database

Although current nano-LC coupled with a tandem mass spectrometry (MS/ MS) has the throughput ability of 4000 peptides per run (2 hours; Ishihama,

2005), it is not able to analyse a complex peptide mixture from a whole cell lysate. Therefore, additional steps are required to reduce the complexity of the peptides. Ultra-centrifuging and the use of sucrose gradients can increase the number of proteins identified by purifying the cellular component of interest (Lee *et al.*, 2002). Size exclusion chromatography, sodium dodecyl sulfate polyacrylamide gel electrophoresis (SDS-PAGE) and isoelectrical focusing have all been used as protein separation. In this project, peptide separation post-digestion will be carried out using a strong cation exchange (SCX) column and reverse phase technologies (Cargile *et al.*, 2004; Winnik and Ortiz, 2008).

1.9 AIMS AND OBJECTIVES OF THE STUDY

1.9.1 THE HYPOTHESIS

The hypothesis for this investigation was three-fold:

1. The use of human respiratory epithelia (normal tracheal-bronchial epithelia) is a viable *in vitro* alternative to the rat lung model (*in vivo*)

2. Exposure of the human respiratory epithelia to tobacco smoke components (vapour and particle phases) causes harm

3. Genomics and proteomics can be utilised to identify biomarkers of exposure and harm in the human respiratory epithelia to tobacco smoke components

1.9.2 PROJECT AIMS AND OBJECTIVES

The objective of the proposed research was to identify intelligent biomarkers, these are genomic/proteomic biomarkers with the corresponding protein and gene expression data in the human respiratory epithelia following exposure to selected particle (e.g. cadmium and nicotine) and vapour phase (e.g. formaldehyde and urethane) tobacco smoke components (TSC). The key

components were selected for their thrombogenic capacity (nicotine), cytotoxicity (cadmium) and production of reactive metabolites during xenobiotic metabolism (formaldehyde and urethane). Thus, providing a holistic approach towards the identification of biomarkers in the pulmonary epithelium (i.e. cells derived from human primary explant tissue) *in vitro*.

Conventional toxicological analysis will be used, at the first instance, to establish the dose of the various TSC required to induce alterations in epithelial resistance, secreted surface proteins and release of inflammatory markers. It was imperative that the final working doses used were sub-toxic, since the objective was to identify the important biomarkers involved with toxicant stress and to avoid studying dead or dying cells. Following the establishment of the dose required to achieve these different biological endpoints, the toxicogenomic investigations will be initiated.

Toxicogenomic experiments will be designed to identify early molecular markers for events in pulmonary injury (i.e. 24 hours). Microarray technology will be employed to compare the patterns of mRNA expression of human genes associated with stress, simultaneously from control and TSC treated lung tissue. The major candidate genes will be classified (e.g. growth factors, inflammation, and xenobiotic metabolism) and associated with the biological endpoints. Stringent lists of candidate genes associated with these changes will be generated, thereby providing data on the mechanisms of the biological endpoints, i.e. biomarkers.

Finally, mRNAs levels do not necessarily predict the levels of the corresponding proteins in a cell. Consequently, proteomic analysis will be used to correlate candidate gene responses with a specific protein. The main interest of the study was the proteins involved in the early stress phase of toxicant challenge. Once a protein function had been identified, this provided an insight into the mechanism of action of the responsive genes or the "intelligent biomarkers" of TSC exposure in lung epithelia (Figure 1.19).
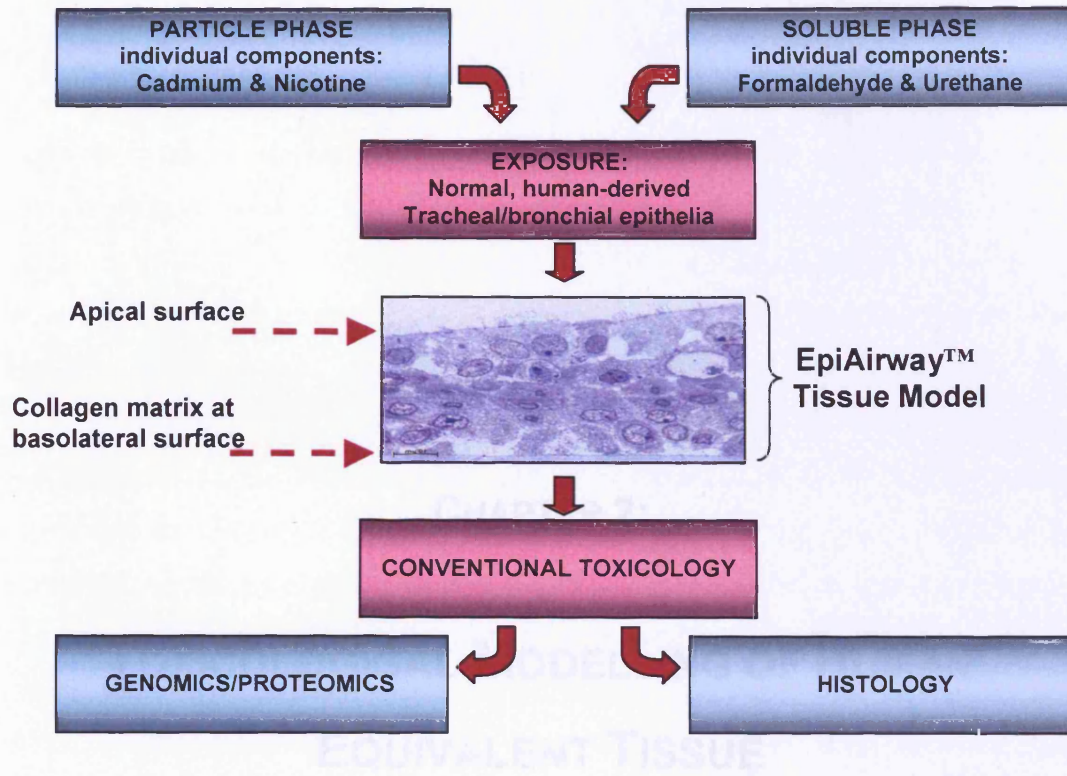
Figure 1.19 The general research project aims. Flowchart of the project aims involved in identification of genomic and protein biomarkers of exposure in the respiratory epithelia to tobacco smoke components. Tissue provided by K.Sexton

CHAPTER 2:

TOXICOLOGICAL MODELLING OF HUMAN EQUIVALENT TISSUE

2.1 INTRODUCTION

Scientific reviews by Coggins (2002 and 2007) of the chronic inhalation studies of mainstream cigarette smoke in all five species of laboratory animals (e.g. rats, mice, hamster, dog, non-human primates) used to evaluate carcinogenic potential, revealed no statistically significant increase in the incidence of malignant lung tumours and atherosclerosis following exposure to smoke. Furthermore, these findings were not consistent with the epidemiological results observed in human smokers. The outcome of the comprehensive animal studies reviewed by Coggins does support the idea that research should focus on the use of human tissue to try to corroborate the epidemiological findings. This obviously limits what can be achieved using acute/chronic exposure studies to cigarette smoke and/or various tobacco components. It is also difficult to study environmental contaminants such as tobacco smoke because of methodological problems in testing entire atmospheres. Most investigations are based on *in vivo* and *in vitro* experiments that use model substances and surrogate mixtures to simulate the real life situation. In this respect, *in vitro* systems, in particular, offer the possibility of using human target cells and comparing the results with human data. This eliminates any difficulties in extrapolating animal data to humans, and reduces the need for animals in testing such atmospheres.

The target tissue for toxic gases and particles in the ambient air is the epithelium lining the upper and lower airways. Therefore, different cells types such as alveolar type II cells, bronchial epithelial cells or macrophages have been used to study the biological activity of airborne substances (e.g. Steimer *et al.*, 2005). However, there are perceived disadvantages of this approach in that cell lines typically exhibit several abnormal characteristics in addition to their immortality and those abnormalities can impede toxicological studies. For example, certain airway cell lines have lost the ability to form tight junctions, thereby eliminating their capacity to produce *in vivo*-like barrier properties (e.g. A549 cell line; Steimer *et al.*, 2005). It would be much better to have a more complex interactive system like the normal human bronchial

epithelium (NHBE; Forbes and Ehrhardt, 2005). The NHBE is a mixed cell population of cells with differing phenotypes representative of the proximal airways. Their primary role is to maintain defence systems e.g. muco-ciliary transport, P450's, cytokines and basal stem cells. In addition, individual cell types may respond quite differently to a complex mixture like tobacco smoke; they may lack biotransformation enzymes which are necessary to produce toxic metabolites (Castell *et al.*, 2005).

In searching to remove these disadvantages, a commercially available, primary, upper airway, culture has become available, known as the EpiAirway™ Tissue Model (ETM; MatTek Corp.). ETM consists of cells derived from human primary explant tissue from three donors, requiring no animal tissue/product. It has been cultured to form a pseudo-stratified, highly differentiated, 3-dimensional (3-D) tissue that closely resembles the epithelia of the human respiratory tract. This model is not developed from lung tumours/disease tissue, thus cells are genotypically/phenotypically more representative of normal epithelia than other commonly used models. It provides a novel, toxicological tool that offers a means of assessing various respiratory tract issues while avoiding species extrapolation and the use of laboratory animals (e.g. BéruBé *et al.*, 2006).

In the following work, conventional toxicological analysis (e.g. trans-epithelial electrical resistance [TEER], cell viability [MTT] and protein assay) was used to establish the dose of TSC needed to cause changes in epithelial resistance, secreted surface proteins and release of inflammatory markers. By applying conventional toxicology techniques, a dose-response range could be established and the toxic effect of the TSC thus characterised. This dose range was considered important for gaining an understanding of potential protective mechanisms, and would be utilised in further toxicogenomics and proteomic investigations (Chapters 4 and 5).

A key feature to note is that it was imperative that the final doses used were sub-toxic, since the research objective was to identify important biomarkers involved with toxicant stress, rather than studying dead or dying cells.

2.2 Materials and Stock Solutions

2.2.1 Cells and Materials

Materials:	Supplier:
The EpiAirway™ Tissue Model	MatTek, Ashland, USA
MTT 100 Kit	MatTek, Ashland, USA
Growth Media	MatTek, Ashland, USA
EVOM	World Precision Instruments
ENDOHM-12	World Precision Instruments
Bradford Reagent (B6916)	Sigma-Aldrich
Dulbecco's Phosphate Buffered Saline (+Mg^{2+} + Ca^{2+}; D8662)	Sigma-Aldrich
Cadmium Chloride (28811-1ml-f)	Sigma-Aldrich
RNAlater (R0901)	Sigma-Aldrich
(-) Nicotine (N3876)	Sigma-Aldrich
Formaldehyde (433284)	Sigma-Aldrich
Urethane (U2500)	Sigma-Aldrich
Proteoplex Human (71414-3)	Merck Biosciences, Germany

Table 2.1 Materials used and their suppliers. All suppliers are UK based unless stated

2.2.2 Stock and TSC Solutions

Bovine Serum Albumin (BSA) was supplied as a 2mg/ml stock solution (Sigma; P0834). A dilution range (0-10µg/ml) was prepared as required and stored at 4°C.

Cadmium Chloride was supplied as a 0.1M solution (Sigma; 28811). A series of dilutions (0-400µM) in PBS was prepared as required and stored at 4°C.

Nicotine was supplied as a solution (Sigma; N3876). A dilution range of (0-125mM) was prepared in PBS as required and stored at 4°C.

Formaldehyde was supplied as a 35% weight in water (Sigma; 433284). A series of dilutions (0-25mM) was prepared in PBS as required and stored at 4°C.

Urethane was supplied as a solid (Sigma; U2500). A series of dilutions (0-2M) was prepared in PBS as required and stored at 4°C.

2.3 METHODS

2.3.1 CELLS, CULTURE AND EXPOSURE

Upon receipt of the EpiAirway™ cell cultures from MatTek Corporation in the USA, the cells were handled according to the manufacturer's specifications as follows. Briefly, cells were removed from transport packaging immediately after being received, the basal surfaces rinsed in pre-warmed PBS (37°C) and placed into 0.9ml pre-warmed culture medium (37°C) in a 6-well culture plate. They were equilibrated at 37°C with 4.5% CO_2 for 24 hours. After this time, an initial transepithelial electrical resistance (TEER, Section 2.3.2) value was recorded to assess the tissue integrity. Following this culture preconditioning, the cells were deemed ready for exposure to TSC. Individual TSC were prepared by adding them to sterile phosphate buffered saline with Mg^{2+} and Ca^{2+} (PBS) and shaken to ensure full solubilisation and mixing. The four different TSC solutions were prepared fresh on the day of use. TSC solutions were then warmed to 37°C before use. Apical exposure of the cells (n = 4 wells per dose) consisted of placing a 100µl volume of a solution onto the apical surface. Final working solution concentrations were determined during

the conventional toxicology studies (e.g. TEER and MTT assay [Section 2.3.2 and 2.3.3]).

2.3.2 TRANS-EPITHELIAL ELECTRICAL RESISTANCE

Trans-Epithelial Electrical Resistance (TEER) was used as a primary indicator of tissue stress by measuring the integrity (i.e. maintenance) of the cellular tight junctions. MatTek provides cultures with an established TEER value between 400-500 Ohms cm^2.

Briefly, the electrodes of the Endohm tissue resistance chamber needed to be equilibrated 24 hours before use, by filling the chamber with PBS and connecting the electrodes to the base unit with the power off. Immediately before use (and subsequently every 12 measurements), the calibration is checked and zeroed (if necessary) by altering the potentiometers. Following equilibration, the cultures were washed by placing 2ml of PBS into each well of a 6-well plate and the cultures then placed into these wells, with an additional 0.3ml of PBS added to the apical surface. The wash was subsequently aspirated and retained (Section 2.3.4). A further 0.25ml of PBS was then added to the apical surfaces. A blank culture insert (with 0.25ml PBS on the apical surface) was then placed into the Endohm tissue resistance chamber and a measurement taken (Figure 2.1). The cultures were tested in sequence, with a blank measurement being taken every 6 test measurements.

After TEER measurements, the PBS was aspirated from the culture surface and discarded; the culture was then placed in RNAlater (Chapter 4, Section 4.3.1; unless used for a MTT assay). All cultures were then kept at -20°C until further use in the genomics and proteomics investigations (Chapters 4 and 5).
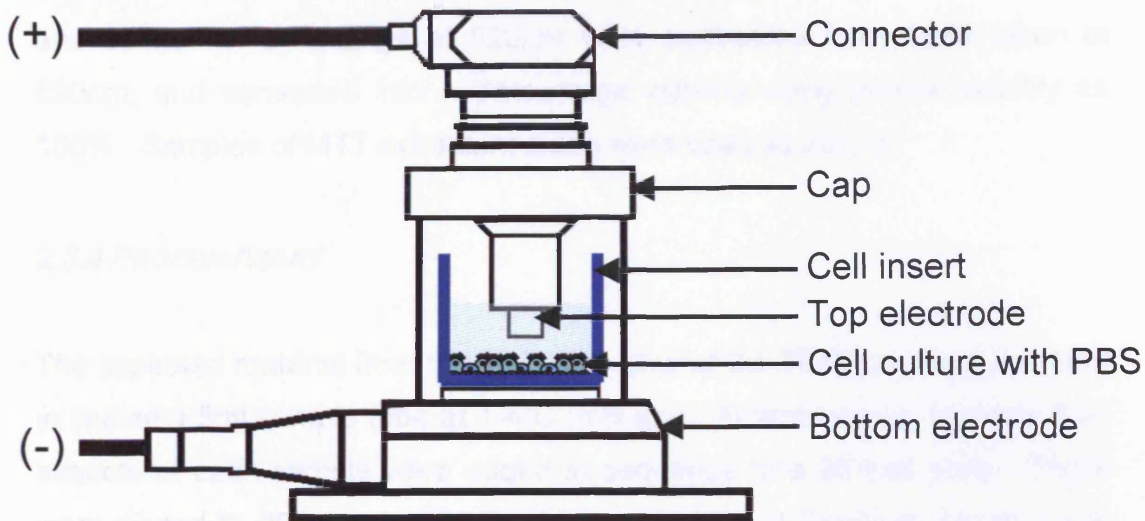
Figure 2.1 Diagrammatic overview of the ENDOHM chamber. This figure displays the EpiAirway™ culture in the ENDOHM chamber for a TEER reading. Control cultures have a TEER value between 400-500 Ohms cm^2, a culture with a loss of cellular integrity will have a TEER value >100 Ohms cm^2

2.3.3 MTT

The MMT [3-(4,5-dimethylthiazol-2-yl)-2,5-diphenyl tetrazolium bromide] assay for cellular growth and survival (Mossman, 1983), was used as an additional indicator of tissue viability. On the day of use, the MTT reagent and diluent (MTT 100 Kit, MatTek Corp.), were warmed to 37°C and kept in the dark. Immediately before use, these solutions were mixed and 300μl of the resultant solution added to the necessary number of wells in a 24-well plate. The cultures were taken from the wash-step of the TEER protocol (Section 2.3.3) and placed in the MTT solution. These were then protected from the light and incubated at 37°C, 4.5% CO_2 for 3 hours. Meanwhile, 2ml of MTT extractant solution was aliquoted into each necessary well of a further 24-well plate, and after the incubation period, the cultures were inserted into the extractant. These were sealed and left in the dark for 24 hours, after which time triplicate 100μl aliquots of solution from each test culture were put into a 96-well assay plate, to each of which was added a further 100μl of MTT

extractant solution. These plates were then read on a plate-reader at 590nm and 620nm. The readings at 620nm were subtracted from those taken at 590nm, and converted into a percentage viability using control viability as 100%. Samples of MTT extractant alone were used as blanks.

2.3.4 PROTEIN ASSAY

The aspirated material from the first wash step of the TEER protocol was kept in sealed 1.5ml sample tube at 1-4°C until use. At time of use, triplicate 50µl aliquots of each sample were added in sequence to a 96-well plate. These were diluted to 200µl using PBS, after which 50µl of Bradford Reagent was added and mixed by pipetting (Bradford, 1976). The plates were sealed and protected from the light for 5 minutes in order to allow the colour to fully develop and then read at 540nm on a plate reader (Opsys MR, Dynex). Results were converted to concentrations using a graph of standards generated by assaying known concentrations of bovine serum albumin (BSA) and the dilution factors were then accounted for. Samples of PBS alone were used as blanks.

2.3.5 CYTOKINE ASSAY

The production and release of endogenous cytokines into the basal medium of the cultures was tested using the Proteoplex™ 16-well Human Cytokine Array. Each well of the Proteoplex™ Array contains an identical microarray of the 12 anti-cytokine capture antibodies, each spotted in quadruplicate (Figure 2.2). The detection strategy is a standard 'sandwich' immunoassay that relies on biotinylated detection antibodies and streptavidin-conjugated fluorophore for detection (Figure 2.3).

The culture medium from each culture post-exposure to TSC (0.9ml) was kept in sealed 1.5ml sample tubes at 1-4°C until use. At time of use, 100µl aliquots of each dose were added in sequence to the microarray and processed as described in the user protocol. Firstly the human cytokine standard was

reconstituted in 1.25ml PBS, the microarray slide was then washed two times with PBS-tween (PBST). The sample and cytokine standard was added to the appropriate well and incubated at room temperate (RT) with gentle agitation for 60min. The sample and cytokine standard was then removed and the slide was washed 4 times with PBST. Detection was carried out using SensiLight™; 100µl was added to each well and incubated at RT for 90min. The SensiLight™ was aspirated and the slide was washed 4 times with PBST. At this point the well support was removed from the glass slide; the slide was then placed in the rinse solution for 10sec. The slide was dried by placing the slide in a slide dryer and where it was centrifuged for 1min at 200x *g*. The microarray was then scanned at 633nm excitation (Ex) and 660nm emission (Em) at 10µm (GenePix 4000B, Molecular Devices). All samples were run in triplicate.

2.3.6 STATISTICAL ANALYSIS

The statistical difference between data points was determined using a two-tailed Student's t-test. Standard deviation was used to represent experimental variation. Significance was accepted at P≤ 0.05.
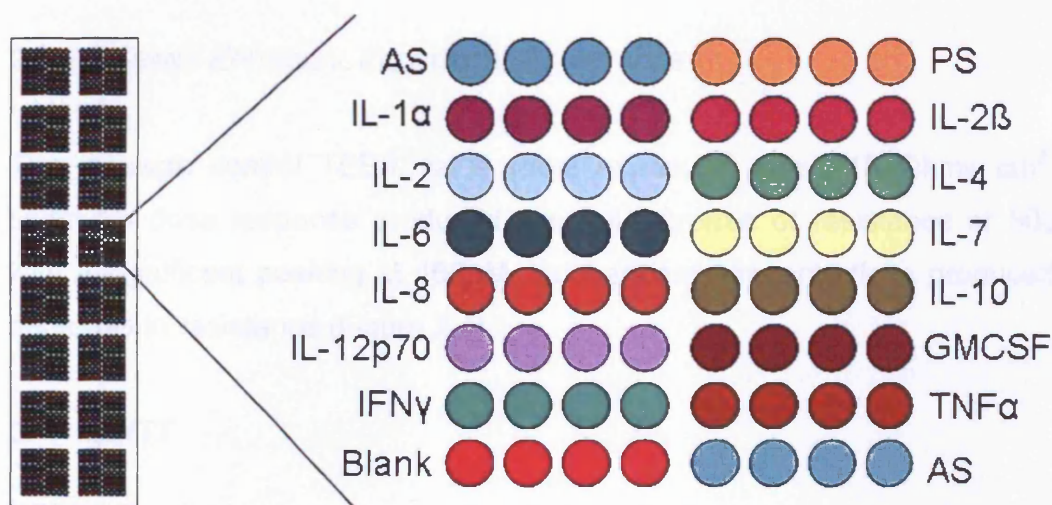
Figure 2.2 Proteoplex™ Microarray layout. 16 identical arrays on each slide and map of each array, showing the arrangement of the 12 capture antibodies, alignment spots (AS), positive control spots (PS) and negative control spots (Blank)
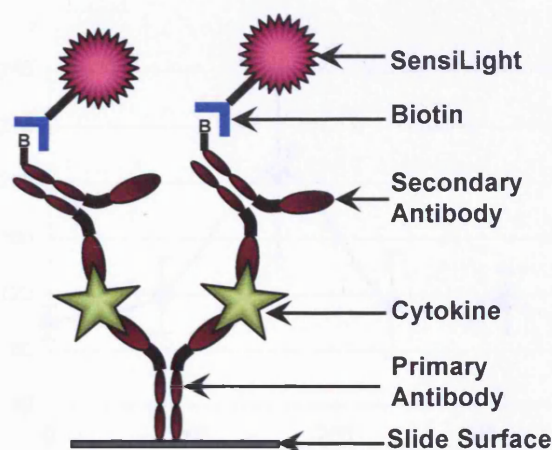
Figure 2.3 'Sandwich' immunoassay format. The detection strategy is a standard immunoassay that relies on biotinylated detection antibodies and streptavidin-conjugated fluorophore for detection

2.4 RESULTS

2.4.1 CADMIUM

A cadmium dose response was established by using a concentration range of 0-400µM.

2.4.1.1 TRANS-EPITHELIAL ELECTRICAL RESISTANCE

The average control TEER value (post exposure) was 210 Ohms cm^2, a cadmium dose response produced a small increase of resistance at 80µM with a significant peaking at 160µM. Subsequent concentrations produced a decrease in resistance (Figure 2.4).

2.4.1.2 MTT

The MTT assay indicated significant decreases in tissue viability with an increased concentration of cadmium. This trend reversed at 240µM with an increase of viability. Subsequent concentrations of cadmium resulted in a decrease of viability (Figure 2.5).
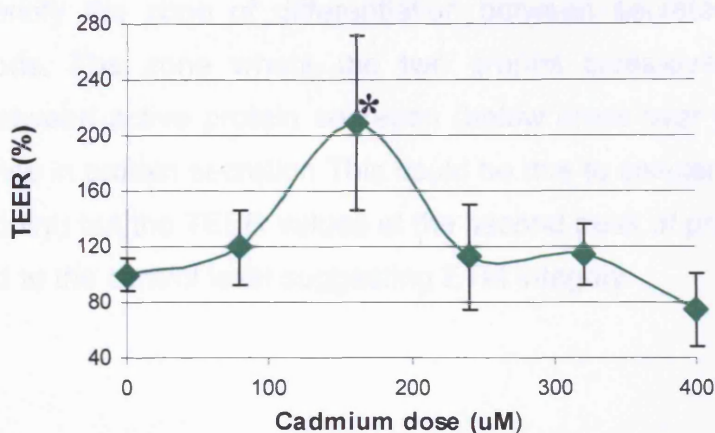
Figure 2.4 Cadmium dose response on TEER readings. The asterisk (*) denotes significant (p≤0.05), I denotes standard deviation and n=3
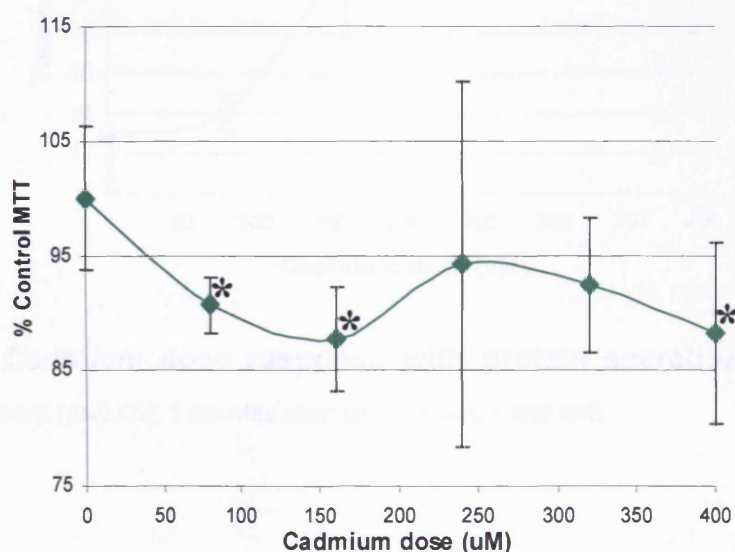
Figure 2.5 Cadmium dose response on cell viability. The asterisk denotes significant (p≤0.05), I denotes standard deviation and n=3

2.4.1.3 PROTEIN SECRETION

At 80µM cadmium, a small increase of protein was detected. Protein secretion increased significantly by 50% at the 160µM dose, followed by a brief plateau before increasing to a second peak of protein secretion at 320µM cadmium (Figure 2.6).

A comparison of the TEER versus protein secretion data (Figure 2.7) could be used to identify the zone of differentiation between secreted protein and cellular debris. The zone where the two graphs cross-over marked the transition between active protein secretion (below cross-over point) and the secondary rise in protein secretion This could be due to cellular debris (above cross-over point) but the TEER values at the second peak of protein secretion had reduced to the control level suggesting ETM integrity.
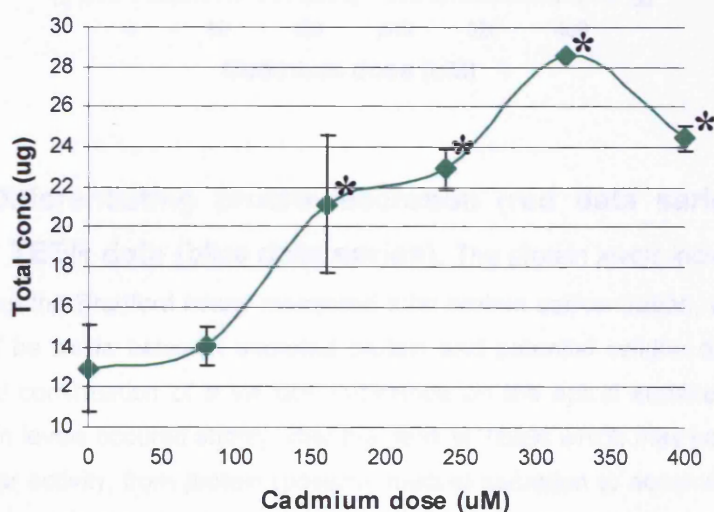
Figure 2.6 Cadmium dose response with protein secretion. The asterisk denotes significant ($p \leq 0.05$), I denotes standard deviation and n=3
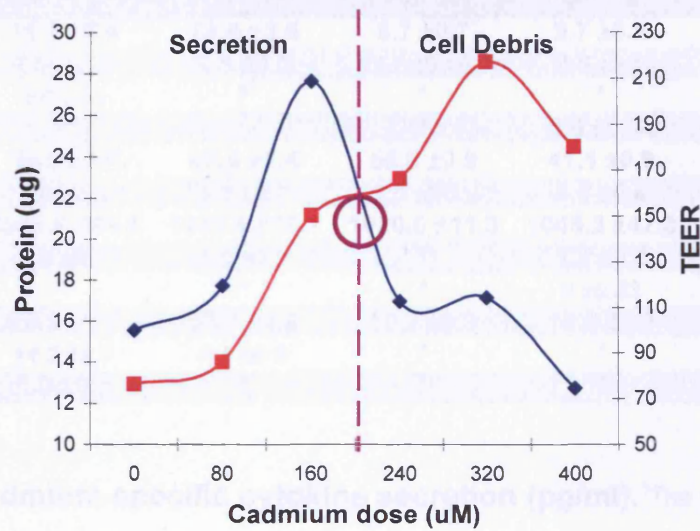
Figure 2.7 Differentiating protein secretion (red data series) and cell debris using TEER data (blue data series). The protein levels increased with TSC concentration, but the Bradford assay measured total protein concentration, and as such, no distinction could be made between secreted protein and potential cellular debris. However, there was visual confirmation of a viscous substance on the apical surface of the cells. A plateau in protein levels occured shortly after the peak in TEER which may have suggested a change in cellular activity; from protein (possibly mucus) secretion to accumulation of limited cell debris. Also the TEER values at this concentration returned to the control level inferring ETM integrity

2.4.1.4 CYTOKINE SECRETION

The cytokine release response following cadmium challenge is depicted in Table 2.2. A standard curve was produced from the human cytokine standard (figure 2.8).

CYTOKINE	CADMIUM DOSE RANGE				
	0 uM	80 uM	160 uM	240uM	400 uM
IL-1a	15.8 ±0.6	26.6 ±2.6	8.7 ±0.7	9.7 ±0.2	15.6 ±1.7
IL-1b	2.6 ±0.2	3.9 ±0.3	1.2 ±0.19	0.5 ±0.1	1.7 ±0.1
IL-2	0.8 ±0.1	*	*	*	1.3 ±0.1
IL-4	*	*	*	0.6 ±0.04	*
IL-6	54.8 ±3.8	60.9 ±2.4	56.8 ±0.9	41.1 ±0.9	89.4 ±12.5
IL-7	1.8 ±0.4	3.3 ±0.7	2.5 ±0.04	5.8 ±0.4	*
IL-8	1045.8 ±41.8	1045.4 ±19.1	1020.6 ±11.3	1045.2 ±42.3	1045.3 ±43.5
IL-10	1.5 ±0.3	1.9 ±0.3	*	1.2 ±0.1	2.2 ±0.3
IL-12	*	*	*	1 ±0.33	*
GMCSF	28.2 ±1.7	38.8 ±1.6	10.7 ±0.9	18.3 ±1.3	51.5 ±4.6
IFN-g	14.3 ±2.4	4.3 ±0.3	*	*	11.4 ±2.1
TNF-a	1.0 ±0.1	*	*	*	1.2 ±0.2

Table 2.2 Cadmium-specific cytokine secretion (pg/ml). The asterisk indicates data point is below the limit of detection, ± indicates SD and data values for which SD is greater than 15% of predicted concentration (italics)
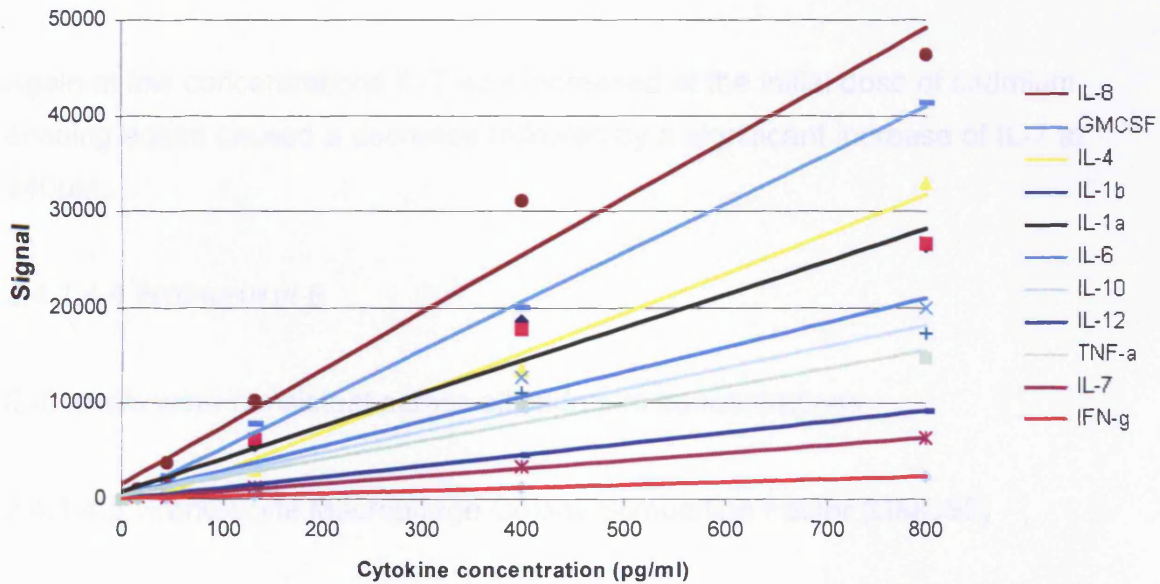
Figure 2.8 Standard curves of the cytokines. The 12 cytokine R^2 values ranged from 0.97-1.00

2.4.1.4.1 INTERLEUKIN-1A & 1B

An increase in cadmium produced a significant increase in Interleukin (IL) -1a followed by significant deceases of IL-1a in relation to the control with subsequent concentrations, finishing at a control level at the highest dose. IL-1b although at low levels showed an initial increase with dose followed by significant decreases with successive concentrations ending with an increase at the final concentration of 400μM.

2.4.1.4.2 INTERLEUKIN-6

A cadmium dose range produced an initial increase in IL-6 with a subsequent decease back to control levels; increased dosing resulted in a significant decrease finishing with a significant increase at the highest concentration.

2.4.1.4.3 INTERLEUKIN-7

Again at low concentrations IL-7 was increased at the initial dose of cadmium, ensuing doses caused a decrease followed by a significant increase of IL-7 at 240μM.

2.4.1.4.4 INTERLEUKIN-8

IL-8 levels were consistent across all cadmium concentrations.

2.4.1.4.5 Granulocyte Macrophage Colony Stimulating Factor (GMCSF)

An initial concentration 80μM cadmium caused an increase of GMCSF; further concentrations of cadmium produced a significant decrease followed by a significant increase at 240μM and a highly significant increase above the control level at 400μM.

2.4.1.4.6 Other Cytokines

IL-2, IL-4, IL-10, IL-12, IFN-g and TNF-α showed a variable response across the cadmium dose range.

2.4.2 Formaldehyde

A FA dose-response was established by using a concentration range of 0-25mM.

2.4.2.1 Trans-Epithelial Electrical Resistance

The average control TEER value (post exposure) was 210 Ohms cm^2, the FA dose-response produced a small decrease in resistance at doses 0.5-1mM with a significant peak at 5mM. Subsequent concentrations produced a decrease in resistance (Figure 2.9).
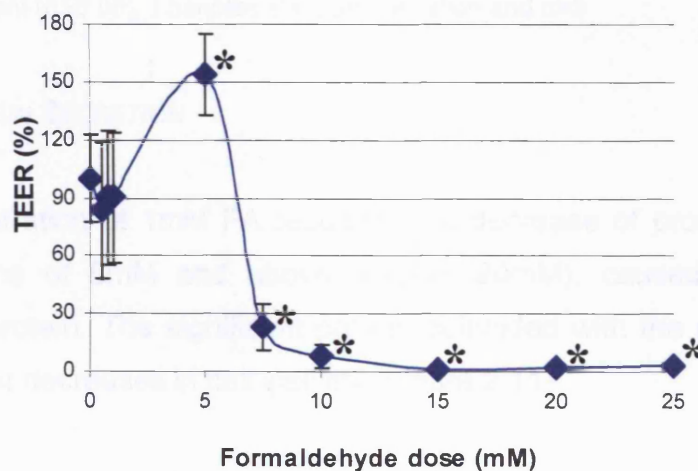
Figure 2.9 Formaldehyde dose response on TEER readings. The asterisk denotes significant (p≤0.05), I denotes standard deviation and n=3

59

2.4.2.2 MTT

The MTT assay indicated decreases in tissue viability with an increased concentration of formaldehyde. Concentrations of 5mM and above resulted in a significant decreases of viability (Figure 2.10).
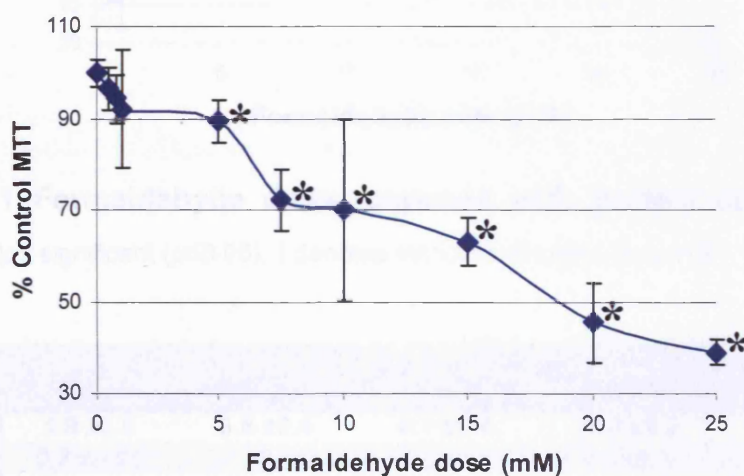
Figure 2.10 Formaldehyde dose response using MTT assay. The asterisk denotes significant ($p \leq 0.05$), I denotes standard deviation and $n=3$

2.4.2.3 PROTEIN SECRETION

Initial concentration of 1mM FA resulted in a decrease of protein secretion. Concentrations of 5mM and above (except 20mM), caused a significant increase of protein. The significant protein coincided with the peak in TEER and significant decreases in cell viability (Figure 2.11).

2.4.2.4 CYTOKINE SECRETION

The cytokine release response following formaldehyde challenge is depicted in Table 2.3.
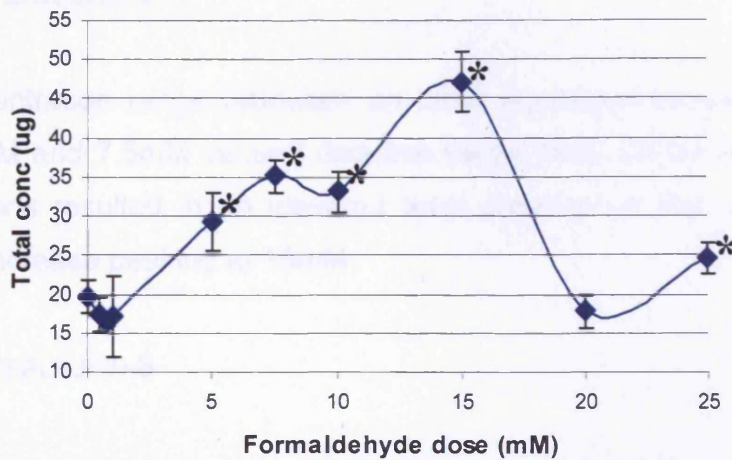
Figure 2.11 Formaldehyde dose response with protein secretion. The asterisk denotes significant (p≤0.05), I denotes standard deviation and n=3

CYTOKINE	FORMALDEHYDE DOSE RESPONSE					
	0 mM	1 mM	5 mM	7.5 mM	10 mM	15 mM
IL-1a	4.9 ±2.6	6.6 ±0.4	8.1 ±0.4	17.3 ±0.6	70.1 ±6.3	46.7 ±2.8
IL-1b	0.7 ±0.04	*	1.0 ±0.2	2.4 ±0.4	4.6 ±0.3	3.1 ±0.1
IL-2	1.6 ±0.1	0.6 ±0.1	1.3 ±0.2	1.0 ±0.2	0.3 ±0.05	0.4 ±0.05
IL-4	*	*	*	0.4 ±0.06	0.4 ±0.05	0.8 ±0.1
IL-6	19.3 ±0.8	22.3 ±0.7	15.1 ±0.6	14.4 ±0.3	18.6 ±0.9	53.3 ±2.7
IL-7	*	*	*	3.1 ±0.2	*	4.9 ±0.4
IL-8	1219.2 ±12.2	1218.6 ±16.4	1219.3 ±12.1	1219.1 ±24.2	1210.8 ±12.2	1218.6 ±14.6
IL-10	1.2 ±0.2	0.8 ±0.2	0.5 ±0.1	1.4 ±0.2	*	0.7 ±0.06
IL-12	2.3 ±0.4	1.8 ±0.3	*	2.2 ±0.4	*	1.6 ±0.3
GMCSF	4.0 ±0.2	*	5.1 ±0.4	3.9 ±0.2	0.6 ±0.4	4.3 ±0.1
IFN-g	33.2 ±8.3	6.7 ±1.1	17.0 ±0.9	20.7 ±1.4	*	3.0 ±0.2
TNF-a	*	*	*	0.6 ±0.1	*	*

Table 2.3 Formaldehyde-specific cytokine secretions (pg/ml). The asterisk indicates data point is below the limit of detection, ± indicates SD and data values for which SD is greater than 15% of predicted concentration (italics)

2.4.2.4.1 INTERLEUKIN-1A & 1B

An increase in FA produced significant increases in IL-1a peaking at 10mM this was followed by significant decline of IL-1a at 15mM. IL-1b although at lower levels showed the same profile with significant increases of IL-1b at concentration 7.5mM and above and a reduction of IL-1b at 15mM.

2.4.2.4.2 INTERLEUKIN-6

A FA concentration range produced an initial significant increase in IL-6 a dose of 5mM and 7.5mM caused decease below initial control levels; further concentrations resulted in an elevated level observed in the control and a significant increase peaking at 15mM.

2.4.2.4.3 INTERLEUKIN-8

IL-8 levels were consistent across all FA dose concentrations.

2.4.2.4.4 OTHER CYTOKINES

IL-2, IL-4, IL-7, IL-10, IL-12, GMCSF, IFN-g and TNF-α showed either low (>2pg) or variable responses across the FA concentration range.

2.4.3 NICOTINE

A nicotine dose response was established by using a concentration range of 0-125mM.

2.4.3.1 TRANS-EPITHELIAL ELECTRICAL RESISTANCE

The average control TEER value (post exposure) was 210 Ohms cm^2, the nicotine dose-response produced a small decrease in resistance at a concentration of 25mM. The resistance later increased with a peak at 50mM. Subsequent concentrations produced a significant decrease in resistance (Figure 2.12).
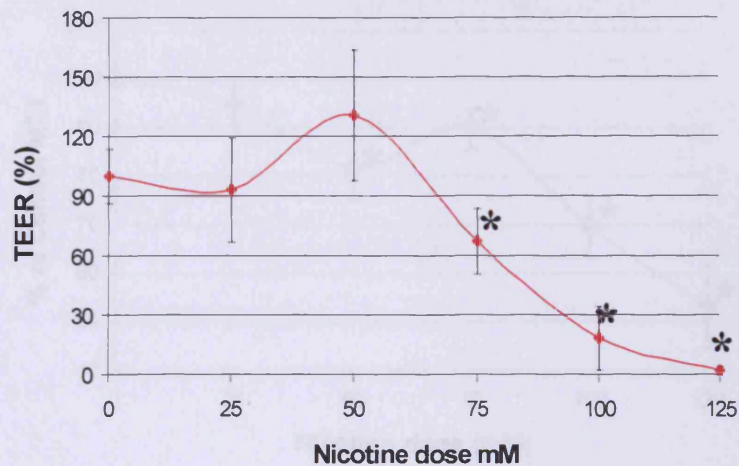
Figure 2.12 Nicotine dose response on TEER readings. The asterisk denotes significant ($p \leq 0.05$), I denotes standard deviation and n=3

### 2.4.3.2 MTT

The MTT assay indicated decreases in tissue viability with an increased concentration of nicotine. A concentration of 75mM created a significant increase in viability; subsequent concentrations resulted in significant decreases of viability (Figure 2.13).

2.4.3.3 PROTEIN SECRETION

Initial concentrations of nicotine resulted in a decrease of protein secretion (0-50mM). Concentrations of 75mM and above caused a significant increase of secreted protein (Figure 2.14).

2.4.3.4 CYTOKINE SECRETION

The cytokine release response following nicotine challenge is depicted in Table 2.4.

63
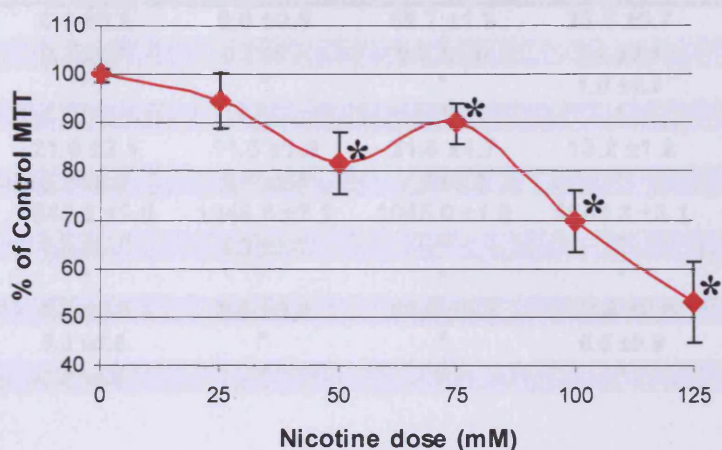
Figure 2.13 Nicotine dose response using MTT assay. The asterisk denotes significant (p≤0.05), I denotes standard deviation and n=3
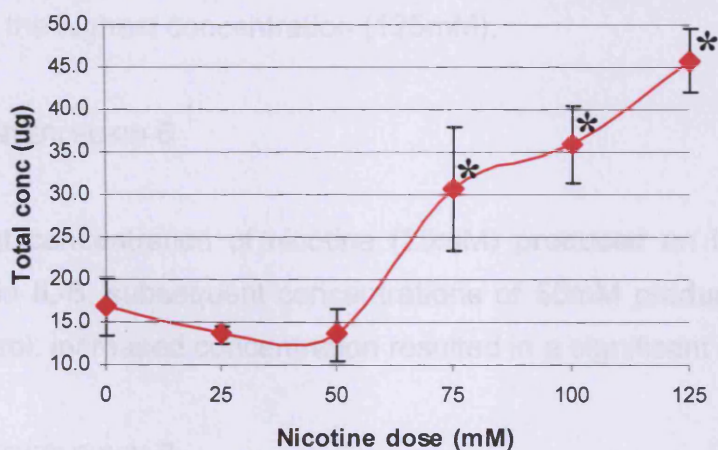
Figure 2.14 Nicotine dose response with protein secretion. The asterisk denotes significant (p≤0.05), I denotes standard deviation and n=3

CYTOKINE	NICOTINE DOSE RANGE				
	0 mM	25 mM	50 mM	75 mM	125 mM
IL-1a	8.4 ±0.6	9.6 ±0.6	69.7 ±1.9	23.6 ±0.7	74.8 ±2.2
IL-1b	*0.7 ±0.1*	*0.5 ±0.1*	5.8 ±1.0	*1.4 ±0.2*	*2.7 ±0.5*
IL-2	*	*	*	*1.0 ±0.2*	*0.9 ±0.1*
IL-4	*	*	*	*	*
IL-6	21.0 ±2.1	11.0 ±1.0	21.6 ±1.7	13.2 ±1.2	14.6 ±0.7
IL-7	*3.7 ±0.6*	*2.1 ±0.4*	*1.3 ±0.2*	*	*3.0 ±0.5*
IL-8	1045.2 ±1.0	1045.6 ±2.1	1045.0 ±1.0	1045.3 ±2.1	1045.4 ±2.1
IL-10	1.5 ±0.1	*1.3 ±0.3*	*	*	1.1 ±0.1
IL-12	*	*	*	*	*
GMCSF	4.2 ±0.3	5.8 ±0.4	54.0 ±5.3	12.4 ±0.6	19.7 ±1.4
IFN-g	*3.5 ±0.6*	*	*	6.5 ±0.9	*
TNF-a	*0.2 ±0.1*	*	*	*	*0.6 ±0.3*

Table 2.4 Nicotine-specific cytokine secretions (pg/ml). The asterisk indicates data point is below the limit of detection, ± indicates SD and data values for which SD is greater than 15% of predicted concentration (italics)

2.4.3.4.1 INTERLEUKIN-1A

An Initial 25mM concentration of nicotine had little effect on IL-1a; subsequent concentrations caused a significant rise followed by a drop in IL-1a before peaking at the highest concentration (125mM).

2.4.3.4.2 INTERLEUKIN-6

The lowest concentration of nicotine (25mM) produced an initial significant decrease in IL-6, subsequent concentrations of 50mM produced levels seen in the control; increased concentration resulted in a significant decreases.

2.4.3.4.3 INTERLEUKIN-8

IL-8 levels were consistent across all nicotine concentrations.

2.4.3.4.4 Granulocyte Macrophage Colony Stimulating Factor

With a similar profile to IL-1a, an initial concentration of nicotine caused a small but significant increase of GMCSF further concentrations caused

another significant rise followed by a decrease and finally rising at the highest concentration.

2.4.1.4.5 OTHER CYTOKINES

IL-1b, IL-2, IL-4, IL-7, IL-10, IL-12, IFN-g and TNF-α showed either low (>2pg) or variable responses across the nicotine concentration range.

2.4.4 URETHANE

The urethane dose response was established by using a concentration range of 0-4M.

### 2.4.4.1 TRANS-EPITHELIAL ELECTRICAL RESISTANCE

The average control TEER value (post exposure) was 210 Ohms cm^2, urethane dose response produced a significant increase in resistance with a significant resistance peak at 500mM. All subsequent concentrations produced a decrease in resistance (Figure 2.15).
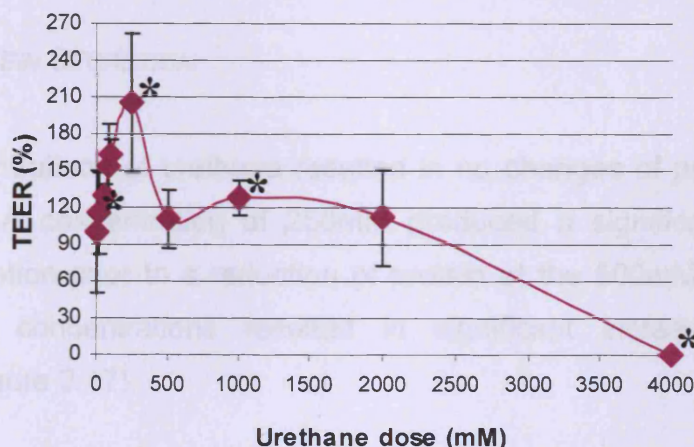
Figure 2.15 Urethane dose response on TEER readings. The asterisk denotes significant (p≤0.05), I denotes standard deviation and n=3

2.4.4.2 MTT

The MTT assay indicated a slight increase in tissue viability with an increased concentration of urethane. A concentration of 2000mM created a decrease in viability that was extended with a 4000mM concentration, resulting in a significant decrease in viability (Figure 2.16).
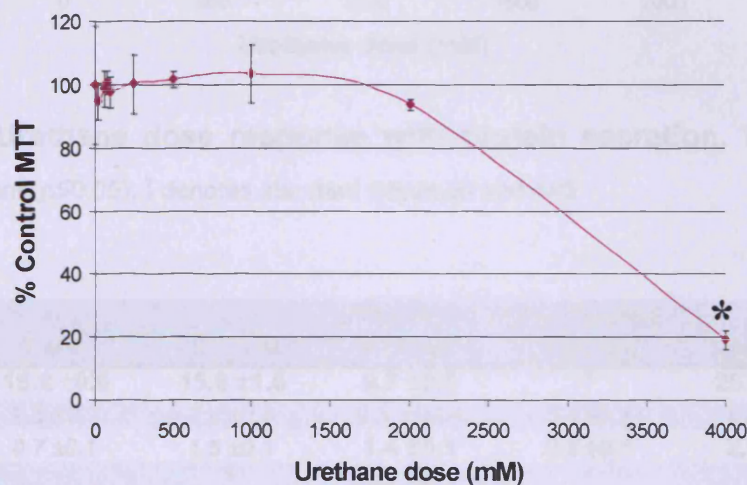

Figure 2.16 Urethane dose response using MTT assay. The asterisk denotes significant (p≤0.05), I denotes standard deviation

2.4.4.3 PROTEIN SECRETION

Initial concentrations of urethane resulted in no changes of protein secretion (0-100mM). A concentration of 250mM produced a significant increase in protein secretion prior to a reduction of protein at the 500mM concentration. Subsequent concentrations resulted in significant increases in protein detected (Figure 2.17).

2.4.4.4 CYTOKINE SECRETION

The cytokine release response following urethane challenge is depicted in Table 2.5.
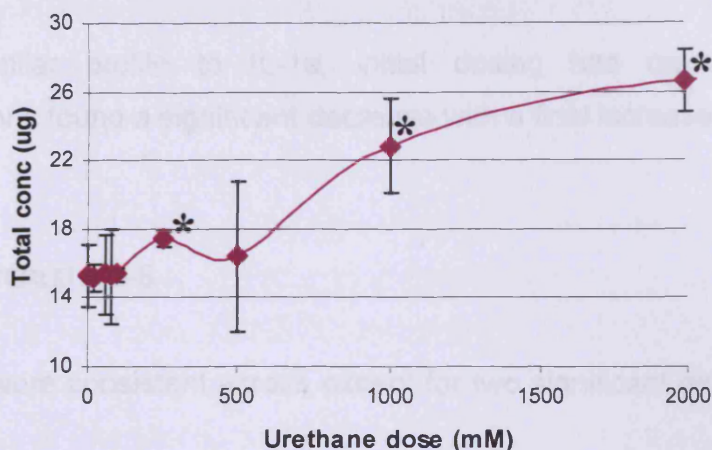
Figure 2.17 Urethane dose response with protein secretion. The asterisk denotes significant (p≤0.05), I denotes standard deviation and n=3

CYTOKINE	URETHANE DOSE RANGE					
	0 mM	100 mM	250 mM	500 mM	2000 mM	4000 mM
IL-1a	15.8 ±0.6	15.9 ±1.6	9.7 ±0.9	*	25.7 ±1.0	99.6 ±8.9
IL-1b	1.3 ±0.1	2.4 ±0.4	0.1 ±0.04	0.4 ±0.1	1.3 ±0.2	4.4 ±0.8
IL-2	0.7 ±0.1	1.5 ±0.3	1.4 ±0.1	0.5 ±0.1	2.1±0.1	1.8 ±0.3
IL-4	*	*	1.1 ±0.1	*	*	1.1 ±0.2
IL-6	33.5 ±2.3	38.9 ±1.6	11.9 ±0.1	4.7 ±0.8	20.0 ±1.4	57.7 ±3.5
IL-7	*	*	8.9 ±0.4	*	*	9.7 ±0.8
IL-8	1471.0 ±58.8	1475.6 ±29.5	1781.1 ±53.4	1514.0 ±53.0	1473.3 ±29.5	1830.0 ±27.5
IL-10	*	*	1.4 ±0.1	*	*	*
IL-12	*	*	1.0 ±0.2	*	1.7 ±0.4	2.1 ±0.4
GMCSF	39.3 ±3.1	42.1 ±2.1	5.1±0.2	*	6.9 ±0.6	18.2 ±0.7
IFN-g	19.2 ±3.1	24.5 ±4.7	27.0 ±0.8	*	26.9 ±1.3	23.0 ±3.7
TNF-a	*	0.8 ±0.1	0.5 ±0.1	*	1.8 ±0.4	0.9 ±0.2

Table 2.5 Urethane-specific cytokine secretions (pg/ml). The asterisk indicates data point is below the limit of detection, ± indicates SD and data values for which SD is greater than 15% of predicted concentration (italics)

2.4.4.4.1 IL-1A

An initial concentration of urethane caused no change in IL-1a; a subsequent concentration of 250mM caused a significant decrease. Increased concentrations of urethane resulted in significant rises, peaking at the highest dose (4M).

2.4.4.4.2 Interleukin-6

With a similar profile to IL-1a, initial dosing had no effect, further concentrations found a significant decrease with a final increase at the highest dose.

2.4.4.4.3 Interleukin-8

IL-8 levels were consistent across except for two significant peaks at 250mM and 4M.

2.4.4.4.4 Granulocyte Macrophage Colony Stimulating Factor

As witnessed in IL-1a and IL-6 an initial dose of 250mM had little effect, subsequent concentration caused a significant decrease that reversed with a peak at the highest dose. This GMCSF level was still below the control level.

2.4.1.4.5 Other cytokines

IL-1b, IL-2, IL-4, IL-7, IL-10, IL-12, IFN-g and TNF-α showed either low (>2pg) or variable responses across the urethane concentration range.

2.5 Discussion

The objective of this study was to use conventional toxicology to measure the responses of a commercial *in vitro*, human tissue equivalent model of respiratory epithelia to well-characterised components of tobacco smoke. To be considered an appropriate model for toxicological studies, it was important that the system originated from normal (non-immortalised) cells. It was equally important to choose a human-derived tissue model, in order to avoid inevitable species-related differences, which would compromise experimental results (Coggins, 2002). The cell-cell interactions that occur *in vivo* (but are not generally present in single-cell cultures) can significantly alter the cellular

effects of many toxins (Andreoli *et al.*, 2003). The range of these effects can only be fully-investigated in a biological system capable of transcribing and translating genes in response to the action of toxins. The ETM consisted of cells derived from healthy, human, primary-explant tissue, normal human bronchial epithelium (NHBE), as opposed to lung tumour or diseased tissue. Consequently, the cells were genotypically and phenotypically more representative of normal epithelia than other commonly used models (e.g. A549; Padar *et al.*, 2005, BEAS-2B; Penn *et al.*, 2005, CALU-3; Grainger *et al.*, 2008, 16HBE14o-; Grumbach *et al.*, 2008). The overiding advantage of this system was that the human tracheo-bronchial epithelium was cultured to form a 3-dimensional, pseudo-stratified state, that exhibited a functional muco-cilliary phenotype with tight junctions (Bérubé *et al.*, 2006); as observed *in vivo*. When compared to standard epithelial monolayer culture, this system much more closely resembled human bronchioles, both morphologically and physiologically (Hermann *et al.*, 2004; BéruBé *et al.*, 2006; Bérubé *et al* 2009).

The comparison of TEER measurements in this study highlighted similar trends with the four TSC, despite differences in their physicochemistry (i.e. vapour or particle phase components). Initial doses caused a small reduction in TEER; this was followed by a significant peak before falling to zero. This reaction pattern was indicative of a loss of cellular tight junctions, and consequently, degradation of the tissue model. This response could be described as biphasic 'hormesis', which is characterised as a low dose stimulation, followed by a high dose inhibition (Rozman and Doull, 2003; Calabrese, 2004; Balharry *et al.*, 2008). This consistent biphasic appearance of the TEER was vital for determining the sub-toxic doses.

The MTT assay for cell viability was used as an additional indicator of cell/ tissue integrity. The MTT data profile was not consistent across the different TSC components. Vapour phase components (formaldehyde and urethane) had no similarities at the lower doses but both components decreased in viability at the higher doses. The particle phase components (cadmium and nicotine) had similar profiles with an initial decrease in viability followed by a

peak before falling to zero. The peaks observed using MTT consistently occurred after the peaks observed with TEER measurements. A comparison of both sets of data led to the conclusion that the TEER readings acted as an early indicator for the deterioration of the tissue model. That is, the loss of tight junctions increased the cell activity but this was not sustained with the increase in dose.

When cells are under stress they often secrete proteins into the culture medium. Following this, more severe damage may occur and membrane components are released and eventually the cell may die. Thus, it is necessary to identify all of these endpoints in relation to the dose of a toxicant. In the case of this investigation, the genomic and proteomic studies would be superior to identify the "intelligent biomarkers" of the early stress response (Chapters 4 and 5).

The protein secretions collected were consistent for all four TSC with almost identical profiles observed; a small decrease in protein was followed by a sharp rise with a subsequent plateau before a final rise in protein. The Bradford assay was used to measure protein concentration, and as such, no distinction was made between secreted protein and potential cellular debris. However, there was visual confirmation of a viscous substance on the apical surface of the cells. This material had the characteristics of mucin, (i.e. clear and thick viscous), as reported by other investigators (Chemuturi *et al.*, 2004; Greenwell *et al.*, 2005; Balharry *et al.*, 2008). It appeared that the pattern of increased TEER followed the rise in secreted proteins. The reduction in TEER corresponded with a secondary increase in proteins detected; this may be explained by the Bradford assay detecting partial cell debris and cellular secretion. This debris/secretion may have been easier to remove by this brief wash step due to the reduction of the TEER and therefore tissue integrity. The potential to differentiate between secreted proteins and cellular debris was investigated further by using immuno-histochemistry (IHC) techniques (Chapter 3).

The levels of cytokines expressed by the ETM were determined as a further measure of cellular activity and cell-cell interactions. Although due to the experimental samples being run as a triplicate it is imperative that these results were considered as being 'trends' rather than empirical data. There were a number of similarities between the four TSC, with the pro-inflammatory cytokines IL-1a, IL-1b, IL-6 and GM-CSF induced by all the TSC. The main difference between the particulate and vapour phase components was that cadmium and nicotine induced IL-7 expression, while formaldehyde and urethane induced IL-2 and IFN-g secretion. Interleukin-2 and IL-7 are both thought to be involved in T-cell homeostasis (Boyman et al., 2007). Therefore, the difference could be due to alternate mechanisms for achieving the same goal, which may be to induce NK-cell activity (Williams et al., 1998). IFN-g is also thought to be indirectly involved in T-cell homeostasis and has been demonstrated to enhance T-cell mediated immune responses (Boyman et al., 2007). The apparent link between elevated cytokine secretion and TEER could be related to the increase in cell numbers within the ETM. Simply, the higher the cell numbers, the greater the concentration of cytokines being expressed (Emad and Emad, 2007). The elevated expression of cytokines suggested that the ETM was functioning in an in vivo-like manner, with the induction of signalling cascades and various immune responses (Kolsuz et al., 2003). This permitted further speculation into whether xenobiotics, such as the TSC, play a role in inducing respiratory defence mechanisms, as well as biotransformation events.

Using these conventional toxicology techniques as a measure of the functionality of the model epithelium, it was possible to compare this new model with established cell culture models (Forbes and Ehrhardt, 2005). In general, the ETM appeared to be more toxicologically resistant to these TSC toxicants than individual cell cultures. For example, IC10 (median inhibition concentration which produces a 10% reduction in cell viability determined by MTT uptake) for cadmium chloride was ten times greater in the ETM than in monolayers of mammalian pulmonary cells (e.g. A549; Watjen et al., 2002). Both nicotine and urethane demonstrated IC50 (50% reduction in cell viability) values that were approximately 100 times higher than in mammalian

monolayer cultures (ICCVAM, 2001). This is probably due to the interactions between the different cell types within the model (e.g. mucus secretion) and was more representative of the situation in the human lung than monolayer cultures. However, the protective response to formaldehyde was induced by only two-fold compared to a monolayer of A549 cells (Lestari *et al.*, 2005).

It was also important to note that the concentrations of TSC used in this study are much higher than the concentrations in mainstream smoke. The amount of these compounds inhaled from a single cigarette can vary greatly depending on the type of cigarette and the smoking habits of an individual (Andreoli *et al.*, 2003). Numerous studies have shown a wide range of concentrations for each TSC: nicotine; 1-3mg/cigarette (Willems *et al.*, 2006), cadmium; 0-6.67µg/cigarette (Smith *et al.*, 1997), urethane; 20-48ng/cigarette (Zimmerli *et al.*, 1991), formaldehyde; 3.4-283µg/cigarette (Smith *et al.*, 2000). In each case the maximum concentration was used to calculate the daily intake of a 20-a-day smoker (mg/m^2 lung tissue) and compared to the experimental dose (mg/m^2 ETM) required to generate an IC10 (determined by MTT). Both the particulate phase compounds (nicotine and cadmium) were overdosed by approximately 20,000 times (roughly equivalent to a lifetime dose, assuming 50 years of smoking 20-a-day). However, the vapour phase compounds were strikingly different from both the particulate phase compounds, and each other. Formaldehyde was dosed approximately 400 times more than the daily intake of a smoker (roughly 40 times less than a lifetime dose). By contrast, urethane required dosing at over a million times the daily dose of a smoker. Despite the ETM having known metabolic capacity (Hayden *et al.*, 2006), this extreme over-dosing could be due to the absence or lack of activation of the specific P450 (CYP2E1) required to metabolise urethane to its active form, vinyl carbamate.

Despite the physical differences between the particulate and vapour phase TSC, this model has shown no real distinction between the two phases. The only area in which there was an obvious difference in the concentrations required to elicit the desired toxic response. This may be partially due to the protective response (increased mucus secretion resulting from hyperplasia

and hypertrophy and cytokine mediated immune responses) observed in the model, the bioavailability of the TSC or possibly the lack of activation of specific metabolism mechanisms. Subtle differences between the particle and vapour phase components may have been masked by the requirement to solubilise the TSC and application to the apical cell surface in liquid form.

Despite the drawback of limited P450 activity, the model hallmark was the ease of its use. The model arrived fully-differentiated and screened for metabolic activity and tissue integrity prior to dispatch. The ETM was low maintenance, only requiring feeding every other day with EpiAirway™ maintenance medium (included), to provide viable tissue for up to 27 days (Hayden *et al.*, 2006). The multi-well (24-well/96-well) format was ideal for multiple dosing experiments and screening; with easy access to both the apical and basal surfaces of the cells. This model had the added advantage of derivation from normal human tissue, thus circumventing the need for extrapolation of data from *in vivo* studies in different species. As such, the ETM could provide a novel, toxicological tool to assess various respiratory tract issues while avoiding species extrapolation and the use of laboratory animals.

2.6 CONCLUSION

TSC induce a toxic response within the EpiAirway™ model causing loss of cell viability, tight junction degradation and stimulation of secretory processes. At the sub-toxic doses, a reaction to the compounds was induced which may result in protection against toxicity. This response has not been reported in single-cell cultures, which suggested that the ETM model may generate a closer representation of the human *in vivo* environment resulting from cross-talk between cells. The nature of the ETM (multi-well plate format) also meant that it was easily accessible for the application of experimental techniques. From this investigation, it appeared that the ETM was a viable *in vitro* alternative for modelling human responses to inhaled toxicants.

Chapter 3:

Morphological Changes in the EpiAirway™ Model

3.1 INTRODUCTION

Morphological analysis was required to complement the conventional toxicology studies (Chapter 2), and to increase the understanding on the mechanisms of TSC's toxicity. The histological assessment involved examination of the changes in the general cell tissue morphology, i.e. maintenance of pseudo-stratification, presence of a mucociliary phenotype and vacuolization, in both control and treated tissues. The primary objectives of the following experimental work presented in this chapter were to examine physiological responses that could not be measured using conventional toxicology, e.g. mucin secretion and cell differentiation. Furthermore, by investigating the morphological and physiological changes involved in differentiation, the cellular kinetics during toxicant challenge could also be deciphered, to provide better resolution of the mechanisms of toxicity.

3.2 MATERIALS AND STOCK SOLUTIONS

3.2.1 MATERIAL AND SUPPLIERS

Materials:	Supplier:
Araldite CY212 (R1040)	Agar Scientific
Glutaraldehyde (25 %) (R1010)	Agar Scientific
Osmium Tetroxide (R1015)	Agar Scientific
Propylene Oxide (R1080)	Agar Scientific
Leica Q550IW Image Analysis System	Leica Ltd.
Leica DM2500 Light Microscope	Leica Ltd.
Leica RM2135 Microtome	Leica Ltd.
Leica EG1140 Embedding Centre	Leica Ltd.
Vacuum Tissue Processor	Leica Ltd.
Leica DFC320 Camera	Leica Ltd.
Aqueous Eosin (1%) (LAMB/100-D)	R A Lamb
Mayers Hematoxylin (S1275)	Sigma-Aldrich

Materials:	Supplier:
PBS pH 7.4 with 0.05% Tween (P3813)	Sigma-Aldrich
BSA in PBS pH 7.4 with 0.05% Tween (P3688)	Sigma-Aldrich
Toluidine Blue Stain (198161)	Sigma-Aldrich
Tracheobronchial Mucin (sc-52329)	SantaCruz Biotechnology, USA
Mouse ABC Staining System (sc-2017)	SantaCruz Biotechnology, USA
p63 4A4 (559951)	BD Pharmingen
Mouse Anti-Human Cytokeratin 5/6 (M7237)	Dako
Biotinylated Goat Anti-Mouse (E0433)	Dako
Streptavidin AB/HRP (K0377)	Dako
DAB (K3466)	Dako
Normal Goat Serum (X0907)	Dako

Table 3.1 Materials used and their suppliers. All suppliers are UK based unless stated)

3.2.2 STOCK SOLUTIONS

Neutral Buffered Formalin (NBF; 10%) was prepared by the Cardiff School of Biosciences Histology Unit.

Glutaraldehyde Fixative was prepared as a 1x working solution containing 3% Glutaraldehyde, 0.1M Cacodylate and 3mM Calcium Chloride. Fixative was made as required and stored at 4°C.

3.3 METHODS

3.3.1 FIXING THE ETM

The exposed ETM (Chapter 2) were immersed in 10% NBF and placed at 4°C for 24 hours. The ETM was then excised from the Millicell insert (Chapter 2,

Section 2.3.2) in preparation for paraffin embedding and sectioning. Tissue processing, i.e. paraffin embedding, sectioning and staining, was carried out by a histotechnologist, Mr Derek Scarborough, at the School of Biosciences, Cardiff University. A brief overview of these procedures has been outlined below in Sections 3.3.2 to 3.3.5.

3.3.2 Tissue Processing

Once the tissue has been fixed (Section 3.3.1), it must be processed into a form in which it can be made into thin microscope sections. This was achieved by embedding tissues in paraffin that was similar in density to tissue and could be sectioned between 3 to 10 microns. The main steps in this process, when dealing with wet-fixed tissue, included 'dehydration', 'clearing' and 'paraffin infiltration'.

Wet-fixed tissues, such as ETM samples from this study, can not be directly infiltrated with paraffin. The water from the tissues must be removed by 'dehydration' via a series of alcohols (e.g. 70% to 95% to 100%). Following dehydration, the next step was 'clearing' and consisted of replacement of the dehydrant, i.e. alcohol, with a substance that would be miscible with the paraffin. The common clearing agent was xylene and the tissues were processed through several changes of xylene. The final step in processing was to infiltrate the tissue with molten paraffin wax at 60°C. Tissues were placed in plastic processing cassettes prior to loading on the automatic processing machine. All the above processes were automated using a fully-enclosed Vacuum Tissue Processor (Leica, UK).

3.3.3 Paraffin Embedding

It was important for the tissue to be fully-supported by paraffin wax to prevent the tissue shredding during sectioning. This was achieved by placing the 'cleared' tissue into a vacuum to remove all air pockets. The ETM was then placed into a plastic 'embedding mould', and a Leica EG1140 Embedding Centre was used to embed the tissue in warm paraffin wax. After allowing the

wax to set (30 minutes on a cold plate), the tissue was removed from the embedding mould and the sample was ready for sectioning.

3.3.4 SECTIONING

Following tissue processing and paraffin embedding, the ETM had to be cut into sections that could be placed on a glass slide for the purpose of light microscopy (LM). Sectioning was achieved using a Leica RM2135 Microtome (i.e. a knife with a mechanism for advancing a paraffin block standard distances across it). The embedded lung tissue samples were placed on ice to ensure uniform sections were obtained. The ice hardened the wax and softened the tissue so the entire sample was of the same consistency for sectioning. The tissue was then cut into 5μm sections via the microtome.

Once the sections were cut, they were floated on a warm water bath (40-50°C) that facilitated the removal of any wrinkles and air bubbles produced during sectioning. The paraffin embedded sections of lung tissue were then collected on to a pre-coated glass microscope slide. The slides used were coated in poly-L-lysine to improve adhesion of sections. The samples were then left to bind to the slides on a hot plate for 15-30 minutes, then in an oven at 37-45°C for a minimum of 24 hours.

3.3.5 HAEMATOXYLIN AND EOSIN STAIN

The embedding process must be reversed in order to remove the paraffin wax from the tissue and allow water soluble dyes to penetrate the sections. Therefore, before any staining could be done, the slides were 'deparaffinized' by running them through xylene followed by series of graded alcohol (100% to 70%). The dewaxed tissue sections were stained with Mayer's haematoxylin for 1.5 minutes. Sections were washed in running tap water for 5 minutes, and then stained with 1% aqueous eosin for 10 minutes, and a final 20 second wash in running tap water (Bancroft and Gamble, 2001).

The stained slides were taken through the reverse process that they went through from paraffin section to water, i.e. series of graded alcohol to xylene, at which point the mountant DPX was placed over the section and the coverslip on top of the mountant. The stained sections were then ready to view by LM (Bancroft and Gamble, 2001).

3.3.6 IMMUNO-HISTOCHEMISTRY OF LUNG TISSUE

In order to determine the presence of mucin and kinetic patterns of differentiation, immuno-histochemistry (IHC) techniques were conducted (e.g. p63, cytokeratin 5/6 and tracheobronchial mucin). The removal of paraffin wax from the lung tissue, to allow attachment of a primary antibody and water soluble dyes to penetrate the tissue sections, was carried out as described in Section 3.3.5.

3.3.6.1 TRACHEO-BRONCHIAL MUCIN

The tracheobronchial mucin (TBM) was detected using an immunoperoxidase staining procedure (mouse ABC staining system containing normal blocking serum, biotinylated secondary antibody, avidin and biotinylated horseradish peroxidase), briefly described below. All steps were performed at room temperature. Endogenous peroxidase activity was blocked using 6% H_2O_2 for 10 minutes; slides were then washed in buffer for 5 minutes. To stop non-specific binding of the secondary antibody the cells/tissues were incubated with 1.5% blocking in serum PBS for 60 minutes. Excess serum was removed and replaced with the tracheobronchial mucin antibody (mucin 4, cell surface associated; 2µg/ml) and the tissues were incubated for 60 minutes. The specimens were then washed in buffer wash for 10 minutes and the wash was repeated two more times. The slides were then incubated with biotinylated secondary antibody (1:100) for 30 minutes, and washed in buffer wash for 10 minutes the wash was repeated two more times. Tissues were then incubated with avidin and biotinylated horseradish peroxidase enzyme for 30 minutes, followed by a wash in buffer wash for 10 minutes and washed two more times. Peroxidase/diaminobenzidine reaction (DAB) was then used to identify where

the antibody had bound to the tissue; upon oxidation DAB forms a brown product at the site of the target antigen. The samples were finally washed with distilled water and counterstained with haematoxylin and mounted in DPX (Section 3.5.5).

3.3.6.2 P63

The protein 63 (p63) was detected using an immunoperoxidase staining procedure, briefly described below. All steps were carried out at room temperature. Endogenous peroxidase activity was blocked using 6% H_2O_2 for 10 minutes; slides were then washed in buffer for 5 minutes. To stop non-specific binding of the secondary antibody the tissues were incubated with 20% normal goat serum for 20 minutes. Excess serum was removed and replaced with the p63 antibody (1:100) and the slides were incubated overnight at 4°C. Specimens were then washed in buffer wash for 10 minutes; the wash was repeated two more times. The tissues were then incubated with biotinylated goat anti-mouse secondary antibody (1:100) for 20 minutes, and then washed in buffer wash for 10 minutes; this was repeated two more times. Samples were then incubated with an antibody/streptavidin horseradish peroxidase (AB/HRP) complex for 20 minutes followed by 3 buffer washes for 10 minutes each. DAB was then used to identify where the antibody had bound to the tissue; upon oxidation DAB forms a brown product at the site of the target antigen. Tissues were then washed with distilled water and counterstained with haematoxylin and mounted in DPX (Section 3.5.5).

3.3.6.3 Cytokeratin 5/6

The detection of the cytokeratin 5/6 (CK 5/6) was detected using an immunoperoxidase staining procedure, briefly described below. All steps were carried out at room temperature. Tissues were submerged in 1mM EDTA pH 9.0 and heated until the buffer boiled. Endogenous peroxidase activity was blocked using 0.5% H_2O_2 in methanol for 10 minutes; tissues were then washed in buffer for 5 minutes. To stop non-specific binding of the secondary antibody, the tissues were incubated with 20% normal goat serum for 20

minutes. Excess serum was removed and replaced with the CK 5/6 antibody (1:25) and the tissues were incubated for 60 minutes. Specimens were then washed in buffer (3 times) for 10 minutes. The tissues were incubated with biotinylated goat anti-mouse secondary antibody (1:100) for 20 minutes with 3 buffer washes for 10 minutes. Tissues were then incubated with Streptavidin AB/HRP complex for 20 minutes followed by washing in buffer (3 x 10 minute). Liquid DAB was then used to identify where the antibody had bound to the tissue. Specimens were then washed with distilled water and counterstained with haematoxylin and mounted in DPX (Section 3.5.5).

3.3.7 IMAGE ANALYSIS AND STATISTICAL ANALYSIS

ETM sections were viewed using a DM2500 light microscope (Leica). Image analysis (IA) software was used to capture digitised LM images from a DFC320 digital camera (Leica) of control and treated ETM sections. LM images (x40 and x100 magnification) were saved as TIFF files and imported into the Leica Q550IW IA System, for image processing. IA was also used for the quantification of the total number of the nuclei per unit length (200μm), using the Qwin analysis software to calculate nuclei and cell numbers. Ten TIFF images were captured of random areas of ETM sections for each dose. The resulting data (n=3) was imported into Excel (Microsoft Office 2003). A two-tailed Student's t-test was then applied to determine any statistical differences.

3.3.8 PROCESSING ETM FOR SEMI-THIN SECTIONING

3.3.8.1 FIXATION OF ETM

The ETM were excised from the Millicell plastic insert, as detailed in Section 3.3.1. The ETM was submerged in cold (4°C) glutaraldehyde (3%) fixative for 15 minutes. The ETM was then removed and immersed in more fresh fixative for 1 hour at 4°C. The gluteraldehyde fixative was replaced with phosphate buffer and washed overnight (~12 hours), at 4°C.

3.3.8.2 Tissue Processing

Tissue processing and staining for semi-thin sectioning was carried out by an electron microscopist, Mr Chris von Ruhland, at the Medical Microscopy Sciences, School of Medicine, Cardiff University. A brief overview of these procedures has been outlined in Sections 3.3.10.2 and 3.3.10.3. Once the lung tissue was fixed (Section 3.3.10.1), it had to be processed into a form in which it could be made suitable for semi-thin sectioning. This was achieved by embedding the fixed lung tissue in a resin (Araldite), that acted as a support matrix for the lung tissue, permitting ultra-thin (e.g. 60 to 90 nm) sections to be cut. Prior to tissue processing, a piece of fixed ETM (PTFE membrane and lung tissue) was cut into $4mm^2$ pieces. The tissue was placed into a glass, sample vial that was used to carry the tissue through the various stages of 'dehydration', 'post-fixation' and 'resin infiltration'. The sample vials were kept on a rotating wheel inside a fume cupboard.

Post-fixation was carried out by osmicating (1% osmium tetroxide in phosphate buffer) for 60 minutes at 4°C. The tissue was then passed through a series of graded alcohols (30%-90%: 15 minutes in each, then 2 x 100%: 30 minutes each). Once dehydrated, the lung tissue samples were placed into new sample vials and immersed in propylene oxide for 30 minutes (Glauert and Lewis, 1998). This was followed by overnight (~12 hours) rotation in a fume cupboard in a 50/50 mix of propylene oxide and Araldite CY212. During this time the propylene oxide dissipated leaving only the Araldite. The following day the tissue was infiltrated with Araldite for 8 hours.

The ETM samples were embedded in fresh Araldite. This process involved placing one section of tissue into a plastic/disposable, embedding capsule and topping up the capsule with fresh Araldite. The capsule was then placed into a resin oven and polymerised at 60°C for 48 hours.

3.3.8.3 SECTIONING AND TOLUIDINE BLUE STAINING

Following resin polymerisation, the capsule was cut away from the resin/tissue block using a disposable razor blade. Excess resin was trimmed from the blocks until the tissue was exposed. Semi-thin survey sections (2 μm) were taken using a diamond knife and mounted onto glass slides, and the tissue stained with toluidine blue (TB). TB staining was performed by drying the sections on to the slide by placing them on a slide warmer. Once the slides had dried, several drops of staining solution was placed the sections for 1-2 minutes depending on depth of colour required (slides remained on the slide heater throughout this process). The excess stain was removed by gently rinsing the slide with distilled water, the slides were then air dried and mounted in DPX.

3.3.9 HISTOPATHOLOGY

A series of LM micrographs were produced of the TSC and control exposed ETM (n=3 per slide). The images were then pathologically evaluated by chief pathologist, Dr Martin Foster (Astra Zeneca, Charnwood, Leicestershire. UK).

3.4 RESULTS

3.4.1 GENERAL MORPHOLOGY

For a complete overview of the morphological changes (toluidine blue and Haematoxylin and eosin staining) and physiological changes (cell specific markers) in the ETM model following exposure to TSC, see Table 3.2.

3.4.2 HISTOPAHTHOLOGY OF TSC EXPOSED ETM

Haematoxylin and eosin (H+E) staining was carried out on ETM sections from the five exposures which included PBS, as a visual confirmation to the conventional toxicology (described in Chapter 2); Figure 3.1 and 3.2.

Cell Marker / Stain	Control	Cadmium (uM)				Formaldehyde (mM)			
		80	160	240	320	1	5	7.5	10
H+E (Nuclei)	44 ±3	39 ±2	68 ±7	42 ±4	38 ±3	48 ±2	65 ±4	32 ±1	26 ±3
H+E (Depth δ%)	100	133	100	183	83	133	183	150	83
p63 (+ive)	4 ±1	0	0	0	0	0	5 ±1	8 ±2	0
CK 5 / 6	+	-	--	--	-	++	+++	++	+
TBM	+								
Toluidine blue		FN	BCH	BCH	BCH / FN	RH	BCH	B	CB

Cell Marker / Stain	Control	Nicotine (mM)				Urethane (mM)			
		25	50	75	100	100	250	500	2000
H+E (Nuclei)	44 ±3	48 ±2	37 ±1	21 ±2	17 ±3	45 ±3	52 ±5	42 ±5	19 ±3
H+E (Depth δ%)	100	183	167	200	150	150	167	133	80
p63 (+ive)	4 ±1	8 ±3	10 ±2	22 ±3	10 ±2	29 ±2	0	2 ±1	3 ±1
CK 5 / 6	+	+++	++	+	+	++	++	++	++
TBM	+	-	+++	++	++				
Toluidine blue		C	C	LV	PR	RH	B	B	B

Table 3.2 Overview of the histological analysis. The overview of cell specific markers and histological stains to access morphological and physiological changes to the ETM. Key: Nuclei – the mean number of nuclei counted per unit length (Section 3.3.9), depth δ% - the percentage change in the depth of the tissue compared to the control, p63 – mean number of p63 positives per unit length, CK 5 / 6 and TBM – (--) lowest expression to (+++) highest expression of cell marker / stain, toluidine blue – (FN) focal necrosis, (BCH) basal cell hyperplasia, (RH) regional hypertrophy, (B) Blastoid changes, (CB) cytoplasmic blebbing, (C) cytolysis, (LV) lipid vacuolation, (PR) end stage plaque reaction, (±) Standard deviation

3.4.2.1 CADMIUM

Initial ETM concentrations of 80µM and 160µM cadmium revealed 'normal' pseudo-stratification of three cell layers. In the subsequent concentration of 240µM, the tissue reached its maximum thickness. Mean nuclei (MN) per unit length (MN = 68) suggested the cells appeared to increase in volume, as well as to multiply in number. Further increases in concentration of cadmium led to a thinning of the tissue and a significant reduction of nuclei ($p>0.0001$; NM 320µM = 38; Figure 3.1; Table 3.2).

3.4.2.2 FORMALDEHYDE

A 1mM exposure of formaldehyde demonstrated 'normal' pseudo-stratification of three cell layers. A concentration of 5mM caused the tissue to reach its maximum thickness (MN = 65). Additional increases in formaldehyde concentrations resulted in a breakdown of cellular structure, thinning of the tissue and eventual sloughing of the cells off the insert membrane, leading to a significant reduction of nuclei ($p>0.0001$) (MN 10mM = 26; Figure 3.1; Table 3.2).

3.4.2.3 NICOTINE

A nicotine concentration of 25mM induced an increase in the thickness of the model and a concomitant increase in cell number (MN = 48), causing a doubling in size compared to the control (40µm). Further concentrations of nicotine resulted in a dramatic deterioration of the cellular structure and loss of cell contents, with eventual cell sloughing from the membranes leading to a significant reduction of nuclei ($p>0.0001$) (MN 50mM = 37; MN 75mM = 21; MN 100mM = 17; Figure 3.2; Table 3.2).

3.4.2.4 URETHANE

The 100mM concentration of urethane induced an increase in the thickness of the model, denoted by an increase in cell number (MN = 45). The tissue thickness increased by 150% when compared to the control cultures.

Additional doses of urethane caused destruction of the cellular structure, with a final dose of 2000mM causing a significant thinning of the tissue to two layers ($p > 0.05$; 13μm), featuring cells with reduced size, when compared to the initial dose (100mM; Figure 3.2; Table 3.2).

PBS

Cadmium

Formaldehyde

80µM

160µM

240µM

320µM

1mM

5mM

7.5mM

10mM
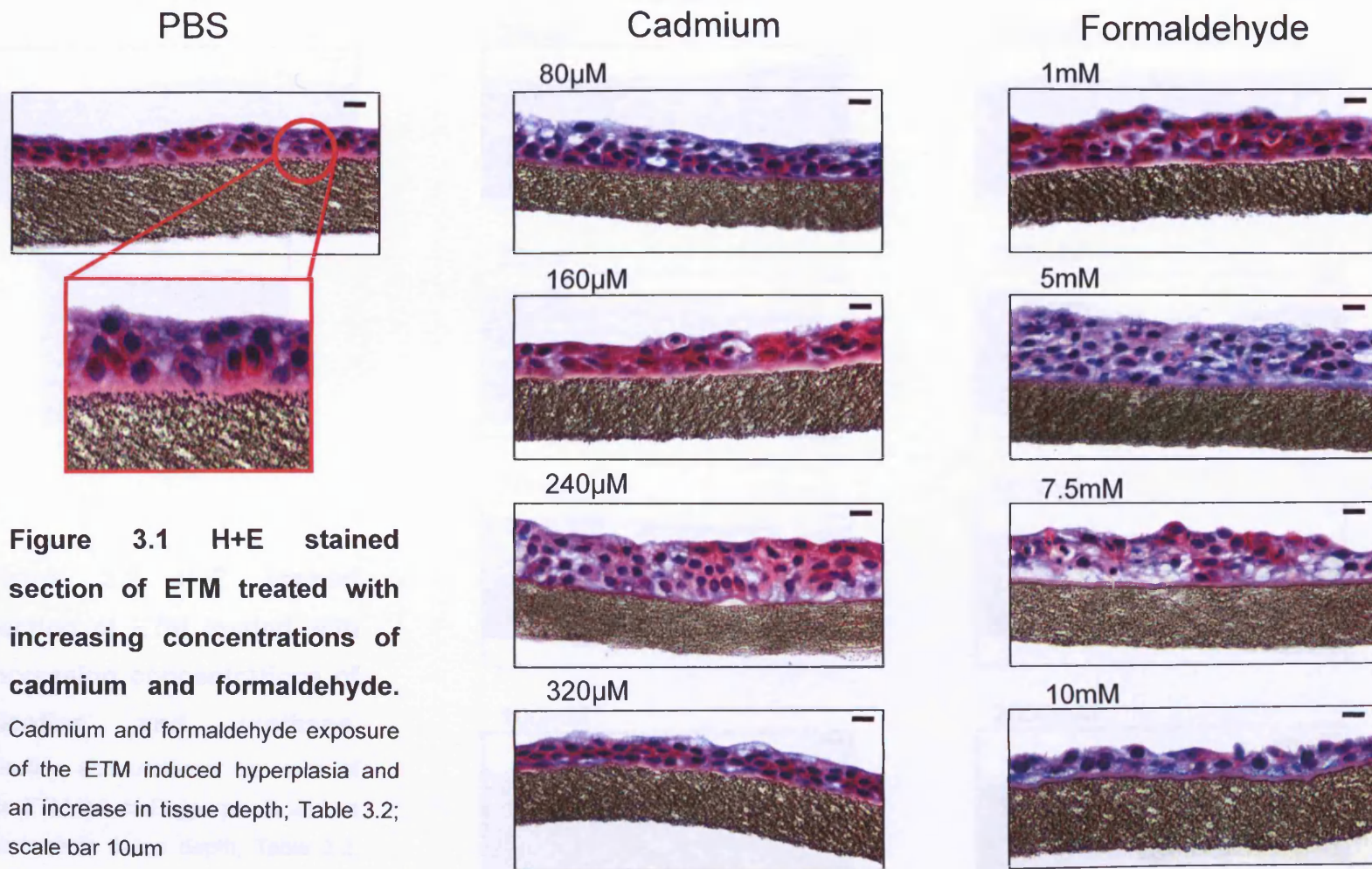
Figure 3.1 H+E stained section of ETM treated with increasing concentrations of cadmium and formaldehyde. Cadmium and formaldehyde exposure of the ETM induced hyperplasia and an increase in tissue depth; Table 3.2; scale bar 10µm

PBS

Nicotine

25mM

50mM

75mM

100mM

Urethane

100mM

250mM

500mM

2000mM
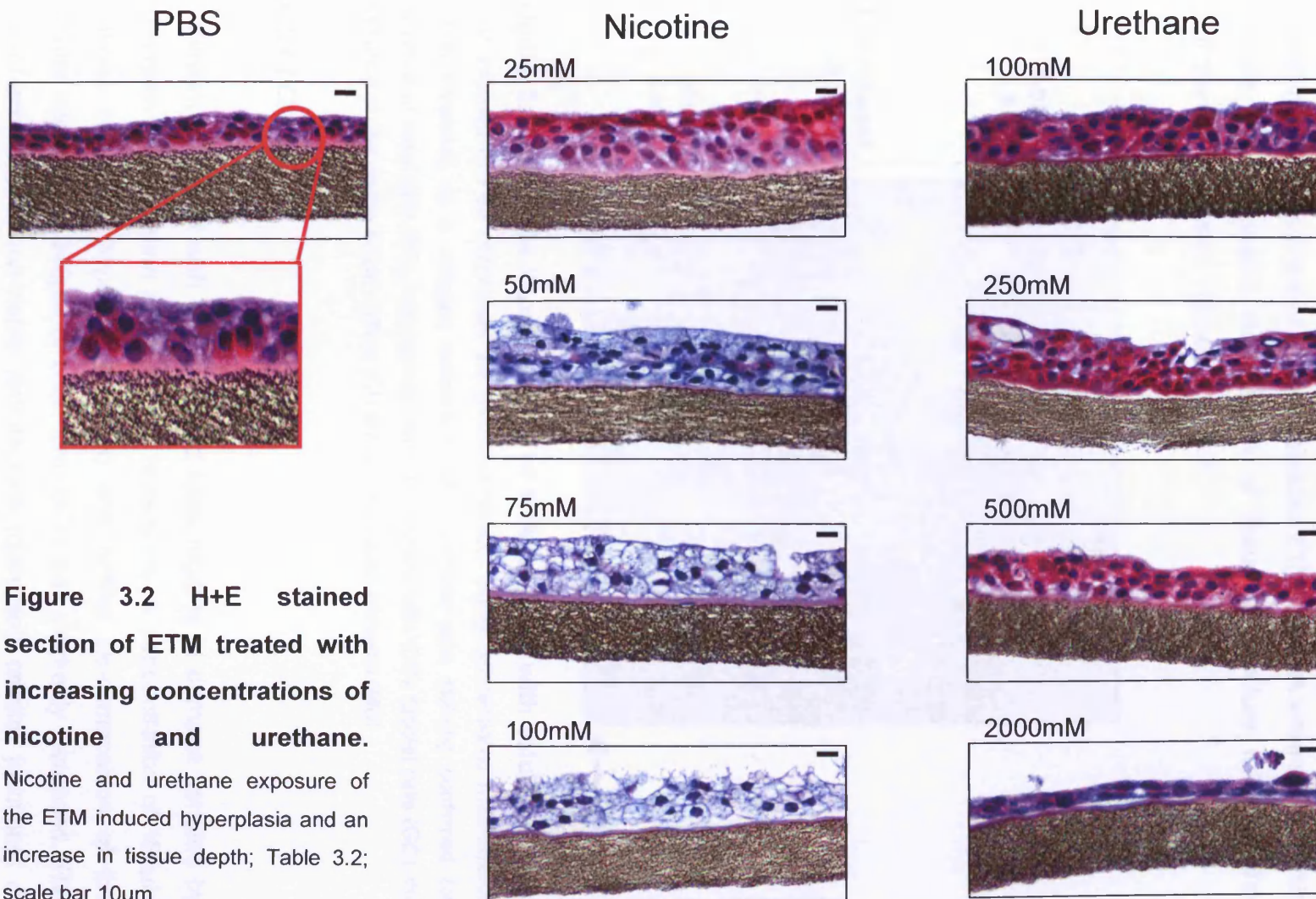
Figure 3.2 H+E stained section of ETM treated with increasing concentrations of nicotine and urethane. Nicotine and urethane exposure of the ETM induced hyperplasia and an increase in tissue depth; Table 3.2; scale bar 10μm

3.4.3 TOLUIDINE BLUE STAINING

Semi-thin survey sections of resin-embedded ETM samples were stained with toluidine blue to enable visualisation of tissue architecture following the control and TSC doses; Figures 3.3 - 3.7.
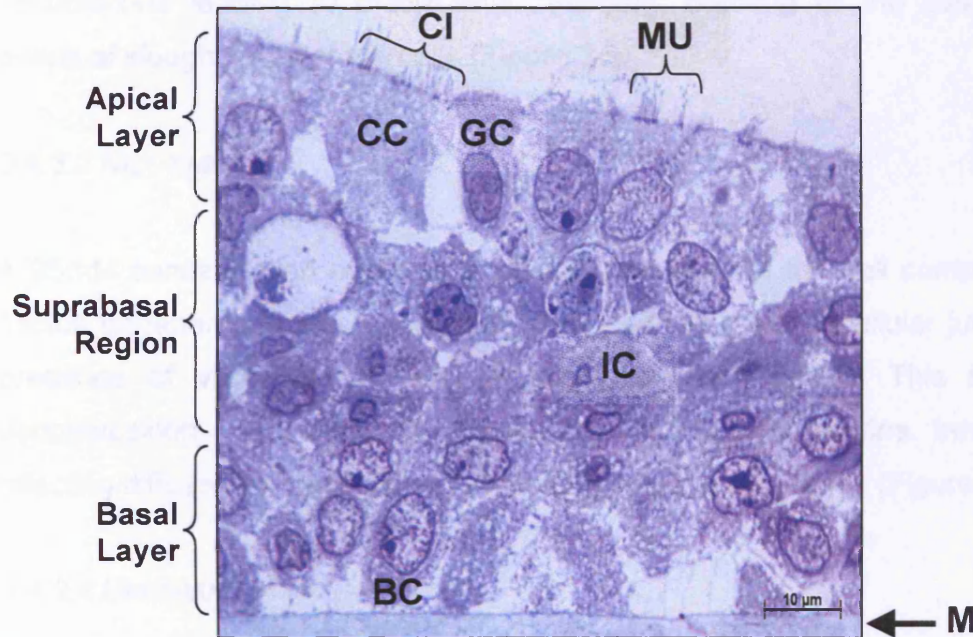
Figure 3.3 Semi-thin (2µm) section of ETM stained with toluidine blue.
ETM exposed to PBS maintained the pseudo-stratified, highly differentiated multi-layered model supported on a collagen membrane (M). Toluidine blue staining confirmed the presence of basal cells (BC), intermediate cells (IC), ciliated cells (CC), Goblet cells (GC), the presence of cilia on the apical surface (CI) and the expulsion of mucin (MU)

3.4.3.1 CADMIUM

Cadmium treatment with 80µM yielded focal regions of damage denoted by chromatin condensation and cytosolic retractions. A concentration of 160µM induced basal cell hyperplasia (BCH) and further de-composition of the cellular integrity. At 240µM of cadmium, BCH was markedly increased. The tissue exhibited a non-viable architecture (disrupted cellular junctions) at 320µM (Figure 3.4).

3.4.3.2 FORMALDEHYDE

A 1mM concentration of formaldehyde created regional hypertrophy (RH; Figure 3.5). A concentration of 5mM initiated early degradation of the tissue along side reactive cell synthesis (Figure 3.5). Further increased challenges caused changes in early cellular development, cell swelling and disruption of the plasma membrane. At the 10mM dose, there was evidence of vacuolations leading to cytoplasmic blebbing, thinning of the tissue and eventual sloughing-off of the cells (Figure 3.5).

3.4.3.3 NICOTINE

A 25mM concentration of nicotine induced cytolysis of the cell components. Tissue degeneration was denoted by disruption of the intracellular junctions, presence of vacuoles and disordered tissue architecture. This form of decomposition continued with further incremental of nicotine treatments effecting diffuse lipid vacuolation and thickening of membranes (Figure 3.6).

3.4.3.4 URETHANE

Diffuse cellular swelling and regional tissue degeneration occurred with a 100mM urethane concentration. Increased concentrations generated region-specific (basal region only) alterations in cells. Quantitative observations of the tissue histopathology suggested that the nucleus-to-cytoplasmic ratios were enlarged (versus lower doses; Figure 3.7).

3.4.4 DETECTION OF P63

Protein 63 staining was carried out on ETM sections from the four TSC exposures and PBS. This was conducted for a visual assessment of the expression of p63 in the basal cells of the ETM; Figure 3.8 and 3.9.

CADMIUM
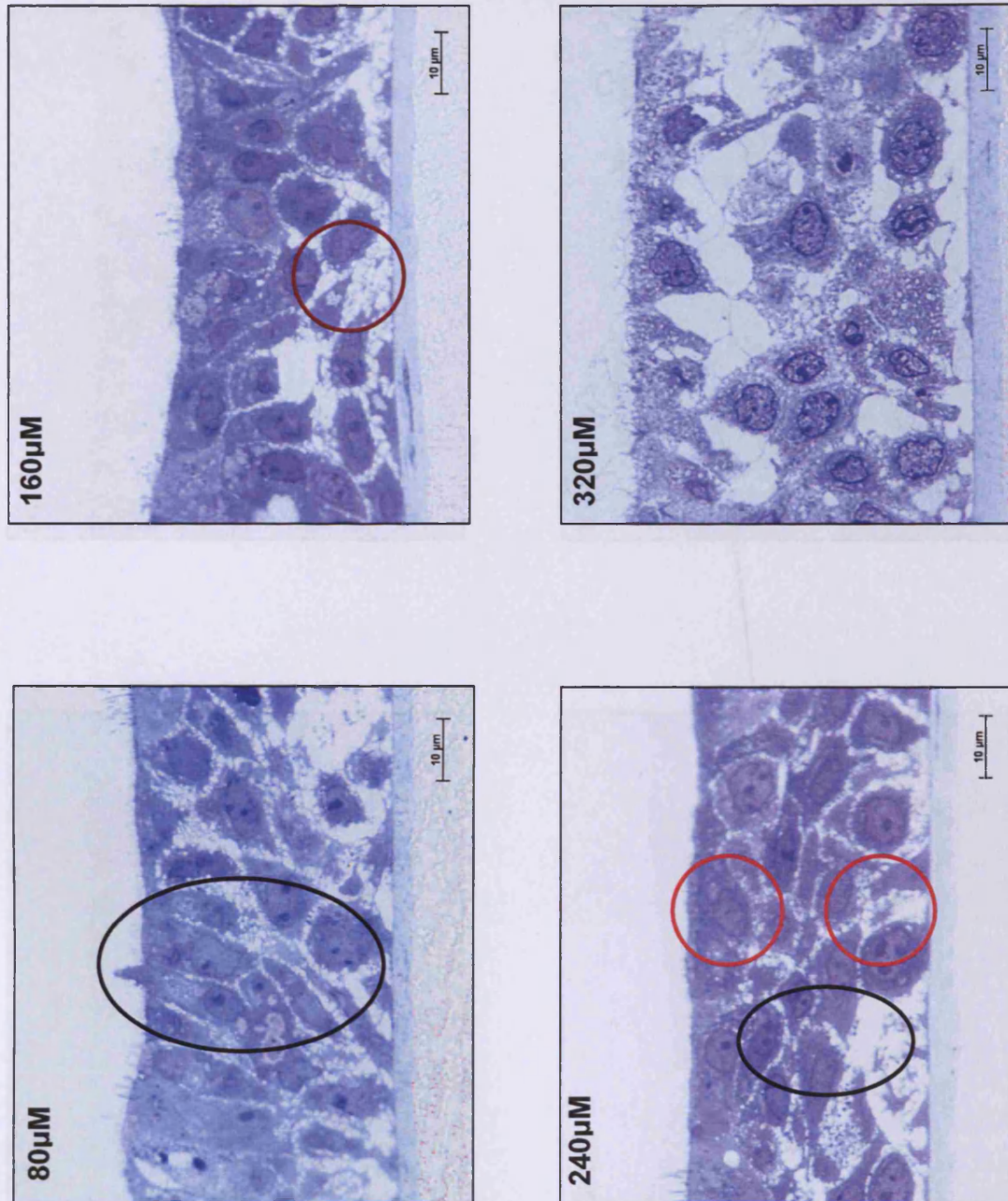
Figure 3.4 Semi-thin (2µm) section of ETM stained with toluidine blue treated with increasing concentrations of cadmium. Black circle (80µM) - focal regions of damage observed (chromatin condensation and cytosolic retractions), purple circle (160µM) – basal cell hyperplasia, black circle (240µM) – area of necrosis, red circle – areas of hyperplasia, complete loss viable architecture at 320µM; scale bar 10µm
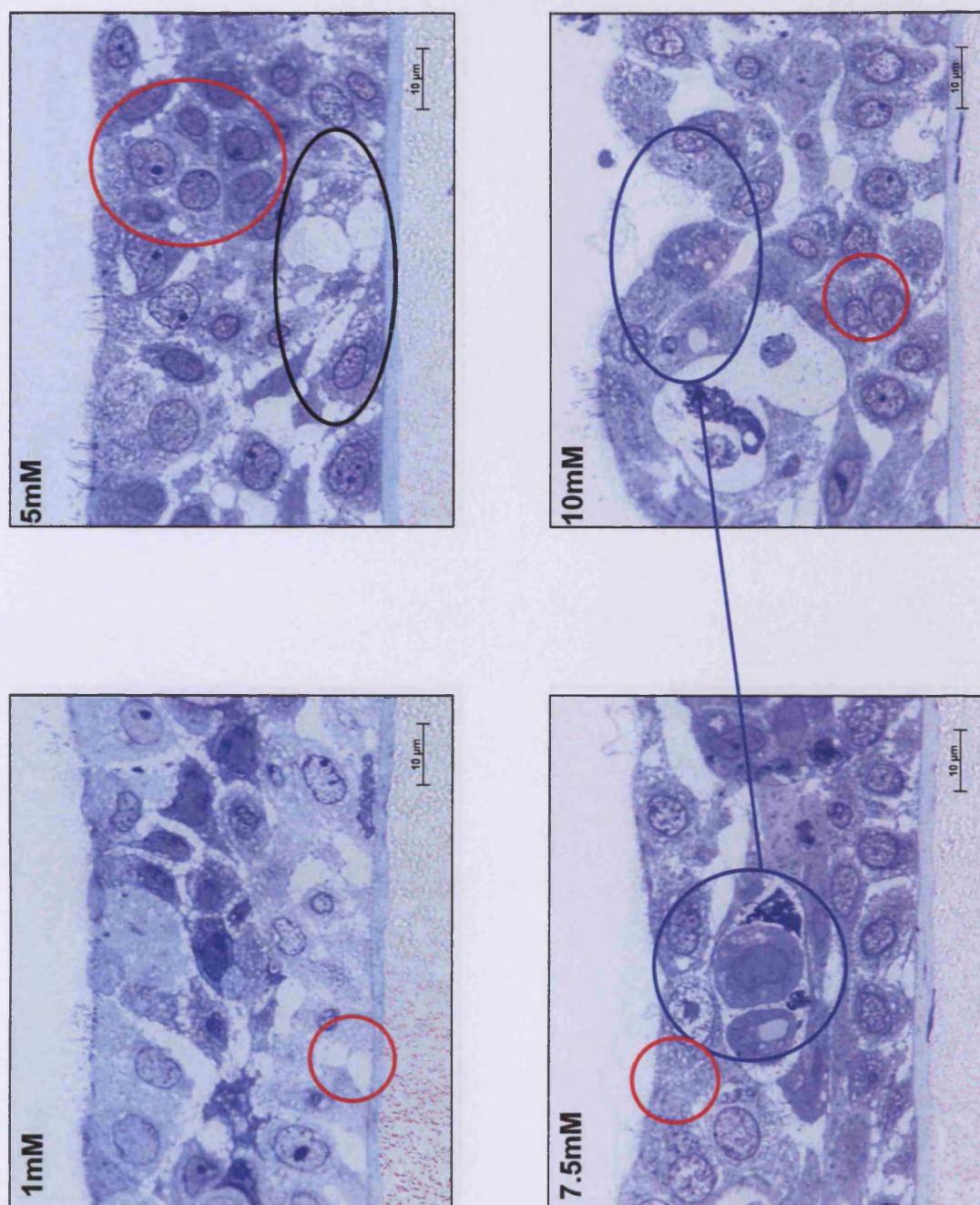
FORMALDEHYDE

Figure 3.5 Semi-thin (2μm) section of ETM stained with toluidine blue treated with increasing concentrations of formaldehyde. Red circle (1mM) - area of regional hypertrophy, red circle (5mM) - area of reactive cell synthesis, black circle (5mM) - area tissue degradation, red circle (7.5mM) – changes in early cellular development, cell swelling and disruption of the plasma membrane leading to early necrosis, blue circles – progression of cytoplasmic blebbing with increased dose, red circle (10mM) – vacuolation; scale bar 10μm

NICOTINE
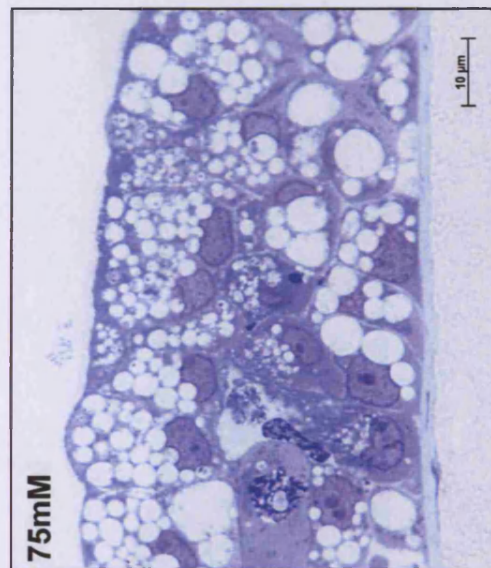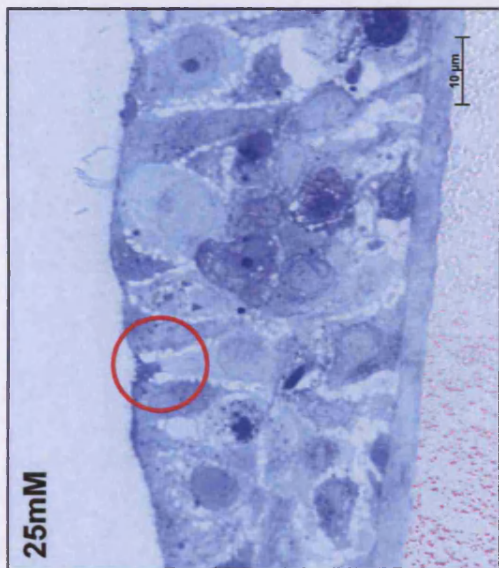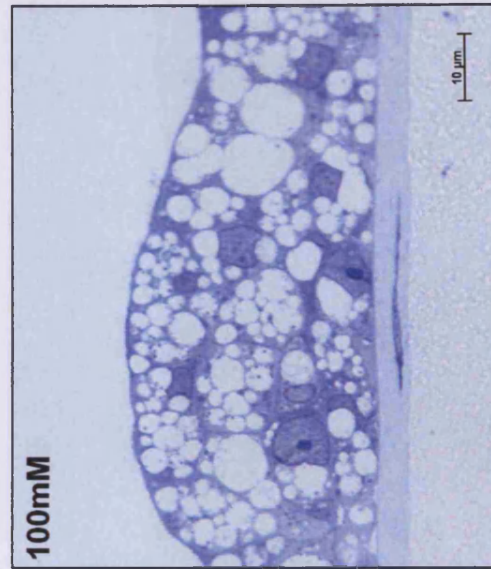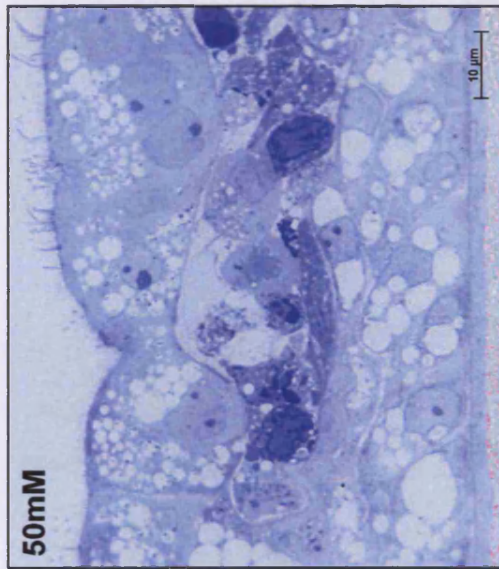
Figure 3.6 Semi-thin (2μm) section of ETM stained with toluidine blue treated with increasing concentrations of nicotine. Red circle (25mM) – (evidence of burst cells due to an osmotic imbalance) cytolysis further increases in nicotine induced disruption of the intracellular junctions and diffuse lipid vacuolation leading to thickening of membranes; scale bar 10μm
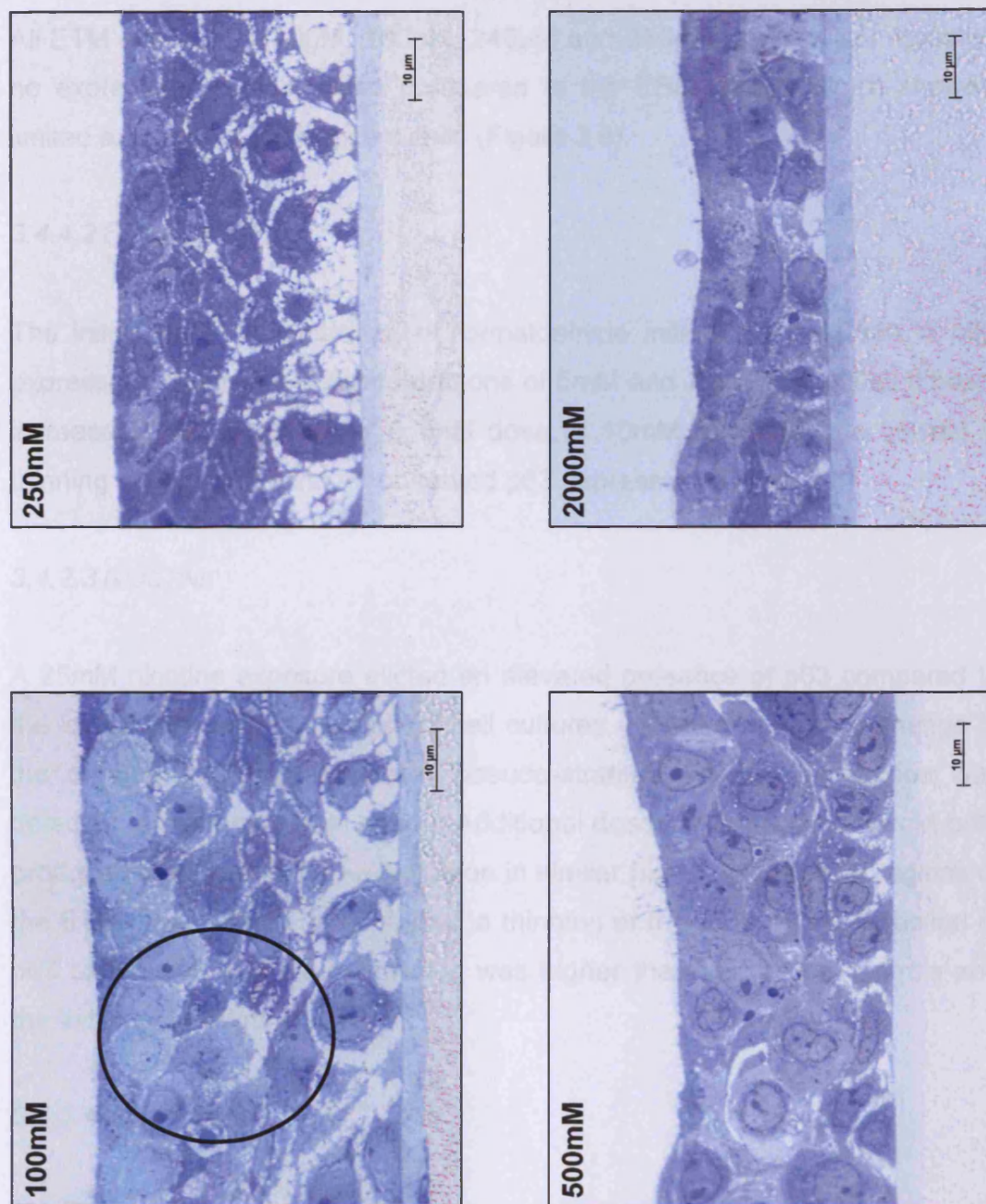
URETHANE

Figure 3.7 Semi-thin (2μm) section of ETM stained with toluidine blue treated with increasing concentrations of urethane. Black circle – indicates diffuse cellular swelling with regional hypertrophy. Additional concentrations (250mM and 500mM) resulted changes in basal cellular development, characterised by expansion of the cytoplasm and enlargement of the cell nucleus; scale bar 10μm

3.4.4.1 CADMIUM

All ETM exposures (80μM, 160μM, 240μM and 320μM) of cadmium revealed no expression of p63, when compared to the PBS control, which showed limited expression, in the basal cells (Figure 3.8).

3.4.4.2 FORMALDEHYDE

The initial 1mM concentration of formaldehyde initiated a reduction in p63 expression. Subsequent concentrations of 5mM and 7.5mM produced a basal increase in p63 expression. A final dose of 10mM formaldehyde caused a thinning of the model and no observed p63 expression (Figure 3.8).

3.4.2.3 NICOTINE

A 25mM nicotine exposure elicted an elevated presence of p63 compared to the levels observed in the control cell cultures. However, due to a change in the organisation of the 'normal' pseudo-stratification, the expression was detected in the suprabasal region. Additional doses of 50mM and 75mM both produced increases in p63 expression in similar higher, suprabasal regions of the ETM. The 100mM dose caused a thinning of the ETM and a reduction of p63 expression, but the expression was higher than that in the controls and the initial dose (Figure 3.9).

3.4.2.4 URETHANE

The ETM exposure of 100mM urethane produced a dramatic increase in p63 expression at the basal and intermediate levels of cell organisation. Doses of 250mM and 500mM urethane resulted in a marked reduction to below the control culture levels of p63. A 2000mM dose caused a thinning of the ETM to a maximum of two cells layers thick but limited expression of p63 was observed (Figure 3.9).

PBS

Cadmium

Formaldehyde

80μM

1mM

160μM

5mM
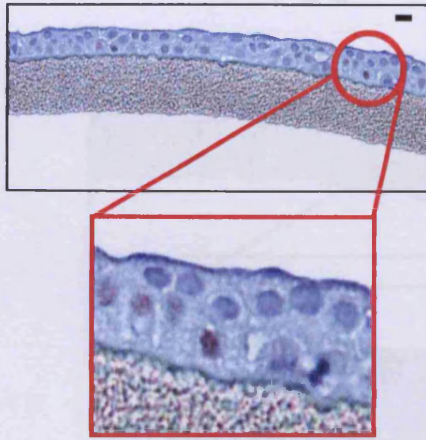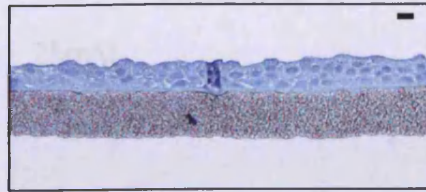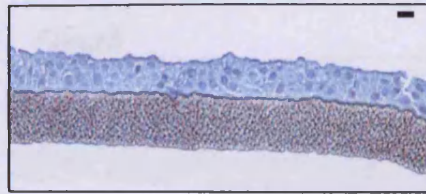
240μM
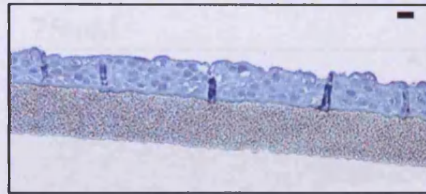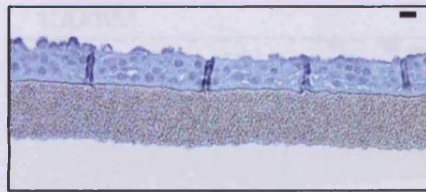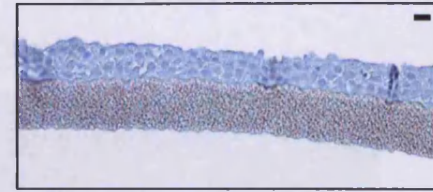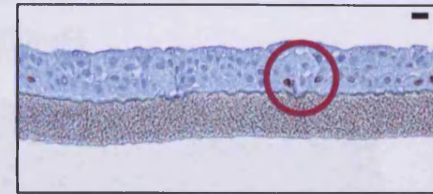
7.5mM

320μM
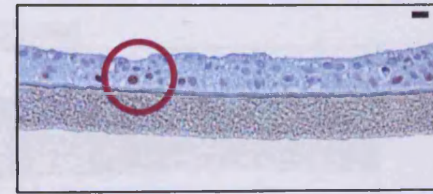
10mM
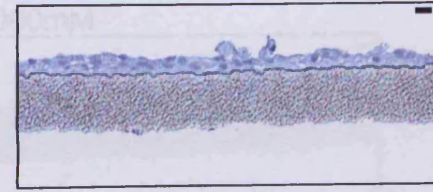
Figure 3.8 p63 stained section of ETM treated with increasing concentrations of cadmium and formaldehyde. p63 stained brown, red circle - p63 positive in the control ETM. Cadmium exposure of the ETM did not inhibit p63 expression and formaldehyde (purple circle) exposure of the ETM induced p63 at the higher concentrations; Table 3.2, scale bar 10μm

PBS

Figure 3.9 p63 stained section of ETM treated with increasing concentrations of nicotine and urethane. p63 stained brown, red circle - p63 positive in the control ETM. Nicotine (blue circle) and urethane (purple circle) exposure of the ETM initially induced p63; Table 3.2, scale bar 10µm

Nicotine

25mM

50mM

75mM

100mM

Urethane

100mM

250mM

500mM

2000mM
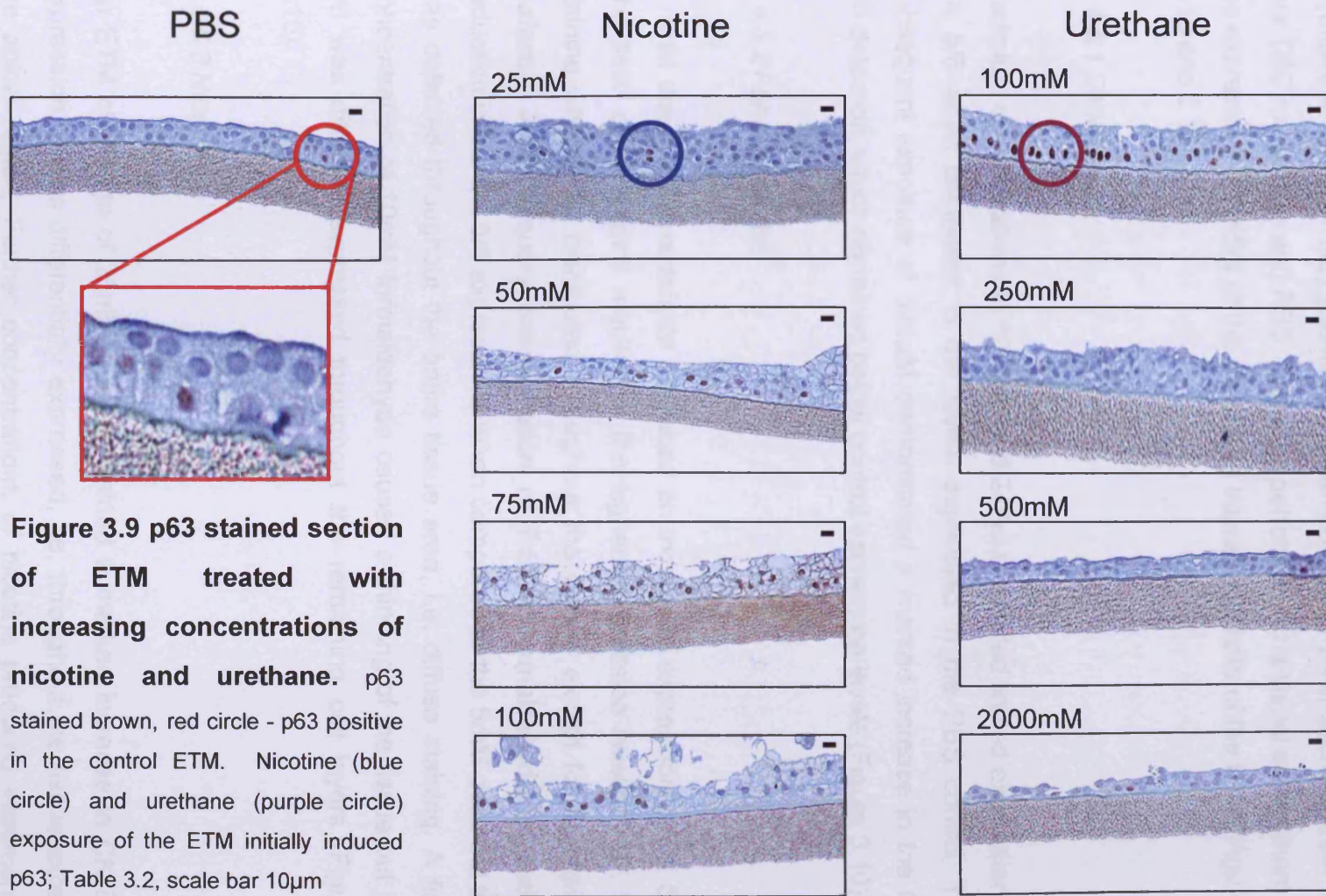
3.4.5 Cytokeratin 5/6 Detection

Cytokeratin 5/6 (CK 5/6) staining was carried out on ETM sections from the four TSC exposures and PBS. This was performed for a visual assessment of the expression of CK5/6 at the basal and suprabasal cells of the ETM; Figures 3.10 and 3.11.

3.4.5.1 Cadmium

Cadmium concentrations of 80, 160 and 240μM revealed limited expression of CK 5/6 when compared to the levels expressed in the PBS control. The subsequent exposure of 320μM demonstated a marked increase in the CK 5/6 detection, which remained below control expression levels (Figure 3.10).

3.4.5.2 Formaldehyde

A 1mM dose of formaldehyde produced an increased expression of CK 5/6. The 5mM concentration resulted in the highest expression levels of CK 5/6 staining which was distributed throughout the tissue, except for the apical surface. A subsequent concentration of 7.5mM formaldehyde caused a reduction in the CK 5/6 expressions when compared to the 5mM dose but this was detected throughout the entire tissue area, i.e. diffuse staining. A final concentration of 10mM formaldehyde caused a thinning of the tissue but CK 5/6 was diffusely expressed throughout the remaining cell layers (Figure 3.10).

3.4.5.3 Nicotine

An ETM challenge of 25mM nicotine yielded a marked increase in CK 5/6 expression. It was differentially expressed, i.e. throughout the tissue except the apical region. Further concentrations of nicotine produced incremental decreases in CK 5/6 positive cells. It was also noted that with increased dose, the location of the expression became more basal (Figure 3.11).

3.4.5.4 URETHANE

A concentration of 100mM urethane produced an increase CK 5/6 expressions throughout the basal and intermediate levels of the tissue. The concentrations of 250mM and 500mM urethane generated a reduction in detection levels but still remained higher than that found in the control cultures. The final concentration of 2000mM urethane thinned the tissue down to two cell layers and the CK 5/6 staining was diffuse i.e. encompassed all tissue (Figure 3.11).

3.4.6 TRACHEO-BRONCHIAL MUCIN VISUALISATION OF TISSUE

Tracheo-bonchial mucin (TBM) staining was carried out on ETM sections from the four exposure and PBS; Figure 3.12.

3.4.6.1 NICOTINE

A 25mM concentration of nicotine did not elicit significant levels of TBM expression. The successive increases in concentration produced tissue wide increases in non-specific staining (Figure 3.12).

PBS
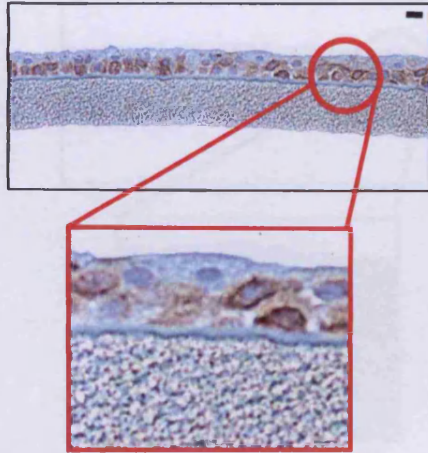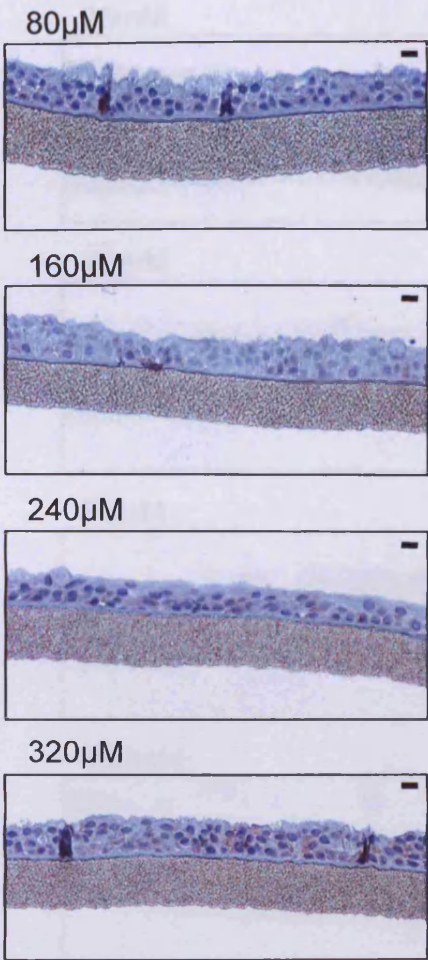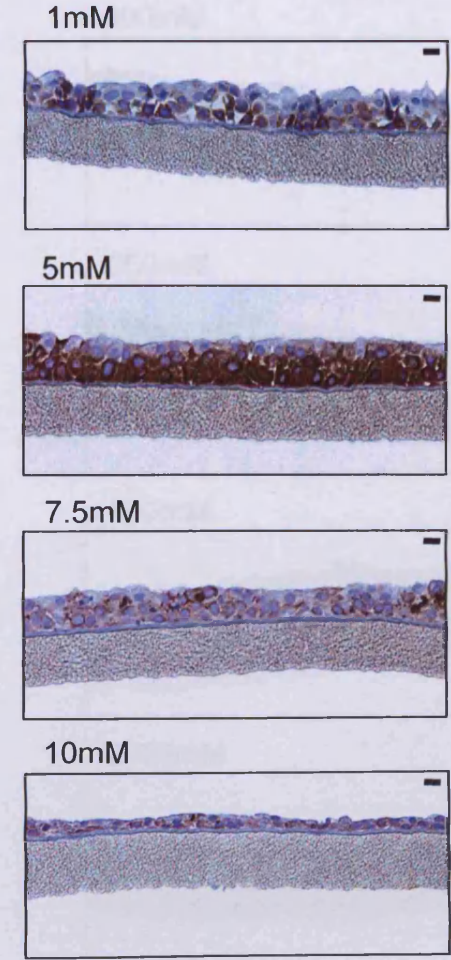
Figure 3.10 Cytokeratin 5/6 stained section of ETM treated with increasing concentrations of cadmium and formaldehyde. CK5/6 expression is denoted by brown stain, cadmium inhibited CK5/6 expression except for the highest dose, formaldehyde induced CK5/6 expression; Table 3.2; scale bar 10µm

Cadmium

80µM

160µM

240µM

320µM

Formaldehyde

1mM

5mM

7.5mM

10mM
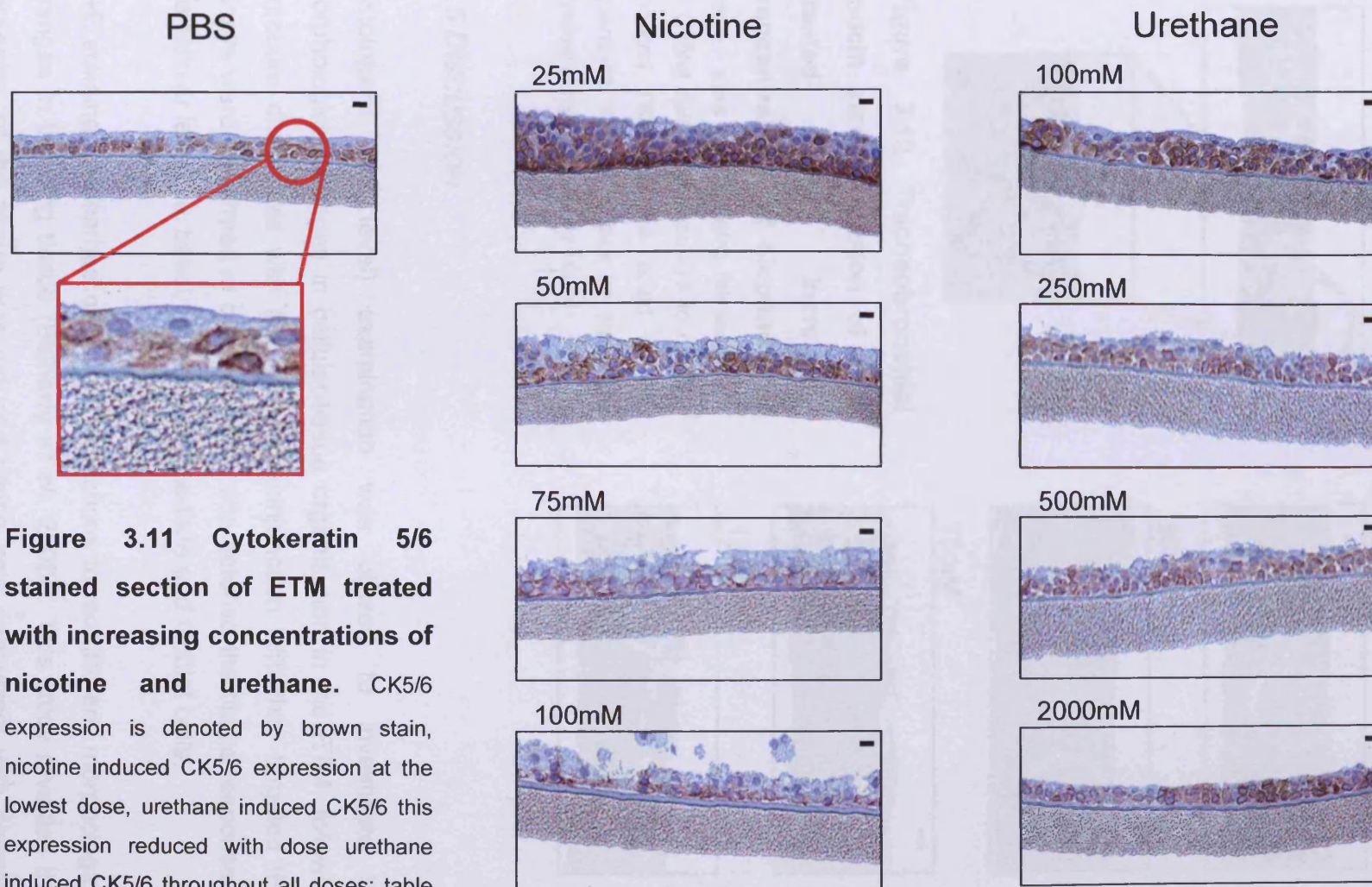
Figure 3.11 Cytokeratin 5/6 stained section of ETM treated with increasing concentrations of nicotine and urethane. CK5/6 expression is denoted by brown stain, nicotine induced CK5/6 expression at the lowest dose, urethane induced CK5/6 this expression reduced with dose urethane induced CK5/6 throughout all doses; table 3.2, scale bar 10µm

PBS

Nicotine

25mM

50mM

75mM

100mM
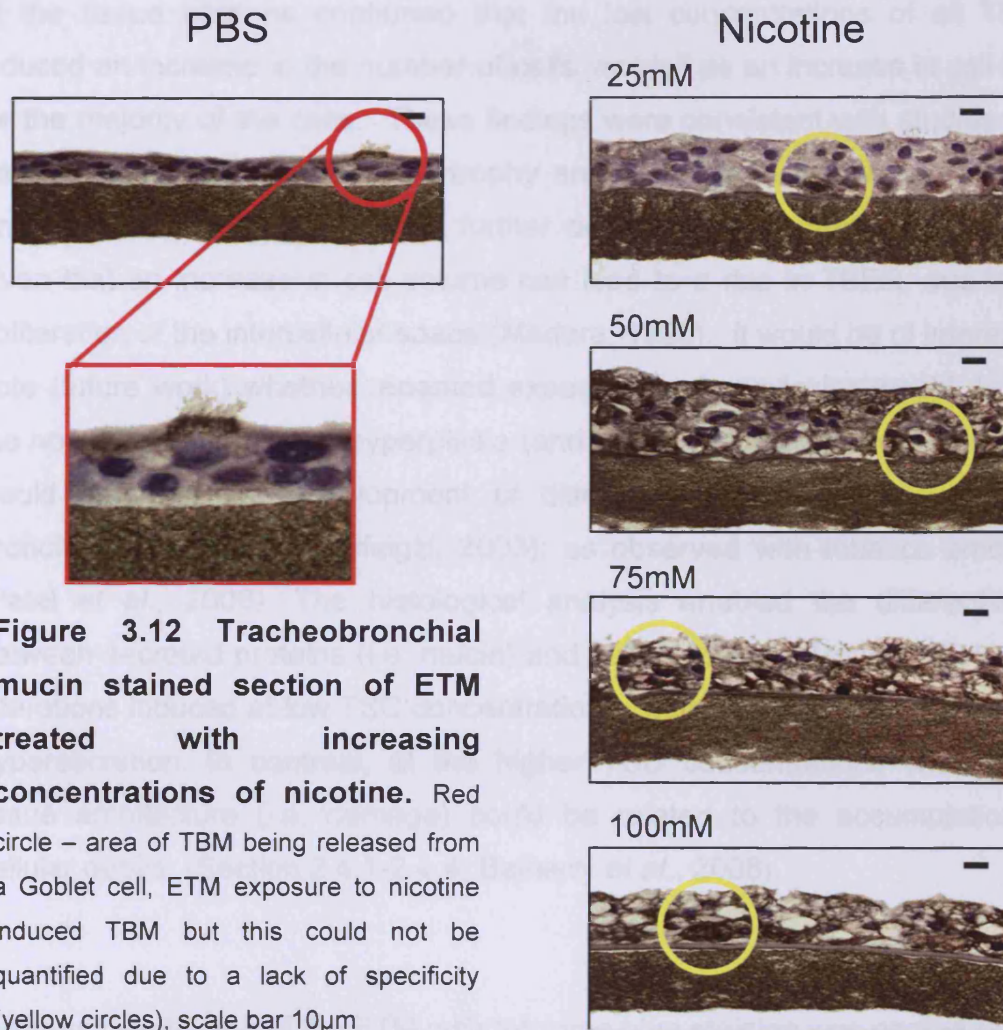
Figure 3.12 Tracheobronchial mucin stained section of ETM treated with increasing concentrations of nicotine. Red circle – area of TBM being released from a Goblet cell, ETM exposure to nicotine induced TBM but this could not be quantified due to a lack of specificity (yellow circles), scale bar 10µm

3.5 DISCUSSION

Histological (LM level) examination was utilised to investigate the morphological changes in cellular-tissue organisation in the ETM, following exposure challenges with the TSC. In conjunction with this, targeted IHC assays were performed in order to better characterise the tissue response at the cellular level, i.e. basal, ciliated, intermediate and Goblet cells.

H+E staining was carried out on ETM sections to monitor any morphological changes in the lung tissue (Balharry *et al*., 2008). This study revealed that thickening of the tissue was induced which was concurrent with elevated TEER outputs (section 2.4.1.1, 2.4.2.1, 2.4.3.1 and 2.4.4.1). Image analysis

of the tissue sections confirmed that the low concentrations of all TSCs induced an increase in the number of cells, as well as an increase in cell size for the majority of the cells. These findings were consistent with studies that have identified Goblet cell hypertrophy and hyperplasia in human smokers (Innes *et al.*, 2006). This could further account for the changes in TEER, given that an increase in cell volume can lead to a rise in TEER, due to an obliteration of the intercellular space (Madara, 1998). It would be of interest to note (future work) whether repeated exposure to these toxins would disrupt the normal progression of hyperplasia (and hence, epithelial recovery), which would result in the development of diseases such as asthma, chronic bronchitis and cancer (Tesfaigzi, 2003); as observed with tobacco smoking (Patel *et al.*, 2008). The histological analysis enabled the differentiation between secreted proteins (i.e. mucin) and cellular debris. The morphological alterations induced at low TSC concentrations could be associated with mucin hypersecretion. In contrast, at the higher TSC concentrations changes in tissue architecture (i.e. damage) could be related to the accumulation of cellular debirs, (Section 2.4.1-2.4.4; Balharry *et al.*, 2008).

Semi-thin sectioning of the ETM with toluidine blue staining was carried out on TSC exposed ETM. This allowed detailed morphological changes of cellular and tissue architecture at more than adequate levels of resolution (i.e. one step below transmission electron microscopy (TEM). On closer examination of the individual TSC, there were four main pathological developments: (1) hyperplasia, (2) hypertrophy, (3) cytolysis, and (4) necrosis. Cadmium exposed ETM revealed evidence of apoptosis and necrosis at the initial dose; this was substantiated by the biochemical mode of action of cadmium on cells resulting in apoptosis and necrosis (Pinot, *et al.*, 2000). Further exposures of cadmium identified evidence of necrosis and focal areas of hyperplasia. The existence of hyperplasia infered that the ETM was attempting to repair and/or regenerate (McDowell *et al.*, 1979; Zahm *et al.*, 1997). Exposure of the lowest concentration of formaldehyde (1mM) to the ETM revealed regional hypertrophy at the basal level. This pathological abnormality was also observed in a study by Innes *et al.*, (2006), where they identified Goblet cell

hypertrophy in smokers compared to non-smokers. Further increments of formaldehyde initiated tissue degeneration and necrosis, as denoted by a loss of the basal and columnar cells; features that have also been observed in inflammatory airway diseases (Trautmann et al., 2005). These observations of hypertrophy and regional degeneration were also noted in the ETM exposed to urethane, where the basal degeneration was very pronounced at the 250mM exposure. Degeneration at this level may suggest the ETM would fail to replenish the cells that had been damaged (Barbieri and Pietenpol, 2005). The presence of cytolysis was only observed in the nicotine treated cells. Previous studies by other investigators, regarding the removal of inflammatory cells from airway tissues, implied that the removal process was solely due to apoptosis (Haslett, 1999; Henson et al., 2001). Investigations conducted by Uller et al., (2004), demonstrated that cells may also be cleared through primary cytolysis, where necrosis was secondary to apoptosis. The mechanism of squamous metaplasia has been described by other researchers (Puchelle et al., 2006) as being a component of the protective response, leading to regeneration and repair post-injury.

IHC analysis was conducted to confirm epithelial differentiation and identification of protective mechanisms (e.g. p63). The first cell-specific marker used was protein 63 (p63), a transcription factor in the development and maintenance of stratified-epithelium. It was investigated since deregulated growth of stratified-epithelium is a major cause lung disease (Barbieri and Pietenpol, 2005). This marker was located in the basal layers of stratified epithelial tissues (Dellavalle et al., 2001). The basal layers were thought to include cells of high proliferative capacity, which replenish the terminally differentiated populations in the suprabasal regions (Pellegrini et al., 2001).

Analysis of the cadmium exposure revealed no expression of p63. The role of p63 in apoptosis remains controversial but studies have demonstrated that an induction of p63 results in a reduction of apoptosis (Barbieri and Pietenpol, 2006; Liefer et al., 2000). The interactions of cadmium on the mitochondria

can lead to apoptosis (Pinot *et al.*, 2000). Therefore, it may be assumed that an increase of apoptosis could decrease p63 expression.

Examination of the ETM exposure to formaldehyde demonstrated an initial down-regulation of p63. This could be indicative of an increase in apoptosis and necrosis. The subsequent doses of formaldehyde produced an increase of p63 expression, suggesting that the model was attempting to repair and counteract apoptotic functions, such as DNA damage (Chilosi *et al.*, 2002). This repair process was deemed to be overwhelmed (e.g. cell swelling and disruption of the plasma membrane), as there was no p63 expression and there was morphological evidence of necrosis with the final formaldehyde exposure.

The response of the ETM to nicotine had a completely different exposure profile. The p63 expression increased with the incremental exposures which have indicated that the ETM was attempting to repair and inhibit the apoptotic functions (Chilosi *et al.*, 2002). The expression location of p63 was altered for each concentration of nicotine exposure, and moved into the suprabasal region. On further examination, it was possible to view structural changes (e.g. disruption of the intracellular junctions, presence of vacuoles) to the ETM and a marked reduction in the pseudo-stratification of the epithelia. The change of structure may be classified as squamous metaplasia, i.e. squamous morphology (Gray *et al.*, 2007). A change in cell structure is not necessarily associated with a specific disease but can be observed in smokers (Peters *et al.*, 1993; Murarescu *et al.*, 2007).

Finally, urethane elicited an increase in p63 expression at the lowest concentration (100mM). It was believed to have an anti-apoptotic protective mechanism, with the model attempting to repair damage by maintaining cellular propagative capacity (Yang *et al.*, 1998). Further increments of urethane exposure created a stark reduction in the p63 expression that corresponded to widespread tissue degradation. It should be noted that urethane (ethyl carbamate) has the capacity to be carcinogenic (Gupta and

Dani, 1989) and deregulation of p63 has been associated with early stages of invasive cancers (Comperat *et al.*, 2007; Urist *et al.*, 2002).

The second cell-specific marker examined was cytokeratin 5/6 expression. Cytokeratins are a family of cytoskeletal proteins in all epithelia (Presland and Dale, 2000). They are expressed in epithelial cells and self-assemble to form a three-dimensional array of filaments that extend from the nucleus to the cell membrane and are significant for maintenance of cell shape and viability (Presland *et al.*, 2002). Cytokeratin 5 is expressed in the basal region of the stratified tissue. This is the region thought to replenish the higher regions (Gomperts *et al.*, 2007). Cytokeratin 6 can be expressed in the suprabasal region; this region is associated with differentiation and is often paired with cytokeratin 16 (Presland and Dale, 2000).

Analysis of the cadmium exposure to the ETM showed limited expression of CK 5/6. This decrease may be indicative of an inhibition of cytokeratin's role in the repair process (Bloor *et al.*, 2001; Gomperts *et al.*, 2007). Increasing concentrations of cadmium increased the expression of CK 5/6 at the suprabasal region but all expression was below the control levels, suggesting that this region had limited differentiation (Chu and Weiss, 2002). Examination at the ETM of the lowest concentration of formaldehyde (1mM) revealed an initial increase in CK 5/6 at the basal region, which may infer that the ETM was viable and attempting to repair via replenishment of the cells injured post-exposure (Pierce *et al.*, 1994; Gomperts *et al.*, 2007). The subsequent concentration of formaldehyde (5mM) caused a dramatic increase of CK 5/6, in the basal and suprabasal regions, which may be interpreted as a repair response to counteract any apoptotic functions (Chilosi *et al.*, 2002). The final formaldehyde concentration (10mM) induced a reduction in CK 5/6 expression back to control level but the model was notably thin in cell layers with eventual sloughing-off of cells, as the repair/maintenance process had been over-whelmed. CK 5/6 expression in nicotine treated cells (25mM) caused an increased expression at the basal and suprabasal regions compared to the control cells. This induction of the repair/maintenance mechanisms was followed by subsequent decreases of expression with increased

concentrations of nicotine (50, 75 and 100mM). This expression pattern was finalised with a control level expression at the basal region of the ETM. However, it was believed that the expression was really suprabasal cytokeratin 6, due to the re-structuring of the ETM post-nicotine exposure. This unique expression was also observed with cadmium and urethane. However, there was one subtle difference with urethane (2000mM) in that CK 5/6 expression was throughout all regions of the post-exposure tissue indicating that the ETM was attempting to 'survive'. Further examination concluded that the apical surface had been sloughed-off, with only the cytokeratin stained regions of viable cells remained.

The final IHC technique used was the detection of TBM. It constituted the most characteristic glycoproteins of mucus and was synthesized by the Goblet cells of the epithelium and the mucosal cells of submucosal glands. TB secretions coat the respiratory tract epithelium and protect the airways by binding or trapping pathogens. Over-expression of this gene could be indicative of a protective mechanism being initiated, due to exposure of a xenobiotic or pathogen (Wang *et al.*, 2008). This IHC technique was not sensitive enough to quantify due to the antibody used was generic (MUC4) rather than a more specific TBM antibody e.g. MUC5B (Kesimer et al., 2009)

3.6 CONCLUSION

Histological evaluations, in conjunction with IHC, enabled identification of the mechanisms of TSC injury and repair. Three discrete zones of tissue injury and repair could be delineated: (1) apical region and its Goblet cells; (2) suprabasal region reactive intermediate cells; and (3) basal zone, where basal cells acted as progenitors cells. The data from this Chapter also confirmed the findings in Chapter 2, in that the concentrations of TSC used in this study were intended to achieve a full range of responses from the ETM, from sub-toxic concentrations to widespread cell death.

CHAPTER 4:

TRANSCRIPTIONAL CHANGES OF ETM EXPOSURE TO TOBACCO SMOKE COMPONENTS

4.1 INTRODUCTION

In Chapter 3, the biological and related morphological responses to TSC in the ETM were evaluated. The conventional toxicological evaluations suggested that the four TSC elicited a similar response from the ETM, i.e. biphasic; Balharry *et al.*, (2008). An alternative approach was now required to assess the early/protective biological responses and highlight potential biomarkers of harm for specific mechanisms of injury attributed to smoking. This could be achieved by using genomics, where the study of transcriptional changes could be determined.

In the following work, the toxicogenomic or transcriptional changes to TSC challenge was determined; thus providing a holistic toxicological approach. The use of human tissue equivalent models of respiratory epithelium provided human mRNA transcript data, allowing identification of biomarkers that could be related to many respiratory diseases (Sexton *et al.*, 2008). To measure potential genomic markers of injury, differential gene expression was investigated using a standard, microarray platform; OligoGEArrays® (SuperArray). The Oligo GEArray® Human Toxicology & Drug Resistance Microarray profiled the expression of 263 genes related to the metabolic processes of cell stress, cell toxicity, drug resistance and metabolism. Genes critical in drug metabolism resistance and, such as those encoding enzymes important for drug transport and phase I metabolism (specifically P450-mediated oxidation) were included.

4.2 MATERIALS AND STOCK SOLUTIONS

4.2.1 MATERIALS AND SUPPLIES

Materials:	Supplier:
QIAzol Lysis Reagent (79306)	Qiagen
RNeasy Mini Kit (74104)	Qiagen
QIAshredders (79654)	Qiagen
QuantiTect® Reverse Transcription Kit (205311)	Qiagen
QuantiTect® SYBR Green PCR Kit (204143)	Qiagen
RNAlater (76104)	Qiagen
Oligo GEArray® Human Toxicology & Drug Resistance Microarray (OHS-401)	SuperArray, USA
cRNA Cleanup Kit (GA-012)	SuperArray, USA
Gene Expression Analysis Suite (GA-022)	SuperArray, USA
Biotin-11-UTP (NEL543001EA)	Perkin Elmer
Significance Analysis of Microarrays	Stanford University, USA
SDS Solution (Ultra Pure) (20%)	National Diagnostics
SSC Solution (Ultra Pure) (20x)	National Diagnostics
Water (W4502)	Sigma-Aldrich
Ethidium Bromide (E1510)	Sigma-Aldrich
Loading Dye (G2526)	Sigma-Aldrich
RNAlater (R0901)	Sigma-Aldrich
NuSieve™ Agarose	Cambrex
StrataClone™ (240205)	Sratagene, Netherlands
Wizard® Plus Miniprep DNA Purification System (A1340)	Promega
Thermo-fast® 96 Detection Plates (AB-0800)	ABgene
Ultra Clear Cap Strips (AB-0866)	ABgene

Table 4.1 Materials used and their suppliers. All suppliers are UK based unless stated

Gene Symbol	Qiagen Ref	Entrez Gene ID	Amplicon (bp)
BAX	QT00031192	581	111
CCND1	QT00495285	595	96
CYP20A1	QT00065394	57404	120
CYP4F3	QT00018039	4051	98
GAPDH	QT01192646	2597	119
HMOX1	QT00092645	3162	99
HSPA8	QT00030079	3312	79
SULT1A1	QT00000112	6817	76
TOP1	QT00085400	116447	92
TNFRSF11A	QT00035434	8792	70

Table 4.2 QuantiTect® Primer Assay for qPCR

4.2.2 STOCK SOLUTIONS

4.2.2.1 MICROARRAY

Wash Solution 1 was prepared as a 1x working solution containing 2x SSC and 1% SDS. This working solution was stored at room temperature.

Wash Solution 2 was prepared as a 1x working solution containing 0.1x SSC and 0.5% SDS. This working solution was stored at room temperature.

Annealing Mix (per sample):

RNA	0.1-3.0µg of total RNA
Truelabeling Primer	1µl
RNase-Free H$_2$O	**to a final volume of 10µl**

Table 4.3 Preparation of annealing mix solution. Microarray procedure detailed in Section 4.3.2.1

cDNA Synthesis Master Mix (per reaction):

RNase-free H$_2$0	4µl
5X cDNA Synthesis Buffer	4µl
RNase Inhibitor	1µl
cDNA Synthesis Enzyme Mix	1µl
Final Volume	**10µl**

Table 4.4 Preparation of cDNA Synthesis Master Mix solution. Microarray procedure detailed in Section 4.3.2.1

Amplification Master Mix (per reaction):

2.5X RNA Polymerase Buffer	16µl
Biotinylated-UTP, 10mM	2µl
RNA Polymerase Enzyme	2µl
Final Volume	**20µl**

Table 4.5 Preparation of Amplification Master Mix solution. Microarray procedure detailed in Section 4.3.2.1

4.2.2.2 QUANTITATIVE PCR

Genomic DNA Elimination Reaction Mix (per reaction):

7X gDNA Wipeout Buffer	2µl
Template RNA	Variable (up to 1µg)
RNase-free Water	Variable
Final Volume	**14µl**

Table 4.6 Preparation of Genomic DNA Elimaination Mix solution. qPCR procedure detailed in Section 4.3.6.1

Reverse Transcription (RT) Reaction Mix (per reaction):

Quantiscript Reverse Transcriptase	1μl
5X Quantiscript RT Buffer	4μl
RT Primer Mix	1μl
Entire genomic DNA elimination reaction	14μl
Final Volume	**20μl**

Table 4.7 Preparation of Reverse Transcription Reaction Mix solution.
qPCR procedure detailed in Section 4.3.6.1

Ligation Reaction Mix (per reaction):

StataClone™ Cloning Buffer	3μl
PCR Product or Control Insert	2μl
StataClone™ Vector Mix	1μl
Final Volume	**6μl**

Table 4.8 Preparation of Ligation Reaction Mix solution. qPCR procedure
detailed in Section 4.3.6.2

SYBR Green PCR Mix (per reaction):

Plasmid DNA	1μl
2X SYBR Green PCR Master Mix	12.5μl
QuantiTect Primer Assay	2.5μl
PCR Grade Water	9μl
Final Volume	**25μl**

Table 4.9 Preparation of SYBR Green PCR Mix solution. qPCR procedure
detailed in Section 4.3.6.1

4.3 METHODS

4.3.1 RNA EXTRACTION AND PREPARATION

4.3.1.1 RNA ISOLATION USING QIAZOL PROTOCOL

RNA from ETM was isolated using QIAzol (Qiagen) as outlined in the QIAzol Lysis Reagent Handbook (Qiagen, 2). This is a single step, liquid phase separation procedure, which allows the simultaneous extraction of RNA, DNA and protein. The technique is based on an extraction outlined by Chomczynski and Sacchi (1987) and works well on large or small amounts of starting material.

Briefly, the cells were harvested then lysed in QIAzol, the sample was homogenised by passing the lysate (several times) through a 20-gauge needle fitted to a syringe, followed by centrifugation (>8,000 x g, two minutes) in a QIAshredder column resulting in a mono-phase solution of guanidine thiocyanate and phenol. All insoluble material and high molecular weight DNA was removed by centrifugation (12,000 x g). After the addition of chloroform, the solution was mixed thoroughly and then centrifuged (12,000 x g). This resulted in the separation of the solution into three layers, a red organic phase (protein), an interphase (DNA) and colourless upper aqueous phase (RNA). The aqueous layer was carefully removed and an equal volume of isopropanol added. After centrifugation (12,000 x g) the RNA precipitate formed a pellet. The pellet was washed in 70% ethanol, and then reformed by centrifugation (7,500 x g). The pellet was air dried to remove all residual ethanol before being resuspended in RNase/DNase-free water (20μl).

4.3.1.2 QUANTIFYING THE RNA ISOLATE

The purity and yield of all RNA samples were assessed using the Ultraspec 2100pro (Amersham). Purity was established by measuring the 260:280nm absorption ratio. A ratio of 2.0 was indicative of a very pure RNA sample (Ultraspec 2100 RNA/DNA Calculator User Manual). However, a ratio of over

1.8 was considered acceptable for subsequent gene analysis. Lower ratios can indicate contamination in the sample. The yield of the sample was calculated from the absorbance of the sample at a wavelength of 260nm.

4.3.1.3 CHECKING INTEGRITY OF RNA: RUNNING AN AGAROSE GEL

A sample of the RNA was run on a 1% agarose gel (0.5g in 50ml 1x TBE with 3μl of 10mg/ml ethidium bromide). Each well was loaded with 500ng RNA, 2μl loading dye, and made up to a total of 10μl in high purity RNase/DNase free water. The gel was electrophoresed (approximately 40 minutes, 90 volts) and viewed under UV using the UVP Gel doc System.

4.3.2 MICROARRAYS

4.3.2.1 PREPARATION OF BIOTIN LABELLED CDNA PROBE

Isolated RNA (500ng) was mixed with Truelabeling primer (1μl). The annealing mix stock (Table 4.3) and RNA were incubated at 70°C for 10mins. The solution was then cooled and cDNA synthesis master mix (Table 4.4) was added to the annealing mix and incubated at 42°C for 50mins followed by 75°C for 5mins then allowed to cool to 37°C. The amplification mix (Table 4.5) was added to the cDNA synthesis master mix and incubated at 37°C overnight.

The reaction mixture contained a large excess of unincorporated nucleotide that would interfere with the calculation of the yield of labelled cRNA product required for the array hybridisation. The Superarray cRNA clean up kit was used for purification. The kit incorporated small scale chromatography and centrifugation to give a quick and reproducible separation of the probe from contaminants. The probe was eluted in 10mM Tris Buffer pH 8.0 and stored on ice prior to quantification of the purified probe (described in Section 4.3.1.2). Each array required 2μg of probe for the hybridisation step to produce a strong signal for chemiluminescent imaging.

4.3.2.2 HYBRIDISATION OF THE PROBE TO THE ARRAY

The microarray membranes were moistened and placed in the supplied hybridisation tube containing 5ml of deionised water. After 5 minutes the water was discarded and replaced with 2ml of pre-warmed (60°C) GEAhyb hybridisation solution. These hybridisation tubes were then placed within standard hybridisation cylinders and placed within the hybridisation oven at 60°C for 60mins at a slow agitation (5rpm).

Target hybridisation mix was prepared by adding 2µg of the biotin-labelled cRNA to 0.75ml GEAhyb hybridisation solution. The pre-hybridisation solution from the hybridisation tube was discarded and was replaced by the target hybridisation mix. This target was hybridised overnight at 60°C with slow agitation (5rpm).

Wash solution 1 and 2 we prepared as described in Section 4.2.2.1, the target was removed from the hybridisation tube and replaced with 5ml wash solution 1. The hybridisation was placed back in the hybridisation oven with a faster agitation (20rpm) for 15mins. This first wash was discarded and replaced with 5ml of wash solution 2 (high stringency) and placed back in the hybridisation oven for 15mins at fast agitation (20rpm). After the allotted time the wash solution was removed and the membrane was allowed to cool to room temperature.

4.3.2.3 CHEMILUMINESCENT DETECTION

All of the following detection steps were carried out at room temperature. The first step of detection was to block the array this was carried out by adding 2ml of GEAblocking solution Q to the hybridisation tube and incubated for 40mins. The blocking solution was discarded; the next step was to bind with alkaline phosphatase-conjugated streptavidin (AP-SA) by adding 2ml AP-SA buffer and incubating for 10mins with gentle agitation (5rpm). The AP-SA buffer was then discarded and the membrane was washed several times with buffer F and buffer G (supplied with array). Finally 1ml of CDP-Star

chemiluminescent substrate was added to the hybridisation tube and incubated for 5mins with gentle agitation (5rpm). Using forceps the membrane was removed and placed into a zip-lock bag prior to imaging.

4.3.2.4 CHEMILUMINESCENT IMAGING

The chemiluminescence was detected using an UVP Biospectrum imaging system. This system incorporated a high resolution Hama 12 bit CCD cooled camera and Visionworks LS software. Images were detected using dynamic integration set to take 20 images over a 20min period maximum sensitivity (1x1). The image was then selected on the parameters of maximum number of spots detected without bleeding/overexposure.

4.3.3 EXPRESSION ANALYSIS OF EXPOSED ETM

Each insert was apically treated/exposed with 100µl warm TSC solution. The dose for each TSC was determined from previous studies (Chapter 2). The doses were as follows: Nicotine: 30mM; Cadmium (cadmium chloride): 0.1mM; Urethane: 70mM; Formaldehyde: 1.2mM. Each dose was replicated (n=5). After 24 hours the toxin (TSC) was removed from the surface and the tissue was stored in RNAlater (Qiagen, UK) prior to RNA isolation (Section 4.3.1.1).

4.3.4 DATA NORMALISATION AND STATISTICAL ANALYSIS

The data obtained from control (PBS), nicotine, FA, urethane and cadmium exposed ETM's were generated using the GEArray Expression Analysis software. The data comprised the intensity of the spot, the background intensity of the membrane and an adjusted intensity that was taken to be a quantitative measure of gene expression (i.e. spot intensity minus background intensity). In order to compare hybridisation signal intensities across the membranes normalised signal intensity for each spot was obtained. Normalisation can be defined as the process of removing certain systematic

biases from microarray data; including corrections for differences in overall array intensity i.e. background noise.

Preliminary statistical analysis using an Anderson Darling test for normality ($p>0.05$) on 30 genes (11%) confirmed the raw array data was normally distributed. Following this step global normalisation between membranes was carried out which involved dividing the spot intensity of each gene by the median spot intensity of the whole array to correct for variations between arrays. As the mean value can be distorted by the effects of a few extreme outliers, the median value was considered the most accurate basis for normalisation, thus reducing the possibility of data variance due to anomalous data points (Balharry *et al.*, 2005). As a final assessment, the data was analysed using SAM (Significance Analysis of Microarrays; Stanford University) analysis. SAM correlates gene expression data to a wide variety of parameters and uses data permutations to provide an estimate of false discovery rates for multiple testing. Changes in gene expression were expressed as a ratio (fold-change). The lower cut off point for identifying relevant genes was set at a ratio of 1.5 (deVos *et al.*, 2003; Treadwell and Singh 2004).

The significance of differentially expressed genes could only result when statistical analyses were applied. The appropriate statistical analysis in this instance was a 2 class unpaired t-test. The two-tailed student's t-test is a test used to examine a difference between mean values of two groups of data. A null hypothesis of no expression-level difference in individual genes between control and nicotine, FA, urethane, cadmium ETM exposure was adopted. The resultant statistical value could then be used to determine which genes were significantly differentially expressed. A p value of ≤ 0.05 was deemed significant. Genes were grouped and annotated according to the functional classification allocated by GEArray Expression Analysis software.

4.3.5 FUNCTIONAL GROUPING

Each of the genes present on the array could be categorised under functional group headings. These groups are listed in Table 4.10. The purpose of looking at the functional groups was to assess whether genes were contributing to the same type of responses.

GEArray® Human Toxicology & Drug Resistance Microarray
Apoptosis
Cell Cycle
Cell growth, Proliferation and Differentiation
Transporters
Response to Stress
Chaperones and Heat Shock Proteins
Transcription Factors and Regulators
Drug Metabolising Enzymes

Table 4.10 The main functional gene classes. The Oligo GEArray® Human Toxicology & Drug Resistance Microarray has eight classes of genes

4.3.6 QUANTITATIVE PCR TO VALIDATE TRANSCRIPTIONAL CHANGES

PCR amplifies DNA exponentially, doubling the number of molecules present with each amplification cycle. The number of amplification cycles and the amount of PCR end-product enables calculation of the initial quantity of genetic material, but numerous factors complicate this calculation.

The ethidium bromide staining typically used to assess a successful PCR prevents further amplification, and is only semi-quantitative. The polymerase chain reaction may not be exponential for the first several cycles, and furthermore, plateaus eventually, so care must be taken to measure the final amount of DNA while the reaction remains in the exponential growth phase. To overcome these difficulties, several different quantitative methods have

been developed. The most sensitive quantification methods are achieved by real-time polymerase chain reaction (qPCR; Figure 4.2), where the amount of DNA is measured after each cycle of PCR by use of fluorescent dyes (SYBR Green; QuantiTect primer assay handbook, Qiagen).

A standard curve was constructed from the starting concentration of cDNA target (1ηg – 1fg) plotted against their CT value, the fractional PCR cycle at which the fluorescent signal significantly rises above the background signal (Figure 4.1). This technique was carried out on ten genes selected by methods outlined in Section 4.3.2.
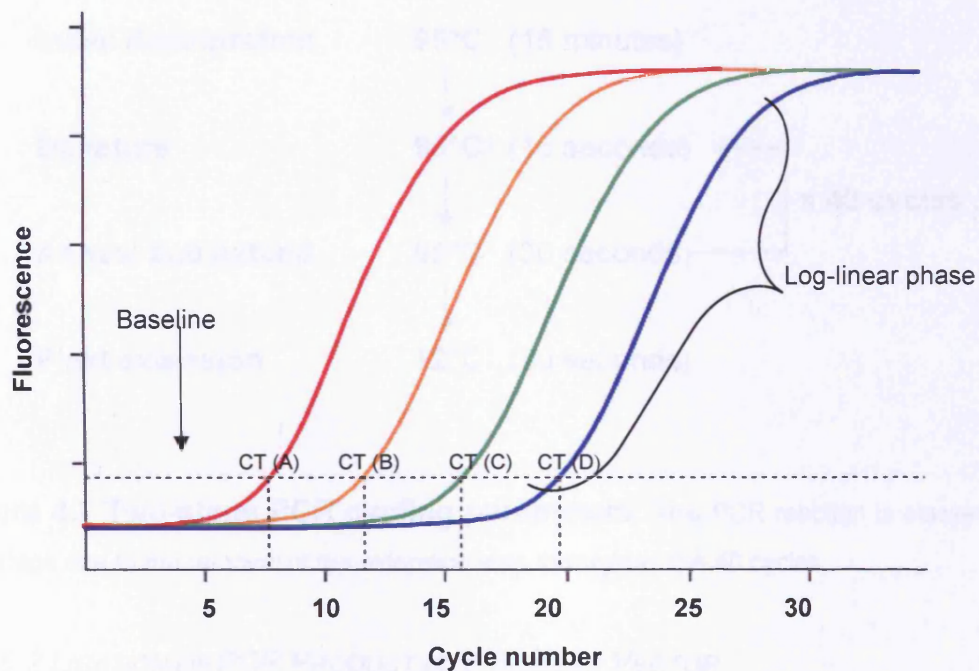
Figure 4.1 Example of data for real-time RT-PCR. Shows an exponential increase in the amount of cDNA present in each sample with sample A having the greatest amount of cDNA target (1ng) and sample D the least amount of cDNA target (1pg)

4.3.6.1 RT-PCR

The samples previously used in the array procedure were used to synthesise cDNA by a reverse transcription reaction. Purified RNA (500ηg) was briefly

incubated in gDNA Wipeout buffer at 42°C for 2 minutes to effectively remove genomic DNA (Table 4.6). The complete genomic DNA elimination reaction was then placed on ice for 10 minutes; it was then added to the reverse transcription reaction (Table 4.7) and incubated at 42°C for 30 minutes. The reaction was terminated by heat inactivating the reverse transcription reaction at 95°C for 3 minutes. Next, a 25µl SYBR Green PCR reaction (Table 4.9) was carried out as detailed in the QuantiTect primer assay handbook (Qiagen, 2007). This involved a two-stage PCR reaction (Figure 4.2). The PCR product was loaded on to a 2% NuSieve™ agarose gel, the product was extracted by excising the resultant band and heating the excised band at 65°C for 2 minutes.

Initial denaturation   **95°C** (15 minutes)

Denature   **95°C** (15 seconds)

                                                              x 40 cycles

Anneal and extend   **55°C** (30 seconds)

Final extension   **72°C** (30 seconds)
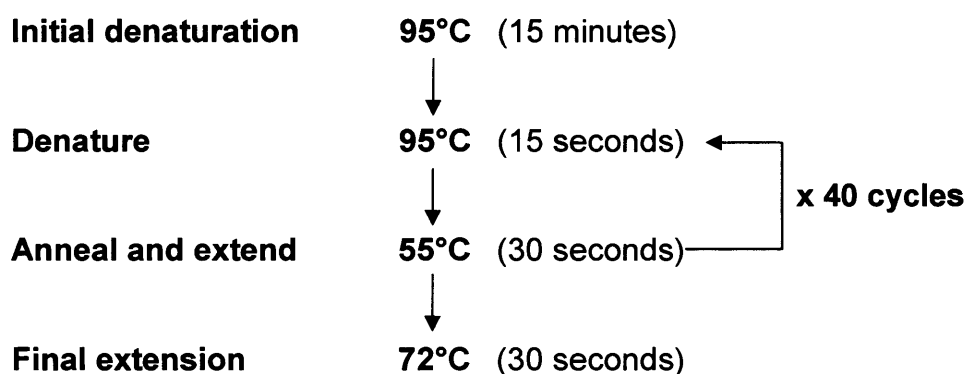
Figure 4.2 Two-stage PCR cycling parameters. This PCR reaction is classed as two-stage due to the removal of the extension step throughout the 40 cycles

4.3.6.2 LIGATION OF PCR PRODUCT INTO PLASMID VECTOR

Purified PCR product was ligated into a StrataClone PCR cloning vector (pSC-A) using the StrataClone PCR cloning kit. This method is detailed in the StrataClone PCR cloning kit manual (Stratagene, 2007). In brief the ligation reaction mix was prepared as detailed in Table 4.8 and incubated at room temperature for 5 minutes.

4.3.6.3 TRANSFORMATION INTO E.COLI

A tube containing StrataClone SoloPack competent cells was thawed on ice for each ligation reaction and 1μl of the ligation prepared in section 4.3.6.2 was added to the competent cells. The transformation mixture was then placed on ice for 20 minutes. The reactions were then heated shocked at 42°C for 45 seconds and then returned to ice for a further 2 minutes. Pre-warmed SOC medium (250μl) was added and then placed at 37°C with gentle agitation to allow the cells to recover for 1 hour. The transformed *E.coli* (100μl) was plated on pre-prepared LB/ampicillin/X-gal agar plates. The plates were then cultured overnight at 37°C.

4.3.6.4 SCREENING TRANSFORMANTS FOR INSERTS

Successful cloning of an insert into the pSC-A vector interrupts the coding sequence of β-galactosidase. This results in a colour change between clones which contain PCR product, and those that do not. Recombinant clones can therefore be identified by a white colouring, compared to uncloned vectors which remain blue.

Luria broth (LB; 10ml) containing 1mg/ml ampicillin was inoculated with a white colony, and incubated overnight at 37°C. The culture containing the recombinant clones was plated onto LB agar/ampicillin plates and sent for sequencing whilst the remainder was stored as a 20% glycerol stock.

4.3.6.5 PLASMID DNA PURIFICATION

Purification of plasmid DNA from the bacterial cells was undertaken using the Wizard *Plus* SV Miniprep DNA Purification System. LB containing the recombinant *E.coli* (1.5ml) was centrifuged (10000 x *g*) for 5 minutes. The resulting pellet was resuspended in 250μl resuspension buffer and vortexed. Cell lysis solution (250μl) was added and mixed by inverting. The sample was incubated at room temperature until the cell suspension had cleared

(maximum of 5 minutes). Alkaline protease solution (10µl) was added and mixed by inverting, then incubated at room temperature for 5 minutes. After incubation, 350µl neutralisation solution was added and immediately mixed by inversion. The sample was then centrifuged at maximum speed for 10 minutes, and the cleared lysate decanted into a prepared spin column. This was centrifuged at maximum speed for 1 minute. The columns were then washed with 750µl column wash solution and centrifuged for a further 1 minute. A final wash was carried out by adding 250µl column wash solution to the column and centrifuging for 2 minutes. To elute the plasmid, 50µl nuclease-free water was added to the column, and centrifuged for one minute. The concentration of DNA in the resultant eluant was measured using a Ultraspec 2100pro (Amersham).

4.3.6.6 SERIAL DILUTIONS OF STANDARDS

When the sequence of the insert was confirmed, standards were created for each gene. The Ultraspec measurement of the eluted DNA (Section 4.3.6.5) was used to calculate the dilution factor necessary to obtain a concentration of 1ng/µl. Serial dilutions were then carried out to obtain a series of standards ranging from 10fg/µl to 100pg/µl.

4.3.6.7 QUANTITATIVE PCR OF EXPERIMENTAL GENES

RNA was isolated from the exposed and control ETM (Section 4.3.1.1), and cDNA was synthesised from this, by a reverse transcription reaction (Section 4.3.6.1). Samples and standards were prepared for qPCR using the QuantiTect SYBR Green PCR Kit (Table 4.9). Each sample and standard was loaded in triplicate (25µl per well) into a Thermofast 96 well PCR detection plate. The plate was analysed on an MJ Research Opticon (BioRad, Hercules, CA).

4.4 RESULTS

4.4.1 RNA PURITY AND INTEGRITY

The integrity and yield of the RNA from control and exposed ETM (n=5) [Table 4.11] indicated that each sample was within the desired ratio with a sufficiently high yield. Isolated RNA was loaded and run on an agarose gel (1%) and viewed under UV (Biospectrum imaging system) to confirm RNA integrity and genomic contamination (Figure 4.3). There was very little or no genomic contamination, with the observed bands free from smears (which is an indication of RNA degradation).

Figure 4.3 Typical agarose gel depicting RNA integrity.

4.4.2 MICROARRAY ANALYSIS

Microarray data from the exposed cell cultures was analysed to show differential gene expression for the different TSC (Table 4.12; Figure 4.8). When comparing gene expression in cadmium, formaldehyde and urethane to PBS, 18 genes were up-regulated by >3-fold. Some of the largest changes, as shown in Table 4.12, were responses to DNA damage stimulus (CHEK2), cell stress (CTPS), chemokines (CXCL10), oxidoreductases (CYP20A1, PTGS). Nine genes with the largest change were seen in genes involved in cell cycle (CCND1).

Exposure of ETM	Absorbance (260nm)	RNA concentration (ng/ul)	Ratio A_{260}/A_{280}
Nicotine[a]	0.234	562	1.7
Nicotine[b]	0.454	1090	1.5
Nicotine[c]	0.377	905	1.8
Nicotine[d]	0.469	1126	2.0
Nicotine[e]	0.350	840	1.8
Cadmium[a]	0.223	535	1.7
Cadmium[b]	0.337	809	1.8
Cadmium[c]	0.144	346	1.8
Cadmium[d]	0.707	1682	1.5
Cadmium[e]	0.683	1639	2.0
Urethane[a]	0.347	833	1.9
Urethane[b]	0.322	773	1.9
Urethane[c]	0.432	1037	1.9
Urethane[d]	0.141	338	1.6
Urethane[e]	0.250	600	1.6
Formaldehyde[a]	0.352	845	1.9
Formaldehyde[b]	0.347	833	1.9
Formaldehyde[c]	0.321	770	1.8
Formaldehyde[d]	0.261	626	1.8
Formaldehyde[e]	0.166	398	1.9
Control[a]	0.500	1200	1.9
Control[b]	0.344	826	1.9
Control[c]	0.323	775	1.9
Control[d]	0.287	689	1.8
Control[e]	0.375	900	1.9

Table 4.11 Concentrations and ratios of RNA. (n=5) isolated from control and exposed ETM

In contrast, when comparing the gene expression of nicotine to PBS fewer changes in mRNA expression were induced with 5 genes being up-regulated by >1.5-fold with the largest change observed in sulfotransferases (SULT2A1). Eleven genes were down regulated by >1.5-fold with the greatest change observed in oxidoreductases (CYP7A1) and transporters (TPMT).

Further analysis placed the genes of interest into functional groups (annotated by SuperArray): drug metabolism; transcription factors & regulators, stress response; cell growth/proliferation & differentiation; and transporters. These groups were common for all compounds. Nicotine also contained the functional group DNA repair (Figure 4.4), and cadmium, urethane and formaldehyde had genes in the apoptosis and cell cycle functional grouping (Figure 4.5, 4.6 and 4.7).

Another technique was used for graphical representation of gene expression data in response to cadmium, FA, nicotine and urethane exposure of the ETM (Table 4.13). The data were plotted on a graph with the gene names along the x-axis and fold-change from the control on the y-axis to determine gene homology and expression trends.
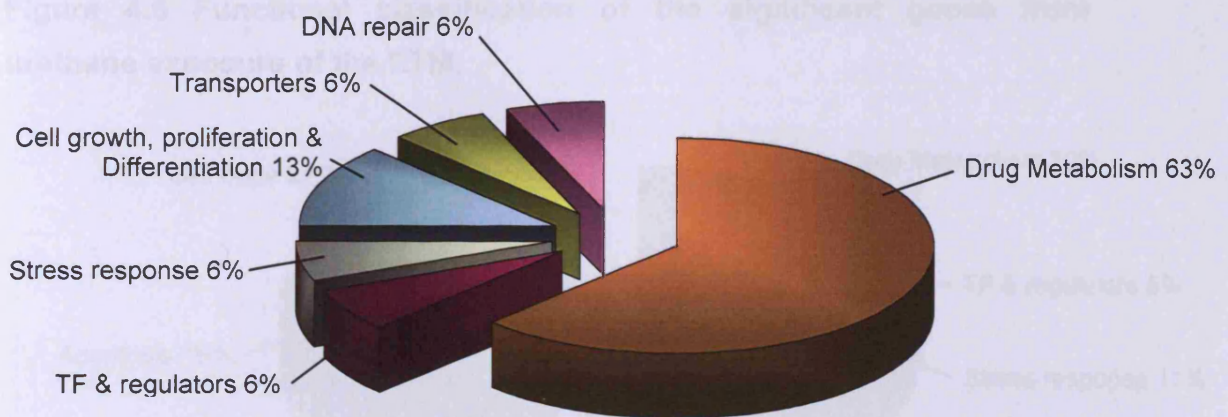
Figure 4.4 Functional classification of the significant genes from nicotine exposure of the ETM. The functional group of DNA repairs genes was unique to nicotine

Cell cycle 19%
Drug Metabolism 23%
Apoptosis 5%
TF & regulators 5%
Transporters 10%
Stress response 14%
Cell growth, proliferation &
Differentiation 24%
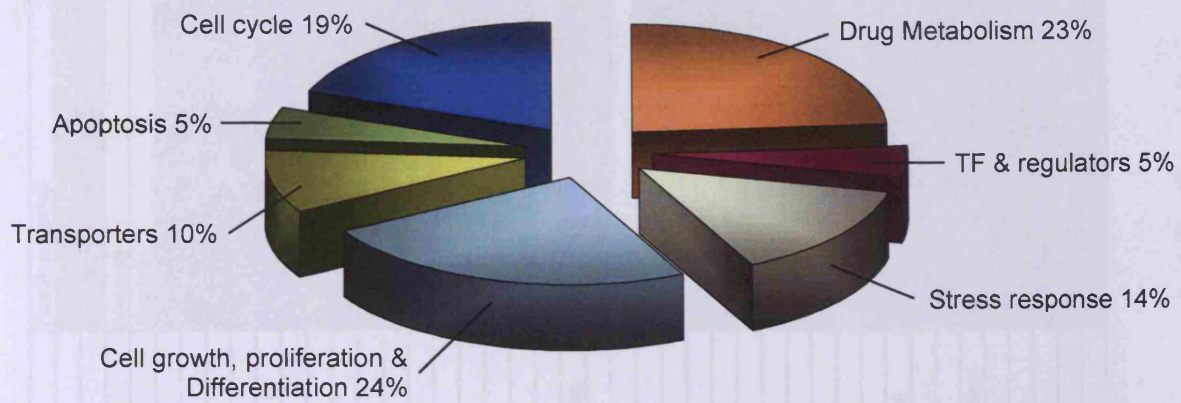
Figure 4.5 Functional classification of the significant genes from cadmium exposure of the ETM.

Cell cycle 13%
Drug Metabolism 18%
Apoptosis 13%
TF & regulators 6%
Transporters 13%
Stress response 13%
Cell growth, proliferation &
Differentiation 24%
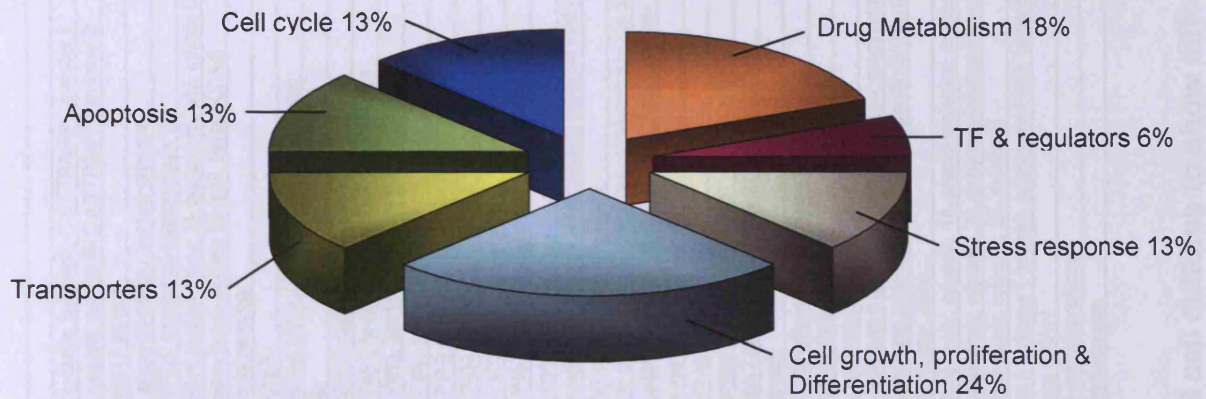
Figure 4.6 Functional classification of the significant genes from urethane exposure of the ETM.

Cell cycle 21%
Drug Metabolism 20%
Apoptosis 16%
TF & regulators 5%
Transporters 11%
Stress response 11%
Cell growth, proliferation &
Differentiation 16%
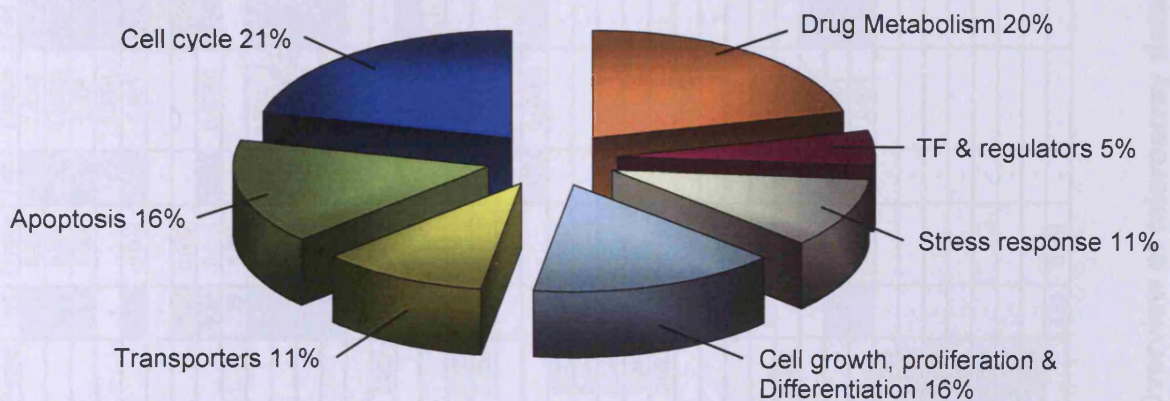
Figure 4.7 Functional classification of the significant genes from formaldehyde exposure of the ETM.

Gene ID	Nicotine		Cadmium		Urethane		Formaldehyde		Gene name	Functional group
	Fold	P-value	Fold	P-value	Fold	P-value	Fold	P-value		
ABCC1	-		5.31	0.010	4.44	0.0002	3.90	0.001	ATP-binding cassette, sub-family C (CFTR/MRP), member 1	Transporters
ABCC2	-		8.37	0.001	7.63	0.00001	6.60	0.000004	ATP-binding cassette, sub-family C (CFTR/MRP), member 2	Transporters
BAX	-		-3.29	0.008	-3.27	0.009	-4.30	0.006	BCL2-associated X protein	Apoptosis
CASP10	-		-		3.82	0.0001	3.80	0.00005	Caspase 10, apoptosis-related cysteine protease	Apoptosis
CCND1	-		-5.27	0.002	-3.68	0.003	-3.91	0.003	Cyclin D1 (PRAD1: parathyroid adenomatosis 1)	Cell Cycle
CDKN2A	-		-		-		-3.04	0.00002	Cyclin-dependent kinase inhibitor 2A (melanoma, p16, inhibits CDK4)	Cell Cycle
CDKN2D	-		-3.12	0.0001	-		-3.00	0.0002	Cyclin-dependent kinase inhibitor 2D (p19, inhibits CDK4)	Cell Cycle
CHEK2	-		18.66	0.015	18.23	0.00001	14.96	0.00002	CHK2 checkpoint homolog	Cell Cycle
CRYAB	-		3.29	0.002	-				Crystallin, alpha B	Cell Growth, Proliferation and Differentiation
CSF2	-		4.34	0.000004	4.18	0.000002	3.67	0.0001	Colony stimulating factor 2 (granulocyte-macrophage)	Cell Growth, Proliferation and Differentiation
CTPS	-		9.31	0.006	8.10	0.00000002	6.19	0.00000003	CTP synthase	Stress Response
CXCL10	-		23.82	0.003	18.84	0.00002	15.46	0.00002	Chemokine (C-X-C motif) ligand 10	Cell Growth, Proliferation and Differentiation
CYP1A1	-		4.21	0.008	4.31	0.00002	4.28	0.001	Cytochrome P450, family 1, subfamily A, polypeptide 1	Drug Metabolism
CYP1B1	-		3.08	0.002	-		-		Cytochrome P450, family 1, subfamily B, polypeptide 1	Drug Metabolism
CYP2E1	-1.99	0.032	-		-		-		Cytochrome P450, family 2, subfamily E, polypeptide 1	Drug Metabolism
CYP20A1	-		11.03	0.0005	9.0	0.000001	7.36	0.00004	Cytochrome P450, family 20, subfamily A, polypeptide 1	Drug Metabolism
CYP4B1	-		-		-		-3.14	0.004	Cytochrome P450, family 4, subfamily B, polypeptide 1	Drug Metabolism
CYP4F3	-2.67	0.037	-		-		-		Cytochrome P450, family 4, subfamily F, polypeptide 3	Drug Metabolism
CYP7A1	-3.73	0.006	-		-		-		Cytochrome P450, family 7, subfamily A, polypeptide 1	Drug Metabolism
E2F1	-		-		-		-4.18	0.00003	E2F transcription factor 1	Apoptosis
EGFR	-		-		-3.32	0.00003	-4.30	0.00002	Epidermal growth factor receptor (erythroblastic leukemia viral (v-erb-b) oncogene homolog)	Cell Growth, Proliferation and Differentiation
ELK1	-1.65	0.001	3.15	0.007	-		-		ELK1, member of ETS oncogene family	Transcription factors & regulators
ERCC3	-1.63	0.014	-		-		-		Excision repair cross-complementing, complementation group 3	DNA repair
HIF1A	-2.16	0.044	-		-		-		Hypoxia-inducible factor 1, alpha subunit (basic helix-loop-helix transcription factor)	Stress Response
HMOX1	-1.80	0.006	-		-		-		Heme oxygenase (decycling) 1	Drug Metabolism
HMOX2	-1.57	0.000	-		-		-		Heme oxygenase (decycling) 2	Drug Metabolism
MET	-		-4.53	0.000002	-3.17	0.000002	-		Met proto-oncogene (hepatocyte growth factor receptor)	Cell Growth, Proliferation and Differentiation
MT3	-		3.15	0.021	-		-		Metallothionein 3 (growth inhibitory factor (neurotrophic))	Cell Growth, Proliferation and Differentiation
MVP	-		3.65	0.035	-		-		Major vault protein	Stress Response
MYC	-		3.14	0.042	-		-		V-myc myelocytomatosis viral oncogene homolog	Cell Cycle
NNMT	-2.6	0.047	-		-		-		Nicotinamide N-methyltransferase	Drug Metabolism
PPARD	-		-		3.49	0.00001	3.95	0.001	Peroxisome proliferative activated receptor, delta	Transcription factors & regulators
PPARGC1A	-		6.80	0.015	5.83	0.001	6.03	0.007	Peroxisome proliferative activated receptor, gamma, coactivator 1	Stress Response
PTGS1	-		11.14	0.013	6.91	0.001	6.15	0.007	Prostaglandin-endoperoxide synthase 1 (prostaglandin G/H synthase and cyclooxygenase)	Drug Metabolism
RARA	1.79	0.023	-		-		-		Retinoic acid receptor, alpha	Cell Growth, Proliferation and Differentiation
SULT1A1	1.78	0.022	-		-		-		Sulfotransferase family, cytosolic, 1A, phenol-preferring, member 1	Drug Metabolism
SULT2A1	2.23	0.038	-		-		-		Sulfotransferase family, cytosolic, 2A, dehydroepiandrosterone (DHEA) -preferring, member 1	Drug Metabolism
SULT2B1	1.70	0.017	-		-		-		Sulfotransferase family, cytosolic, 2B, member 1	Drug Metabolism
TBXAS1	-1.74	0.005	-		-		-		Thromboxane A synthase 1 (platelet, cytochrome P450, family 5, subfamily A)	Drug Metabolism
TOP1	1.84	0.038	-		-		-		Topoisomerase (DNA) I	Cell Growth, Proliferation and Differentiation
TPMT	-2.99	0.018	-		-		-		Thiopurine S-methyltransferase	Transporters
XDH	-		3.53	0.001	-		-		Xanthine dehydrogenase	Drug Metabolism

Table 4.12 Overview of microarray data from exposed cell cultures to show differential gene expression for the various TSCs. Coloured cells highlight gene homology between different exposures
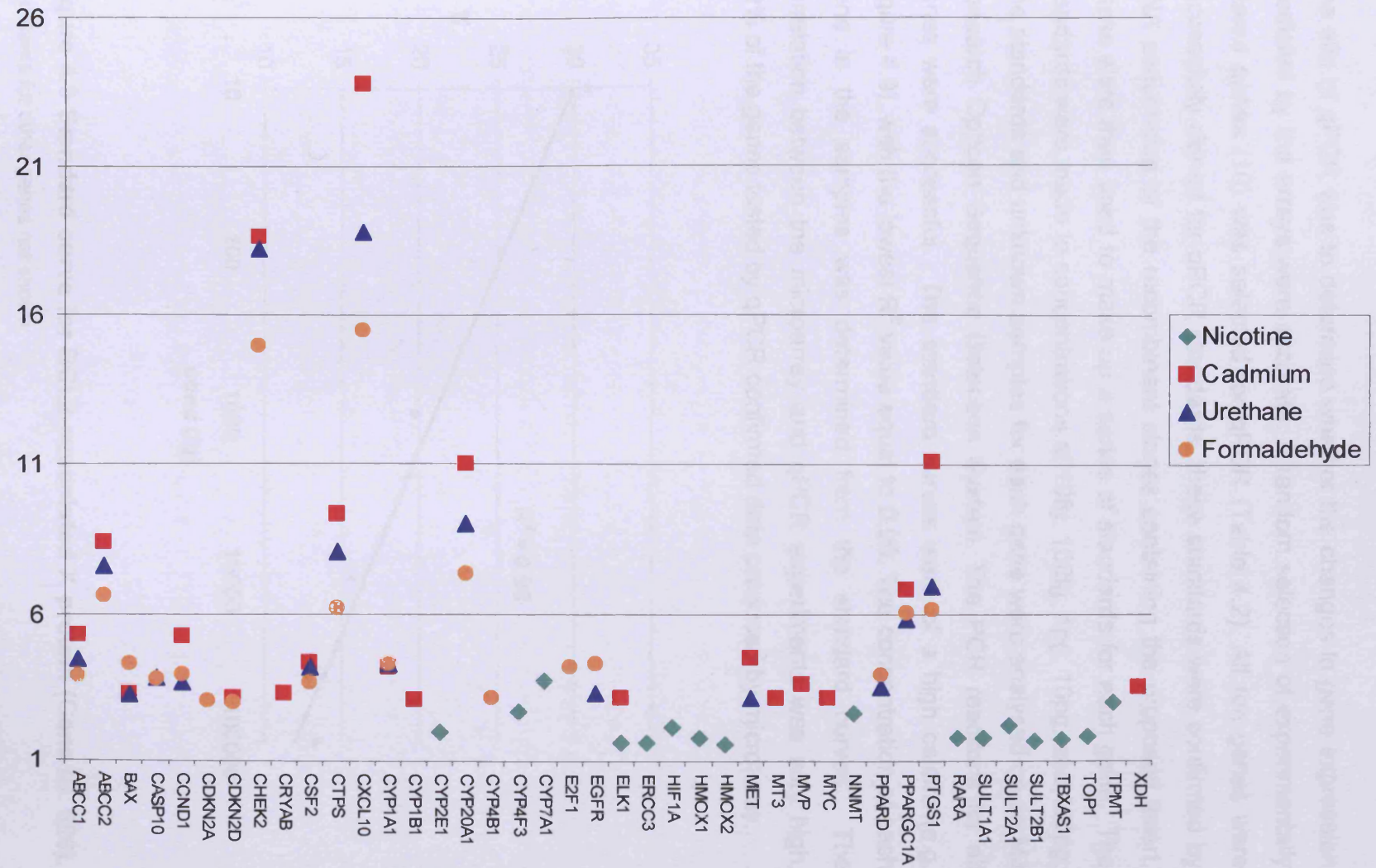
Figure 4.8 Graphical representation of differential gene expression. The comparison of fold-change between the various TSC with PBS controls permitted the determination of gene homology and expression trends

4.4.3 QUANTITATIVE PCR

The aim of qPCR was to determine whether the changes in gene expression predicted by the arrays were accurate. A random selection of experimentally altered genes (10) was selected for qPCR (Table 4.2). All ten genes were successfully cloned for qPCR standards, these standards were confirmed by DNA sequencing of the recombinant clones containing the proposed insert. These were then used to make up a series of standards for each gene. The standards were made to concentrations of 10fg, 100fg, 1pg, 10pg, and 100pg. The standards and unknown samples for each gene were analysed on an MJ Research Opticon Sequence Detection System. The PCR reactions for all genes were successful. The standard curves were of a high calibre (e.g. Figure 4.9), with the lowest R^2 value equal to 0.96. The concentration of each gene in the samples was determined from the standard curves. The correlation between the microarray and qPCR experiments was very high, 80% of the genes tested by qPCR confirmed data produced by microarray.
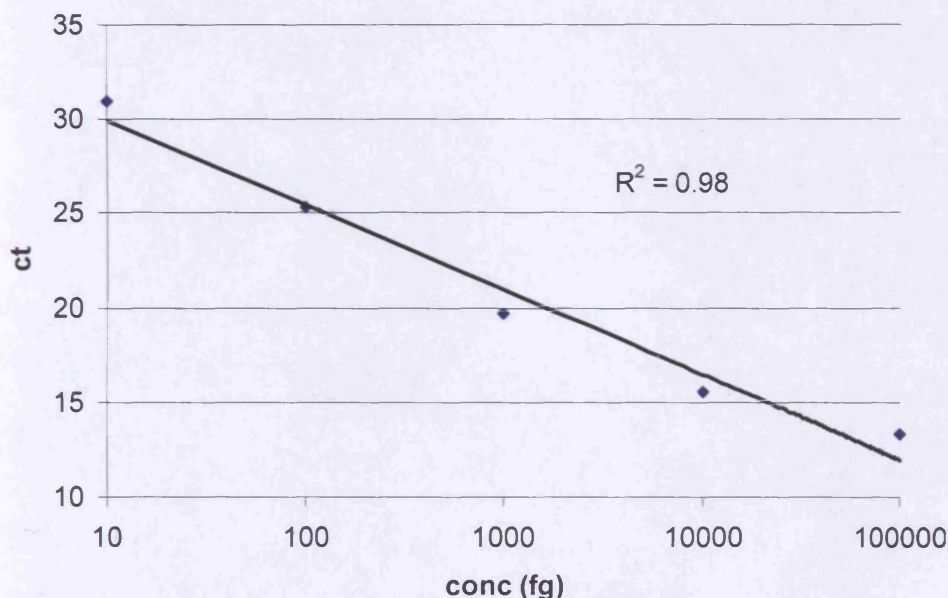
Figure 4.9 Standard curve for BCL2-associated X protein (Gene ID. 596).
Standards for other genes not shown

4.5 DISCUSSION

There are a number of lung related diseases associated with tobacco smoke (Smith *et al.*, 2006). These studies were further complicated by the number of chemicals (~4500; (Andreoli *et al.*, 2003)) used in tobacco and individual smoking habits. Therefore, an alternative approach was required to assess the biological responses and to identify any potential biomarkers of exposure and harm for specific mechanisms of injury attributed to smoking. In this component of the research investigation, a subtoxic dose of nicotine, cadmium, urethane and formaldehyde had significant effects on epithelial gene-expression.

Various methods have been used to assess changes in gene expression, such as quantitative polymerase chain reaction (qPCR), *in situ* hybridisation and Northern blotting. There are, however, problems in selecting which genes to investigate, as important links may be missed between different gene activities. Despite the rapid advances in microarray technology permitting large-scale, chip-based gene profiling, analysis of gene expression patterns by nylon based cDNA microarray remains an important technique in molecular biology (Seliger, 2007; Sexton *et al.*, 2008). The persistence of this technology is partly due to its accessibility (used on the bench-top) and cost (expensive, specialised equipment not required). Importantly, for this study, nylon arrays also have high sensitivity and are useful for experiments with low RNA abundance. Moreover, this methodology has been used successfully in previous genomic studies in our laboratory to investigate toxicant effects in the lung (Balharry *et al.*, 2005; BéruBé *et al.*, 2006; Wise *et al.*, 2006).

The effect of nicotine in the animal and cell system has been comprehensively researched (Yildiz, 2004; Hukkanen *et al.*, 2005). Nicotine has been shown to elicit a variety of physiological effects (i.e. cardiac contractility, mobilisation of blood sugars and increased free fatty acids) but for the purpose of this study only the thrombogenic and atherosclerotic mechanisms of nicotine have been documented. The majority of significantly altered genes from the nicotine

exposure study were involved in drug metabolism; an additional DNA repair gene was expressed but not present in other exposure studies. Further examination of the nicotine gene-list found five of the sixteen genes are involved in atherosclerosis. These could be separated further into anti-atherosclerosis and pro-atherosclerosis.

The anti-atherosclerosis genes *CYP2E1*, *ELK1* and *HIF1A* have different mechanisms of action. The down-regulation of *CYP2E1* would reduce reactive oxygen species (ROS), stabilising the initiation of inflammation (Parke and Sapota, 1996). Decreased expression of *ELK1* in smooth muscle cells leads to an increase in the expression of proteins required for the differentiated function of these cells. Several disease states have been associated with a decrease in these muscle cell proteins e.g. atherosclerosis and asthma (Berger *et al.*, 2002; Zhou *et al.*, 2005). Down regulation of *HIF1A* inhibits foam cell formation, and hence, atherosclerosis (Jiang *et al.*, 2007).

The pro-atherosclerosis genes were *CYP7A1* and *HMOX1*. *CYP7A1* encodes for a protein with a rate-limiting enzyme activity for bile acid synthesis (Cohen *et al.*, 1992). Down regulation of *CYP7A1* would result in a decrease of cholesterol absorption and would be classed as hypercholesterolemic, with a significant increase in the low density lipoprotein fraction (Pullinger *et al.*, 2002; Erickson *et al.*, 2003); likely to result in an individual susceptibility to the development of atherosclerosis (Erickson *et al.*, 2003). *HMOX1* is a cytoprotective gene that reacts to oxidative stress. Induced expression of *HMOX1* is one of the major defence mechanisms against oxidative stress (Brydun *et al.*, 2007). This may indicate that reduced *HMOX1* may be involved in the mechanism of atherosclerosis due to the over-production of ROS and increased inflammatory responses (Griendling and FitzGerald, 2003).

There are many biological effects exerted by cadmium on membranes, mitochondrial structure and function, DNA and gene expression (Pinot *et al.*, 2000). Oxidative stress is initiated by cadmium in many cell types; determined by decreased activity of antioxidants (Manca *et al.*, 1994; Yang *et al.*, 1997). The genes significantly altered by cadmium exposure were investigated for

potential associations to cytotoxicity. Nine of a possible twenty genes were found to have cytotoxic associations; which could be further separated into pro- and anti-cytotoxic.

An anti-cytotoxic (i.e. a protective) mechanism was observed with *ABCC1* and *ABCC2*; elevated levels of these genes in tumour cells leads to resistance to cytotoxic drugs (O'Connor, 2007). Another anti-cytotoxic mechanistic gene was *BAX*, down-regulation of which would inhibit the initiation of mitochondrial dysfunction (Wei *et al.*, 2001). Mitochondrial dysfunction could lead to the release of cytochrome *c* and which activation of DNA damage initiated apoptotic pathways (Shiu *et al.*, 2007). The xenobiotic-metabolizing enzymes play a crucial role in the detoxification processes and bioactivation of several xenobiotic compounds (Lieber, 1997). *CYP1A1* was elevated in this study, suggesting a cytoprotective role. Metallothioneins play a vital role in defending cells against heavy metals and oxidative stress (Kagi and Schaffer, 1988). In this study *MT3* was elevated by 3-fold, similar to the results of a previous study with *MT2A* and cadmium exposure to lens epithelial cells, This resulted in a 20% protection against cadmium-induced oxidative stress (Hawse *et al.*, 2006). *MVP* is also known as a lung-resistance protein (Scheffer *et al.*, 1995), has a proposed role in drug resistance (Kowalski *et al.*, 2007), and an up regulation may suggest a protective role.

Pro-cytotoxic genes, such as *CCND1* is consistently inhibited in chemotherapy drug tests, when investigating development of resistance (Hernandez-Vargas *et al.*, 2007). *MET* is also known as human growth factor receptor, protects cells from apoptosis (Kakazu *et al.*, 2004), but in this study was down-regulated; indicating a decrease in protection against apoptosis. *XDH* is associated with the reductive activation of chemotherapeutic agents and elevation of this gene observed in this study could lead to a greater rate of formation of oxygen radicals and significantly increased cytotoxicity (Yee and Pritsos, 1997).

Extensive research has been prompted into the potential biological effects of urethane given its tumourigenesis in humans (Ritchie *et al.*, 2007;

Strathopoulos *et al.*, 2007). The principle targets/sites are the liver and lung (Siemiatycki *et al.*, 2004) in animals, which has prompted extensive research into its mechanisms of action. The genes significantly altered by urethane exposure were investigated for potential associations to carcinogenicity. The urethane exposure study found ten of a possible sixteen significantly altered genes associated with carcinogenicity. Further analysis differentiated genes into pro- and anti-carcinogenicity.

Anti-carcinogenicity genes comprised of 90% of the significantly altered genes was demonstrated by *BAX*, also known as *BCL2*-associated X protein which suppresses DNA repair (Jin *et al.*, 2006). In this investigation it was to be found the gene down-regulated, increasing genetic stability and inhibiting DNA damage. Inhibition of *CASP10* is associated with the pathogenesis of trophoblast tumourigenesis (Fong *et al.*, 2006), but in this study it was found at elevated levels, demonstrating anti-carcinogenicity. The *CCND1* gene is elevated in human breast cancers (Wang *et al.*, 2003), and yet it was observed to be inhibited. *CHEK2* has been reported as an important signal transducer of cellular responses to DNA damage and a candidate tumour marker (Nevanlinna and Bartek, 2006). Significantly elevated levels of this gene would suggest increased anti-carcinogenicity. As observed in this study, elevated expression of *CXCL10* has been to shown to limit the cancerous process (Palmer *et al.*, 2001; Ben-Baruch, 2006). Also associations between increased *EGFR* and pulmonary adenocarcinomas have been reported (Nakamura *et al.*, 2007). Down-regulation of this gene was observed, which could indicate an anti-carcinogenicity mechanistic action. This down-regulation was also observed with *MET* (also known as *HGFR*), with similar consequences of an anti-carcinogenicity mechanistic role (Shia *et al.*, 2005).

There were only two pro-carcinogenicity genes significantly altered in this investigation, *CYP1A1* and *PPARD*. *PPARD* is a nuclear receptor implicated in tumourigenesis by the activation *PTGS2*; a rate limiting enzyme for prostaglandin synthesis and tumour growth (Xu *et al.*, 2006). Pro-carcinogens are substrates for *CYP1A1*, and up-regulation was observed in this study, and as such, thought to be associated to pro-carcinogenicity (Nebert and Dalton,

2006). The low number of pro-carcinogenicity genes could be due to the bioavailability of the TSC or possible lack of activation of specific metabolic mechanisms (Balharry *et al.*, 2008).

Formaldehyde is mutagenic and genotoxic (de Serres and Brockman, 1999). The mutagenic and genotoxic potential of formaldehyde is consistent with its ability to form cross-linkages between protein and single-stranded DNA (Merk and Speit, 1998). The genes significantly altered by formaldehyde exposure were investigated for potential associations to mutagenicity. The formaldehyde exposure study found six of a possible nineteen significantly altered genes associated with mutagenicity. Further analysis differentiated genes into pro- and anti-mutagenicity.

As mentioned previously, *BAX* suppresses DNA repair (Jin *et al.*, 2006), and in this work, this gene down-regulated increased genetic stability and inhibited DNA damage. Investigation of the cell cycle regulatory protein *CCND1* suggested that it was found at elevated levels in tumour progression. The down-regulation of this gene inferred an anti-mutagenic role. *CYP4B1* activates amines that can be carcinogenic (Imaoka *et al.*, 2001), and any down-regulation of this gene would be indicative of an inhibited activation of amine activity. Elevated *E2F1* has been associated with increased sensitivity to apoptosis (Roos *et al.*, 2007) and down-regulation of this gene may have an anti-mutagenic role.

Two genes of significant change have been associated with pro-mutagenicity (*CDKN2A* and *CYP1A1*). Inhibition of *CDKN2A* has been linked to specific activities that allow cells to evade differentiation processes; properties linked to malignancy (Berman *et al.*, 2005). In comparison to literature searches on carcinogenicity of urethane, *CYP1A1* has been associated with the mediation of ROS, which in turn creates an environment favourable to DNA damage (Hansen *et al.*, 2007).

One specific gene (*PTGS1*) was not associated to the literature searches but was significantly induced in three out of the four compounds. *PTGS1* is

thought to be responsible for the production of prostaglandins that are responsible for a host of physiological responses (e.g. inflammation and platelet aggregation; Park *et al.*, 2006).

This study identified nine genes; *CCND1*, *CDKN2A*, *CYP7A1*, *CYP1A1*, *HMOX1*, *MET*, *PPARD*, *PTGS1* and *XDH* that could be linked directly to the specific mechanisms of toxicity identified in this study (i.e. carcinogenic, cytotoxic, mutagenic and thrombogenic). These genes all have potential to act as genomic biomarkers for the onset and development of many respiratory diseases. Of these nine potential genomic biomarkers, three were of particular interests (*CYP7A1*, *HMOX1* and *PTGS1*). Two genes were unique to a specific disease pathway, whilst the third was very highly up-regulated across three of the compounds. These genes have also been used previously in clinical research studies. *CYP7A1* has been documented as an adult liver cell marker (Cai *et al.*, 2007). *HMOX1*, the enzyme responsible for the synthesis of CO, is suppressed in lymphocytic bronchitis and airway luminal occlusion after transplantation (Minamoto *et al.*, 2005). Inhibited *PTGS1* (also known as *COX1*) has been known to increase side-effects of nonsteroidal anti-inflammatory drugs (NSAIDs). Limited inhibition of *COX1* increases the drug tolerability (Asero, 2007). This may support *COX1* as a vital player in future drug development.

4.6 CONCLUSION

The microarray analysis has provided transcriptional data on the exposure of the ETM to TSC. The technique has been shown to be highly-reproducible between replicates, confirmed by qPCR. This study has identified nine genes with the potential as genomic biomarkers of specific disease mechanisms associated with tobacco smoke. Another potential genomic biomarker has been identified which has not previously been related to tobacco smoke; *PTGS1*, the key enzyme in prostaglandin biosynthesis. This could result in a disruption of tissue homeostasis and the onset of disease. It represents a major genomic biomarker for TSC-related lung injury.

CHAPTER 5:

PROTEOMIC ANALYSIS IN THE ETM AFTER EXPOSURE TO TOBACCO SMOKE COMPONENTS

5.1 INTRODUCTION

Transcription omics (Chapter 4) is widely-used to compare changes in gene-expression levels between a diseased and control state. Whilst this data is useful, differences in gene-expression do not necessarily correspond to differences in protein levels (Bye et al., 2008). There are also high-degrees of variability between mRNA and protein concentrations (Greenbaum et al., 2003). Post-translational modifications, such as phosphorylation, can not be quantified or identified when examining the mRNA levels. In reality, the measurement of protein compared to nucleic acid expression could lead to a better understanding of disease processes and the identification of biomarkers (Hanash, 2003).

Functional proteomics, combined with mass spectrometry (MS), provides the tools required to study the response of cells to stimuli, i.e. xenobiotics, by identifying protein expression changes in the test and control scenarios (Conrads et al., 2001). Standard approaches to proteomics have been 1-/2 dimensional electrophoresis followed by MS. In this gel-based system, proteins are separated by their isoelectric point (pI) and/or molecular weights, detected by staining, excised from the gel and digested prior to identification by MS. This approach requires extensive optimisation and is prone to experimental errors (Righetti et al., 2004). Although advances in differential-in-gel-electrophoresis (DIGE) technology have aided this technology, by allowing multiplexing for three separate protein mixtures (Wu et al., 2005).

In the following work, the proteomic change following TSC challenge was determined. The use of human tissue equivalent models of respiratory epithelium provided human protein data for identification of biomarkers that could be related to many respiratory diseases (Sexton et al., 2008). To measure differential protein expression, state-of-the-art tandem MS Time of Flight (TOF/TOF) Analyzer, Nano-LC (Dionex Ultimate 3000, Probot Microfraction Collector and Global Proteome Server (GPS) Explorer Software

v3.6) and iTRAQ was utilised. The peptide analysis was carried out using MASCOT software.

5.2 MATERIALS AND STOCK SOLUTIONS

5.2.1 PROTEIN EXTRACTION, LABELLING AND IDENTIFICATION

Materials:	Supplier
Triethylammonium Bicarbonate (T7408)	Sigma
Nonidet P40 (74385)	Fluka
Phenylmethylsulfonyl Fluoride (93482)	Fluka
Bovine Serum Albumin (B8667)	Sigma
iTRAQ Reagents multiplex kit (4352135)	Applied Biosystems
Trypsin (4352157)	Applied Biosystems
Ethanol	Fisher
Ultimate 3000 Nano-LC	Dionex
Bio-SCX	Dionex
PepMap100	Dionex
PepMap75μm	Dionex
Acetonitrile (43,913-4)	Aldrich
Probot microfraction collector	Dionex
CHCA (C2020)	Sigma
4800 MALDI TOF/TOF	Applied Biosystems
Trifluoroacetic acid (91709)	Fluka
[Glu^1] – Fibrinopeptide B (F3261)	Sigma

Table 5.1 Materials used and their suppliers. All suppliers are UK based unless stated

5.2.2 WESTERN AND ANTIBODY DETECTION

Materials:	Supplier:
X-cell SureLock^{TM} Mini-Cell SDS-PAGE Apparatus	Invitrogen

Materials:	Supplier:
X-cell II™ Blot Module Western Blot Apparatus	Invitrogen
Hybond-P polyvinylidenedifluoride (PVDF) membrane	Amersham
Chromatography Paper 3MM	Whatman
P200 Gel Loading Tips	Alpha Laboratories
Powerpac 300 Power Suppliers	Biorad
X-OMAT™ LS Kodak Film 18 x 24 cm	Amersham
NuPAGE 4-12% Bis-Tris 1mm x 12 well (NP 0322 BOX)	Invitrogen
Immobilon Western HRP Substrate (WBKLS0100)	Millipore
Actin Primary Antibody (A-2066)	Sigma
COX1 Primary Antibody (sc-19998)	Santa Cruz, USA
Cystatin-A Primary Antibody (sc-32803)	Santa Cruz, USA
Goat Anti-Rabbit IgG, HRP-linked Antibody (7074)	Cell Signalling
Goat Anti-Mouse IgG, HRP-linked Antibody (7076)	Cell Signalling

Table 5.2 Materials used and their suppliers. All suppliers are UK based unless stated

5.2.3 STOCK SOLUTIONS

MALDI matrix was prepared by making a CHCA (Sigma; C2020) 2mg/ml solution in 70% (v/v) acetonitrile in 0.1% (v/v) Trifluoroacetic acid (TFA) containing 10fmol/µl Glu-Fib); this solution was prepared as required.

Electrophoresis running buffers for pre-cast gels – MOPS (Invitrogen; NP0001) were diluted appropriately to 1x for use and were stored at room temperature.

Transfer buffer was prepared as a 1x working solution containing 25mM Tris-HCl, 192mM glycine and 20% (v/v) analysis grade methanol (Fisher). This 1x working solution was stored at room temperature.

Pre-stained SeeBlue Plus 2® molecular weight marker (Invitrogen; LC5925) was supplied as a ready-to-use protein marker and were stored in aliquots at 4°C.

PBS-Tween containing 0.1% Tween-20 detergent (v/v) in 1x PBS was prepared and stored at room temperature.

Blocking buffer was prepared as a 1x working solution containing 0.2% I-block (Tropix. Inc) and 0.02% (v/v) sodium azide (NaN_3) supplemented in PBS-Tween. The blocking buffer was stored for up to 1 month at 4°C.

Immobilon Western HRP Substrate (Millipore) was supplied as two separate solutions stored at 4°C. Equal volumes of solution A and B (5ml total) were warmed to room temperature and mixed then allowed to stand for 5 minutes prior to its application to the membrane (Section 5.3.7).

MESNA stripping buffer was prepared as a 1x working solution containing 62.5mM Tris-HCl pH 6.8, 2% w/v SDS and 50mM 2-mercaptoethanosulfonate (MESNA; Sigma M-1511). MESNA stripping buffer was kept for no longer than two weeks and was stored at 4°C.

Trifluoroacetic acid (TFA) buffers: A = 2% acetonitrile in water with 0.05% (v/v) Trifluoroacetic acid (TFA) and B = 90% acetonitrile in water with 0.01% (v/v) TFA.

5.3 METHODS

5.3.1 PROTEIN EXTRACTION AND PREPARTION

The following techniques were all carried out at the Central Biotechnology Services, Cardiff University. The Protein from the TSC exposed and control ETM (NHBE cells) was isolated and labelled using the iTRAQ reagents (Applied Biosystems), as outlined in the Applied Biosystems (AB) iTRAQ

Reagents Chemistry Reference Guide (2004). This labelling system consisted of isobaric tags with a charged reporter group that was unique to each of the four reagents (Figure 5.1). The four reagents had the same mass and upon fragmentation in MS/MS gave rise to four unique reporter ions (m/z = 114-117; Zieske, 2006). This technique was developed by Darryl Pappin at AB (Ross *et al.*, 2004) and could be used for multiplexed profiling of up to four different samples.

Isobaric Tag
(Total mass = 145)

Reporter
(Mass = 114 thru 117)

PRG   = MS/MS fragmentation

Balance
(Mass = 31 thru 28)
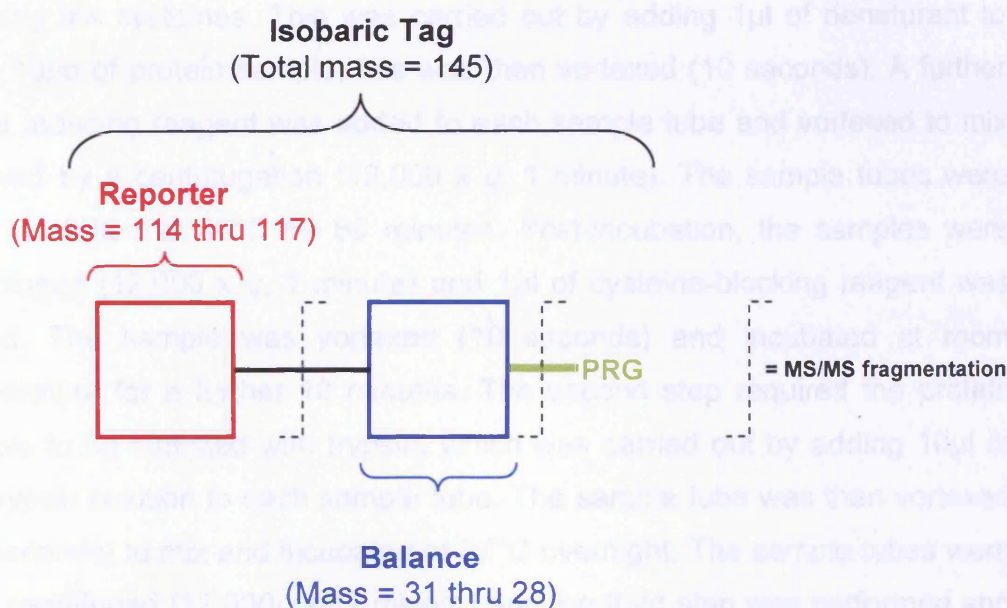
Figure 5.1 iTRAQ™ Reagent Structure. iTRAQ reagents were non-polymeric, isobaric tagging reagents consisting of a reporter group, a balance group and a peptide reactive group (PRG; adapted from AB iTRAQ Reagents, 2008)

5.3.1.1 PROTEIN ISOLATION AND QUANTIFICATION

Frozen cell pellets were resuspended in 10mM triethylammonium bicarbonate with 1% (v/v) Nonidet P40 (NP®-40) and 10mM phenylmethylsulfonyl fluoride (PMSF) and incubated for 15 minutes on ice. Lysates were clarified by centrifugation (10,000 x *g*, 5 minutes) and quantified using the Bradford assay (Bradford, 1976). Briefly, sets of standards were made up using bovine serum albumin (BSA) (0 to 20µg/ml). Cell lysate was diluted 10-fold in 0.1% NP®-40 and 200µl of sample was added to each well in a 96-well plate. Bradford

reagent (50µl) was added to each sample and the absorbance was read at 590nm using a plate reader. Assays were performed in triplicate for each cell lysate and the mean value recorded.

5.3.1.2 PROTEIN LABELLING

There were four main steps in the process of iTRAQ labelling (Figure 5.2). The first step required reducing and denaturing the sample, followed by blocking the cysteines. This was carried out by adding 1µl of denaturant to each 10µg of protein sample; this was then vortexed (10 seconds). A further 2µl of reducing reagent was added to each sample tube and vortexed to mix followed by a centrifugation (12,000 x g, 1 minute). The sample tubes were then incubated at 60°C for 60 minutes. Post-incubation, the samples were centrifuged (12,000 x g, 1 minute) and 1µl of cysteine-blocking reagent was added. The sample was vortexed (10 seconds) and incubated at room temperature for a further 10 minutes. The second step required the protein sample to be digested with trypsin, which was carried out by adding 10µl of the trypsin solution to each sample tube. The sample tube was then vortexed (10 seconds) to mix and incubated at 37°C overnight. The sample tubes were then centrifuged (12,000 x g, 1 minute) and the third step was performed and involved the labelling of the protein digests with the iTRAQ reagents. The iTRAQ reagents needed to be at room temperature, and were reconstituted with 70µl of ethanol, vortexed for 1 minute followed by centrifugation (12,000 x g, 1 minute). The content of one iTRAQ reagent was transferred to one sample tube, the sample tubes were then vortexed (10 seconds) and centrifuged (12,000 x g, 1 minute) prior to an incubation at room temperature for 60 minutes. The final step in the labelling process was to combine the iTRAQ reagent-labelled sample tubes into one fresh tube, with a final vortex (10 seconds) and centrifugation (12,000 x g, 1 minute).

5.3.2 LC SEPARATION OF iTRAQ REAGENT LABELLED PEPTIDES

Equal volumes of the digested peptides labelled with different iTRAQ reagents were mixed and peptides corresponding to 2µg of undigested protein were
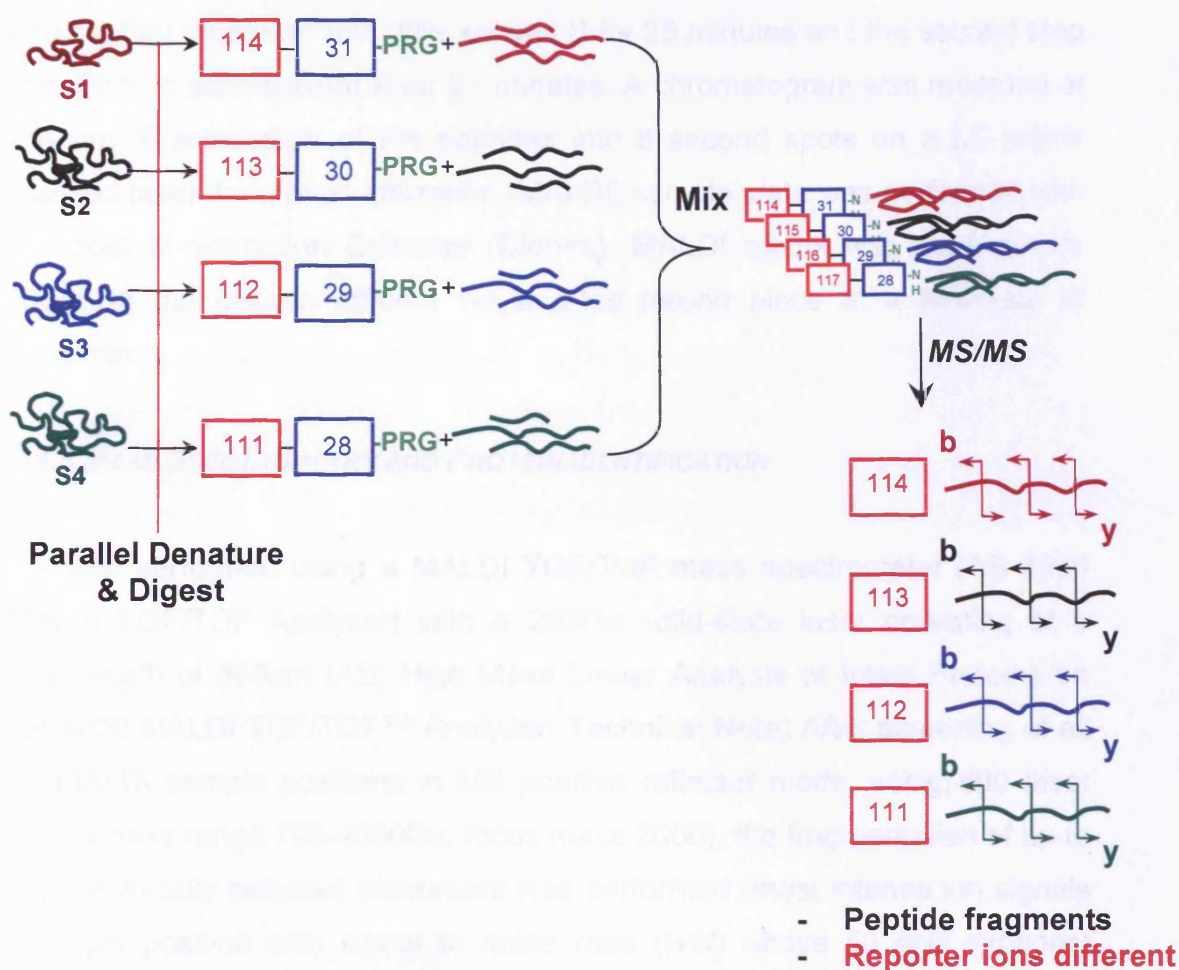
Figure 5.2 Schematic overview of a multiplex iTRAQ reaction. General workflow for four samples (S1-S4), each sample is reduced, alkylated and ezymatically digested with trypsin, the peptides are then labelled and combined and analysed by LC-MS/MS. The resultant mixture provided a set of single precursor ions, for the identification of single proteins from a known sample (adapted from Zieske, 2006)

separated on a nano-LC system using a two-dimensional salt plug method. Peptides were applied to a SCX cartridge (BioX-SCX, 500µm, 15mm, 5µm) that was plumbed upstream of the RP desalting cartridge (PepMap100, 300µm, 5mm, 100 Å). Samples were separated on the SCX cartridge using 20µl step elutions with increasing concentrations of NaCl (100mM, 200mM, 400mM, 800mM, and 1M). Each step elution was loaded onto the RP desalting column where the eluting peptides were desalted. Peptides were then separated using a C18 column (PepMap75µm id, 30cm, 3µm, 100 Å) at

a flow rate of 300nl/min. Peptides were separated using a two-step gradient with the first step from 5 to 20% solvent B for 25 minutes and the second step from 20% to 50% solvent B for 21 minutes. A chromatogram was recorded at 214 nm. Fractionation of the peptides into 8 second spots on a LC-matrix assisted laser desorption ionization (MALDI) sample plate was performed with a Probot Microfraction Collector (Dionex). MALDI matrix was continuously added to the column effluent via a μ-tee mixing piece at a flow rate of 1.4μl/min.

5.3.3 MASS SPECTROMETRY AND PROTEIN IDENTIFICATION

MS was performed using a MALDI TOF/TOF mass spectrometer (AB 4800 MALDI TOF/TOF Analyzer) with a 200Hz solid-state laser operating at a wavelength of 355nm (AB; High Mass Linear Analysis of Intact Proteins on the 4800 MALDI TOF/TOF™ Analyzer: Technical Note) After screening of all LC-MALDI sample positions in MS positive reflector mode, using 800 laser shots (mass range 700-4000Da; focus mass 2000), the fragmentation of up to 6 automatically selected precursors was performed (most intense ion signals per spot position with signal to noise ratio (S/N) above 50 and strongest analysed first). Internal calibration of each spot in MS was achieved against the Glu-Fib added to the matrix. Common trypsin autolysis peaks and matrix ion signals and precursors within 300 resolution of each other were excluded from the selection. In MS/MS positive ion mode 4000 spectra were averaged with 1kV collision energy (collision gas was air at a pressure of 1.6×10^{-6} Torr) and default calibration.

5.3.4 DATA AND STATISTICAL ANALYSIS

MS/MS queries were performed using the MASCOT Database search engine v2.1 (Matrix Science Ltd), embedded into Global Proteome Server (GPS) Explorer software v3.6 on the Swiss-Prot database (O'Donovan et al., 2002). Searches were restricted to the human taxonomy with trypsin specificity (one missed cleavage allowed); the tolerances set for peptide identification searches was 0.3 Da for MS/MS. Cysteine modification by

methylmethanethiosulfonate (MMTS) and iTRAQ modification of the N-terminus and lysines was employed as a fixed modification. Quantitation based on signature-ion peak areas was performed using GPS-Explorer software. Fold-changes (FC) between the treated samples and the reference control samples were calculated by the software for each of the quantified peptides of the same protein. Search results were evaluated by protein and peptide score confidence intervals (CI) % calculated in the GPS-Explorer software and based on the MASCOT score (Glückmann *et al.*, 2007). In order to get average FC, all single peptide expression values with minimum CI% above 50, were normalized for each protein on the median. Protein identification results with CI% score above 95 were accepted, all the identifications in (Table 5.5) were additionally manually inspected for correctness. Data from three independent biological replicates were examined for consistent protein changes that were more than 2-fold altered.

The significance of differentially expressed proteins could only be resolved following statistical analyses (Glückmann *et al.*, 2007). The appropriate statistical analysis in this instance was a 2 Class Unpaired t-test (Tian *et al.*, 2008). The two-tailed Student's t-test is a test used to examine a difference between mean values of two groups of data. A Null Hypothesis of no expression-level difference in individual proteins between control and nicotine, FA, urethane and cadmium ETM exposure was adopted. The resultant statistical value could then be used to determine which proteins were significantly differentially expressed. A p value of ≤ 0.05 was deemed significant. The statistically differentially expressed proteins identified, were processed using the Genecodis (Carmona-Saez *et al.*, 2007), to determine the molecular function data of each protein.

5.3.5 1D SDS PAGE

Pre-cast gels (Invitrogen) were prepared by rinsing the gel cassette with its storage buffer and by carefully removing the tape covering the slot at the back of the gel cassette and the well comb. The exposed loading wells were then

rinsed with 1x electrophoresis running buffer. The gel cassette was inserted into the lower buffer chamber assembled with the gel tension wedge, adjacent to the buffer core. Wells were filled with 1x electrophoresis running buffer. Protein samples to be loaded onto the gels were first prepared. Following the quantification of protein concentration, an equal volume of 2x GSB (100mM Tris-Cl pH6.8, 20% Glycerol, 0.2M DTT, 4% SDS, 0.02% bromophenol blue) was added and the samples were heated at 100°C for 5 minutes on a dry heating block. These samples, along with a pre-stained molecular weight marker, were loaded onto the gels by pipetting under the running buffer using the P200 gel loading tips. Gels were run at 200V for 50 minutes to 1 hour.

5.3.6 WESTERNS

Hybond-P polyvinylidenedifluoride (PVDF) membrane was soaked in analysis grade methanol before use and then equilibrated in transfer buffer. Polyacrylamide gels were placed onto the membranes between two pieces of Whatman 3MM filter paper soaked in transfer buffer in a blotting cassette. Western blotting was carried out using an X-cell II™ Blot module inserted into an X-cell SureLock™ Mini-Cell unit (Invitrogen) at 30V, 250mA for 60 minutes. The blots were then washed in PBS-Tween.

5.3.7 ANTIBODY DETECTION

Western Blots were incubated in a sealed polyethylene bag with approximately 15ml-20ml of blocking buffer for 1 hour at room temperature on an orbital shaker (Stuart-Scientific). The blocking buffer was then replaced with 10-20ml of primary antibody diluted to the required concentration in blocking buffer (Table 5.3). To fully utilise each blot they were cut into three sections, this was permitted by the differences in MW of COX1, Actin and Cystatin-A (Figure 5.3). The blots were incubated with primary antibody overnight at 4°C. Post-incubation, blots were then washed three times for at least 10 minutes in PBS-Tween. Subsequently, the blots were incubated for 1 hour with 10-20ml of appropriate horseradish peroxidise (HRP)-conjugated

secondary antibody diluted to 1/10,000 with blocking buffer (see Table 5.3). Blots were then washed again three times for at least 10 minutes in PBS-Tween. Following this, the blots were incubated with Immobilon Western HRP Substrate for 5 minutes in a section of polyethylene film. Any excess reagent was removed and blots were exposed to autoradiograph film; through a new section of polyethylene film. Following exposure each section of the blot was stripped and placed incubated in a sealed polyethylene bag with approximately 15ml-20ml of MESNA stripping buffer for 30 minutes at 50°C.

Figure 5.3 Schematic overview of a Western blot. The western blot was cut into three sections to allow simultaneous antibody detection of three different antibodies; the scissors indicate where the cuts were made

1° ANTIBODY	DILUTION	MW	2° ANTIBODY	DILUTION
Cox1	1:200	72KDA	MOUSE	1:10000
ACTIN	1:10000	45KDA	RABBIT	1:10000
CYSTATIN-A	1:200	11KDA	MOUSE	1:10000

Table 5.3 Primary and secondary antibodies for Westerns. Overview of the primary (1°) and secondary (2°) antibodies with their optimised dilution factor used in an antibody detection of a western technique for proteomic validation (Section 5.3.7)

5.4 RESULTS

5.4.1 PROTEIN CONCENTRATION

The protein from control and TSC exposed ETM cells (n=3; Table 5.4), indicated that the protein yield for each sample was sufficient for proteomic analysis.

Exposure of ETM	Abs A (590nm)	Abs B (590nm)	Abs Av (590nm)	µl for 100µg protein
Nicotine[a]	1.025	0.898	0.962	79.4
Nicotine[b]	0.93	0.935	0.933	84.7
Nicotine[c]	0.817	0.667	0.742	80.68*
Cadmium[a]	1.016	0.977	0.997	73.5
Cadmium[b]	0.925	0.94	0.933	84.7
Cadmium[c]	0.829	0.687	0.758	77.7*
Urethane[a]	1.006	0.837	0.922	86.2
Urethane[b]	0.965	0.919	0.942	82.0
Urethane[c]	0.85	0.723	0.786	72.9*
Formaldehyde[a]	0.929	0.938	0.934	84.7
Formaldehyde[b]	0.963	0.875	0.919	87.7
Formaldehyde[c]	0.924	0.854	0.889	59.2*
Control[a]	0.934	0.832	0.883	96.2
Control[b]	0.865	0.841	0.853	104.2
Control[c]	0.954	0.962	0.958	79.4

Table 5.4 Bradford assay data and the volume required for a total protein concentration of 100µg. Absorbance (590nm) values of a Bradford assay to determine protein concentrations (n=3) isolated from control and TSC exposed ETM; * indicates values were taken from a secondary standard curve

5.4.2 MASS SPECTROMETRY AND PROTEIN IDENTIFICATION ANALYSIS

Analysed MS data (n=7) from the exposed cell cultures was analysed to show differential protein expression for the four different TSC (Table 5.5). When comparing protein expression in cadmium, formaldehyde and urethane to PBS, 413 proteins were identified. This number was reduced to 250 protein identifications when the parameter of two or more peptides was imposed for an individual identification. The Gene Ontology information, prepared using Genecodis (Carmona-Saez *et al.*, 2007), for molecular function was carried out on all proteins identified in each TSC (Figure 5.4).

When placing the final stringent parameters (Section 5.3.4), which included data from three independent biological replicates, consistent protein changes altered by more than 2-fold identified 10 proteins (Table 5.5). Some of the largest changes, as shown in Table 5.5, were defence proteins (cystatin-A, ubiquitin and protein plunc precursor), inflammatory proteins (complement-C3 and protein plunc precursor) and structural/development proteins (cornifin-B and calmodulin).

When comparing the protein expression of the TSCs to PBS; two proteins (cystatin-A and ubiquitin) were consistently induced by 2 fold or more across all TSC. Cystatin-A and ubiquitin proteins also exhibited the greatest inductions (Table 5.5). Cadmium, formaldehyde and urethane had fewer numbers of proteins with a 2-fold expression, compared with nicotine, which had nine proteins altered by 2-fold or more.

Further analysis placed all the proteins identified into the following functional and molecular groups (annotated by Genecodis): (1) protein binding, (2) nucleotide binding, (3) oxidoreductase activity, (4) calcium ion binding, (5) ATP binding, (6) Nucleotide binding with ATP binding, (7) Structural molecule activity and (8) Nucleotide binding with protein binding. These groups were common for all compounds, with the protein binding being the functional group containing the greatest numbers of proteins (Figure 5.4).

151
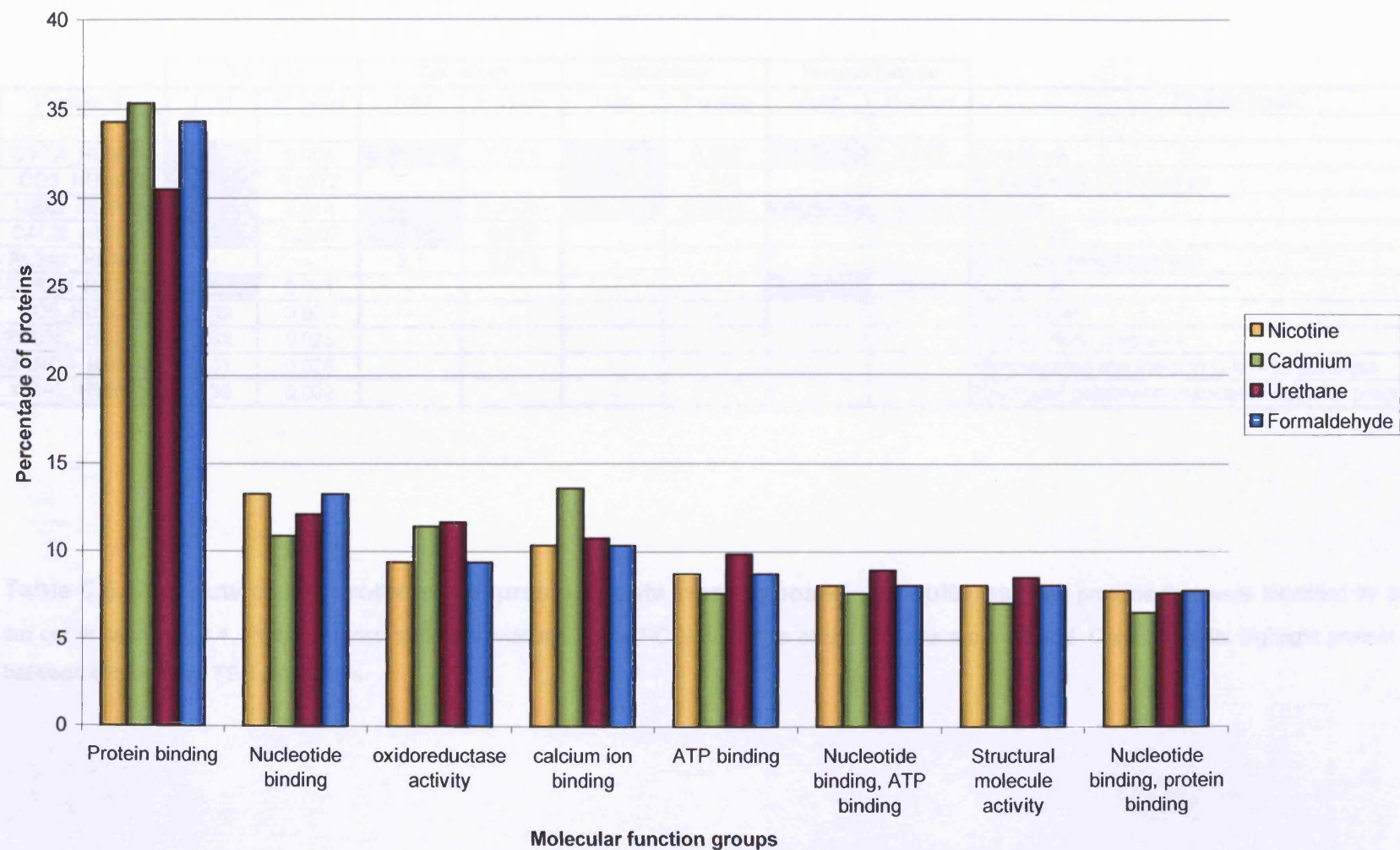
Figure 5.4 Molecular function grouping of all the proteins identified from TSC exposures. Genecodis was used to obtain the gene oncology for all proteins that were identified by parameters set out in Section 5.3.4. All proteins, regardless of fold-change, were used in this analysis

Protein ID	Nicotine		Cadmium		Urethane		Formaldehyde		Protein name
	Fold	P-value	Fold	P-value	Fold	P-value	Fold	P-value	
CYTA_HUMAN	5.23	0.005	6.7	0.011	3.29	0.003	3.8	0.042	Cystatin-A
CO3_HUMAN	2.97	0.0072	-	-	2.66	0.044	-	-	Complement C3 precursor
UBIQ_HUMAN	3.27	0.014	3.86	0.00001	2.42	0.00001	3.45	0.021	Ubiquitin
CALM_HUMAN	2.33	0.0007	3.56	0.018	-	-	-	-	Calmodulin
AL3A1_HUMAN	-	-	2.1	0.015	-	-	-	-	Aldehyde dehydrogenase
SPR1B_HUMAN	2.37	0.041	-	-	-	-	5.63	0.00001	Cornifin-B
CD9_HUMAN	3.09	0.003	-	-	-	-	-	-	CD9 antigen
PLUNC_HUMAN	2.62	0.025	-	-	-	-	-	-	Protein Plunc precursor
MARCS_HUMAN	2.36	0.026	-	-	-	-	-	-	Myristoylated alanine-rich C-kinase substrate
NGAL_HUMAN	2.38	0.002	-	-	-	-	-	-	Neutrophil gelatinase-associated lipocalin precursor

Table 5.5 Overview of the proteomic expression data from exposed cell cultures. The proteins that were identified by parameters set out in section 5.3.4. Protein names and abbreviations in the NCBI database of the proteins are indicated. Coloured cells highlight protein homology between two or more TSC exposures

5.4.3 WESTERN BLOT ANALYSIS

The aim of Western blot analysis was to determine whether the changes in protein expression predicted by the nano-LC and MS were accurate. COX1, actin, and cystatin-A were selected for Western blotting analysis from the list of experimentally altered proteins (Figure 5.5). COX1 was selected due to the elevated gene expression data observed in cadmium, formaldehyde and urethane (Section 4.4.2), actin was used for normalisation of the blot. Western blots were then scanned and the densitometry of the bands quantified by using Genetools software (Table 5.6)
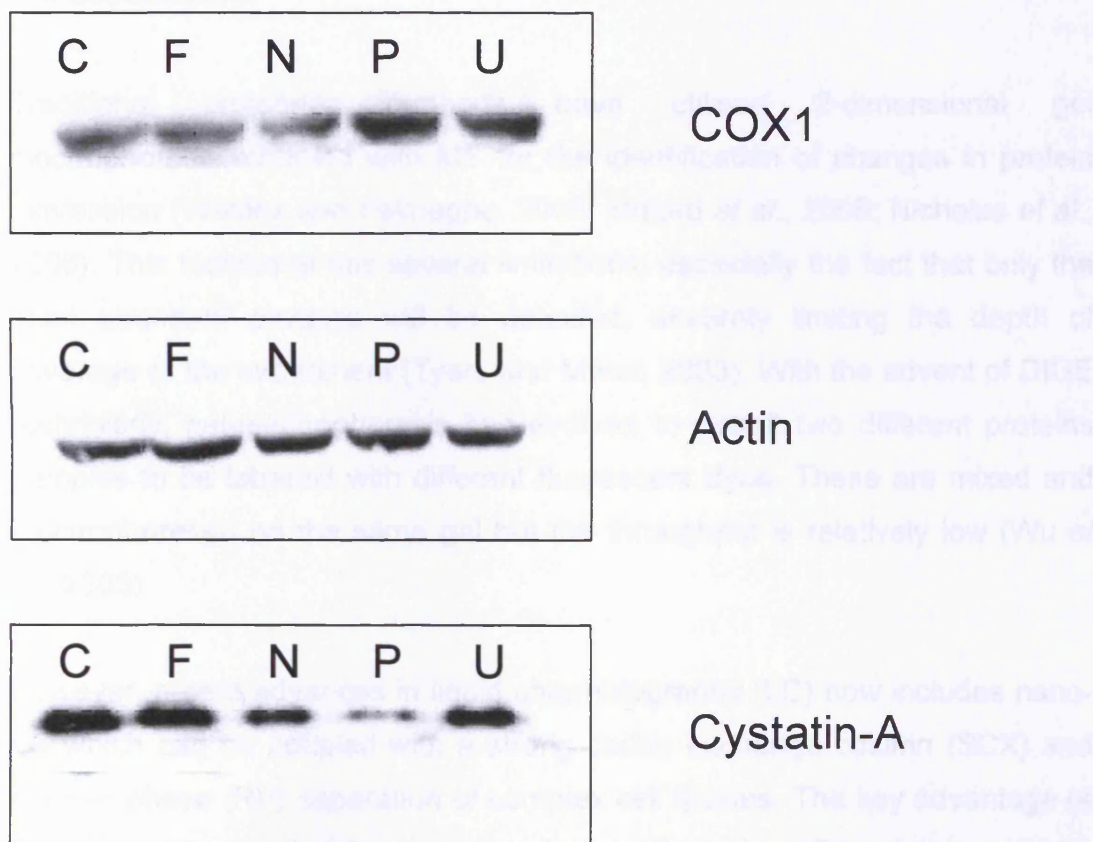
Figure 5.5 Analysis of four proteins by western blotting. Whole cells extracts were generated from TSC exposed of the MatTek EpiAirway tissue samples. They were resolved by 1D SDS-PAGE electrophoresis followed by Western blotting. Resolved proteins were analysed by immunoblotting using primary antibodies specific to COX1, actin and cystatin-A. Key: C-cadmium, F-formaldehyde, N-nicotine, P-PBS control and U-urethane

TSC	CYSTATIN-A INDUCTION	COX1 INDUCTION
CADMIUM	4.2	0.9
FORMALDEHYDE	3.1	0.7
NICOTINE	2.5	0.8
URETHANE	4.0	1.0

Table 5.6 Quantification of protein induction by immunoblotting. Western blots were scanned and the bands quantified by densitometry using Genetools software (n=3). The cystatin-A induction result concurs with the data from the iTRAQ, experiment

5.5 DISCUSSION

Traditional proteomic methods have utilised 2-dimensional gel electrophoresis, coupled with MS for the identification of changes in protein expression (Wattiez and Falmagne, 2005; Malard *et al.*, 2005; Nicholas *et al.*, 2006). This technique has several limitations, especially the fact that only the most abundant proteins will be detected, severely limiting the depth of coverage of the experiment (Tyers and Mann, 2003). With the advent of DIGE technology, gel-electrophoresis has evolved to permit two different proteins samples to be labelled with different fluorescent dyes. These are mixed and electrophoresed on the same gel but the throughput is relatively low (Wu *et al.*, 2005).

However, recent advances in liquid chromatography (LC) now includes nano-LC which can be coupled with a strong cation exchange column (SCX) and reverse phase (RP) separation of complex cell lysates. The key advantage of this approach was that the peptides resolved from the SCX column could be directly placed into the MS/MS system (Wu *et al.*, 2005). As proteomic techniques become more established, the need to move from the qualitative to the quantitative is ever increasing. The type of proteomic study utilised for this research project involved a differential expression analysis. This approach included comparative analysis of protein expression in the normal and

exposed tissue, where these identified changes in protein expression may represent markers (Pan *et al.*, 2008; Joo Lee *et al.*, 2008). To perform this study we required multiplexing, broad-proteome coverage and absolute quantification and iTRAQ met these criteria.

Applied Biosystems iTRAQ reagents were a multiplexed set of four isobaric reagents (same mass) which are amine specific and yield labelled peptides that were identical in mass, and hence, also identical in single MS mode. However, they produced strong, diagnostic, low-mass MS/MS signature ions allowing for quantitation of up to four different samples simultaneously (Aggarwal *et al.*, 2006).

A complementary approach was required to evaluate the biological responses post-genomics (Chapter 4), as means to compare protein function with the identified biomarkers of exposure and harm, for specific mechanisms of lung injury attributed to smoking. In this study, a subtoxic dose of nicotine, cadmium, urethane and formaldehyde had significant effects on lung epithelial protein expression.

As described in Chapter 4, the effect of nicotine in the animal and cell system has been comprehensively researched (Yildiz, 2004; Hukkanen *et al.,* 2005). For the purpose of this study, only the thrombogenic and atherosclerotic mechanisms of nicotine were investigated. The majority of significantly altered proteins identified were involved in 'binding' and was consistent for all exposures carried-out (e.g. ANXA1; Skrahina *et al.*, 2008). A total of nine proteins were identified (cystatin-A, complement C3, ubiquitin, calmodulin, cornifin-B, CD9 antigen, protein plunc, myristoylated alanine-rich protein kinase C substrate and neutrophil gelatinase-associated lipocalin) of which seven could be associated with atherosclerosis.

There were two proteins not directly related to atherosclerosis, one of which was a plunc protein. Plunc is classed as a defence protein believed to function in the innate immune response and involved in inflammatory responses to irritants in the upper airways (Bingle and Craven, 2002). This finding has also

been observed by other researchers (e.g. Lindahl *et al.*, 2001) for inhaled xenobiotics (i.e. exposed to epoxy). This protein may be used as marker of irritancy. The second protein with no associations to atherosclerosis was cornifin-B. Cornifin-B is expressed in squamous tissue and normally absent in normal mucociliary epithelium but increased levels were expressed when exposed to environmental toxicants (Tesfaigzi and Carlson, 1999). The same study also indicated that this protein could be induced under certain states of cell proliferation. No link to atherosclerosis has been published.

The remaining significantly altered proteins (cystatin-A, complement C3, ubiquitin, calmodulin, CD9 antigen, myristoylated alanine-rich protein kinase C substrate and neutrophil gelatinase-associated lipocalin) could be separated further into anti-atherosclerosis and pro-atherosclerosis associations.

The anti-atherosclerosis protein cystatin-A is another defence protein that was induced. Cystatin-A inhibits cysteine proteases, which play a central role in extracellular matrix (ECM) remodelling. ECM remodelling has been implicated in the progression of cardiovascular diseases (Bengtsson *et al.*, 2008; Lutgens *et al.*, 2007). Ubiquitin is a regulatory protein that labels proteins for proteasomal degradation; other functions equally important include stability and function of many proteins (Ventii and Wilkinson, 2008). Ubiquitin is also involved in a number of biological processes (e.g. inflammation and apoptosis), that contribute to atherosclerosis. The induction of ubiquitin proteins has also been related to the production of coronary plaques (Herrmann *et al.*, 2002). Myristoylated alanine-rich protein kinase C substrate (MARCKS) is involved in the airway homeostatic process, since it is one of the molecules regulating the secretion of the mucin (Park *et al.*, 2008). A recent study by Guo (2007), highlighted the rapid recruitment of MARCKS to membrane rafts that would mediate S1P stimulation, and enhanced endothelial barrier integrity; failure of this barrier could result in atherosclerosis. Neutrophil gelatinase-associated lipocalin (NGAL) is a protein capable of binding small lipophilic substances (Flower, 1994). NGAL is also expressed by epithelial cells during inflammation or injury (Gwira *et al.*, 2005). It is thought that NGAL can be induced by a number of xenobiotics but this

induction would act as an anti-apoptotic effect (Tong, 2005). Recent studies have indicated NGAL as a marker of several diseases (Moniaux *et al.*, 2008; Bennett *et al.*, 2008) but this was not due to the detrimental effect of the protein on the disease. In the case of atherosclerosis, its induction has been associated with vascular repair (Bu *et al.*, 2006).

The remaining proteins (complement C3, calmodulin and CD9) can be classed has having pro-atherosclerosis associations. Studies have shown that atherosclerosis is an inflammatory disease (Ross, 1999) and C3 is a mediator of the inflammatory process (Muller-Eberhard, 1988). Past studies have indicated the elevated concentration of C3 in patients with atherosclerosis (Geertinger and Sorensen, 1973). Recent investigations have corroborated these findings with the added information that induced C3 was involved in the progression of atherosclerosis (Szeplaki *et al.*, 2004). Calmodulin plays a role in several biological processes such as inflammation, metabolism, apoptosis and muscle contraction. Calmodulin is vital for proteins unable to bind calcium, and as such, use calmodulin as a calcium sensor and signal transducer (Stevens, 1983). Calmodulin is thought to be constitutively-expressed in eukaryotic cells; however, expression can vary during the cell cycle (Koller and Strehler, 1993). Atherosclerosis can be characterised by the presence of lesions called atheromatous plaques (Gamble, 2006). It has been suggested that one of the processes of this disease is the calcium precipitation which binds the cholesterol with the plaque precursor matrix; one of the components of this matrix is calmodulin (Gamble, 2006). By inducing calmodulin, its increase triggers (up-regulate) plaque precursor matrix and initiates the atherosclerosis process (Chen *et al.*, 2002). CD9, a cell surface protein that plays a role in cell development, regulation and growth, modulates cell adhesion and migration (Maecker *et al.*, 1997; Berditchevski, 2001). It has also been implicated in platelet activation and aggregation events (Jennings *et al.*, 1990). CD9 can be found expressed on macrophages and has been shown to enhance the juxtacrine mitogenic activity, which in turn, can lead to the development of atherosclerosis (Ouchi *et al.*, 1997).

As previously described in Chapter 4, there are many biological effects exerted by cadmium on membranes. The majority of candidate proteins identified from the cadmium exposure study were involved in protein binding. This was consistent for all exposures, although the molecular function profiles were very similar for all compounds there was an increase in calcium ion binding. The four proteins (cystatin-A, ubiquitin, calmodulin and aldehyde dehydrogenase) significantly altered by cadmium exposure were investigated for potential associations to cytotoxicity. Of the four significantly altered proteins, three proteins (cystatin-A, ubiquitin, calmodulin) had also been induced by nicotine but all four had no associations with cytotoxicity. Cystatin-A is a protease inhibitor and studies have shown it to suppresses ultraviolet B-induced apoptosis (Takahashi et al., 2007), indicating the protective/anti-apoptosis mechanisms. Ubiquitin is in the centre of cellular proteolysis and using its degradative capacity has become integral to processes in the cell (i.e. DNA repair; McBride et al., 2003). Oxidative stress is initiated by cadmium in many cell types, as determined by decreased activity of antioxidants (Manca et al., 1994; Yang et al., 1997). The response of ubiquitin to oxidative stressors has been examined by Grunge (2005) and increased levels of oxidative stress induced the degradation rate of the oxidised proteins (Grune et al., 1995). As mentioned previously in this section, calmodulin plays a role in several biological processes such as inflammation and apoptosis (Stevens, 1983) but exposure to reactive oxygen intermediates (ROI) can activate signalling pathways that are considered to prevent cell death. The mechanism to prevent apoptosis is thought to be the ROI-induced phosphorylation of calmodulin, leading to the inhibition of calmodulin-dependent kinases (Franklin et al., 2006). The final protein significantly and uniquely altered by the cadmium exposure was aldehyde dehydrogenase (ALDH-2), which plays a major role in the detoxification of aldehydes. Research of ALDH-2 has concentrated on its deficiency in the oxidative stress-related diseases (Ren, 2007; Wenzel et al., 2008). The up-regulation of this protein would benefit the anti-oxidant defensive mechanism.

The biological effects and target tissues of urethane have been documented (Siemiatycki et al., 2004) and the proteins that have been significantly-altered,

post-urethane exposure, have been investigated for potential associations to carcinogenicity. Two principle proteins can be classed as being anti-carcinogenic and include cystatin-A (also known as stefin-A) and ubiquitin. Cystatin-A functions as a cysteine protease inhibitor and has the potential to be a biomarker (Kehinde *et al.*, 2008). Its up-regulation in lung tumour samples compared to normal lung tissue suggests it is able to counteract (suppress) harmful tumour-associated proteolytic activity (Parker *et al.*, 2008; Werle *et al.*, 2006). Ubiquitin's ubiquitinous (and hence its name) functions of degradation, proliferation and apoptosis reveals the importance of its role in carcinogenesis (Voutsadakis, 2008; Wolf and Hilt, 2004). In this work, its regulation once again pointed to a role in defensive/protection for cell survival (Sun *et al.*, 2004).

The remaining protein identified by exposure to urethane could be classified as being pro-carcinogenic. Complement C3 plays a vital role in the activation of the inflammatory process, especially in airway hyper-responsiveness (Walters *et al.*, 2002). There is evidence that links inflammation to cancer development (e.g. Crohn's disease; Weitzman and Gordon, 1990; Shacter and Weitzman, 2002). Also users of anti-inflammatory drugs have a reduced development of cancer (Williams *et al.*, 1999; Meier *et al.*, 2002). These observations may indicate therapeutic strategies. Nevertheless, a study by de Visser (2004) lends serious doubt regarding the actual function of C3, and it's accumulation in inflammatory cells.

Formaldehyde has the potential to be mutagenic and genotoxic due to the ability to form cross-linkages between protein and single stranded DNA (Merk and Speit, 1998). The proteins significantly altered by FA exposure (cystatin-A, ubiquitin and cornifin-B) were investigated for potential associations to mutagenicity. Cystatin-A, ubiquitin and cornifin-B all have anti-mutagenic/protection properties (Parker *et al.*, 2008; Tesfaigzi and Carlson, 1999; Sun *et al.*, 2004).

One specific gene (*PTGS1*), highlighted in Chapter 4, was significantly induced in three out of the four compounds. *PTGS1/COX1*, is thought to be responsible for the production of prostaglandins, which in turn are responsible for a host of physiological responses (e.g. inflammation and platelet aggregation; Park *et al.,* 2006). Western blot analysis indicated a decreased induction of protein expression, except for urethane, which induced no change in protein expression, despite the highly significant changes at the gene level. This result was also observed by Martey *et al.,* (2004). This study examined the effect of cigarette smoke on lung fibroblasts, in particular, *COX2* and prostaglandin E2 (*PGE2*). The conclusion of that investigation was *COX2* and not COX1, was the key enzyme responsible to the induction of *PGE2* after exposure of cigarette smoke.

5.6 CONCLUSION

The proteomic analysis utilising iTRAQ™, nano-LC and MALDI TOF/TOF MS has provided protein data on the exposure of the ETM to different TSC. The technique has been shown to be reproducible between replicates and this has been confirmed by using Western blotting and antibody detection. Two proteins were identified (cystatin-A and ubiquitin) to be significantly induced for all TSC exposures and could be described as 'defence proteins'; due to their protective properties and mechanisms. Consequently, they represent potential biomarkers of general lung injury. This work also identified three proteins (complement C3, calmodulin and CD9) that could be used as biomarkers of specific disease mechanisms (e.g. platelet activation and aggregation associated with tobacco smoke, e.g. atherosclerosis). The protein COX1 was also analysed, using Western blotting with antibody detection, due to its significant induction at the genomic level. There was no significant change at the protein level to indicate that COX1 could not be used as a potential protein biomarker.

CHAPTER 6:

GENERAL DISCUSSION

6.1 OVERVIEW

The overall objective of this research was to identify intelligent biomarkers in human respiratory epithelia following exposure to selected particle (e.g. cadmium and nicotine) and vapour phase (e.g. formaldehyde and urethane) tobacco smoke components (TSC). The key components were selected for their thrombogenic capacity (nicotine), cytotoxicity (cadmium) and production of reactive metabolites during xenobiotic metabolism (formaldehyde and urethane), to provide a holistic approach towards the identification of biomarkers in the pulmonary epithelium (i.e. cells derived from human primary explant tissue) *in vitro*.

Scientific reviews of the chronic inhalation studies of mainstream cigarette smoke in all five species of laboratory animals (e.g. rats, mice, hamster, dog, non-human primates) used to evaluate carcinogenic potential, revealed no statistically significant increase in the incidence of malignant lung tumours and atherosclerosis following exposure to smoke. Furthermore, these findings were not consistent with the epidemiological results observed in human smokers. The outcome of the comprehensive animal studies reviewed does support the idea that research should focus on the use of human tissue to corroborate the epidemiological findings. This obviously limits what can be achieved using acute/chronic exposure studies to cigarette smoke and/or various tobacco components. It is also difficult to study environmental contaminants such as tobacco smoke because of methodological problems in testing entire atmospheres. Most investigations are based on *in vivo* and *in vitro* experiments that use model substances and surrogate mixtures to simulate the real life situation. In this respect, *in vitro* systems, in particular, offer the use of human target cells and comparing the results with human data. This eliminates any difficulties in extrapolating animal data to humans, and reduces the need for animals in testing such atmospheres.

An important research objective was to carry out conventional toxicological analysis to establish the dose of the various TSC required to induce

alterations in epithelial resistance, secreted surface proteins and release of inflammatory markers. It was imperative that the final working doses used were sub-toxic, since the aim was to identify the important biomarkers involved with toxicant stress and avoid studying dead or dying cells.

The first hypothesis for this study was concerned with the premise that the *"use of human respiratory epithelia (normal tracheal-bronchial epithelia) was a viable in vitro alternative to the rodent (e.g. rat) lung model (in vivo)"*. When compared to a standard, epithelial, mono-layer culture, this system more closely resembled human bronchioles, both morphologically and physiologically, and therefore, deemed a viable alternative to the rat lung model (*in vivo*) [e.g. Hermann *et al.*, 2004; Grainger *et al.*, 2006; BéruBé *et al.*, 2009]. For the system to be judged as a viable alternative to a rat lung model for toxicological studies, it was important that the system originated from normal (non-immortalised) cells. It was equally important to choose a human-derived tissue model in order to avoid the inevitable species-related differences that could compromise experimental results. The cell-cell interactions that occur *in vivo* (but not generally present in single-cell cultures), can significantly alter the cellular effects of many toxins. The range of these effects can only be fully-investigated in a biological system capable of transcribing and translating genes in response to the action of toxins. The ETM (i.e. EpiAirway™ Tissue) consisted of cells derived from healthy, human, primary, explant tissue (i.e. normal human bronchial epithelium; NHBE), as opposed to lung tumour or diseased tissue. Consequently, the cells were genotypically and phenotypically more representative of normal epithelia than other commonly used models (e.g. A549 [Padar *et al.*, 2005] and BEAS-2B [Penn *et al.*, 2005]). The overriding advantage of this *in vitro* tissue model was that the epithelium was cultured to form a 3-dimensional, pseudo-stratified state which exhibited a functional mucocilliary phenotype with tight junctions, as observed *in vivo*.

The second hypothesis was based upon the supposition that *"exposure of the human respiratory epithelia to tobacco smoke components (vapour and particle phases) caused harm"*. This was indeed, the circumstance,

whereby acute, sub-toxicological exposures of the ETM to the four different TSCs evoked analogous biochemical and physiological responses; as measured by conventional toxicology assays and complimentary histopathology and IHC). The responses induced cell proliferation, increased protein secretion, elevated cell viability, electrical resistance and cytokine expression. These communal response patterns could be likened to a protective response or potentially an over-correction to the damaged airway epithelium. This so-called, "protective response", was typified by an immediate peak in all the measured toxicological parameters, followed by a subsequent decline, as the TSC concentrations were increased. This dose-response relationship can also be described as a hormetic response but toxicological thinking has so far been hesitant to accept the existence of this response (Calabrese, 2004). At high concentrations of the TSC, the elevated responses were over-whelmed and all the biomarkers of toxicity rapidly deteriorated, i.e. decreased cell numbers, cell viability, electrical resistance and cytokine expression. The only exception to this was the increased levels of protein released into the apical surface wash. Detailed morphological changes in the cellular and tissue architecture for each TSC concentration investigated revealed four key pathological modifications: (1) hyperplasia, (2) hypertrophy, (3) cytolysis and, (4) necrosis. In conjunction with these findings, targeted IHC assays also resolved three discrete zones of tissue injury and repair: (1) the apical region and its Goblet cells; (2) the suprabasal region reactive intermediate cells; (3) the basal zone.

The third hypothesis considered the postulation that *"genomics and proteomics can be utilised to identify biomarkers of exposure and harm in the human respiratory epithelia to tobacco smoke components"*. This hypothesis was resolved to be correct in that a complementary approach was required to evaluate the biological responses post-genomics. The proteomic analysis high-lighted post-translational modifications identifying potential biomarkers of harm for specific mechanisms of injury attributed to smoking. There were also high degrees of variability between mRNA and protein concentrations. Post-translational modifications, such as phosphorylation, can not be quantified or identified when examining the mRNA levels. The

measurement of protein rather than nucleic acid expression lead to a better understanding of disease processes and the consequent identification of biomarkers. Recent advances in mass spectrometry and the development of tags permitting proteomic quantification (e.g. iTRAQ™) has moved proteomic analysis towards direct mass spectrometry. The methods utilised in this study were very successful, with the identification of over four hundred proteins. At the onset of this research project, it had been envisioned that a gel-based method which involved using two-dimensional gel-electrophoresis would be implemented. There were limitations with this technique, with regard to sensitivity, reproducibility and quantification but technology has progressed to ease these shortfalls, i.e. the development of DIGE. Also once the spot of interest had been selected; it was digested into peptides and identified by using mass spectrometry. Moreover, the cost of analysing each protein spot was expensive, and prohibitive, when large sample numbers were required to be analysed.

The move to nano-LC, coupled with strong, cation, exchange columns (SCX) and reverse phase (RP) separation to permit partitioning of complex cell lysates, was not without its problems. To work within the time limitations and financial constraints of this research project, membrane proteins were not isolated, i.e. proteins that were fundamental in biological processes such as cell signalling. However, the identification and quantification of membrane proteins may be regarded as a different branch of proteomics. The ability to analyse intact proteins, pin-point the region and orientation, along with integration into a membrane, represent enormous challenges that today's researchers face.

6.2 CONCLUSIONS

In conclusion, the holistic experimental approach undertaken in this study identified a number of correlative biomarkers, at the biochemical, morphological, immunological and inter-omic levels, in the human respiratory

epithelia following exposure to TSC. The many findings from this study included:

Key deductions from conventional toxicology:

- A biphasic response was observed when measuring TEER, with low concentrations of the TSC eliciting a large and significant increase in TEER above the control level, followed by a decrease in TEER as the concentration of the TSC increased

- All TSC elicited a similar dose response in cell viability that differed from the membrane resistance in a characteristic manner. In each case, the peak in cell viability occurred at a higher concentration than that required to induce the peak of TEER. After this distinctive peak, cell viability decreased with increasing concentration

- The four TSC induced similar pro-inflammatory cytokine expression profiles, where cadmium and nicotine induced IL-7 expression and formaldehyde and urethane induced IL-2 and IFN-g secretion

- Comparison of the ETM with other (academic and commercial) cell culture systems indicated that it was more impervious to toxicants than single-cell cultures

- A TD_{10} was established for all four TSC exposures to the ETM which disclosed the early protective mechanisms of toxicity

Key deductions from histopathology and IHC:

- H+E staining indicated tissue thickening that coincided with peaks in TEER

- Evidence of cell/tissue hypertrophy was resolved using H+E staining

- The differentiation between secreted protein and cell debris could be elucidated by H+E staining

- The p63 expression profiles were TSC-specific and enabled the clarification of their different modes of action in disease and repair

- Protein 63 expression patterns at the supra-basal tissue region inferred a squamatous metaplastic disease status

- Cytokeratin 5/6 expression was consistently higher at the lowest TSC doses, with the exception of cadmium (versus control), which was suggestive of a protective mechanism

- Morphological analysis at the LM and TEM levels made evident four main pathological cell/tissue states; hyperplasia, hypertrophy, cytolysis, and necrosis

Key deductions from genomics:

- 42 mRNA transcripts were altered significantly by TSC exposure

- Functional group analysis demonstrated a notably high homology when compared to nicotine

- The DNA repair functional group was a prominent feature of the nicotine exposures

- Cadmium, formaldehyde and urethane exposures induced 18 genes by greater than 3-fold

- Nicotine exposures induced 5 genes by greater than 1.5-fold

- Nine genes were identified as potential genomic markers for the early onset of pulmonary injury

- *CYP7A1* and *HMOX1* transcriptomic patterns were specific to nicotine and resolved to be a robust biomarker for tobacco smoke exposure and harm

- Cadmium, formaldehyde and urethane exposures up-regulated *PTGS1* (also known as *COX1*)

Key deductions from proteomics:

- Four hundred and thirteen proteins were verified that had one or more associated peptide identifications

- Two hundred and fifty proteins were resolved to have two or more associated peptide identifications

- Three main protein functionalities were recognised: (i) defence (cystatin-A, ubiquitin and protein plunc precursor), (ii) inflammatory (complement-C3 and protein plunc precursor) and, (iii) structural-development (cornifin-B and calmodulin)

- Nicotine exposure to the ETM induced the highest number of protein changes

- The defence proteins cystatin-A and ubiquitin were consistently induced and observed in all exposures

- Complement-C3, myristoylated alanine-rich protein kinase C substrate and neutrophil gelatinase-associated lipocalin correlated with the tobacco smoking-related disease, atherosclerosis

- Western blotting and antibody detection of the highly-expressed gene, COX1, disclosed that its' expression was not induced at the protein level

6.3 ULTIMATE OBJECTIVE

Inter-omic analysis unveiled unknown functional mechanisms of TSC-induced toxicity (Table 6.1). The dysregulation in responsive lung genes could be correlated with injury mechanisms for a number of pulmonary disorders. Furthermore, the related post-translational modifications in responsive proteins uncovered pathways leading to cardiac disease. It is self-evident that extrapolation of these results to exposures using whole cigarette smoke could induce parallel adverse transcriptional changes. Further classification of the intelligent biomarkers, revealed a preponderance of genes and proteins involved in 'anti-disease' mechanisms; a TD_{10} was employed to examine 'early protective mechanisms' of TSC toxicity and not cell death.

There was no overlap of gene and protein biomarkers, which was understandable, when considering the study utilised a 'stress and toxicology' gene-array and not the full-human genome. Furthermore, the limitations in current proteomic technology, which is still in its infancy of development, should not detract from the utility of searching for protein biomarkers. In these studies, identification of responsive proteins provided complimentary information ('anti-disease' mechanisms) and supplementary information (biomarkers for cardiovascular disease).

6.4 FUTURE WORK

6.4.1 EPIAIRWAY™ TISSUE MODEL

The EpiAirway™ Tissue Model utilised had a 'limited shelf-life', i.e. 72 hours post-conditioning. Regardless of a researcher's country of shipping

Disease	Pro-disease		Anti-disease	
	Gene	Protein	Gene	Protein
Atherosclerosis	CYP7A1 HMOX-1	Complement C3 Calmodulin CD9	CYP2E1 ELK-1 HIF1A	Cystatin-A Ubiquitin MARCKS NGAL
Cytotoxicity	CCND-1 MVT XDH		ABCC1 ABCC2 BAX CYP1A1 MT3 MVP	Cystatin-A Ubiquitin Calmodulin ALDH-2
Carcinogenicity	PPARD	Complement C3	BAX CASP10 CCND-1 CHEK-2 CXCL10 CYP1A1 EGFR MET HGFR	Cystatin-A Ubiquitin
Mutagenicity	CDKN2A CYP1A1		BAX CCND-1 CYP4B1 E2F1	Cystatin-A Ubiquitin Cornifin-B

Table 6.1 Overview of biomarkers identified using inter-omic analysis. A summary of the combined responsive gene and protein biomarkers related to functional mechanisms for the on-set of cardio-pulmonary injury and disease; Sexton *et al.,* (2008)

destination, the model would be posted on a Monday from the USA and arrive 48 hours later via special courier delivery (e.g. arrived in the UK on Wednesdays). The model would need to be used within four days of delivery for optimised viability; this also included a 24 hour pre-conditioning step.

When searching for a suitable dose range, the small experimental window prevented cost-effective searches. The concentration of TSC required to obtain a TD_{10} (in 24 hours) was particularly high, as well as being comparable to a lifetime exposure for certain components. In retrospection, the assessment of membrane integrity and cell viability would have been best evaluated by a gene-specific approach. This approach would utilise a gene previously deemed specific to a particular TSC, as determined by peer-reviewed literature searches. This gene expression would then be monitored via Q-PCR across the dose range. Subsequently, the dose which generated significant TSC-specific gene activity would be employed in impending experiments. This could prove to be a more robust (sensitive) tactic and ascertain practical (i.e. lower) responsive doses when compared to the MTT benchmark.

6.4.2 EXPERIMENTAL DEVELOPEMENT

The tracheo-bronchial mucin assay was not as sensitive/specific as required and it is recommended that further optimisation must be undertaken and/or an alternative method sourced. One particular alternative option for the mucin assay could be the lectin-based mucin assay. The lectin-based assay used a modified standard 'sandwich' immuno-assay and the sensitivity would allow for increased detection and quantification (using a standard spectrophotometer; Jackson et al., 2002).

One of the major functions of epithelial cells is secretion. This critical defensive mechanism is carried out by the release of pro-inflammatory mediators (Gabay and Kushner, 1999; Parsanejad et al., 2008). The Oligo GEArray® Human Toxicology & Drug Resistance Microarray was restrictive in the number of early-response, inflammatory genes such as IL-8 and Osteopontin which it could measure. If there were unlimited funds, it would have been beneficial to of used one of the full-spectrum, human genome, microarray systems for a comprehensive transcriptomic screen.

6.4.3 TOBACCO SMOKE

In a continuation of this work, the human lung tissue model would be re-utilised to examine early genetic responses following exposure to whole tobacco smoke (TS). The objectives would be three-fold: (i) discovery of unknown TS biomarkers, (ii) corroboration of existing biomarkers from this study for further validation of their role in exposure and harm and, (iii) determine whether epigenetic modifications regulated the gene changes accounting for specific biomarker expression. The term 'epigenetics' refers to heritable changes in gene expression without accompanying alterations in DNA sequence. Their misdirection by toxin exposure leads to disease and cancer by distinct mechanisms that appear intricately related in initiating and sustaining epigenetic modifications: micro-RNA mediated silencing, DNA methylation and histone modification. TS induced epigenetic signals would be characterised to dissect-out the precise biological pathway(s) of TS action within the lung environment. The added value of this research workflow would be the unique endpoint data, which lend themselves to dictating clinical and therapeutic directions. This would not be limited to the tobacco sciences and health research but would also impact other forms of ambient aerosol pollutants and health research (e.g. solid and vapour phase components of anthropogenic combustion processes).

REFERENCES

Aardema, M. J., and MacGregor, J. T. (2002). Toxicology and genetic toxicology in the new era of "toxicogenomics": impact of "-omics" technologies. Mutat Res **499**:13-25.

Abbott, A. (1999). The promise of proteomics. Nature **402**:715-720.

Adamek, R., Florek, E., Piekoszewski, W., Anholcer, A., and Kaczmarek, E. (2005). Effect of exposure to tobacco smoke and selected socioeconomic factors in occurrence of low birth weight. Przegl Lek (Article in Polish) **62**:965-9.

Afshari, C. A. (2002). Perspective: microarray technology, seeing more than spots. Endocrinology **143**:1983-9.

Agency for Toxic Substances and Disease Registry 1999 Toxicological profile for cadmium.

Agency for Toxic Substances and Disease Registry 1999 Toxicological profile for formaldehyde. Department of Health and Human Services, Public Health Service.

Agency for Toxic Substances and Disease Registry 2006 Toxicological profile for formaldehyde. Department of Health and Human Services, Public Health Service.

Aggarwal, K., Choe, L. H., and Lee, K. H. (2006). Shotgun proteomics using the iTRAQ isobaric tags. Brief Funct Genomic Proteomic **5**:112-20.

Anderson, P. J., Wilson, J. D., and Hiller, F. C. (1989). Particle size distribution of mainstream tobacco and marijuana smoke. Analysis using the electrical aerosol analyzer. Am Rev Respir Dis **140**:202-5.

Andreoli, C., Gigante, D., and Nunziata, A. (2003). A review of in vitro methods to assess the biological activity of tobacco smoke with the aim of reducing the toxicity of smoke. Toxicol In Vitro **17**:587-94.

Applied Biosystems (2004). www3.appliedbiosystems.com/cms/groups/psm_marketing/documents/generaldo cuments/cms_041463.pdf.

Asero, R. (2007). Etoricoxib challenge in patients with chronic urticaria with NSAID intolerance. Clin Exp Dermatol **32**:661-3.

Ashakumary, L., and Vijayammal, P. (1991). Lipid peroxidation in nicotine treated rats. J. Ecotoxicol. Environ. Monit. **1**:283-290.

Bach, P. 2007. The cost of respiratory medicines in the USA, Cambridge Antibody Technologies.

Balharry, D., Oreffo, V., and Richards, R. (2005). Use of toxicogenomics for identifying genetic markers of pulmonary oedema. Toxicol Appl Pharmacol **204**:101-8.

Balharry, D., Sexton, K., and BeruBe, K. A. (2008). An in vitro approach to assess the toxicity of inhaled tobacco smoke components: nicotine, cadmium, formaldehyde and urethane. Toxicology **244**:66-76.

Barbieri, C. E., and Pietenpol, J. A. (2005). p53 family members: similar biochemistry, different biology. Cancer Biol Ther **4**:419-20.

Baron, J., Burke, J., Guengerick, F., Jakoby, W., and Voight, J. (1988). Sites for xenobiotic activation and detoxication within the respiratory tract: Implications for chemically induced toxicity. Toixicol. Appl. Pharmacol. **93**:493-505.

Beall, J., and Ulsamer, A. (1984). Formaldehyde and hepatotoxicity: a review. J Toxicol Environ Health **14:**1-21.

Ben-Baruch, A. (2006). The multifaceted roles of chemokines in malignancy. Cancer Metastasis Rev **25:**357-71.

Bengtsson, E., Nilsson, J., and Jovinge, S. (2008). Cystatin C and cathepsins in cardiovascular disease. Front Biosci **13:**5780-6.

Bennett, M., Dent, C. L., Ma, Q., Dastrala, S., Grenier, F., Workman, R., Syed, H., Ali, S., Barasch, J., and Devarajan, P. (2008). Urine NGAL predicts severity of acute kidney injury after cardiac surgery: a prospective study. Clin J Am Soc Nephrol **3:**665-73.

Benninger, M. (1999). The impact of cigarette smoking and environmental tobacco smoke on nasal and sinus disease: a review of the literature. Am J Rhinol **13:**435-8.

Benowitz, N., Fitzgerald, G., Wilson, M., and Zhang, Q. (1993). Nicotine effects on eicosanoid formation and hemostatic function: comparison of transdermal nicotine and cigarette smoking. J Am Coll Cardiol **22:**1159-67.

Benowitz, N., Jacob, P., 3rd, Fong, I., and Gupta, S. (1994). Nicotine metabolic profile in man: comparison of cigarette smoking and transdermal nicotine. J. Pharmacol. Exp. Ther. **268:**296-303.

Benowitz, N. L. (1988). Nicotine and smokeless tobacco. CA Cancer J Clin **38:**244-7.

Benson, R., and Beland, F. (1997). Modulation of urethane carcinogenicity by ethyl alcohol. Int J Toxicol **16:**521-544.

Berditchevski, F. (2001). Complexes of tetraspanins with integrins: more than meets the eye. J Cell Sci **114**:4143-51.

Berman, H., Zhang, J., Crawford, Y. G., Gauthier, M. L., Fordyce, C. A., McDermott, K. M., Sigaroudinia, M., Kozakiewicz, K., and Tlsty, T. D. (2005). Genetic and epigenetic changes in mammary epithelial cells identify a subpopulation of cells involved in early carcinogenesis. Cold Spring Harb Symp Quant Biol **70**:317-27.

Berube, K., Balharry, D., Jones, T., Moreno, T., Hayden, P., Sexton, K., Hicks, M., and Merolla, L. 2006. Characterisation of airborne particulate matter and related mechanisms of toxicity: An experimental approach, p. 69-110. *In* R. Maynard (ed.), Air pollution and health, vol. 3. Imperial college press, London.

Bhalla, D. K., Hirata, F., Rishi, A. K., and Gairola, C. G. (2009). Cigarette smoke, inflammation, and lung injury: a mechanistic perspective. J Toxicol Environ Health B Crit Rev **12**:45-64.

Bingle, C. D., and Craven, C. J. (2002). PLUNC: a novel family of candidate host defence proteins expressed in the upper airways and nasopharynx. Hum Mol Genet **11**:937-43.

Bloor, B. K., Seddon, S. V., and Morgan, P. R. (2001). Gene expression of differentiation-specific keratins in oral epithelial dysplasia and squamous cell carcinoma. Oral Oncol **37**:251-61.

Bolt, H. (1987). Experimental toxicology of formaldehyde. J Cancer Res Clin Oncol **113**:305-9.

Bonsack, J. 8/03/1881 1881. Cigarette machine. United States.

Borgerding, M., Bodnar, J., Chung, H., Mangan, P., Morrison, C., Risner, C., Rogers, J., Simmons, D., Uhrig, M., Wendelboe, F., Wingate, D., and Winkler, L. (1998). Chemical and biological studies of a new cigarette that primarily heats tobacco. Part 1. Chemical composition of mainstream smoke. Food Chem Toxicol **36**:169-82.

Borgerding, M., and Klus, H. (2005). Analysis of complex mixtures--cigarette smoke. Exp Toxicol Pathol **57 Suppl 1**:43-73.

Boston Biochem 2005 http://www.bostonbiochem.com/upp.php.

Boyman, O., Purton, J., Surh, C., and Sprent, J. (2007). Cytokines and T-cell homeostasis. Curr Opin Immunol **19**:320-6.

Bradford, M. M. (1976). A rapid and sensitive method for the quantitation of microgram quantities of protein utilizing the principle of protein-dye binding. Anal Biochem **72**:248-54.

Bradley, J., Bacharier, L., Bonfiglio, J., Schechtman, K., Strunk, R., Storch, G., and Castro, M. (2005). Severity of respiratory syncytial virus bronchiolitis is affected by cigarette smoke exposure and atopy. Pediatrics **115**:7-14.

Brandage, S., and Lindblom, L. (1979). The enzyme 'aldehyde oxidase' is an iminium oxidase. Reaction with nicotine delta1'(5') iminium ion. Biochem. Biophys. Res. Commun. **91**:991-996.

Brown and Williamson. 2000. The 1999 Massachusetts benchmark study: A final report. Philip Morris.

Brown, C. P., Spivey, G. H., Valentine, J. L., and Browdy, B. L. (1980). Cigarette smoking and lead levels in occupationally exposed lead workers. J Toxicol Environ Health **6**:877-83.

Bryd, G., Chang, J., and deBethizy, J. (1992). Evidence of urinary excretion of of glucuronide conjugates of nicotine, cotinine and trans-3-hydroxycotinine in smokers. Drug. Metab. Dispos.

Brydun, A., Watari, Y., Yamamoto, Y., Okuhara, K., Teragawa, H., Kono, F., Chayama, K., Oshima, T., and Ozono, R. (2007). Reduced expression of heme oxygenase-1 in patients with coronary atherosclerosis. Hypertens Res **30**:341-8.

Bu, D. X., Hemdahl, A. L., Gabrielsen, A., Fuxe, J., Zhu, C., Eriksson, P., and Yan, Z. Q. (2006). Induction of neutrophil gelatinase-associated lipocalin in vascular injury via activation of nuclear factor-kappaB. Am J Pathol **169**:2245-53.

Bye, A., Langaas, M., Hoydal, M. A., Kemi, O. J., Heinrich, G., Koch, L. G., Britton, S. L., Najjar, S. M., Ellingsen, O., and Wisloff, U. (2008). Aerobic capacity-dependent differences in cardiac gene expression. Physiol Genomics **33**:100-9.

Cai, J., Zhao, Y., Liu, Y., Ye, F., Song, Z., Qin, H., Meng, S., Chen, Y., Zhou, R., Song, X., Guo, Y., Ding, M., and Deng, H. (2007). Directed differentiation of human embryonic stem cells into functional hepatic cells. Hepatology **45**:1229-39.

Camilo, R., Capelozzi, V. L., Siqueira, S. A., and Del Carlo Bernardi, F. (2006). Expression of p63, keratin 5/6, keratin 7, and surfactant-A in non-small cell lung carcinomas. Hum Pathol **37**:542-6.

Cannon, V. T., Barfuss, D. W., and Zalups, R. K. (2000). Molecular homology and the luminal transport of Hg2+ in the renal proximal tubule. J Am Soc Nephrol **11**:394-402.

Cannon, V. T., Zalups, R. K., and Barfuss, D. W. (2001). Amino acid transporters involved in luminal transport of mercuric conjugates of cysteine in rabbit proximal tubule. J Pharmacol Exp Ther **298**:780-9.

Cargile, B. J., Talley, D. L., and Stephenson, J. L., Jr. (2004). Immobilized pH gradients as a first dimension in shotgun proteomics and analysis of the accuracy of pI predictability of peptides. Electrophoresis **25**:936-45.

Carmona-Saez, P., Chagoyen, M., Tirado, F., Carazo, J. M., and Pascual-Montano, A. (2007). GENECODIS: a web-based tool for finding significant concurrent annotations in gene lists. Genome Biol **8**:R3.

Casanova, M., Deyo, D., and Heck, H. (1989). Covalent binding of inhaled formaldehyde to DNA in the nasal mucosa of Fischer 344 rats: analysis of formaldehyde and DNA by high-performance liquid chromatography and provisional pharmacokinetic interpretation. Fundam Appl Toxicol **12**:397-417.

Casanova, M., Heck, H., Everitt, J., Harrington, W., and Popp, J. (1988). Formaldehyde concentrations in the blood of rhesus monkeys after inhalation exposure. Food Chem Toxicol **26**:715-6.

Casanova, M., Morgan, K., Steinhagen, W., Everitt, J., Popp, J., and Heck, H. (1991). Covalent binding of inhaled formaldehyde to DNA in the respiratory tract of rhesus monkeys: pharmacokinetics, rat-to-monkey interspecies scaling, and extrapolation to man. Fundam Appl Toxicol **17**:409-28.

Casanova-Schmitz, M., Starr, T., and Heck, H. (1984). Differentiation between metabolic incorporation and covalent binding in the labeliing of macromolecules

in the rat nasal mucosa and bone marrow by inhaled [14C] and [3H]formaldehyde. Toxicol. Appl. Pharmacol. **76**:26-44.

Cashman, J., Park, S., Yang, Z., Wrighton, S., Jacob, P., 3rd, and Benowitz, N. (1992). Metabolism of nicotine by human liver microsomes: stereoselective formation of trans-nicotine N'-oxide. Chem Res Toxicol **5**:639-46.

Castell, J. V., Donato, M. T., and Gomez-Lechon, M. J. (2005). Metabolism and bioactivation of toxicants in the lung. The in vitro cellular approach. Exp Toxicol Pathol **57 Suppl 1**:189-204.

Chan-Yeung, M., and Dimich-Ward, H. (2003). Respiratory health effects of exposure to environmental tobacco smoke. Respirology **8**:131-9.

Chemuturi, N., Hayden, P., Klausner, M., and Donovan, M. (2004). Presented at the American Association of Pharmaceutical Scientists Annual Meeting, Baltimore, MD.

Chen, K. H., Chang, B. H., Younan, P., Shlykov, S. G., Sanborn, B. M., and Chan, L. (2002). Increased intracellular calcium transients by calmodulin antagonists differentially modulate tumor necrosis factor-alpha-induced E-selectin and ICAM-1 expression. Atherosclerosis **165**:5-13.

Chen, Y., Li, W., and Yu, S. (1986). Influence of passive smoking on admissions for respiratory illness in early childhood. Br Med J (Clin Res Ed) **293**:303-6.

Chilosi, M., Poletti, V., Murer, B., Lestani, M., Cancellieri, A., Montagna, L., Piccoli, P., Cangi, G., Semenzato, G., and Doglioni, C. (2002). Abnormal re-epithelialization and lung remodeling in idiopathic pulmonary fibrosis: the role of deltaN-p63. Lab Invest **82**:1335-45.

Chu, P. G., and Weiss, L. M. (2002). Keratin expression in human tissues and neoplasms. Histopathology **40**:403-39.

Clark, J., Dalbey, W., and Stephenson, K. (1980). Effect of sufur dioxide on the morphology and mucin biosynthesis by the rat trachea. J. Environ. Pathol. Toxicol. **4**:197-207.

Coggins, C. R. (2002). A minireview of chronic animal inhalation studies with mainstream cigarette smoke. Inhal Toxicol **14**:991-1002.

Coggins, C. R. (2007). An updated review of inhalation studies with cigarette smoke in laboratory animals. Int J Toxicol **26**:331-8.

Coggon, D., Harris, E., Poole, J., and Palmer, K. (2003). Extended follow-up of a cohort of british chemical workers exposed to formaldehyde. J Natl Cancer Inst **95**:1608-15.

Cohen, J. C., Cali, J. J., Jelinek, D. F., Mehrabian, M., Sparkes, R. S., Lusis, A. J., Russell, D. W., and Hobbs, H. H. (1992). Cloning of the human cholesterol 7 alpha-hydroxylase gene (CYP7) and localization to chromosome 8q11-q12. Genomics **14**:153-61.

Coles, S., Levine, L., and Reid, L. (1979). Hypersecretion of mucus glycoproteins in rat airways induced by tobacco smoke. Lab. Invest. **97**:459-472.

Comperat, E., Bieche, I., Dargere, D., Ferlicot, S., Laurendeau, I., Benoit, G., Vieillefond, A., Verret, C., Vidaud, M., Capron, F., Bedossa, P., and Paradis, V. (2007). p63 gene expression study and early bladder carcinogenesis. Urology **70**:459-62.

Conrads, T. P., Alving, K., Veenstra, T. D., Belov, M. E., Anderson, G. A., Anderson, D. J., Lipton, M. S., Pasa-Tolic, L., Udseth, H. R., Chrisler, W. B.,

Thrall, B. D., and Smith, R. D. (2001). Quantitative analysis of bacterial and mammalian proteomes using a combination of cysteine affinity tags and 15N-metabolic labeling. Anal Chem **73**:2132-9.

Cook, D., and Strachan, D. (1997). Health effects of passive smoking. 3. Parental smoking and prevalence of respiratory symptoms and asthma in school age children. Thorax **52**:1081-94.

Cook, D., Strachan, D., and Carey, I. (1998). Health effects of passive smoking. 9. Parental smoking and spirometric indices in children. Thorax **53**:884-93.
Cooper, J., and Kini, M. (1962). Biochemical aspects of methanol poisoning. Biochem Pharmacol **11**:405-16.

Cozens, A. L., Yezzi, M. J., Kunzelmann, K., Ohrui, T., Chin, L., Eng, K., Finkbeiner, W. E., Widdicombe, J. H., and Gruenert, D. C. (1994). CFTR expression and chloride secretion in polarized immortal human bronchial epithelial cells. Am J Respir Cell Mol Biol **10**:38-47.

Craft, T., Bermudez, E., and Skopek, T. (1987). Formaldehyde mutagenesis and formation of DNA-protein crosslinks in human lymphoblasts in vitro. Mutat Res **176**:147-55.

Crosby, R., Richardson, K., Craft, T., Benforado, K., Liber, H., and Skopek, T. (1988). Molecular analysis of formaldehyde-induced mutations in human lymphoblasts and E. coli. Environ Mol Mutagen **12**:155-66.

Dani, J., and Heinemann, S. (1996). Molecular and cellular aspects of nicotine abuse. Neuron **16**:905-8.

de Serres, F. J., and Brockman, H. E. (1999). Comparison of the spectra of genetic damage in formaldehyde-induced ad-3 mutations between DNA repair-

proficient and -deficient heterokaryons of Neurospora crassa. Mutat Res **437**:151-63.

de Visser, K. E., Korets, L. V., and Coussens, L. M. (2004). Early neoplastic progression is complement independent. Neoplasia **6**:768-76.

Dellavalle, R. P., Egbert, T. B., Marchbank, A., Su, L. J., Lee, L. A., and Walsh, P. (2001). CUSP/p63 expression in rat and human tissues. J Dermatol Sci **27**:82-7.

deVos, S., Hofmann, W., Grogan, T., Krug, U., Schrage, M., Miller, T., Braun, J., Wachsman, W., Koeffler, H., and aid, J. (2003). Gene expression profile of serial samples of transformed B-cell lymphomas. Lab Invest **83**:271-285.

Duan, M., Yu, L., Savanapridi, C., Jacob, P., 3rd, and Benowitz, N. (1991). Disposition kinetics and metabolism of nicotine-1'-N-oxide in rabbits. Drug Metab Dispos **19**:667-72.

Dunn-Rankin, D. (2006). Presented at the Tobaaco harm reduction and perception of risk, Vienna, Austria.

Elinder, C. G., Lind, B., Kjellstrom, T., Linnman, L., and Friberg, L. (1976). Cadmium in kidney cortex, liver, and pancreas from Swedish autopsies. Estimation of biological half time in kidney cortex, considering calorie intake and smoking habits. Arch Environ Health **31**:292-302.

Emad, A., and Emad, Y. (2007). Increased in CD8 T lymphocytes in the BAL fluid of patients with sulfur mustard gas-induced pulmonary fibrosis. Respir Med **101**:786-92.

Erickson, S. K., Lear, S. R., Deane, S., Dubrac, S., Huling, S. L., Nguyen, L., Bollineni, J. S., Shefer, S., Hyogo, H., Cohen, D. E., Shneider, B., Sehayek, E., Ananthanarayanan, M., Balasubramaniyan, N., Suchy, F. J., Batta, A. K., and Salen, G. (2003). Hypercholesterolemia and changes in lipid and bile acid metabolism in male and female cyp7A1-deficient mice. J Lipid Res **44**:1001-9.

Europa 2001 Proposal for a directive of the eurpean parliment and of the council amending Council Directive 86/609/EEC on the approximation of laws, regulations and administrative provisions of the Member States regarding the protection of animals used for experimental and other scientific purposes.http://europa.eu.int/eurlex/lex/LexUriServ/site/en/com/2001/com2001_0 703en01.pdf

Evans, M., Cox, R., Shami, S., Wilson, B., and Plopper, C. (1989). The role of basal cells in the attachment of columnar cells to the basal lamina of the trachea. Am. J. Respir. Cell. Med. Biol **1**:463-469.

Evans, M., Johnson, L., Stephans, R., and Freeman, G. (1976). Renewal of terminal bronchiolar epithelium in the rat following exposure to NO2 and O3 . Lab. Invest. **35**:246-257.

Fergusson, D., and Horwood, L. (1985). Parental smoking and respiratory illness during early childhood: a six-year longitudinal study. Pediatr Pulmonol **1**:99-106.

Field, K. J., and Lang, C. M. (1988). Hazards of urethane (ethyl carbamate): a review of the literature. Lab Anim **22**:255-62.

Fields, W. R., Leonard, R. M., Odom, P. S., Nordskog, B. K., Ogden, M. W., and Doolittle, D. J. (2005). Gene expression in normal human bronchial

epithelial (NHBE) cells following in vitro exposure to cigarette smoke condensate. Toxicol Sci **86**:84-91.

Fiorentino, D. F., Zlotnik, A., Vieira, P., Mosmann, T. R., Howard, M., Moore, K. W., and O'Garra, A. (1991). IL-10 acts on the antigen-presenting cell to inhibit cytokine production by Th1 cells. J Immunol **146**:3444-51.

Flower, D. R. (1994). The lipocalin protein family: a role in cell regulation. FEBS Lett **354**:7-11.

Folts, J., and Bonebrake, F. (1982). The effects of cigarette smoke and nicotine on platelet thrombus formation in stenosed dog coronary arteries: inhibition with phentolamine. Circulation **65**:465-70.

Fong, P. Y., Xue, W. C., Ngan, H. Y., Chiu, P. M., Chan, K. Y., Tsao, S. W., and Cheung, A. N. (2006). Caspase activity is downregulated in choriocarcinoma: a cDNA array differential expression study. J Clin Pathol **59**:179-83.

Forbes, B., and Ehrhardt, C. (2005). Human respiratory epithelial cell culture for drug delivery applications. Eur J Pharm Biopharm **60**:193-205.

Foster, K. A., Avery, M. L., Yazdanian, M., and Audus, K. L. (2000). Characterization of the Calu-3 cell line as a tool to screen pulmonary drug delivery. Int J Pharm **208**:1-11.

Fowler, R. (1954). Redetermination of ionisation constants of nicotine. J. Appl. Chem. **4**:449-452.

Franklin, R. A., Rodriguez-Mora, O. G., Lahair, M. M., and McCubrey, J. A. (2006). Activation of the calcium/calmodulin-dependent protein kinases as a consequence of oxidative stress. Antioxid Redox Signal **8**:1807-17.

Gamble, W. (2006). Atherosclerosis: the carbonic anhydrase, carbon dioxide, calcium concerted theory. J Theor Biol **239**:16-21.

Geertinger, P., and Sorensen, H. (1973). Complement and arteriosclerosis. Atherosclerosis **18**:65-71.

Gerlach, K., Cummings, K., Hyland, A., and Giplin, E. (1998). Presented at the Health effects and trends, Bethesda, MD.

Germann, W., and Stanfield, C. 2004. Principles of Human Physiology, Principles of Human Physiology. Benjamin Cummings, New York.

Gething, M. J., Blond-Elguindi, S., Buchner, J., Fourie, A., Knarr, G., Modrow, S., Nanu, L., Segal, M., and Sambrook, J. (1995). Binding sites for Hsp70 molecular chaperones in natural proteins. Cold Spring Harb Symp Quant Biol **60**:417-28.

Glover, E., and Glover, P. (1992). The smokeless tobacco problem: Risk groups in North America. Presented at the Smokeless Tobacco, Bethesda, MD.

Gluckmann, M., Fella, K., Waidelich, D., Merkel, D., Kruft, V., Kramer, P. J., Walter, Y., Hellmann, J., Karas, M., and Kroger, M. (2007). Prevalidation of potential protein biomarkers in toxicology using iTRAQ reagent technology. Proteomics **7**:1564-74.

Gomperts, B. N., Belperio, J. A., Fishbein, M. C., Keane, M. P., Burdick, M. D., and Strieter, R. M. (2007). Keratinocyte growth factor improves repair in the injured tracheal epithelium. Am J Respir Cell Mol Biol **37**:48-56.

Gonzales, F. (1998). The study of xenobiotic-metabolising enzymes and their role in toxicity in vivo using targeted gene disruption. Toxicol Lett **102-103**:161-166.

Gonzales, F., and Kimura, S. (1999). Role of gene knockout mice in understanding the mechanisms of chemical toxicity and carcinogenesis. Cancer Lett **143**:199-204.

Grainger, C. I., Greenwell, L. L., Lockley, D. J., Martin, G. P., and Forbes, B. (2006). Culture of Calu-3 cells at the air interface provides a representative model of the airway epithelial barrier. Pharm Res **23**:1482-90.

Gray, A. C., McLeod, J. D., and Clothier, R. H. (2007). A review of in vitro modelling approaches to the identification and modulation of squamous metaplasia in the human tracheobronchial epithelium. Altern Lab Anim **35**:493-504.

Green, C. R., and Rodgman, A. (1996). The tobacco chemists' research conference; A half century of advances in analytical methodology of tobacco and its products. Recent Adv. Tob. Sci. **22**:131-304.

Greenbaum, D., Colangelo, C., Williams, K., and Gerstein, M. (2003). Comparing protein abundance and mRNA expression levels on a genomic scale. Genome Biol **4**:117.

Greenwell, L., Carthew, P., Westmoreland, C., and Fentem, J. (2005). Presented at the 5th World Congress on Alternatives and Animal Use in the Life Sciences, Berlin, Germany.

Griendling, K. K., and FitzGerald, G. A. (2003). Oxidative stress and cardiovascular injury: Part I: basic mechanisms and in vivo monitoring of ROS. Circulation **108**:1912-6.

Gruenert, D. C., Finkbeiner, W. E., and Widdicombe, J. H. (1995). Culture and transformation of human airway epithelial cells. Am J Physiol **268**:L347-60.

Grune, T., Merker, K., Jung, T., Sitte, N., and Davies, K. J. (2005). Protein oxidation and degradation during postmitotic senescence. Free Radic Biol Med **39**:1208-15.

Grune, T., Reinheckel, T., Joshi, M., and Davies, K. J. (1995). Proteolysis in cultured liver epithelial cells during oxidative stress. Role of the multicatalytic proteinase complex, proteasome. J Biol Chem **270**:2344-51.

Guo, Y., Singleton, P. A., Rowshan, A., Gucek, M., Cole, R. N., Graham, D. R., Van Eyk, J. E., and Garcia, J. G. (2007). Quantitative proteomics analysis of human endothelial cell membrane rafts: evidence of MARCKS and MRP regulation in the sphingosine 1-phosphate-induced barrier enhancement. Mol Cell Proteomics **6**:689-96.

Gupta, R., and Dani, H. M. (1989). In vitro formation of organ-specific ultimate carcinogens of 4-dimethylaminoazobenzene and urethan by microsomes. Toxicol Lett **45**:49-54.

Gusbin, N., Garzaniti, N., and Louis, R. (2006). Asthma and tobacco. Rev Med Liege (Article in French) **61**:81-6.

Gustafson, P., Barregard, L., Strandberg, B., and Sallsten, G. (2007). The impact of domestic wood burning on personal, indoor and outdoor levels of 1,3-butadiene, benzene, formaldehyde and acetaldehyde. J Environ Monit **9**:23-32.

Gutierrez-Castillo, M., Roubicek, D., and Cebrian-Garcia, M. (2006). Effect of chemical composition on the induction of DNA damage by urban airborne particulate matter. Environ Mol Mutagen **47**:199-211.

Gwira, J. A., Wei, F., Ishibe, S., Ueland, J. M., Barasch, J., and Cantley, L. G. (2005). Expression of neutrophil gelatinase-associated lipocalin regulates epithelial morphogenesis in vitro. J Biol Chem **280**:7875-82.

Hanash, S. (2003). Disease proteomics. Nature **422**:226-32.

Hansen, J., and Olsen, J. (1995). Formaldehyde and cancer morbidity among male employees in Denmark. Cancer Causes Control **6**:354-60.

Hansen, T., Seidel, A., and Borlak, J. (2007). The environmental carcinogen 3-nitrobenzanthrone and its main metabolite 3-aminobenzanthrone enhance formation of reactive oxygen intermediates in human A549 lung epithelial cells. Toxicol Appl Pharmacol **221**:222-34.

Haslett, C. (1999). Granulocyte apoptosis and its role in the resolution and control of lung inflammation. Am J Respir Crit Care Med **160**:S5-11.

Hauptmann, M., Lubin, J., Stewart, P., Hayes, R., and Blair, A. (2004). Mortality from solid cancers among workers in formaldehyde industries. Am J Epidemiol **159**:1117-30.

Hawse, J. R., Padgaonkar, V. A., Leverenz, V. R., Pelliccia, S. E., Kantorow, M., and Giblin, F. J. (2006). The role of metallothionein IIa in defending lens

epithelial cells against cadmium and TBHP induced oxidative stress. Mol Vis
12:342-9.

Hayden, P., Bolmarcich, J., Stolper, G., Jackson, G., and Klausner, M.
(2006). Presented at the American Thoracic Society Meeting, San Diego, CA.

Hayes, R., Blair, A., Stewart, P., Herrick, R., and Mahar, H. (1990). Mortality of
U.S. embalmers and funeral directors. Am J Ind Med **18**:641-52.

Heck, H., and Casanova, M. (2004). The implausibility of leukemia induction by
formaldehyde: a critical review of the biological evidence on distant-site toxicity.
Regul Toxicol Pharmacol **40**:92-106.

**Heck, H., Casanova-Schmitz, M., Dodd, P., Schachter, E., Witek, T., and
Tosun, T.** (1985). Formaldehyde (CH_2O) concentrations in the blood of humans
and Fischer-344 rats exposed to CH_2O under controlled conditions. Am Ind Hyg
Assoc J **46**:1-3.

Heck, H., Chin, T., and Schmitz, M. (1983). Presented at the Formaldehyde
toxicity, Washington, DC.

Heck, H., White, E., and Casanova-Schmitz, M. (1982). Determination of
formaldehyde in biological tissues by gas chromatography/mass spectrometry.
Biomed Mass Spectrom **9**:347-53.

Hellberg, D., and Stendahl, U. (2005). The biological role of smoking, oral
contraceptive use and endogenous sexual steroid hormones in invasive
squamous epithelial cervical cancer. Anticancer Res **25**:3041-6.

Henry, C. (2002). Genomics and the chemical industry.
http://dels.nas.edu/emergingissues/docs/Henry.pdf

Henson, P. M., Bratton, D. L., and Fadok, V. A. (2001). Apoptotic cell removal. Curr Biol **11:**R795-805.

Hermanns, M. I., Unger, R. E., Kehe, K., Peters, K., and Kirkpatrick, C. J. (2004). Lung epithelial cell lines in coculture with human pulmonary microvascular endothelial cells: development of an alveolo-capillary barrier in vitro. Lab Invest **84:**736-52.

Hernandez-Vargas, H., Rodriguez-Pinilla, S. M., Julian-Tendero, M., Sanchez-Rovira, P., Cuevas, C., Anton, A., Rios, M. J., Palacios, J., and Moreno-Bueno, G. (2007). Gene expression profiling of breast cancer cells in response to gemcitabine: NF-kappaB pathway activation as a potential mechanism of resistance. Breast Cancer Res Treat **102:**157-72.

Herrmann, J., Edwards, W. D., Holmes, D. R., Jr., Shogren, K. L., Lerman, L. O., Ciechanover, A., and Lerman, A. (2002). Increased ubiquitin immunoreactivity in unstable atherosclerotic plaques associated with acute coronary syndromes. J Am Coll Cardiol **40:**1919-27.

Hoffler, U., El-Masri, H. A., and Ghanayem, B. I. (2003). Cytochrome P450 2E1 (CYP2E1) is the principal enzyme responsible for urethane metabolism: comparative studies using CYP2E1-null and wild-type mice. J Pharmacol Exp Ther **305:**557-64.

Hong, K. U., Reynolds, S. D., Watkins, S., Fuchs, E., and Stripp, B. R. (2004). In vivo differentiation potential of tracheal basal cells: evidence for multipotent and unipotent subpopulations. Am J Physiol Lung Cell Mol Physiol **286:**L643-9.

http://www.lotrel.com (2005). Understanding hypertension.

Hukkanen, J., Gourlay, S., Kenkare, S., and Benowitz, N. (2005). Influence of menstrual cycle on cytochrome P450 2A6 activity and cardiovascular effects of nicotine. Clin Pharmacol Ther **77**:159-69.

Hukkanen, J., Jacob, P., 3rd, and Benowitz, N. L. (2005). Metabolism and disposition kinetics of nicotine. Pharmacol Rev **57**:79-115.

Hunter, T. C., Andon, N. L., Koller, A., Yates, J. R., and Haynes, P. A. (2002). The functional proteomics toolbox: methods and applications. J Chromatogr B Analyt Technol Biomed Life Sci **782**:165-81.

IARC. (1993). Beryllium, Cadmium, Mercury and exposures in glass manufacturing industry. Monographs on the evaluation of carcinogenic risk of chemicals to humans **58**.

IARC. (1982). Formaldehyde. Monographs on the evaluation of carcinogenic risk of chemicals to humans **29**:345-389.

IARC. (1974). Monographs on the evaluation of the carcinogenic risk of chemicals to man:. **7**:111-140.

IARC. (1987). Overall evaluation of carcinogenicity. Updating monographs volumes 1-42 **Supp 7**.

IARC. (2005). Preamble to the IARC monographs. http://monographs.iarc.

IARC. (2004). Tobacco smoke and involuntary smoking. IARC monographs on the evaluation of carcinogenic risks to humans **83**.

IARC. (1986a). Tobacco smoking. IARC Monographs on the evaluation of carcinogenic risk of chemicals to humans **38**.

IARC. (1995). Wood dust and formaldehyde. Monographs on the evaluation of carcinogenic risk of chemicals to humans **62**:217-375.

ICCVAM 2001 Report of the international workshop on in vitro methods for assessing acute systemic toxicity.
http://iccvam.niehs.nih.gov/methods/invidocs/finalall.pdf

ICCVAM 1993 Revitalization act of 1993 "Plan for use of Animals in research". [Online] http://iccvam.niehs.nih.gov/about/pl103_43.pdf

Imaoka, S., Yoneda, Y., Sugimoto, T., Ikemoto, S., Hiroi, T., Yamamoto, K., Nakatani, T., and Funae, Y. (2001). Androgen regulation of CYP4B1 responsible for mutagenic activation of bladder carcinogens in the rat bladder: detection of CYP4B1 mRNA by competitive reverse transcription-polymerase chain reaction. Cancer Lett **166**:119-23.

Innes, A. L., Woodruff, P. G., Ferrando, R. E., Donnelly, S., Dolganov, G. M., Lazarus, S. C., and Fahy, J. V. (2006). Epithelial mucin stores are increased in the large airways of smokers with airflow obstruction. Chest **130**:1102-8.

Inoue, D., Kubo, H., Watanabe, M., Sasaki, T., Yasuda, H., Numasaki, M., Sasaki, H., and Yamaya, M. (2008). Submucosal gland cells in human lower airways produce MUC5AC protein. Respirology **13**:285-7.

Jackson, A., Kemp, P., Giddings, J., and Sugar, R. (2002). Development and validation of a lectin-based assay for the quantitation of rat respiratory mucin. Novartis Found Symp **248**:94-105; discussion 106-12, 277-82.

Jenkins, R., Guerin, M., and Tomkins, B. 2000. Minstream and sidestream smoke, 2nd ed. Lewis Publishers, FL.

Jennings, L. K., Fox, C. F., Kouns, W. C., McKay, C. P., Ballou, L. R., and Schultz, H. E. (1990). The activation of human platelets mediated by anti-human platelet p24/CD9 monoclonal antibodies. J Biol Chem **265**:3815-22.

Jermini, C., Weber, A., and Grandjean, E. (1976). Quantitative determination of various gas-phase components of the side-stream smoke of cigarettes in the room air as a contribution to the problem of passive-smoking (author's transl). Int Arch Occup Environ Health **36**:169-81.

Jiang, G., Li, T., Qiu, Y., Rui, Y., Chen, W., and Lou, Y. (2007). RNA interference for HIF-1alpha inhibits foam cells formation in vitro. Eur J Pharmacol **562**:183-90.

Jin, T., Lu, J., and Nordberg, M. (1998). Toxicokinetics and biochemistry of cadmium with special emphasis on the role of metallothionein. Neurotoxicology **19**:529-35.

Jin, Z., May, W. S., Gao, F., Flagg, T., and Deng, X. (2006). Bcl2 suppresses DNA repair by enhancing c-Myc transcriptional activity. J Biol Chem **281**:14446-56.

Johnson, W. R., Hale, R. W., Clough, S. C., and Chen, P. H. (1973). Chemistry of the conversion of nitrate nitrogen to smoke products. Nature **243**:223-5.

Joo Lee, E., Ho In, K., Hyeong Kim, J., Yeub Lee, S., Shin, C., Jeong Shim, J., Ho Kang, K., Hwa Yoo, S., Hwan Kim, C., Kim, H. K., Lee, S. H., and Sub Uhm, C. (2008). Proteomic Analysis in Lung Tissue of Smokers and Chronic Obstructive Pulmonary Disease Patients. Chest.

Jumarie, C. (2002). Cadmium transport through type II alveolar cell monolayers: contribution of transcellular and paracellular pathways in the rat ATII and the human A549 cells. Biochim Biophys Acta **1564**:487-99.

Kagi, J. H., and Schaffer, A. (1988). Biochemistry of metallothionein. Biochemistry **27**:8509-15.

Kakazu, A., Chandrasekher, G., and Bazan, H. E. (2004). HGF protects corneal epithelial cells from apoptosis by the PI-3K/Akt-1/Bad- but not the ERK1/2-mediated signaling pathway. Invest Ophthalmol Vis Sci **45**:3485-92.

Karas, M., and Hillenkamp, F. (1988). Laser desorption ionization of proteins with molecular masses exceeding 10,000 daltons. Anal Chem **60**:2299-301.

Kehinde, E. O., Maghrebi, M. A., and Anim, J. T. (2008). The importance of determining the aggressiveness of prostate cancer using serum and tissue molecular markers. Can J Urol **15**:3967-74.

Kemp, P. A., Sugar, R. A., and Jackson, A. D. (2004). Nucleotide-mediated mucin secretion from differentiated human bronchial epithelial cells. Am J Respir Cell Mol Biol **31**:446-55.

Kennedy, R. T., Oates, M. D., Cooper, B. R., Nickerson, B., and Jorgenson, J. W. (1989). Microcolumn separations and the analysis of single cells. Science **246**:57-63.

Kennedy, S. (2001). Proteomic profiling from human samples: the body fluid alternative. Toxicology Letters **120**.

Kerns, W., Pavkov, K., Donofrio, D., Gralla, E., and Swenberg, J. (1983). Carcinogenicity of formaldehyde in rats and mice after long-term inhalation exposure. Cancer Res **43**:4382-92.

Kershbaum, A., and Bellet, S. (1964). Cigarette Smoking and Blood Lipids. Jama **187**:32-6.

Kesimer, M., Kirkham, S., Pickles, R. J., Henderson, A. G., Alexis, N. E., Demaria, G., Knight, D., Thornton, D. J., and Sheehan, J. K. (2009). Tracheobronchial air-liquid interface cell culture: a model for innate mucosal defense of the upper airways? Am J Physiol Lung Cell Mol Physiol **296**:L92-L100.

Kilaru, S., Frangos, S., Chen, A., Gortler, D., Dhadwal, A., Araim, O., and Sumpio, B. (2001). Nicotine: a review of its role in atherosclerosis. J Am Coll Surg **193**:538-46.

Koller, M., and Strehler, E. E. (1993). Functional analysis of the promoters of the human CaMIII calmodulin gene and of the intronless gene coding for a calmodulin-like protein. Biochim Biophys Acta **1163**:1-9.

Kowalski, M. P., Dubouix-Bourandy, A., Bajmoczi, M., Golan, D. E., Zaidi, T., Coutinho-Sledge, Y. S., Gygi, M. P., Gygi, S. P., Wiemer, E. A., and Pier, G. B. (2007). Host resistance to lung infection mediated by major vault protein in epithelial cells. Science **317**:130-2.

Kvasnicka, F. (2003). Proteomics: general strategies and application to nutritionally relevant proteins. J Chromatogr B Analyt Technol Biomed Life Sci **787**:77-89.

Lam, C. F., Caterina, P., Filion, P., van Heerden, P. V., and Ilett, K. F. (2002). The ratio of polymorphonuclear leucocytes (PMN) to non-PMN cells - a novel method of assessing acute lung inflammation. Exp Toxicol Pathol **54**:187-91.

Lee, H., Griffin, T. J., Gygi, S. P., Rist, B., and Aebersold, R. (2002). Development of a multiplexed microcapillary liquid chromatography system for high-throughput proteome analysis. Anal Chem **74**:4353-60.

Lee, H., Guo, H., Lee, S., Jeon, B., Jun, C., Lee, S., Park, M., and Kim, E. (2005). Effects of nicotine on proliferation, cell cycle, and differentiation in immortalized and malignant oral keratinocytes. J Oral Pathol Med **34**:436-43.

Lee, Y. C., Chuang, C. Y., Lee, P. K., Lee, J. S., Harper, R. W., Buckpitt, A. B., Wu, R., and Oslund, K. (2008). TRX-ASK1-JNK signaling regulation of cell density-dependent cytotoxicity in cigarette smoke-exposed human bronchial epithelial cells. Am J Physiol Lung Cell Mol Physiol **294**:L921-31.

Lestari, F., Hayes, A., Green, A., and Markovic, B. (2005). In vitro cytotoxicity of selected chemicals commonly produced during fire combustion using human cell lines. Toxicol In Vitro **19**:653-63.

Lieber, C. S. (1997). Cytochrome P-4502E1: its physiological and pathological role. Physiol Rev **77**:517-44.

Liebler, D. 2002. Introduction to Proteomics Tools for the New Biology. Humana Press Inc.

Liefer, K. M., Koster, M. I., Wang, X. J., Yang, A., McKeon, F., and Roop, D. R. (2000). Down-regulation of p63 is required for epidermal UV-B-induced apoptosis. Cancer Res **60**:4016-20.

Lindahl, M., Stahlbom, B., and Tagesson, C. (2001). Identification of a new potential airway irritation marker, palate lung nasal epithelial clone protein, in human nasal lavage fluid with two-dimensional electrophoresis and matrix-assisted laser desorption/ionization-time of flight. Electrophoresis **22:**1795-800.

Liotta, L. A., Ferrari, M., and Petricoin, E. (2003). Clinical proteomics: written in blood. Nature **425:**905.

Lutgens, S. P., Cleutjens, K. B., Daemen, M. J., and Heeneman, S. (2007). Cathepsin cysteine proteases in cardiovascular disease. Faseb J **21:**3029-41.

MacNee, W. (2001). Oxidative stress and lung inflammation in airways disease. Eur J Pharmacol **429:**195-207.

Madara, J. L. (1998). Regulation of the movement of solutes across tight junctions. Annu Rev Physiol **60:**143-59.

Maecker, H. T., Todd, S. C., and Levy, S. (1997). The tetraspanin superfamily: molecular facilitators. Faseb J **11:**428-42.

Malard, V., Prat, O., Darrouzet, E., Berenguer, F., Sage, N., and Quemeneur, E. (2005). Proteomic analysis of the response of human lung cells to uranium. Proteomics **5:**4568-80.

Manca, D., Ricard, A. C., Tra, H. V., and Chevalier, G. (1994). Relation between lipid peroxidation and inflammation in the pulmonary toxicity of cadmium. Arch Toxicol **68:**364-9.

Martey, C. A., Pollock, S. J., Turner, C. K., O'Reilly, K. M., Baglole, C. J., Phipps, R. P., and Sime, P. J. (2004). Cigarette smoke induces cyclooxygenase-2 and microsomal prostaglandin E2 synthase in human lung

fibroblasts: implications for lung inflammation and cancer. Am J Physiol Lung Cell Mol Physiol **287**:L981-91.

Mathia, N. R., Timoszyk, J., Stetsko, P. I., Megill, J. R., Smith, R. L., and Wall, D. A. (2002). Permeability characteristics of calu-3 human bronchial epithelial cells: in vitro-in vivo correlation to predict lung absorption in rats. J Drug Target **10**:31-40.

Mauderly, J. L. (1993). Toxicological approaches to complex mixtures. Environ Health Perspect **101 Suppl 4**:155-65.

Maunders, H., Patwardhan, S., Phillips, J., Clack, A., and Richter, A. (2007). Human bronchial epithelial cell transcriptome: gene expression changes following acute exposure to whole cigarette smoke in vitro. Am J Physiol Lung Cell Mol Physiol **292**:L1248-56.

McBride, W. H., Iwamoto, K. S., Syljuasen, R., Pervan, M., and Pajonk, F. (2003). The role of the ubiquitin/proteasome system in cellular responses to radiation. Oncogene **22**:5755-73.

McDowell, E. M., Becci, P. J., Schurch, W., and Trump, B. F. (1979). The respiratory epithelium. VII. Epidermoid metaplasia of hamster tracheal epithelium during regeneration following mechanical injury. J Natl Cancer Inst **62**:995-1008.

McKennis, H., Turnbull, L., and Bowman, E. (1963). N-Methylation of nicotine ad cotinine in vivo. J Biol Chem **238**:719-23.

Meier, C. R., Schmitz, S., and Jick, H. (2002). Association between acetaminophen or nonsteroidal antiinflammatory drugs and risk of developing ovarian, breast, or colon cancer. Pharmacotherapy **22**:303-9.

Melnick, R. L. (2002). Carcinogenicity and mechanistic insights on the behavior of epoxides and epoxide-forming chemicals. Ann N Y Acad Sci **982**:177-89.

Merk, O., and Speit, G. (1998). Significance of formaldehyde-induced DNA-protein crosslinks for mutagenesis. Environ Mol Mutagen **32**:260-8.

Messina, E., Tyndale, R., and Sellers, E. (1997). A major role for CYP2A6 in nicotine C-oxidation by human liver microsomes. J Pharmacol Exp Ther **282**:1608-14.

Millard, P. J., Roth, B. L., Thi, H. P., Yue, S. T., and Haugland, R. P. (1997). Development of the FUN-1 family of fluorescent probes for vacuole labeling and viability testing of yeasts. Appl Environ Microbiol **63**:2897-905.

Miller, W. J., Blackmon, D. M., Gentry, R. P., and Pate, F. M. (1969). Effect of dietary cadmium on tissue distribution of 109cadmium following a single oral dose in young goats. J Dairy Sci **52**:2029-35.

Minamoto, K., Harada, H., Lama, V. N., Fedarau, M. A., and Pinsky, D. J. (2005). Reciprocal regulation of airway rejection by the inducible gas-forming enzymes heme oxygenase and nitric oxide synthase. J Exp Med **202**:283-94.

Moniaux, N., Chakraborty, S., Yalniz, M., Gonzalez, J., Shostrom, V. K., Standop, J., Lele, S. M., Ouellette, M., Pour, P. M., Sasson, A. R., Brand, R. E., Hollingsworth, M. A., Jain, M., and Batra, S. K. (2008). Early diagnosis of pancreatic cancer: neutrophil gelatinase-associated lipocalin as a marker of pancreatic intraepithelial neoplasia. Br J Cancer **98**:1540-7.

Moore, W., Jr., Stara, J. F., and Crocker, W. C. (1973). Gastrointestinal absorption of different compounds of 115m cadmium and the effect of different concentrations in the rat. Environ Res **6**:159-64.

Morselt, A. F. (1991). Environmental pollutants and diseases. A cell biological approach using chronic cadmium exposure in the animal model as a paradigm case. Toxicology **70**:1-132.

Muller-Eberhard, H. J. (1988). Molecular organization and function of the complement system. Annu Rev Biochem **57**:321-47.

Murarescu, E. D., Iancu, R., and Mihailovici, M. S. (2007). Morphological changes positive correlates with oxidative stress in COPD. Preliminary data of an experimental rat model--study and literature review. Rom J Morphol Embryol **48**:59-65.

Nakajima, M., Yamamoto, T., Nunoya, K., Yokoi, T., Nagashima, K., Inoue, K., Funae, Y., Shimada, N., Kamataki, T., and Kuroiwa, Y. (1996). Role of human cytochrome P4502A6 in C-oxidation of nicotine. Drug Metab Dispos **24**:1212-7.

Nakamura, H., Kawasaki, N., Taguchi, M., and Kato, H. (2007). Epidermal growth factor receptor gene mutations in early pulmonary adenocarcinomas. Ann Thorac Cardiovasc Surg **13**:87-92.

National Institutes of Health 2000 The National Toxicology Program's 9th Report on Carcinogens. www.nih.gov/news/pr/may2000/niehs-15.htm

National Toxicology Program 2000 Ethyl carbamate. http://ntp.niehs.nih.gov/

Nebert, D. W., and Dalton, T. P. (2006). The role of cytochrome P450 enzymes in endogenous signalling pathways and environmental carcinogenesis. Nat Rev Cancer **6**:947-60.

Nettleship, A., Henshaw, P., and Meyer, H. (1943). Induction of pulmonary tumours in mice with ethyl carbamate J Natl Cancer Inst **4**:309-319.

Nevanlinna, H., and Bartek, J. (2006). The CHEK2 gene and inherited breast cancer susceptibility. Oncogene **25**:5912-9.

Nicholas, B., Skipp, P., Mould, R., Rennard, S., Davies, D. E., O'Connor, C. D., and Djukanovic, R. (2006). Shotgun proteomic analysis of human-induced sputum. Proteomics **6**:4390-401.

Norman, M., Holly, E., Ahn, D., Preston-Martin, S., Mueller, B., and Bracci, P. (1996). Prenatal exposure to tobacco smoke and childhood brain tumors: results from the United States West Coast childhood brain tumor study. Cancer Epidemiol Biomarkers Prev **5**:127-33.

Oberdorster, G. (1992). Pulmonary deposition, clearance and effects of inhaled soluble and insoluble cadmium compounds. IARC Sci Publ:189-204.

O'Connor, R. (2007). The pharmacology of cancer resistance. Anticancer Res **27**:1267-72.

O'Donovan, C., Martin, M. J., Gattiker, A., Gasteiger, E., Bairoch, A., and Apweiler, R. (2002). High-quality protein knowledge resource: SWISS-PROT and TrEMBL. Brief Bioinform **3**:275-84.

Olden, K. (2004). Genomics in environmental health research--opportunities and challenges. Toxicology **198**:19-24.

Olivieri, M., Bodini, A., Peroni, D. G., Costella, S., Pacifici, R., Piacentini, G. L., Boner, A. L., and Zuccaro, P. (2006). Passive smoking in asthmatic children: effect of a "smoke-free house" measured by urinary cotinine levels. Allergy Asthma Proc **27**:350-3.

Ouchi, N., Kihara, S., Yamashita, S., Higashiyama, S., Nakagawa, T., Shimomura, I., Funahashi, T., Kameda-Takemura, K., Kawata, S., Taniguchi, N., and Matsuzawa, Y. (1997). Role of membrane-anchored heparin-binding epidermal growth factor-like growth factor and CD9 on macrophages. Biochem J **328 (Pt 3)**:923-8.

Padar, S., Bose, D. D., Livesey, J. C., and Thomas, D. W. (2005). 2-Aminoethoxydiphenyl borate perturbs hormone-sensitive calcium stores and blocks store-operated calcium influx pathways independent of cytoskeletal disruption in human A549 lung cancer cells. Biochem Pharmacol **69**:1177-86.

Palmer, K., Hitt, M., Emtage, P. C., Gyorffy, S., and Gauldie, J. (2001). Combined CXC chemokine and interleukin-12 gene transfer enhances antitumor immunity. Gene Ther **8**:282-90.

Pan, J., Chen, H. Q., Sun, Y. H., Zhang, J. H., and Luo, X. Y. (2008). Comparative proteomic analysis of non-small-cell lung cancer and normal controls using serum label-free quantitative shotgun technology. Lung **186**:255-61.

Pandey, A., and Mann, M. (2000). Proteomics to study genes and genomes. Nature **405**:837-46.

Park, G. Y., and Christman, J. W. (2006). Involvement of cyclooxygenase-2 and prostaglandins in the molecular pathogenesis of inflammatory lung diseases. Am J Physiol Lung Cell Mol Physiol **290**:L797-805.

Park, J., Fang, S., Crews, A. L., Lin, K. W., and Adler, K. B. (2008). MARCKS regulation of mucin secretion by airway epithelium in vitro: interaction with chaperones. Am J Respir Cell Mol Biol **39**:68-76.

Park, J. Y., Pillinger, M. H., and Abramson, S. B. (2006). Prostaglandin E2 synthesis and secretion: the role of PGE2 synthases. Clin Immunol **119**:229-40.

Park, S., Jacob, P., 3rd, Benowitz, N., and Cashman, J. (1993). Stereoselective metabolism of (S)-(-)-nicotine in humans: formation of trans-(S)-(-)-nicotine N-1'-oxide. Chem Res Toxicol **6**:880-8.

Parke, D. V., and Sapota, A. (1996). Chemical toxicity and reactive oxygen species. Int J Occup Med Environ Health **9**:331-40.

Parker, B. S., Ciocca, D. R., Bidwell, B. N., Gago, F. E., Fanelli, M. A., George, J., Slavin, J. L., Moller, A., Steel, R., Pouliot, N., Eckhardt, B. L., Henderson, M. A., and Anderson, R. L. (2008). Primary tumour expression of the cysteine cathepsin inhibitor Stefin A inhibits distant metastasis in breast cancer. J Pathol **214**:337-46.

Pellegrini, G., Dellambra, E., Golisano, O., Martinelli, E., Fantozzi, I., Bondanza, S., Ponzin, D., McKeon, F., and De Luca, M. (2001). p63 identifies keratinocyte stem cells. Proc Natl Acad Sci U S A **98**:3156-61.

Penn, A., Murphy, G., Barker, S., Henk, W., and Penn, L. (2005). Combustion-derived ultrafine particles transport organic toxicants to target respiratory cells. Environ Health Perspect **113**:956-63.

Pennie, W. D. (2000). Use of cDNA microarrays to probe and understand the toxicological consequences of altered gene expression. Toxicol Lett **112-113**:473-7.

Pennie, W. D., and Kimber, I. (2002). Toxicogenomics; transcript profiling and potential application to chemical allergy. Toxicol In Vitro **16**:319-26.

Pennie, W. D., Tugwood, J. D., Oliver, G. J., and Kimber, I. (2000). The principles and practice of toxigenomics: applications and opportunities. Toxicol Sci **54**:277-83.

Pera, M., Manterola, C., Vidal, O., and Grande, L. (2005). Epidemiology of esophageal adenocarcinoma. J Surg Oncol **92**:151-9.

Permana, P., and Snapka, R. (1994). Aldehyde-induced protein-DNA crosslinks disrupt specific stages of SV40 DNA replication. Carcinogenesis **15**:1031-6.

Peters, E. J., Morice, R., Benner, S. E., Lippman, S., Lukeman, J., Lee, J. S., Ro, J. Y., and Hong, W. K. (1993). Squamous metaplasia of the bronchial mucosa and its relationship to smoking. Chest **103**:1429-32.

Peyton, J., Benowitz, N., and Shulgin, A. (1988). Recent studies of nicotine metabolism in humans. Pharmacol. Biochem. Behav. **30**:131-141.

Pfueller, S. L., Burns, P., Mak, K., and Firkin, B. G. (1988). Effects of nicotine on platelet function. Haemostasis **18**:163-9.

Pierce, G. F., Yanagihara, D., Klopchin, K., Danilenko, D. M., Hsu, E., Kenney, W. C., and Morris, C. F. (1994). Stimulation of all epithelial elements during skin regeneration by keratinocyte growth factor. J Exp Med **179**:831-40.

Pinkerton, L. E., Hein, M. J., and Stayner, L. T. (2004). Mortality among a cohort of garment workers exposed to formaldehyde: an update. Occup Environ Med **61**:193-200.

Pinot, F., Kreps, S. E., Bachelet, M., Hainaut, P., Bakonyi, M., and Polla, B. S. (2000). Cadmium in the environment: sources, mechanisms of biotoxicity, and biomarkers. Rev Environ Health **15**:299-323.

Pinot, F., Kreps, S. E., Bachelet, M., Hainaut, P., Bakonyi, M., and Polla, B. S. (2000). Cadmium in the environment: sources, mechanisms of biotoxicity, and biomarkers. Rev Environ Health **15**:299-323.

Polla, B. S., Bonventre, J. V., and Krane, S. M. (1988). 1,25-Dihydroxyvitamin D3 increases the toxicity of hydrogen peroxide in the human monocytic line U937: the role of calcium and heat shock. J Cell Biol **107**:373-80.

Polla, B. S., Kantengwa, S., Francois, D., Salvioli, S., Franceschi, C., Marsac, C., and Cossarizza, A. (1996). Mitochondria are selective targets for the protective effects of heat shock against oxidative injury. Proc Natl Acad Sci U S A **93**:6458-63.

Pope, C. A., 3rd, Burnett, R. T., Thun, M. J., Calle, E. E., Krewski, D., Ito, K., and Thurston, G. D. (2002). Lung cancer, cardiopulmonary mortality, and long-term exposure to fine particulate air pollution. Jama **287**:1132-41.

Pozzi, R., De Berardis, B., and Paoletti, L. (2005). Winter urban air particles from Rome (Italy): effects on the monocytic-macrophagic RAW 264.7 cell line. Environ Res **99**:344-54.

Presland, R. B., and Dale, B. A. (2000). Epithelial structural proteins of the skin and oral cavity: function in health and disease. Crit Rev Oral Biol Med **11**:383-408.

Presland, R. B., and Jurevic, R. J. (2002). Making sense of the epithelial barrier: what molecular biology and genetics tell us about the functions of oral mucosal and epidermal tissues. J Dent Educ **66**:564-74.

Promega. (2007). Wizard® Plus Minipreps DNA Purification System.

Puchelle, E., Zahm, J. M., Tournier, J. M., and Coraux, C. (2006). Airway epithelial repair, regeneration, and remodeling after injury in chronic obstructive pulmonary disease. Proc Am Thorac Soc 3:726-33.

Pullinger, C. R., Eng, C., Salen, G., Shefer, S., Batta, A. K., Erickson, S. K., Verhagen, A., Rivera, C. R., Mulvihill, S. J., Malloy, M. J., and Kane, J. P. (2002). Human cholesterol 7alpha-hydroxylase (CYP7A1) deficiency has a hypercholesterolemic phenotype. J Clin Invest 110:109-17.

Qiagen. (2007). Isolation of genomic DNA and/or proteins from fatty tissue samples treated with QIAzol™ Lysis Reagent.

Qiagen. (2007). QuantiTect Primer Assay Handbook.

Ragan, H. A. (1977). Effects of iron deficiency on the absorption and distribution of lead and cadmium in rats. J Lab Clin Med 90:700-6.

Raherison, C., Penard-Morand, C., Moreau, D., Caillaud, D., Charpin, D., Kopfersmitt, C., Lavaud, F., Taytard, A., and Annesi-maesano, I. (2007). In utero and childhood exposure to parental tobacco smoke, and allergies in schoolchildren. Respir Med 101:107-17.

Ramirez, R. D., Sheridan, S., Girard, L., Sato, M., Kim, Y., Pollack, J., Peyton, M., Zou, Y., Kurie, J. M., Dimaio, J. M., Milchgrub, S., Smith, A. L., Souza, R. F., Gilbey, L., Zhang, X., Gandia, K., Vaughan, M. B., Wright, W. E., Gazdar, A. F., Shay, J. W., and Minna, J. D. (2004). Immortalization of human bronchial epithelial cells in the absence of viral oncoproteins. Cancer Res 64:9027-34.

Rastogi, T., Jha, P., Reddy, K., Prabhakaran, D., Spiegelman, D., Stampfer, M. J., Willett, W. C., and Ascherio, A. (2005). Bidi and cigarette smoking and

risk of acute myocardial infarction among males in urban India. Tob Control 14:356-8.

Recio, L., Sisk, S., Pluta, L., Bermudez, E., Gross, E., Chen, Z., Morgan, K., and Walker, C. (1992). p53 mutations in formaldehyde-induced nasal squamous cell carcinomas in rats. Cancer Res 52:6113-6.

Reddel, R. R., Salghetti, S. E., Willey, J. C., Ohnuki, Y., Ke, Y., Gerwin, B. I., Lechner, J. F., and Harris, C. C. (1993). Development of tumorigenicity in simian virus 40-immortalized human bronchial epithelial cell lines. Cancer Res 53:985-91.

Reed, C. E. (1999). The natural history of asthma in adults: the problem of irreversibility. J Allergy Clin Immunol 103:539-47.

Ren, J. (2007). Acetaldehyde and alcoholic cardiomyopathy: lessons from the ADH and ALDH2 transgenic models. Novartis Found Symp 285:69-76; discussion 76-9, 198-9.

Righetti, P. G., Castagna, A., Antonucci, F., Piubelli, C., Cecconi, D., Campostrini, N., Antonioli, P., Astner, H., and Hamdan, M. (2004). Critical survey of quantitative proteomics in two-dimensional electrophoretic approaches. J Chromatogr A 1051:3-17.

Rikans, L. E., and Yamano, T. (2000). Mechanisms of cadmium-mediated acute hepatotoxicity. J Biochem Mol Toxicol 14:110-7.

Riley, M. R., Boesewetter, D. E., Turner, R. A., Kim, A. M., Collier, J. M., and Hamilton, A. (2005). Comparison of the sensitivity of three lung derived cell lines to metals from combustion derived particulate matter. Toxicol In Vitro 19:411-9.

Ring, H., Lou, X., Thorn, C., and Benowitz, N. 2005 Nicotine Metabolism Pathway.

Roberts, D. L. (1988). Natural tobacco flavour. Adv. Tob. Sci **14**:49-81.

Roos, W. P., Christmann, M., Fraser, S. T., and Kaina, B. (2007). Mouse embryonic stem cells are hypersensitive to apoptosis triggered by the DNA damage O(6)-methylguanine due to high E2F1 regulated mismatch repair. Cell Death Differ **14**:1422-32.

Ross, P. L., Huang, Y. N., Marchese, J. N., Williamson, B., Parker, K., Hattan, S., Khainovski, N., Pillai, S., Dey, S., Daniels, S., Purkayastha, S., Juhasz, P., Martin, S., Bartlet-Jones, M., He, F., Jacobson, A., and Pappin, D. J. (2004). Multiplexed protein quantitation in Saccharomyces cerevisiae using amine-reactive isobaric tagging reagents. Mol Cell Proteomics **3**:1154-69.

Ross, R. (1999). Atherosclerosis is an inflammatory disease. Am Heart J **138**:S419-20.

Rozman, K. K., and Doull, J. (2003). Scientific foundations of hormesis. Part 2. Maturation, strengths, limitations, and possible applications in toxicology, pharmacology, and epidemiology. Crit Rev Toxicol **33**:451-62.

Russel, M., Jarvis, M., Iyer, R., and Feyerabend, C. (1980). Relation of nicotine yield of cigarettes to blood nicotine concentrations in smokers. Br. Med. J. **280**:972-976.

Russell, W., and Burch, R. 1959. The Principles of Humane Experimental Technique. Methuen, London.

Satir, P., and Sleigh, M. A. (1990). The physiology of cilia and mucociliary interactions. Annu Rev Physiol **52**:137-55.

Scheffer, G. L., Wijngaard, P. L., Flens, M. J., Izquierdo, M. A., Slovak, M. L., Pinedo, H. M., Meijer, C. J., Clevers, H. C., and Scheper, R. J. (1995). The drug resistance-related protein LRP is the human major vault protein. Nat Med **1**:578-82.

Schevelbein, H. (1962). Nicotin Rauchen und organismus-Beitr. Tabakforsch:199-274.

Schevelbein, H. (1982). Nicotine, resorption and fate. Pharm. Ther. **18**:233-248.

Schevelbein, H., Eberhardt, R., Loeschenkohl, K., and Ralhlfs, J. (1973). Absorption of nicotine through the oral mucosa; measurement of nicotine concentration in the blood after application of nicotine and total particulate matter. Agents and actions **3/4**:259-264.

Schick, S., and Glantz, S. (2005). Philip Morris toxicological experiments with fresh sidestream smoke: more toxic than mainstream smoke. Tob Control **14**:396-404.

Schlatter, J., and Lutz, W. K. (1990). The carcinogenic potential of ethyl carbamate (urethane): risk assessment at human dietary exposure levels. Food Chem Toxicol **28**:205-11.

Schwarze, P. E., Johnsen, N. M., Samuelsen, J. T., Thrane, E. V., Lund, K., Lag, M., Refsnes, M., Kongerud, J., Becher, R., Boe, J., Holme, J. A., and Wiger, R. (1996). The use of isolated lung cells in in vitro pulmonary toxicology: studies of DNA damage, apoptosis and alteration of gene expression. Cent Eur J Public Health **4 Suppl**:6-10.

Seliger, H. (2007). Introduction: array technology-an overview. Methods Mol Biol 381:1-36.

Serabjit-Singh, C., Nishio, S., Philpot, R., and Plopper, C. (1988). The distribution of cytochrome P-450 monooxygenase in cells of the rabbit lung. Mol. Pharmacol. 33:279-289.

Sexton, K., Balharry, D., and BeruBe, K. A. (2008). Genomic biomarkers of pulmonary exposure to tobacco smoke components. Pharmacogenet Genomics 18:853-60.

Shacter, E., and Weitzman, S. A. (2002). Chronic inflammation and cancer. Oncology (Williston Park) 16:217-26, 229; discussion 230-2.

Shia, S., Stamos, J., Kirchhofer, D., Fan, B., Wu, J., Corpuz, R. T., Santell, L., Lazarus, R. A., and Eigenbrot, C. (2005). Conformational lability in serine protease active sites: structures of hepatocyte growth factor activator (HGFA) alone and with the inhibitory domain from HGFA inhibitor-1B. J Mol Biol 346:1335-49.

Shiu, L. Y., Chang, L. C., Liang, C. H., Huang, Y. S., Sheu, H. M., and Kuo, K. W. (2007). Solamargine induces apoptosis and sensitizes breast cancer cells to cisplatin. Food Chem Toxicol.

Siemiatycki, J., Richardson, L., Straif, K., Latreille, B., Lakhani, R., Campbell, S., Rousseau, M. C., and Boffetta, P. (2004). Listing occupational carcinogens. Environ Health Perspect 112:1447-59.

Skoczynska, A. (1997). [Lipid peroxidation as a toxic mode of action for lead and cadmium]. Med Pr 48:197-203.

Skrahina, T., Piljic, A., and Schultz, C. (2008). Heterogeneity and timing of translocation and membrane-mediated assembly of different annexins. Exp Cell Res **314**:1039-47.

Slade, J. (1997). Historical notes on Tobacco. Prog. respir. Res **28**:1-11.

Sleigh, M., Blake, J., and Liron, M. (1988). The propulsion of mucus by cilia. Am. Rev. Respir. Dis. **137**:726-731.

Smith, C., Livingston, S., and Doolittle, D. (1997). An international literature survey of "IARC Group I carcinogens" reported in mainstream cigarette smoke. Food Chem Toxicol **35**:1107-30.

Smith, C., Perfetti, T., Rumple, M., Rodgman, A., and Doolittle, D. (2000). "IARC group 2A Carcinogens" reported in cigarette mainstream smoke. Food Chem Toxicol:371-83.

Smith, C. J., Perfetti, T. A., and King, J. A. (2006). Perspectives on pulmonary inflammation and lung cancer risk in cigarette smokers. Inhal Toxicol **18**:667-77.

Snyder, R., and Van Houten, B. (1986). Genotoxicity of formaldehyde and an evaluation of its effects on the DNA repair process in human diploid fibroblasts. Mutat Res **165**:21-30.

Soffritti, M., Maltoni, C., Maffei, F., and Biagi, R. (1989). Formaldehyde: an experimental multipotential carcinogen. Toxicol Ind Health **5**:699-730.

Soloway, S. (1976). Naturally occuring insecticides. Environ. Heal. Perspec. **14**:109-117.

Speit, G., and Merk, O. (2002). Evaluation of mutagenic effects of formaldehyde in vitro: detection of crosslinks and mutations in mouse lymphoma cells. Mutagenesis **17**:183-7.

Spencer. 1985. Pathology of the Lung. Permagon Press, Oxford.

Spira, A., Schembri, F., Beane, J., Shah, V., Liu, G., and Brody, J. S. (2004). Impact of cigarette smoke on the normal airway transcriptome. Chest **125**:115S.

Steimer, A., Haltner, E., and Lehr, C. M. (2005). Cell culture models of the respiratory tract relevant to pulmonary drug delivery. J Aerosol Med **18**:137-82.

Stevens, F. C. (1983). Calmodulin: an introduction. Can J Biochem Cell Biol **61**:906-10.

Stoeppler, M. 1991. Metals and their compounds in the environment, p. 803-851. *In* E. Merian (ed.), New York.

Stratagene. (2007). StrataClone™ PCR Cloning Kit.

Sun, X. M., Butterworth, M., MacFarlane, M., Dubiel, W., Ciechanover, A., and Cohen, G. M. (2004). Caspase activation inhibits proteasome function during apoptosis. Mol Cell **14**:81-93.

Szeplaki, G., Prohaszka, Z., Duba, J., Rugonfalvi-Kiss, S., Karadi, I., Kokai, M., Kramer, J., Fust, G., Kleiber, M., Romics, L., and Varga, L. (2004). Association of high serum concentration of the third component of complement (C3) with pre-existing severe coronary artery disease and new vascular events in women. Atherosclerosis **177**:383-9.

Takahashi, H., Komatsu, N., Ibe, M., Ishida-Yamamoto, A., Hashimoto, Y., and Iizuka, H. (2007). Cystatin A suppresses ultraviolet B-induced apoptosis of keratinocytes. J Dermatol Sci **46**:179-87.

Takeuchi, T., and Ishii, D. (1981). Application of ultra-micro high-performance liquid chromatography to trace analysis. J. Chromatogr. **218**:199-208.

Takeuchi, T., and Ishii, D. (1980). Ultra-micro high-performance liquid chromatography. J. Chromatogr. **190**:150-155.

Taylor, B., and Wadsworth, J. (1987). Maternal smoking during pregnancy and lower respiratory tract illness in early life. Arch Dis Child **62**:786-91.

Tesfaigzi, J., and Carlson, D. M. (1999). Expression, regulation, and function of the SPR family of proteins. A review. Cell Biochem Biophys **30**:243-65.

Tesfaigzi, Y. (2003). Processes involved in the repair of injured airway epithelia. Arch Immunol Ther Exp (Warsz) **51**:283-8.

Thornton, I. (1992). Sources and pathways of cadmium in the environment. IARC Sci Publ:149-62.

Tian, Z., Greene, A. S., Pietrusz, J. L., Matus, I. R., and Liang, M. (2008). MicroRNA-target pairs in the rat kidney identified by microRNA microarray, proteomic, and bioinformatic analysis. Genome Res **18**:404-11.

Tomizawa, M., and Casida, J. (2003). Selective toxicity of neonicotinoids attributable to specificity of insect and mammalian nicotinic receptors. Annu. Rev. Entomol. **48**:339-64.

Tong, Z., Wu, X., Ovcharenko, D., Zhu, J., Chen, C. S., and Kehrer, J. P. (2005). Neutrophil gelatinase-associated lipocalin as a survival factor. Biochem J **391**:441-8.

Tonstad, S., and Svendsen, M. (2005). Premature coronary heart disease, cigarette smoking, and the metabolic syndrome. Am J Cardiol **96**:1681-5.

Trautmann, A., Kruger, K., Akdis, M., Muller-Wening, D., Akkaya, A., Brocker, E. B., Blaser, K., and Akdis, C. A. (2005). Apoptosis and loss of adhesion of bronchial epithelial cells in asthma. Int Arch Allergy Immunol **138**:142-50.

Treadwell, J., and Singh, S. (2004). Microarray analysis of mouse brain gene expression following acute ethanol treatment. Neurochem Res **29**:257-269.

Trink, B., Osada, M., Ratovitski, E., and Sidransky, D. (2007). p63 transcriptional regulation of epithelial integrity and cancer. Cell Cycle **6**:240-5.

Tyers, M., and Mann, M. (2003). From genomics to proteomics. Nature **422**:193-7.

Uller, L., Andersson, M., Greiff, L., Persson, C. G., and Erjefalt, J. S. (2004). Occurrence of apoptosis, secondary necrosis, and cytolysis in eosinophilic nasal polyps. Am J Respir Crit Care Med **170**:742-7.

Urist, M. J., Di Como, C. J., Lu, M. L., Charytonowicz, E., Verbel, D., Crum, C. P., Ince, T. A., McKeon, F. D., and Cordon-Cardo, C. (2002). Loss of p63 expression is associated with tumor progression in bladder cancer. Am J Pathol **161**:1199-206.

Van Laethem, A., Nys, K., Van Kelst, S., Claerhout, S., Ichijo, H., Vandenheede, J. R., Garmyn, M., and Agostinis, P. (2006). Apoptosis signal regulating kinase-1 connects reactive oxygen species to p38 MAPK-induced mitochondrial apoptosis in UVB-irradiated human keratinocytes. Free Radic Biol Med **41**:1361-71.

Ventii, K. H., and Wilkinson, K. D. (2008). Protein partners of deubiquitinating enzymes. Biochem J **414**:161-75.

Villar, J., Edelson, J. D., Post, M., Mullen, J. B., and Slutsky, A. S. (1993). Induction of heat stress proteins is associated with decreased mortality in an animal model of acute lung injury. Am Rev Respir Dis **147**:177-81.

Voutsadakis, I. A. (2008). The ubiquitin-proteasome system in colorectal cancer. Biochim Biophys Acta.

Waddell, W. J., Marlowe, C., and Pierce, W. M., Jr. (1987). Inhibition of the localization of urethane in mouse tissues by ethanol. Food Chem Toxicol **25**:527-31.

Waisberg, M., Joseph, P., Hale, B., and Beyersmann, D. (2003). Molecular and cellular mechanisms of cadmium carcinogenesis. Toxicology **192**:95-117.

Waldum, H., Nilsen, O., Nilsen, T., Rorvik, H., Syversen, V., Sanvik, A., Haugen, O., Torp, S., and Brenna, E. (1996). Long-term effects of inhaled nicotine. Life Sci **58**:1339-46.

Walters, D. M., Breysse, P. N., Schofield, B., and Wills-Karp, M. (2002). Complement factor 3 mediates particulate matter-induced airway hyperresponsiveness. Am J Respir Cell Mol Biol **27**:413-8.

Wang, C., Pattabiraman, N., Zhou, J. N., Fu, M., Sakamaki, T., Albanese, C., Li, Z., Wu, K., Hulit, J., Neumeister, P., Novikoff, P. M., Brownlee, M., Scherer, P. E., Jones, J. G., Whitney, K. D., Donehower, L. A., Harris, E. L., Rohan, T., Johns, D. C., and Pestell, R. G. (2003). Cyclin D1 repression of peroxisome proliferator-activated receptor gamma expression and transactivation. Mol Cell Biol **23**:6159-73.

Wang, K., Wen, F. Q., and Xu, D. (2008). Mucus hypersecretion in the airway. Chin Med J (Engl) **121**:649-52.

Wanner, A., Salathe, M., and O'Riordan, T. G. (1996). Mucociliary clearance in the airways. Am J Respir Crit Care Med **154**:1868-902.

Waters, M. D., Olden, K., and Tennant, R. W. (2003). Toxicogenomic approach for assessing toxicant-related disease. Mutat Res **544**:415-24.

Watjen, W., Cox, M., Biagioli, M., and Beyersmann, D. (2002). Cadmium-induced apoptosis in C6 glioma cells: mediation by caspase 9-activation. Biometals. Biometals **15**:15-25.

Wattiez, R., and Falmagne, P. (2005). Proteomics of bronchoalveolar lavage fluid. J Chromatogr B Analyt Technol Biomed Life Sci **815**:169-78.

Wei, M. C., Zong, W. X., Cheng, E. H., Lindsten, T., Panoutsakopoulou, V., Ross, A. J., Roth, K. A., MacGregor, G. R., Thompson, C. B., and Korsmeyer, S. J. (2001). Proapoptotic BAX and BAK: a requisite gateway to mitochondrial dysfunction and death. Science **292**:727-30.

Weitzman, S. A., and Gordon, L. I. (1990). Inflammation and cancer: role of phagocyte-generated oxidants in carcinogenesis. Blood **76**:655-63.

Wenzel, P., Muller, J., Zurmeyer, S., Schuhmacher, S., Schulz, E., Oelze, M., Pautz, A., Kawamoto, T., Wojnowski, L., Kleinert, H., Munzel, T., and Daiber, A. (2008). ALDH-2 deficiency increases cardiovascular oxidative stress--evidence for indirect antioxidative properties. Biochem Biophys Res Commun **367**:137-43.

Werle, B., Schanzenbacher, U., Lah, T. T., Ebert, E., Julke, B., Ebert, W., Fiehn, W., Kayser, K., Spiess, E., Abrahamson, M., and Kos, J. (2006).

Cystatins in non-small cell lung cancer: tissue levels, localization and relation to prognosis. Oncol Rep **16**:647-55.

Wester, R. C., Maibach, H. I., Sedik, L., Melendres, J., DiZio, S., and Wade, M. (1992). In vitro percutaneous absorption of cadmium from water and soil into human skin. Fundam Appl Toxicol **19**:1-5.

Widdicomb, J., and Pack, R. (1982). The clara cell. Eur. J. Respir. Dis. **63**:202-220.

Wierzchos, J., De Los Rios, A., Sancho, L. G., and Ascaso, C. (2004). Viability of endolithic micro-organisms in rocks from the McMurdo Dry Valleys of Antarctica established by confocal and fluorescence microscopy. J Microsc **216**:57-61.

Willems, E., Rambali, B., Vleeming, W., Opperhuizen, A., and van Amsterdam, J. (2006). Significance of ammonium compounds on nicotine exposure to cigarette smokers. Food Chem Toxicol **44**:678-88.

Williams, C., Shattuck-Brandt, R. L., and DuBois, R. N. (1999). The role of COX-2 in intestinal cancer. Ann N Y Acad Sci **889**:72-83.

Williams, N., Klem, J., Puzanov, I., Sivakumar, P., Schatzle, J., Bennett, M., and Kumar, V. (1998). Natural killer cell differentiation: insights from knockout and transgenic mouse models and in vitro systems. Immunol Rev **165**:47-61.

Winton, H. L., Wan, H., Cannell, M. B., Gruenert, D. C., Thompson, P. J., Garrod, D. R., Stewart, G. A., and Robinson, C. (1998). Cell lines of pulmonary and non-pulmonary origin as tools to study the effects of house dust mite proteinases on the regulation of epithelial permeability. Clin Exp Allergy **28**:1273-85.

Wise, H., Balharry, D., Reynolds, L. J., Sexton, K., and Richards, R. J. (2006). Conventional and toxicogenomic assessment of the acute pulmonary damage induced by the instillation of Cardiff PM10 into the rat lung. Sci Total Environ **360**:60-7.

Wolf, D. H., and Hilt, W. (2004). The proteasome: a proteolytic nanomachine of cell regulation and waste disposal. Biochim Biophys Acta **1695**:19-31.

Wolz, L., Krause, G., Scherer, G., Aufderheide, M., and Mohr, U. (2002). In vitro genotoxicity assay of sidestream smoke using a human bronchial epithelial cell line. Food Chem Toxicol **40**:845-50.

Wong, C. G., Bonakdar, M., Mautz, W. J., and Kleinman, M. T. (1996). Chronic inhalation exposure to ozone and nitric acid elevates stress-inducible heat shock protein 70 in the rat lung. Toxicology **107**:111-9.

Wonnacott, S. 1999. Synopsis of Nicotine Presentations at the Montreal meeting. *In* B. A. Tobacco (ed.).

World health organisation. (1989). Presented at the International programme on chemical safety, Geneva.

Woutersen, R., Appelman, L., Wilmer, J., Falke, H., and Feron, V. (1987). Subchronic (13-week) inhalation toxicity study of formaldehyde in rats. J Appl Toxicol **7**:43-9.

Wu, Y. J., Chen, J. J., and Cheng, Y. Y. (2005). A sensitive and specific HPLC-MS method for the determination of sophoridine, sophocarpine and matrine in rabbit plasma. Anal Bioanal Chem **382**:1595-600.

Xu, L., Han, C., Lim, K., and Wu, T. (2006). Cross-talk between peroxisome proliferator-activated receptor delta and cytosolic phospholipase A(2)alpha/cyclooxygenase-2/prostaglandin E(2) signaling pathways in human hepatocellular carcinoma cells. Cancer Res **66**:11859-68.

Yamamoto, H., Horiuchi, S., Adachi, Y., Taniguchi, H., Nosho, K., Min, Y., and Imai, K. (2004). Expression of ets-related transcriptional factor E1AF is associated with tumor progression and over-expression of matrilysin in human gastric cancer. Carcinogenesis **25**:325-32.

Yamamoto, T., Pierce, W. M., Jr., Hurst, H. E., Chen, D., and Waddell, W. J. (1988). Inhibition of the metabolism of urethane by ethanol. Drug Metab Dispos **16**:355-8.

Yang, C. F., Shen, H. M., Shen, Y., Zhuang, Z. X., and Ong, C. N. (1997). Cadmium-induced oxidative cellular damage in human fetal lung fibroblasts (MRC-5 cells). Environ Health Perspect **105**:712-6.

Yang, J. P., Glickman, A. M., Edwards, V., Boyer, M. I., and Bowen, C. V. (1998). An ultrastructural study of the intimal hyperplasia in healing microarterial anastomoses. Microsurgery **18**:391-6.

Yee, S. B., and Pritsos, C. A. (1997). Reductive activation of doxorubicin by xanthine dehydrogenase from EMT6 mouse mammary carcinoma tumors. Chem Biol Interact **104**:87-101.

Yildiz, D. (2004). Nicotine, its metabolism and an overview of its biological effects. Toxicon **43**:619-32.

Yu, M. C., and Yuan, J. M. (2004). Environmental factors and risk for hepatocellular carcinoma. Gastroenterology **127**:S72-8.

Zahm, J. M., Kaplan, H., Herard, A. L., Doriot, F., Pierrot, D., Somelette, P., and Puchelle, E. (1997). Cell migration and proliferation during the in vitro wound repair of the respiratory epithelium. Cell Motil Cytoskeleton **37**:33-43.

Zalups, R. K., and Ahmad, S. (2003). Molecular handling of cadmium in transporting epithelia. Toxicol Appl Pharmacol **186**:163-88.

Zeegers, M., Kellen, E., Buntinx, F., and van den Brandt, P. (2004). The association between smoking, beverage consumption, diet and bladder cancer: a systematic literature review. World J Urol **21**:392-401.

Zhou, J., Hu, G., and Herring, B. P. (2005). Smooth muscle-specific genes are differentially sensitive to inhibition by Elk-1. Mol Cell Biol **25**:9874-85.

Zieske, L. R. (2006). A perspective on the use of iTRAQ reagent technology for protein complex and profiling studies. J Exp Bot **57**:1501-8.

Zimmerli, B., and Schlatter, J. (1991). Ethyl carbamate: analytical methodology, occurrence, formation, biological activity and risk assessment. Mutat Res **259**:325-50.

APPENDIX 1

ELSEVIER

An in vitro approach to assess the toxicity of inhaled tobacco smoke components: Nicotine, cadmium, formaldehyde and urethane

Dominique Balharry [*], Keith Sexton, Kelly A. BéruBé

Cardiff School of Biosciences, Cardiff University, Museum Avenue, Cardiff, South Glamorgan, CF10 3US, UK

Abstract

One of the first lines of defence to inhaled toxins is the barrier formed by the tracheobronchial epithelium, making this the ideal region for studying the toxicity of inhaled substances. This study utilises a highly differentiated, three-dimensional, in vitro model of human upper respiratory tract epithelium (EpiAirway-100) to measure the acute toxicological responses to well-characterised tobacco smoke components.

To determine the suitability of this model for screening inhaled toxicants, the EpiAirway tissue model (ETM) was treated apically with tobacco smoke components (nicotine, formaldehyde, cadmium, urethane) which are known to induce a variety of toxic effects (e.g. cytotoxic, thrombogenic, carcinogenic). A range of concentrations were used to model different mechanisms and severity of toxicity which were then compared to known in vivo responses.

Similar trends in stress response occurred, with distinct alterations to the tissue in response to all four toxins. At high concentrations, cell viability decreased and tight junctions were degraded, but at sub-toxic concentrations epithelial resistance (indicating tissue integrity) increased 20–60% from control. This peak in resistance coincided with an increase in secreted protein levels, elevated cytokine release and goblet cell hyperplasia and hypertrophy.

In conclusion, acute exposure to tobacco smoke components induces measurable toxic responses within human respiratory epithelium. Sub-toxic concentrations appear to illicit a protective response by increasing mucus secretion and mediating immune responses via cytokine release. These responses are comparable to human in vivo responses, indicating potential for the ETM as a tool for screening the toxicity of inhaled compounds.
© 2007 Elsevier Ireland Ltd. All rights reserved.

Keywords: Nicotine; Cadmium; Formaldehyde; Urethane; EpiAirway; In vitro toxicity

1. Introduction

The respiratory tract is constantly exposed to an array of gases, solids and liquids suspended in the air. Exposure to any number of these substances has the potential to damage the pulmonary epithelium. For example, long-term inhalation of ambient airborne particulate matter is an important factor in the development of cardiopulmonary disease and lung cancer (Pope et al., 2002). One of the greatest challenges when studying respiratory toxicology is the complex nature of inhaled air which consists of a wide mixture of substances with varying chemical, physical and biological characteristics.

* Corresponding author. Tel.: +44 29 20874125; fax: +44 29 20875211.
E-mail address: balharry@cardiff.ac.uk (D. Balharry).

Traditionally, in vivo studies are used to investigate toxicant effects in the lung, however, public opinion and government legislation is leading to a decrease in the popularity of animal testing. A growing number of scientists are now working towards the Three R's principles of Russell and Burch (1959); the "reduction, refinement and replacement" of animal experiments. Consequently, viable alternatives need to be developed which can reproduce in vitro, toxic events that may occur in the human lung.

The tissue initially affected by toxic gases and particles in the ambient air is the epithelial lining of the upper airways. As such, the biological activity of airborne substances is usually studied using bronchial epithelial cells or macrophages (Steimer et al., 2005). There are a number of well-known cell models which all have different advantages, and selection of the most appropriate model to address a specific question in a study can provide extremely valuable information, but there are also some perceived disadvantages to this approach. It is difficult to isolate and culture functional cells from human pulmonary tissue (Schwarze et al., 1996), and despite attempts to immortalise human pulmonary cells they can have a limited lifespan. In contrast, transformed cell lines have an unlimited lifespan allowing prolonged studies, but may not accurately represent the in vivo situation, as the phenotype of transformed cells differs from that of normal cells (Foster et al., 2000). In addition, individual cell types may respond quite differently to a complex mixture like tobacco smoke (Andreoli et al., 2003), as they may lack the requisite biotransformation enzymes (e.g. P450s) (Castell et al., 2005). Similarly, cell lines may show altered expression of a range of secretory and signalling molecules (Forbes and Ehrhardt, 2005). Overall, there are in-built biases when using these kinds of experimental systems. The advent of mixed population cultures and multi-differentiated cultures generates in vivo-like characteristics by enabling further cell–cell interactions. A highly differentiated, three-dimensional system is desirable because it models not only the different effects of toxins on specific cell types, but also the interaction between the cells. Moreover, epithelium cultured at the air–liquid interface would facilitate in vivo-like chemical exposures. These requirements are met by a human derived, primary, upper airway, culture known as the EpiAirway tissue model (MatTek Corporation). The EpiAirway tissue model (ETM) consists of normal, tracheobronchial epithelial cells derived from human primary explant tissue. It is cultured to form a pseudostratified, highly differentiated tissue with a mucociliary phenotype that closely resembles the epithelia of the human respiratory tract (Fig. 1).
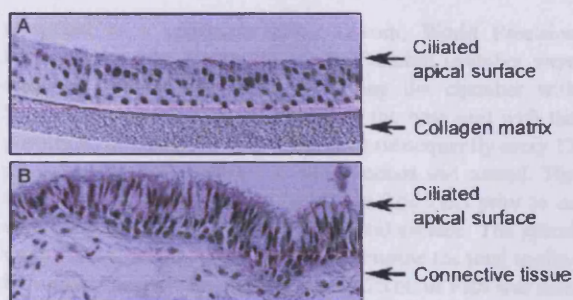

Fig. 1. H&E stained sections at 10× magnification, showing the pseudostratified phenotype common to both (A) EpiAirway tissue and (B) normal human bronchiole. Images reproduced with kind permission from MatTek.

This study is designed to investigate the potential of the ETM to screen the toxicity of inhaled compounds. This can range from airborne particulate matter (e.g. diesel, pollen) to prescription medication (e.g. asthma inhaled medication). Among various inhaled toxins, one of the most common is tobacco smoke, which affects not only smokers, but also anyone coming into contact with environmental tobacco smoke (ETS). ETS is implicated in the exacerbation of many respiratory diseases including asthma and chronic obstructive pulmonary disease, as well as the development of lung cancer (Ambrose and Barua, 2004; Dhala et al., 2006). It has even been indicated that ETS is more toxic than mainstream smoke inhaled by the smoker (Schick and Glantz, 2005). Children are particularly at risk due to their higher respiratory rate which results in increased ETS inhalation. This can result in numerous respiratory tract infections and impaired pulmonary function (Li et al., 1999), behavioural and cognitive problems (DiFranza et al., 2004), and has been linked to sudden infant death syndrome (Anderson and Cook, 1997). Despite the large number of compounds found in tobacco smoke (at least 4000 bioactive compounds) (Andreoli et al., 2003) the toxicological effects of a number of the compounds have been well characterised. Four of these were investigated in this study: nicotine is known mainly for its addictive nature; however it is also thought to have thrombogenic capacity (Hioki et al., 2001); cadmium is a human carcinogen (Smith et al., 1997) and also exerts cytotoxic effects by inducing oxidative stress (Pinot et al., 2000); formaldehyde is also classified as a human carcinogen by the International Agency for Research on Cancer (IARC) and is both mutagenic and genotoxic (de Serres and Brockman, 1999); urethane (also known as ethyl carbamate) generates reactive metabolites (e.g. vinyl carbamate, vinyl carbamate epoxide) during xenobiotic metabolism which

are genotoxic and carcinogenic (Zimmerli and Schlatter, 1991).

The ETM, representing human tracheobronchial tissue, was used to determine the acute toxicological responses to these well-characterised tobacco smoke components (TSC). Epithelial integrity (trans-epithelial electrical resistance; TEER), cell viability (mitochondrial activity; MTT assay), protein (Bradford assay) and cytokine (Proteoplex Array Merck) expression were considered as measures of toxicity. Histological analysis was also carried out to assess structural modifications to the tissue model. A number of morphological and physiological changes were identified and compared to known toxicity mechanisms which occur in humans in vivo. The consistencies/inconsistencies between the in vivo and in vitro studies help identify the potential of this model for screening of inhaled toxicants.

2. Methods

2.1. Cells, culture and exposure conditions

The EpiAirway cell cultures were transported from MatTek in the US in a 24-well plate. Each well contains a 12 mm Millipore insert on which the ETM is cultured at the air–liquid interface for approximately 25 days prior to dispatch. This allows for differentiation of the model into a pseudostratified structure, containing basal, ciliated and goblet cells, which closely resembles the human tracheobronchial region (Fig. 1). On arrival, the cells were handled according to the manufacturer's specifications as follows. Briefly, each insert was placed into 0.9 ml pre-warmed culture medium (serum free DMEM enriched with various growth factors and hormones, provided by MatTek) in six-well culture plates. The cells were equilibrated at 37 °C with 4.5% CO_2 for 24 h. After this time, initial TEER values were recorded (see below) to confirm tissue integrity. Following this culture preconditioning, acute exposure (24 h) of ETM cells to TSC solutions was carried out at the air–liquid interface. TSC solutions were made up in sterile PBS (supplemented with magnesium and calcium) and warmed to 37 °C before 100 μl was applied to the apical surface of the insert. A series of concentrations were selected for each TSC to determine sub-toxic and toxic effects. The concentrations were as follows: nicotine: 0, 25, 50, 75, 100, 125 mM; cadmium (cadmium chloride): 0, 0.08, 0.16, 0.24, 0.32, 0.4 mM; urethane: 0, 100, 250, 500, 2000, 4000 mM; formaldehyde: 0, 1, 5, 7.5, 10, 15 mM. Each concentration was carried out in triplicate. After 24 h the toxin (TSC) was removed from the surface and TEER, MTT, cytokine and protein assays were carried out (see below).

2.2. Trans-epithelial electrical resistance

TEER measurements were taken using an Endohm tissue resistance chamber (World Precision Instruments) which

is linked to a resistance meter (Evom; World Precision Instruments). The electrodes of the Endohm chamber were equilibrated 24 h before use by filling the chamber with PBS and connecting the electrodes to the base unit with the power off. Immediately before use (and subsequently every 12 measurements) the calibration was checked and zeroed. The cultures ($n = 3$) were washed basally in 2 ml PBS prior to an additional 0.3 ml PBS wash of the apical surface. The apical wash was aspirated and retained to determine the total acellular surface protein content. A further 0.25 ml of PBS was then added to the apical surface for TEER measurement. An empty culture insert (containing 0.25 ml PBS) was used as a "blank" and subtracted from each subsequent sample reading (Duff et al., 2002). TEER measurements were taken at time zero and 24 h after exposure and are presented as resistance values (in ohms, Ω).

2.3. MTT

MTT reagent (3-[4,5-dimethylthiazol-2-yl]-2,5-diphenyl tetrazolium bromide) was warmed to 37 °C and 300 μl added to each well of a 24-well plate (Mosmann, 1983). After measuring TEER the ETM inserts were placed in the MTT solution ($n = 3$). These were protected from light and incubated at 37 °C in 4.5% CO_2 for 3 h. After this, the cultures were immersed in 2 ml MTT extracting solution (containing acidified isopropanol) and incubated in the dark for a further 24 h. Triplicate 100 μl aliquots of MTT extractant from each culture were assayed on a platereader at a wavelength of 590 nm.

2.4. Protein assay

The aspirated material from the first apical surface wash was stored at 1–4 °C until use within 48 h. The total amount of protein (μg) contained in each sample ($n = 3$) was then identified using the Bradford (1976) assay for protein.

2.5. Cytokine assay

The production and release of endogenous cytokines into the basal medium of the ETM was measured using the Proteoplex Human Cytokine Array (Merck Biosciences). The Proteoplex Array consists of 16 wells each of which contain an identical microarray of 12 anti-cytokine capture antibodies, spotted in quadruplicate (Barchet et al., 2006). Detection is based on a standard 'sandwich' immunoassay and relies on biotinylated detection antibodies and streptavidin-conjugated fluorophores.

The samples ($n = 3$) were processed as described in the user protocol, briefly outlined below. The Proteoplex wells were washed with PBST (provided) prior to adding aliquots of the basal media. These were incubated for 1 h at room temperature with gentle agitation before washing again with PBST. A detection antibody cocktail (provided) was added to each well and incubated for an hour, then washed with PBST. A solution containing the fluorophore (SensiLight; provided) was incu-

bated with the samples for 90 min. After a final wash in PBST the array was washed in rinse solution (provided) and then dried. The Proteoplex Array was then shipped to the 'Proteo-Plex Slide Analysis Service' (Nottingham, UK) for scanning and analysis.

2.6. Histology

The ETM from concurrent experiments were fixed in 10% neutral-buffered formalin for a minimum of 24 h prior to paraffin embedding and sectioning. The embedded ETM were cut into 5 μm sections using a microtome and stained with haematoxylin and eosin (H&E). The sections were finally analysed by light microscopy. Random areas of each section were selected and the number of nuclei (cell number) along a 40 μm length of the ETM were counted ($n = 6$).

2.7. Statistical analysis

All data are represented with error bars illustrating the standard deviation. Significance has been calculated using a Student's t-test, with $p \leq 0.05$ deemed significant and $p \leq 0.01$ being highly significant.

3. Results

3.1. TEER

Prior to treatment with TSC the ETM samples consistently generated a TEER of over 700 Ω. This indicated that the integrity of the epithelial membrane was good, and that the cells were healthy. Post-exposure, the TEER measurements were dramatically altered, with all TSC exhibiting similar trends in response to treatment (Fig. 2). A biphasic response was observed with the low concentrations eliciting a large and significant (nicotine: $p = 0.009$, cadmium: $p = 0.005$, urethane: $p = 0.048$, formaldehyde: $p = 0.014$) increase above the control level (Table 1), followed by a steady decrease in TEER as the concentration increased.

3.2. MTT

The MTT assay, which measures mitochondrial activity in viable cells, was carried out on all the samples 24 h after treatment with the toxins. All TSC elicited
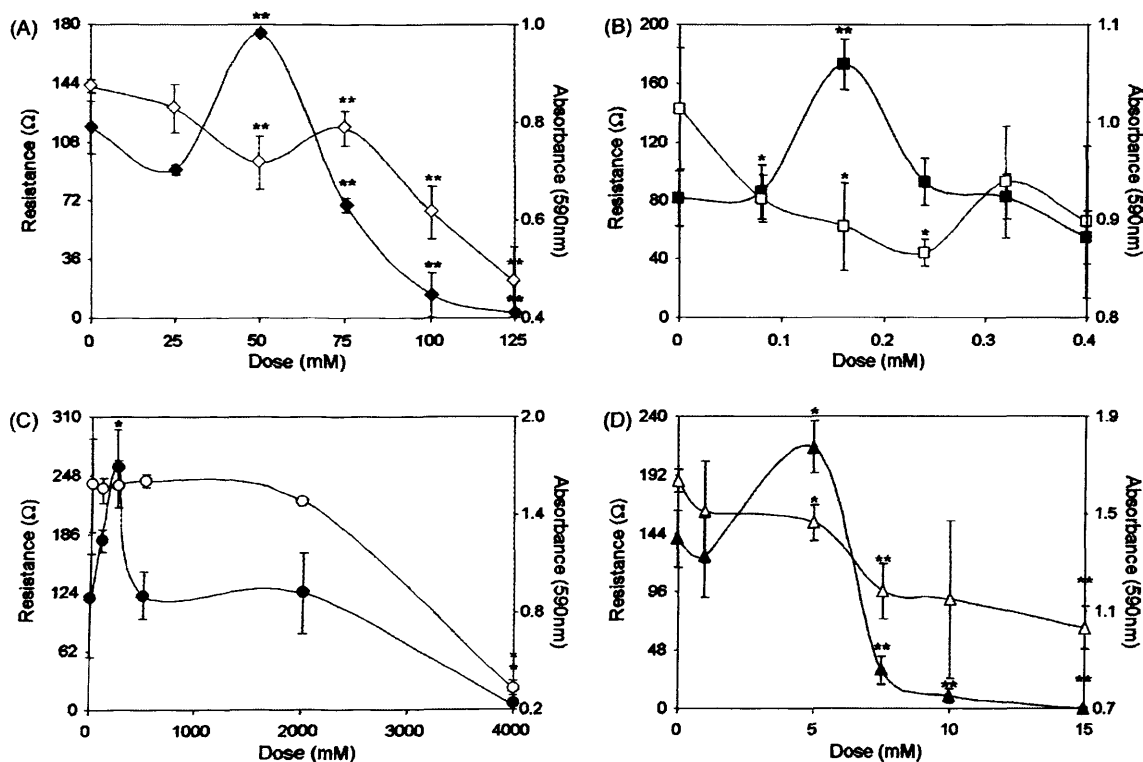
Fig. 2. The response of ETM to a range of TSC concentrations. TEER (black) is measured as resistance (ohms, Ω). Significant (*$p \leq 0.05$) and highly significant (**$p \leq 0.01$). Cell viability (white) is determined by MTT uptake and measured using absorbance (590 nm). Significant (*$p \leq 0.05$) and highly significant (**$p \leq 0.01$). (A) Nicotine; (B) cadmium; (C) urethane; (D) formaldehyde. Standard deviation is indicated by error bars.

Table 1
Summary of toxicology data for ETM dosed with nicotine, cadmium, urethane and formaldehyde

	TEER peak (mM)	MTT rise (mM)	Protein plateau (mM)	TD10/TD50 (mM)
Nicotine	50	75	75	75/125
Cadmium	0.16	0.32	0.16	0.35/–
Urethane	250	500	250	2100/3000
Formaldehyde	5	5	7.5	5/18

The dose at which each event (e.g. TEER peak) is given. TD10 and TD50 are determined by MTT assay.

a similar dose response that differed from the TEER response in one distinct way (Fig. 2). In each case, the peak in cell viability occurred at a higher concentration than that required to induce the peak of TEER (Table 1). After this peak, cell viability decreased with increasing concentration. The MTT values were used to calculate TD10 and TD50 values (concentration required to kill 10 and 50% of cells, respectively) for each of the TSC (Table 1).

3.3. Protein assay

A Bradford assay was carried out on the apical surface wash of all the samples. This wash contained all proteins secreted onto the apical surface, as well as any cellular debris. All the toxins induced similar patterns of change in protein levels, with two slightly different profiles observed (Fig. 3). Protein levels reached a maximum of 45 µg (induced by nicotine and formalde-
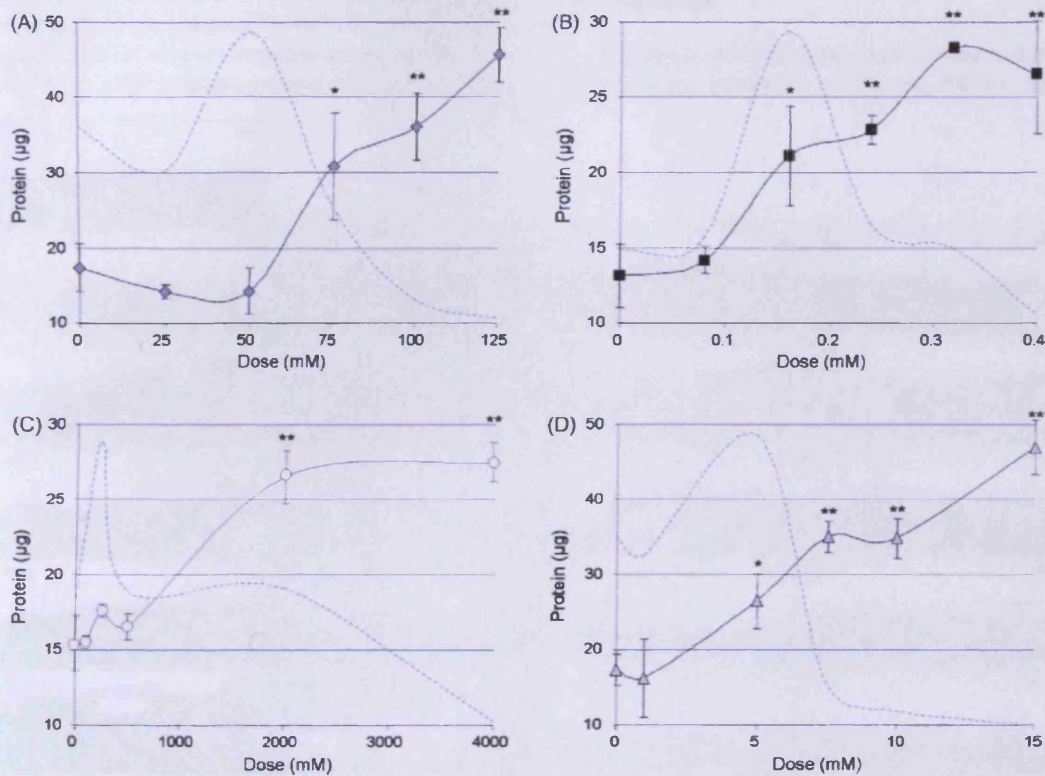
Fig. 3. Amount of total protein present in the initial 0.3 ml apical surface wash in response to a range of TSC concentrations. Protein detected using Bradford assay. (A) Nicotine (grey diamond); (B) cadmium (black square); (C) urethane (white circle); (D) formaldehyde (grey triangle). Significant ($^{*}p \leq 0.05$) and highly significant ($^{**}p \leq 0.01$). Standard deviation is indicated by error bars. TEER is shown for comparison (dashed line).

Table 2
List of cytokines that are significantly altered from control levels in response to TSC

Cadmium	Nicotine	Formaldehyde	Urethane
IL-1α	IL-1α	IL-1α	IL-1α
IL-1β	IL-1β	IL-1β	IL-1β
–	–	IL-2	IL-2
IL-6	IL-6	IL-6	IL-6
–	IL-7	–	–
IL-10	–	IL-10	–
GM-CSF	GM-CSF	GM-CSF	GM-CSF
–	–	IFN-γ	IFN-γ

hyde) or 27 µg (induced by cadmium and urethane) in the apical wash. A "plateau effect" occurred closely after (nicotine, formaldehyde) or coinciding with (cadmium, urethane) the concentration range where TEER was at its peak.

3.4. Cytokine assay

The level of endogenous cytokines found in the basal medium of all the samples was measured. Several of the cytokines (Table 2) showed concentration dependant changes in expression induced by the TSC. In all cases the greatest levels of expression occurred for interleukin (IL) 1α, IL-6 and granulocyte-macrophage colony-

stimulating factor (GM-CSF); ranging from ~20 pg/ml to a concentration dependant peak of ~70 pg/ml. A trend was noted, with maximum cytokine expression corresponding with the peak of TEER for over 70% of the cytokines. The remaining cytokines were found in concentrations of between 1 and 5 pg/ml depending on TSC concentration.

3.5. Histology

All the TSC seemed to illicit similar changes to the morphology of the ETM (Fig. 4). Even the lowest concentration of each TSC appeared to induce thickening of the tissue in comparison to the control. The tissue reached it's maximum thickness at the second concentration (Fig. 4B–D[ii]), coincident with the peak of TEER. At this point, the cells within the tissue appeared to increase in volume, as well as multiplying in number (Fig. 5). Subsequent increases in concentration led to a break down of the cellular structure, thinning of the tissue due to reduced cell swelling and cell numbers, and eventual sloughing off of the cells.

4. Discussion

The objective of this study was to determine the acute toxicological responses of human derived bronchial
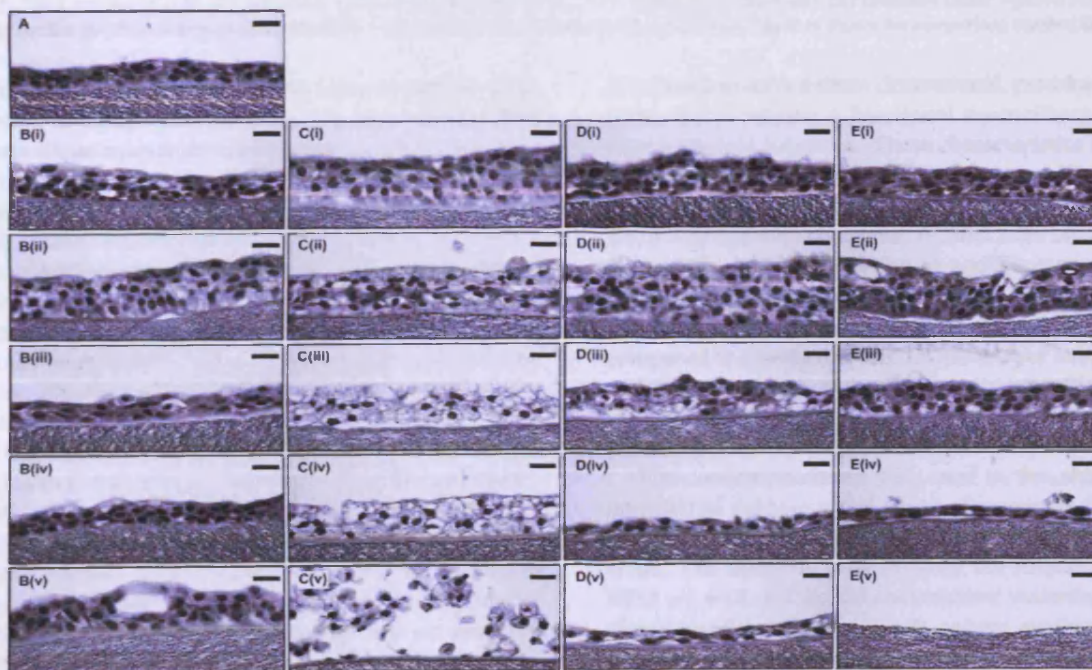

Fig. 4. H&E stained sections of ETM treated with increasing concentrations of (A) PBS; (B) cadmium: (i) 0.08, (ii) 0.16, (iii) 0.24, (iv) 0.32, (v) 0.4 mM; (C) nicotine: (i) 25, (ii) 50, (iii) 75, (iv) 100, (v) 125 mM; (D) formaldehyde: (i) 1, (ii) 5, (iii) 7.5, (iv) 10, (v) 15 mM; (E) urethane: (i) 100, (ii) 250, (iii) 500, (iv) 2000, (v) 4000 mM.
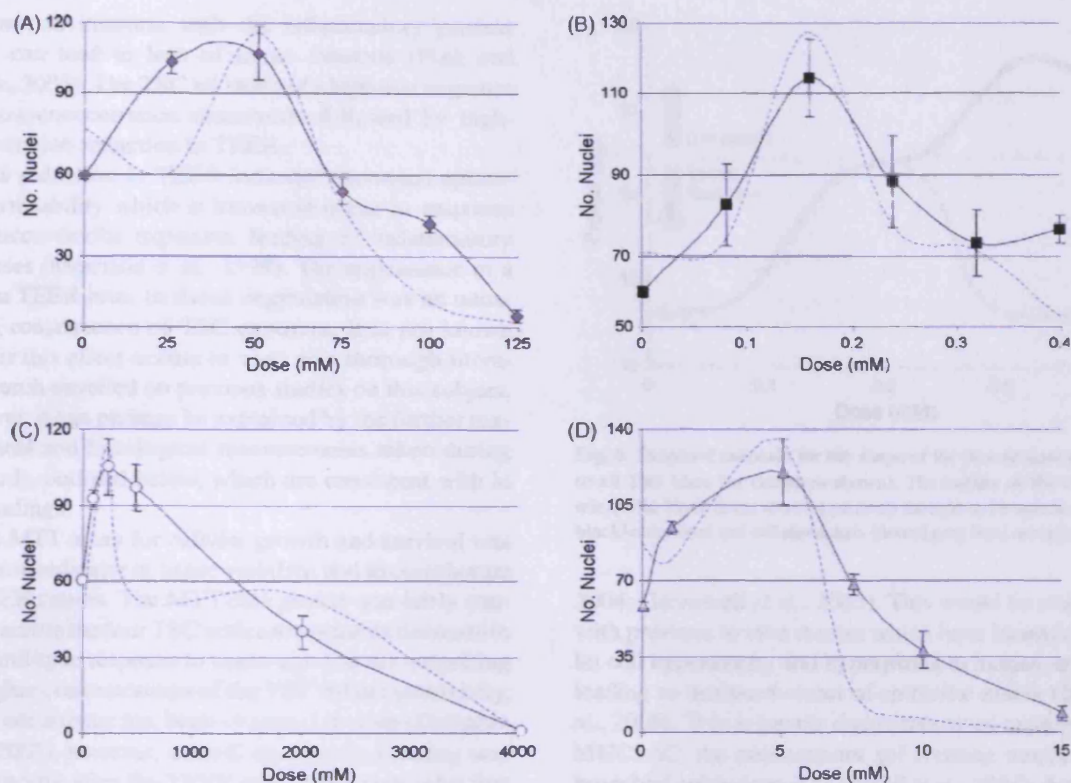
Fig. 5. Total number of cells counted along a 40 μm length of the ETM. (A) Nicotine (grey diamond); (B) cadmium (black square); (C) urethane (white circle); (D) formaldehyde (grey triangle). Standard deviation is indicated by error bars. TEER is shown for comparison (dashed line).

epithelium to well-characterised tobacco smoke components in comparison to known in vivo effects. This human tissue equivalent of respiratory epithelia is a commercially engineered in vitro model used by researchers in industry and academia for inhalation toxicology (Agu et al., 2006; BéruBé et al., 2006; Chen et al., 2006). This model circumvents any potential species-related differences that could compromise the interpretation of experimental results (Coggins, 2002), by utilising normal (non-immortalised) human tissue to derive the model. The range of toxic effects can only be fully investigated in a biological system capable of transcribing and translating genes in response to the action of toxins, as cell–cell interactions that occur in vivo can significantly alter the cellular effects of many toxins (Ekwall et al., 1990). The ETM consists of cells derived from healthy human primary explant tissue (normal human bronchial epithelium (NHBE) as opposed to lung tumour or diseased tissue). Consequently, the cells are genotypically and phenotypically more representative of normal epithelia than other commonly used models (e.g. Calu-3: carcinoma derived, BEAS-2B: transformed). The overriding advantage of this system is that the epithelium

is cultured to form a three-dimensional, pseudostratified state which exhibits a functional mucocilliary phenotype with tight junctions. These characteristics are vital in the normal functioning of the human epithelium in vivo (Chilvers and O'Callaghan, 2000; Godfrey, 1997). The ETM contains columnar, ciliated cells interspersed with goblet cells, in addition to undifferentiated basal cells which have the potential to act as progenitor cells for damaged epithelium (Inayama et al., 1988). When compared to standard epithelial monolayer culture, this system more closely resembles human bronchial tissue, both morphologically and physiologically (Pampaloni et al., 2007).

The concentrations of TSC used in this study were intended to achieve a full range of responses from the ETM, from sub-toxic concentrations to widespread cell death. The methods used to study the response of the ETM are well established conventional toxicology techniques used in numerous cell culture studies. TEER was used as the primary indicator of tissue stress by measuring the integrity of cellular tight junctions, and hence epithelial permeability. Breakdown of tight junctions is an early indication of cellular degradation and

is known to interfere with the inflammatory process which can lead to loss of tissue function (Fink and Delude, 2005). The TSC all induced a biphasic response with low-concentration stimulation followed by high-concentration reduction in TEER.

This reduction in TEER indicates increased epithelial permeability which is known to occur in response to tobacco smoke exposure, leading to inflammatory responses (Morrison et al., 1999). The appearance of a peak in TEER prior to tissue degradation was an unexpected consequence of TSC exposure. It is not known whether this effect occurs in vivo, as a thorough literature search unveiled no previous studies on this subject. However, it can perhaps be explained by the further toxicological and histological measurements taken during this study, outlined below, which are consistent with in vivo findings.

The MTT assay for cellular growth and survival was used as an indicator of tissue viability, and to corroborate the TEER results. The MTT data profile was fairly consistent across the four TSC with a measurable decrease in cell viability in response to treatment. It is not surprising that higher concentrations of the TSC led to cytotoxicity, as this occurrence has been observed in vivo (Gelbman et al., 2007), however, a small increase in viability was noted shortly after the TEER peak. This may infer that a loss of tight junctions (indicated by increased TEER) leads to an acute increase in cellular activity (and therefore increased MTT metabolism). Alternatively, it could be that increased cell numbers (known to occur in vivo) (Innes et al., 2006) leads to increased MTT conversion generating a false impression of increased viability. A comparison of the TEER and MTT data (and other toxicological measurements detailed below) implies that the peak in TEER readings may act an early indicator for toxicity and deterioration of the tissue model.

The epithelium of the upper respiratory tract secretes a large number of proteins involved in protecting and stabilising the ciliated surface (Ali and Pearson, 2007). These mucin-rich proteins (mucus) scavenge, immobilise or kill pathogens that come into contact with the apical surface of the tissue (Sheehan et al., 2006). The total amount of protein accumulated on the surface of the ETM was measured to monitor the occurrence of protein secretion. The protein levels appeared to increase with TSC concentration, but the Bradford assay measures total protein concentration, and as such, no distinction was made between secreted protein and cellular debris. However, there was visual confirmation of a viscous substance on the apical surface of the cells. This material had the characteristics of mucin, i.e. clear and viscous, as reported in by other investigators (Chemuturi et al.,
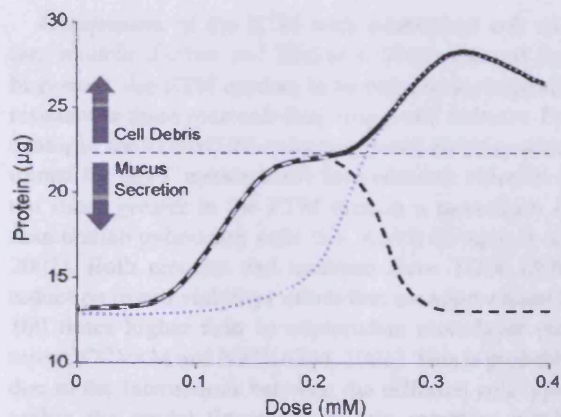
Fig. 6. Proposed rationale for the shape of the protein dose response to all TSC (data for cadmium shown). The outline of the total protein (solid black line), secreted proteins thought to be mucins (dashed black/white line) and cellular debris (dotted grey line) are represented.

2004; Greenwell et al., 2005). This would be consistent with previous in vivo studies which have identified goblet cell hypertrophy and hyperplasia in human smokers, leading to increased stores of epithelial mucin (Innes et al., 2006). This is largely due to increased expression of MUC5AC, the predominant gel forming mucin of the bronchial epithelium (O'Donnell et al., 2004). A plateau in protein levels occurs shortly after the peak in TEER which may suggest a change in cellular activity, from protein (possibly mucus) secretion to accumulation of cell debris (Fig. 6). If this is the case, this could partially explain the TEER peak, as mucus on the cell surface could increase the electrical resistance of the tissue.

H&E staining was carried out on ETM sections to monitor morphological changes to the tissue. This confirmed that thickening of the tissue was induced, concurrent with the elevated TEER. Image analysis of the sections showed that the low concentrations bring about an increase in the number of cells, as well as the observed increase in the size of many of the cells. These findings appear consistent with previous studies which have identified goblet cell hypertrophy and hyperplasia in human smokers (Innes et al., 2006). This could further account for the changes in TEER as increasing cell volume can lead to a rise in TEER due to the obliteration of the intercellular space (Madara, 1998). It would be interesting to note whether repeated exposure to these toxins may disrupt the normal progression of hyperplasia (and hence epithelial recovery), which could result in the development of diseases such as asthma, chronic bronchitis and cancer (Tesfaigzi, 2003) as observed with tobacco smoking. The histology also verified the high-concentration tissue degradation (and break down of

tight junctions) indicated by decreases in the TEER and MTT assays. Taken in overview, the histological analysis seems to confirm the postulated differentiation between secreted proteins (possibly mucins) and cell debris; with hyper secretion of protein at low concentrations, and cell breakdown leading to further protein release at high concentrations (Fig. 6), but further studies involving mucin assays would be required to substantiate these observations.

The levels of cytokines expressed by the ETM were determined as a further measure of cellular activity and cell–cell interactions. There were a number of similarities between the four TSC, with the pro-inflammatory cytokines IL-1α, IL-1β, IL-6 and GM-CSF induced by all the compounds. The main difference between the TSC was that cadmium and nicotine induced IL-7 expression, while formaldehyde and urethane induced IL-2 and IFN-γ secretion. Interleukin-2 and -7 are both thought to be involved in T-cell homeostasis (Boyman et al., 2007), so this difference could be due to alternate mechanisms for achieving the same goal. IFN-γ is also thought to be indirectly involved in T-cell homeostasis and has been demonstrated to enhance T-cell mediated immune responses (Boyman et al., 2007). The apparent link between elevated cytokine secretion and TEER could be related to the increase in cell numbers within the ETM. Simply; the higher the cell numbers, the greater concentrations of cytokines are expressed. The elevated expression of cytokines suggest that the ETM was functioning in an in vivo-like manner, with the induction of signalling cascades and various immune responses (Chung, 2001). This permits further investigation into whether xenobiotics, such as the TSC, play a role in inducing respiratory defence mechanisms as well as biotransformation events.

The four TSC all appear to illicit a similar response from the ETM. The low concentrations seem to be sub-toxic, inducing cell proliferation, increased protein secretion, cell viability and electrical resistance as well as elevated cytokine expression. This reaction could be linked to a protective response or potentially an overcorrection to the damage caused to the airway epithelium. This response peaks then declines as the concentrations increase. At high concentrations of the TSC the elevated responses are overwhelmed, and all the markers of toxicity rapidly decline, with a drop in cell viability and TEER, limited cytokine expression and reduced cell numbers. The only exception to this is the increasing levels of protein released into the apical surface wash. This is believed to be due to the degradation of the tissue and discharge of the protein contents of the cells as they disintegrate.

Comparison of the ETM with established cell culture models (Forbes and Ehrhardt, 2005) showed that in general, the ETM appears to be more toxicologically resistant to these toxicants than single-cell cultures. For example, the TD10 (10% reduction in cell viability determined by MTT metabolism) for cadmium chloride is ten times greater in the ETM than in a monolayer of mammalian pulmonary cells (i.e. A549) (Watjen et al., 2002). Both nicotine and urethane show TD50 (50% reduction in cell viability) values that are approximately 100 times higher than in mammalian monolayer cultures (ICCVAM and NICEATM, 2001). This is probably due to the interactions between the different cell types within the model (increased protein secretion resulting from hyperplasia and hypertrophy, and cytokine mediated immune responses). However, the protective response to formaldehyde is induced by only two-fold compared to a monolayer of A549 cells (Lestari et al., 2005). This difference in response may be partially due to the bioavailability of the TSC, or possibly the lack of activation of specific metabolism mechanisms. A further benefit of the ETM is the ease of use. The model is fully differentiated, and screened for metabolic activity and tissue integrity (P450 activity, mucin dot blot, TEER ≥ 270) prior to dispatch (MatTek, 2007) and can provide viable tissue for up to 27 days (Hayden et al., 2006). The multi-well (24-well/96-well) format is ideal for multiple exposure experiments and screening, with easy access to both the apical and basal surfaces of the cells. This model has the added advantage of derivation from normal human tissue, circumventing the need for extrapolation of data from in vivo studies in different species. As such, the ETM could provide a tool to assess respiratory tract toxicity while avoiding species extrapolation and the use of laboratory animals.

In conclusion, acute exposure to TSC induces toxic responses within the ETM causing loss of cell viability, tight junction degradation and stimulation of secretory processes. These changes are preceded by a rapid increase in TEER which has consequently been identified as a potential early marker of toxicity. The toxins induce increased protein secretion, resulting from cell hyperplasia and hypertrophy, and initiate immune responses via altered cytokine expression. These changes closely mimic documented changes in the human bronchial epithelium indicating that, after validation, this model could prove useful for screening inhaled toxins and for further respiratory toxicology studies.

Conflict of interest

The authors declare no known conflict of interest.

Acknowledgement

References

Agu, R.U., Valiveti, S., Paudel, K.S., Klausner, M., Hayden, P.J., Stinchcomb, A.L., 2006. Permeation of WIN 55,212-2, a potent cannabinoid receptor agonist, across human tracheo-bronchial tissue in vitro and rat nasal epithelium in vivo. J. Pharm. Pharmacol. 58, 1459–1465.

Ali, M.S., Pearson, J.P., 2007. Upper airway mucin gene expression: a review. Laryngoscope 117, 932–938.

Ambrose, J.A., Barua, R.S., 2004. The pathophysiology of cigarette smoking and cardiovascular disease: an update. J. Am. Coll. Cardiol. 43, 1731–1737.

Anderson, H.R., Cook, D.G., 1997. Passive smoking and sudden infant death syndrome: review of the epidemiological evidence. Thorax 52, 1003–1009.

Andreoli, C., Gigante, D., Nunziata, A., 2003. A review of in vitro methods to assess the biological activity of tobacco smoke with the aim of reducing the toxicity of smoke. Toxicol. In Vitro 17, 587–594.

Barchet, W., Price, J.D., Cella, M., Colonna, M., MacMillan, S.K., Cobb, J.P., Thompson, P.A., Murphy, K.M., Atkinson, J.P., Kemper, C., 2006. Complement-induced regulatory T cells suppress T-cell responses but allow for dendritic-cell maturation. Blood 107, 1497–1504.

BéruBé, K.A., Balharry, D., Jones, T.P., Moreno, T., Hayden, P., Sexton, K., Hicks, M., Merolla, L., Timblin, C., Shukla, A., Mossman, B.T., 2006. Characterisation of airborne particulate matter and related mechanisms of toxicity. In: Ayres, J., Maynard, R.L., Richards, R.J. (Eds.), Air Pollution and Health. Imperial College Press, London, pp. 69–110.

Boyman, O., Purton, J.F., Surh, C.D., Sprent, J., 2007. Cytokines and T-cell homeostasis. Curr. Opin. Immunol. 19, 320–326.

Bradford, M.M., 1976. A rapid and sensitive method for the quantitation of microgram quantities of protein utilising the principle of protein–dye binding. Anal. Biochem. 72, 248–254.

Castell, J.V., Donato, M.T., Gomez-Lechon, M.J., 2005. Metabolism and bioactivation of toxicants in the lung. The in vitro cellular approach. Exp. Toxicol. Pathol. 57 (Suppl. 1), 189–204.

Chemuturi, N., Hayden, P., Klausner, M., Donovan, M., 2004. Localization of P-glycoprotein in human tracheal/bronchial epithelial cell culture (EpiAirway™). American Association of Pharmaceutical Scientists Annual Meeting. J. Pharm. Sci. 94 (9), 1976–1985.

Chen, S.C., Eiting, K., Cui, K., Leonard, A.K., Morris, D., Li, C.Y., Farber, K., Sileno, A.P., Houston Jr., M.E., Johnson, P.H., Quay, S.C., Costantino, H.R., 2006. Therapeutic utility of a novel tight junction modulating peptide for enhancing intranasal drug delivery. J. Pharm. Sci. 95, 1364–1371.

Chilvers, M.A., O'Callaghan, C., 2000. Local mucociliary defence mechanisms. Paediatr. Respir. Rev. 1, 27–34.

Chung, K.F., 2001. Cytokines in chronic obstructive pulmonary disease. Eur. Respir. J. Suppl. 34, 50s–59s.

Coggins, C.R., 2002. A minireview of chronic animal inhalation studies with mainstream cigarette smoke. Inhal. Toxicol. 14, 991–1002.

de Serres, F.J., Brockman, H.E., 1999. Comparison of the spectra of genetic damage in formaldehyde-induced ad-3 mutations between DNA repair-proficient and -deficient heterokaryons of *Neurospora crassa*. Mutat. Res. 437, 151–163.

Dhala, A., Pinsker, K., Prezant, D.J., 2006. Respiratory health consequences of environmental tobacco smoke. Clin. Occup. Environ. Med. 5, 139–156.

DiFranza, J.R., Aligne, C.A., Weitzman, M., 2004. Prenatal and postnatal environmental tobacco smoke exposure and children's health. Pediatrics 113, 1007–1015.

Duff, T., Carter, S., Feldman, G., McEwan, G., Pfaller, W., Rhodes, P., Ryan, M., Hawksworth, G., 2002. Transepithelial resistance and inulin permeability as endpoints in in vitro nephrotoxicity testing. Altern. Lab. Anim. 30 (Suppl. 2), 53–59.

Ekwall, B., Silano, A., Paganuzzi-Stammati, A., Zucco, F., 1990. Toxicity tests with mammalian cell cultures. In: Bourdeau, P. (Ed.), Short-term Toxicity Tests for Non-genotoxic Effects. John Wiley & Sons Ltd., pp. 75–97.

Fink, M.P., Delude, R.L., 2005. Epithelial barrier dysfunction: a unifying theme to explain the pathogenesis of multiple organ dysfunction at the cellular level. Crit. Care Clin. 21, 177–196.

Forbes, B., Ehrhardt, C., 2005. Human respiratory epithelial cell culture for drug delivery applications. Eur. J. Pharm. Biopharm. 60, 193–205.

Foster, K.A., Avery, M.L., Yazdanian, M., Audus, K.L., 2000. Characterization of the Calu-3 cell line as a tool to screen pulmonary drug delivery. Int. J. Pharm. 208, 1–11.

Gelbman, B.D., Heguy, A., O'Connor, T.P., Zabner, J., Crystal, R.G., 2007. Upregulation of pirin expression by chronic cigarette smoking is associated with bronchial epithelial cell apoptosis. Respir. Res. 8, 10.

Godfrey, R.W., 1997. Human airway epithelial tight junctions. Microsc. Res. Tech. 38, 488–499.

Greenwell, L.L., Carthew, P., Westmoreland, C., Fentem, J., 2005. Modelling the human bronchi and its responses in vitro. In: 5th World Congress on Alternatives and Animal Use in the Life Sciences, Berlin, Germany.

Hayden, P.J., Bolmarcich, J., Stolper, G., Jackson, G.R., Klausner, M., 2006. Drug/xenobiotic-metabolizing enzyme (XME) expression in the EpiAirway™ in vitro human airway model: utility for assessing tracheal/bronchial biotransformation of inhaled pharmaceuticals and environmental chemicals. In: American Thoracic Society Meeting, San Diego, CA.

Hioki, H., Aoki, N., Kawano, K., Homori, M., Hasumura, Y., Yasumura, T., Maki, A., Yoshino, H., Yanagisawa, A., Ishikawa, K., 2001. Acute effects of cigarette smoking on platelet-dependent thrombin generation. Eur. Heart J. 22, 56–61.

ICCVAM, NICEATM, 2001. Report of the International Workshop on In Vitro Methods for Assessing Acute Systemic Toxicity (NIH Publication No. 01-4499). Available at: http://iccvam.niehs.nih.gov/methods/invidocs/finalall.pdf. Accessed on 30 July 2006.

Inayama, Y., Hook, G.E., Brody, A.R., Cameron, G.S., Jetten, A.M., Gilmore, L.B., Gray, T., Nettesheim, P., 1988. The differentiation potential of tracheal basal cells. Lab. Invest. 58, 706–717.

Innes, A.L., Woodruff, P.G., Ferrando, R.E., Donnelly, S., Dolganov, G.M., Lazarus, S.C., Fahy, J.V., 2006. Epithelial mucin stores are increased in the large airways of smokers with airflow obstruction. Chest 130, 1102–1108.

Lestari, F., Hayes, A.J., Green, A.R., Markovic, B., 2005. In vitro cytotoxicity of selected chemicals commonly produced during fire combustion using human cell lines. Toxicol. In Vitro 19, 653–663.

Li, J.S., Peat, J.K., Xuan, W., Berry, G., 1999. Meta-analysis on the association between environmental tobacco smoke (ETS) expo-

sure and the prevalence of lower respiratory tract infection in early childhood. Pediatr. Pulmonol. 27, 5–13.

Madara, J.L., 1998. Regulation of the movement of solutes across tight junctions. Annu. Rev. Physiol. 60, 143–159.

MatTek, 2007. EpiAirway Technical Specification (AIR-100). Available at: http://www.mattek.com/pages/products/epiairway/specification. Accessed on 30 July 2007.

Morrison, D., Rahman, I., Lannan, S., MacNee, W., 1999. Epithelial permeability, inflammation, and oxidant stress in the air spaces of smokers. Am. J. Respir. Crit. Care Med. 159, 473–479.

Mosmann, T., 1983. Rapid colorimetric assay for cellular growth and survival: application to proliferation and cytotoxicity assays. J. Immunol. Methods 65, 55–63.

O'Donnell, R.A., Richter, A., Ward, J., Angco, G., Mehta, A., Rousseau, K., Swallow, D.M., Holgate, S.T., Djukanovic, R., Davies, D.E., Wilson, S.J., 2004. Expression of ErbB receptors and mucins in the airways of long term current smokers. Thorax 59, 1032–1040.

Pampaloni, F., Reynaud, E.G., Stelzer, E.H., 2007. The third dimension bridges the gap between cell culture and live tissue. Nat. Rev. Mol. Cell. Biol. 8, 839–845.

Pinot, F., Kreps, S.E., Bachelet, M., Hainaut, P., Bakonyi, M., Polla, B.S., 2000. Cadmium in the environment: sources, mechanisms of biotoxicity, and biomarkers. Rev. Environ. Health 15, 299–323.

Pope, C.A., Burnett, R.T., Thun, M.J., Calle, E.E., Krewski, D., Ito, K., Thurston, G.D., 2002. Lung cancer, cardiopulmonary mortality, and long-term exposure to fine particulate air pollution. JAMA 287, 1132–1141.

Russell, W., Burch, R., 1959. The Principles of Humane Experimental Technique. Methuen, London.

Schick, S., Glantz, S., 2005. Philip Morris toxicological experiments with fresh sidestream smoke: more toxic than mainstream smoke. Tob. Control 14, 396–404.

Schwarze, P.E., Johnsen, N.M., Samuelsen, J.T., Thrane, E.V., Lund, K., Lag, M., Refsnes, M., Kongerud, J., Becher, R., Boe, J., Holme, J.A., Wiger, R., 1996. The use of isolated lung cells in in vitro pulmonary toxicology: studies of DNA damage, apoptosis and alteration of gene expression. Cent. Eur. J. Public Health Suppl. 4, 6–10.

Sheehan, J.K., Kesimer, M., Pickles, R., 2006. Innate immunity and mucus structure and function. Novartis Found. Symp. 279, 155–166 (Discussion 167–169, 216–219).

Smith, C.J., Livingston, S.D., Doolittle, D.J., 1997. An international literature survey of "IARC Group I carcinogens" reported in mainstream cigarette smoke. Food Chem. Toxicol. 35, 1107–1130.

Steimer, A., Haltner, E., Lehr, C.M., 2005. Cell culture models of the respiratory tract relevant to pulmonary drug delivery. J. Aerosol Med. 18, 137–182.

Tesfaigzi, Y., 2003. Processes involved in the repair of injured airway epithelia. Arch. Immunol. Ther. Exp. (Warsz) 51, 283–288.

Watjen, W., Cox, M., Biagioli, M., Beyersmann, D., 2002. Cadmium-induced apoptosis in C6 glioma cells: mediation by caspase 9-activation. Biometals 15, 15–25.

Zimmerli, B., Schlatter, J., 1991. Ethyl carbamate: analytical methodology, occurrence, formation, biological activity and risk assessment. Mutat. Res. 259, 325–350.

APPENDIX 2

Genomic biomarkers of pulmonary exposure to tobacco smoke components

Keith Sexton, Dominique Balharry and Kelly A. BéruBé

Background Associations between smoking and the development of tobacco-related diseases in humans have historically been assessed by epidemiological studies. These studies are further complicated by the number of chemicals used in tobacco and individual smoking habits. An alternative approach is required to assess the biological responses.

Objective Toxicogenomics was carried out to identify early molecular markers for events in pulmonary injury resulting from tobacco smoke components (TSC) exposure.

Materials and methods EpiAirway-100 cells were exposed at the air/liquid interface to representative particle (nicotine; cadmium) and vapour phase [formaldehyde (FA) and ethyl carbamate] components of cigarette smoke. Microarray technology was used to compare expression profiles of human genes associated with toxicity and drug resistance, from control and TSC-treated respiratory epithelium ($n = 5$/dose).

Results Using the GEArray 'toxicology and drug resistance' microarray followed by significance analysis of microarray analysis, 42 mRNA transcripts were found to be significantly altered by the TSC exposure. The vapour [ethyl carbamate, FA and particle (nicotine, cadmium)] phase TSC exhibited differential transcriptional responses that could not be attributed to their chemical phase. The transcriptional changes could be classified according to a functional family, where ethyl carbamate, FA and cadmium classified as carcinogens, demonstrated the highest gene homology when compared with the noncarcinogen, nicotine.

Discussion Analysis of the microarray data and further confirmation (reverse transcriptase-PCR) identified three potential biomarkers for TSC-induced injury. These three genes (*CYP7A1*, *HMOX1* and *PTGS1*) are highly upregulated and have been linked with mechanistic pathways of disease. *Pharmacogenetics and Genomics* 18:853–860 © 2008 Wolters Kluwer Health | Lippincott Williams & Wilkins.

Cardiff School of Biosciences, Cardiff University, Museum Avenue, Cardiff, Wales, UK

Correspondence to Keith Sexton, Cardiff School of Biosciences, Museum Avenue, Cardiff, Wales CF10 3US, UK
Tel: +1 29 20874125; fax: +1 29 20875211;
e-mail: Sextonk@cardiff.ac.uk

Introduction

The respiratory tract of humans is constantly exposed to an array of gases, solids and liquids suspended in the air. Exposure to any number of these substances has the potential to damage the pulmonary epithelium. For example, long-term inhalation of airborne particulate is an important factor in the development of cardiopulmonary disease and lung cancer [1–4]. Most of the early studies performed on tobacco smoke [5] were complicated by the vast number of the tobacco chemical components; approximately 10^{15} reactive species in the gas phase [6] with varying chemical, physical and biological characteristics [7].

Traditionally, *in vivo* studies are used to investigate toxicant effects in the lung, however, public opinion and government legislation [8,9] is leading to a decrease in the popularity of animal testing. A growing number of scientists are now working towards the three R's

principles of [10] 'Reduction, Refinement and Replacement' of animal experiments. Consequently, viable alternatives need to be developed which can reproduce *in vitro*, toxic events that may occur in the human lung.

The EpiAirway tissue model (ETM, MatTek Corp., Ashland, Massachusetts, USA) is a commercially available *in vitro* model used by researchers in industry and academia for lung toxicology [11–13]. This model eliminates any potential species-related differences that could compromise the interpretation of experimental results [5], by utilizing normal (nonimmortalized) human tissue to derive the model. The range of toxic effects can only be fully investigated in a biological system capable of transcribing and translating genes in response to the action of toxins, as cell–cell interactions that occur *in vivo* can significantly alter the cellular effects of many toxins [14]. The ETM consists of cells derived from healthy human primary explant tissue (normal human bronchial

epithelium as opposed to lung tumour or diseased tissue). Consequently, the cells are genotypically and phenotypically more representative of normal epithelia than other commonly used models (e.g. Calu-3: carcinoma derived, BEAS-2B: transformed). The primary advantage of this system is that the epithelium is cultured to form a three-dimensional, pseudostratified state, which exhibits a functional mucocilliary phenotype with tight junctions. These characteristics are vital in the normal functioning of the human epithelium *in vivo* [15,16]. When compared with standard epithelial monolayer culture, this system more closely resembles human bronchial tissue, both morphologically and physiologically [17].

The development of successful biomarkers requires the combination of a number of disciplines and skills, such as models of different types of toxicity to generate regiospecific biomarkers, analytical/bioinformatic capability to identify and characterize them, and ability to develop and validate appropriate assays to confirm 'fit for purpose'. Validated biomarkers are needed to replace insensitive functional and labour intensive pathological methods, which only reflects advanced toxicity.

The objective of this study was to utilize the Oligo GEArray Human Toxicology and Drug Resistance (Super-Array, Bethesda, Maryland, USA) Microarray to compare the patterns of mRNA expression of human genes associated with toxicity and drug resistance, from control and treated respiratory epithelia. To achieve this objective, the ETM must maintain certain levels of functionality, with cellular interactions and relatively low levels of cell death [toxic dose 20% (dose required to kill 20% of cells)]. The compounds were selected from the particle phase (e.g. cadmium and nicotine) and vapour phase [e.g. formaldehyde (FA) and ethyl carbamate] of tobacco smoke and exhibit a variety of known mechanisms of toxicity (e.g. thrombogenic, carcinogenic, mutagenic and cytotoxic). The combination of human tissue equivalent models of respiratory epithelia and microarray technology provides human mRNA transcript data allowing identification of biomarkers that could be related to many respiratory diseases.

Methods
Cells, culture and exposure conditions
The EpiAirway cell cultures were transported from MatTek in the USA in a 24-well plate format. Each insert was basally attached to an agarose/media preservation matrix, the inserts were then covered with a wetted gauze and sealed before transport. Transport took 24 h at 4°C. Each well contains a 12 mm millipore insert on which the ETM is grown. On arrival, the cells were handled according to the manufacturer's specifications as follows: briefly, the basal surface of the ETM was rinsed with prewarmed [phosphate buffered saline (PBS)

supplemented with magnesium and calcium, 37°C)] and each insert was placed into 0.9 ml prewarmed culture medium (37°C) in six-well culture plates. The cells were equilibrated at 37°C with 4.5% CO_2 for 24 h. Following this culture preconditioning, acute exposure (24 h) of ETM cells to tobacco smoke component (TSC) solutions was carried out at the air–liquid interface. TSC solutions were made up in sterile PBS (+ Mg and Ca) and warmed to 37°C before dosing. Each insert was apically dosed with 100 µl warm TSC solution. A dose for each TSC was determined from earlier studies described in Ref. [18]. The doses were as follows: nicotine: 30 mmol/l; cadmium (cadmium chloride): 0.1 mmol/l; ethyl carbamate: 70 mmol/l; FA: 7 mmol/l. Each dose was replicated ($n = 5$). After 24 h the toxin (TSC) was removed from the surface and the tissue was stored in RNA later (Qiagen, Crawley, UK) before processing for genomics (see below).

Microarray of EpiAirway tissue model
The Oligo GEArray Human Toxicology and Drug Resistance Microarray profiles the expression of 263 genes related to the metabolic processes of cell stress, cell toxicity, drug resistance and drug metabolism. Genes critical in drug metabolism and resistance such as those encoding enzymes important for drug transport and phase I metabolism (specifically P450-mediated oxidation) are included.

The nylon membrane array matrix is a permeable support with a high DNA binding capacity. Carefully designed 60-mer oligonucleotide probes printed on each microarray minimizes any cross-hybridization between spots on the same array despite the representation of closely related members of the same gene families.

The microarray procedure was performed on control (PBS), nicotine, FA, ethyl carbamate and cadmium-treated ETM ($n = 5$) in accordance with the GEArray Human Toxicology and Drug Resistance Microarray manual (GA-034). In brief, total RNA was isolated from the exposed ETM (QIAZOL, Qiagen). This was then enzymatically converted into a biotinylated cRNA target using the TrueLabeling-AMP 2.0 kit (SuperArray). The resultant-labelled target was hybridized to individual GEArray microarrays in HybTubes (GEArray OHS-401) in a standard hybridization oven. The detection of the microarray was carried out with chemiluminescent detection kit reagents and a chemi-doc imaging system (CCD camera).

Microarray data analysis
Initial acquisition of the array data was carried out using GEArray Expression Analysis Suite Software. The resulting raw data was found to be normally distributed according to the Anderson–Darling statistical test. The

Table 1 Overview of microarray data from exposed cell cultures to show differential gene expression for the various TSC

Gene ID	Nicotine Fold	Nicotine P value	Cadmium Fold	Cadmium P value	Urethane Fold	Urethane P value	Formaldehyde Fold	Formaldehyde P value	Gene name
ABCC1	*		5.31	0.010	4.44	0.0002	3.90	0.001	ATP-binding cassette, subfamily C (CFTR/MRP), member 1
ABCC2	*		8.37	0.001	7.63	0.00001	6.60	0.000004	ATP-binding cassette, subfamily C (CFTR/MRP), member 2
BAX	*		-3.29	0.008	-3.27	0.009	-4.30	0.006	BCL2-associated X protein
CASP10	*		*		3.82	0.0001	3.80	0.00005	Caspase 10, apoptosis-related cysteine protease
CCND1	*		-5.27	0.002	-3.68	0.003	-3.91	0.003	Cyclin D1 (PRAD1: parathyroid adenomatosis 1)
CDKN2A	*		*		*		-3.04	0.00002	Cyclin-dependent kinase inhibitor 2A (melanoma, p16, inhibits CDK4)
CDKN2D	*		-3.12	0.0001	*		-3.00	0.0002	Cyclin-dependent kinase inhibitor 2D (p19, inhibits CDK4)
CHEK2	*		18.66	0.015	18.23	0.00001	14.96	0.00002	CHK2 checkpoint homolog
CRYAB	*		3.29	0.002	*		*		Crystallin, α B
CSF2	*		4.34	0.000004	4.18	0.000002	3.67	0.0001	Colony stimulating factor 2 (granulocyte-macrophage)
CTPS	*		9.31	0.006	8.10	0.00000002	6.19	0.00000003	CTP synthase
CXCL10	*		23.82	0.003	18.84	0.00002	15.46	0.00002	Chemokine (C-X-C motif) ligand 10
CYP1A1	*		4.21	0.008	4.31	0.00002	4.28	0.001	Cytochrome P450, family 1, subfamily A, polypeptide 1
CYP1B1	*		3.08	0.002	*		*		Cytochrome P450, family 1, subfamily B, polypeptide 1
CYP2E1	-1.99	0.032	*		*		*		Cytochrome P450, family 2, subfamily E, polypeptide 1
CYP20A1	*		11.03	0.0005	9.0	0.000001	7.36	0.00004	Cytochrome P450, family 20, subfamily A, polypeptide 1
CYP4B1	*		*		*		-3.14	0.004	Cytochrome P450, family 4, subfamily B, polypeptide 1
CYP4F3	-2.67	0.037	*		*		*		Cytochrome P450, family 4, subfamily F, polypeptide 3
CYP7A1	-3.73	0.006	*		*		*		Cytochrome P450, family 7, subfamily A, polypeptide 1
E2F1	*		*		*		-4.18	0.00003	E2F transcription factor 1
EGFR	*		*		-3.32	0.00003	-4.30	0.00002	Epidermal growth factor receptor (erythroblastic leukemia viral (verbb) oncogene homolog)
ELK1	-1.85	0.001	3.15	0.007	*		*		ELK1, member of ETS oncogene family
ERCC3	-1.63	0.014	*		*		*		Excision repair cross-complementing, complementation group 3
HIF1A	-2.16	0.044	*		*		*		Hypoxia-inducible factor 1, α subunit (basic helix-loop-helix transcription factor)
HMOX1	-1.80	0.006	*		*		*		Heme oxygenase (decycling) 1
HMOX2	-1.57	0.000	*		*		*		Heme oxygenase (decycling) 2
MET	*		-4.53	0.000002	-3.17	0.000002	*		Met protooncogene (hepatocyte growth factor receptor)
MT3	*		3.15	0.021	*		*		Metallothionein 3 (growth inhibitory factor (neurotrophic))
MVP	*		3.65	0.035	*		*		Major vault protein
MYC	*		3.14	0.042	*		*		V-myc myelocytomatosis viral oncogene homolog
NNMT	-2.6	0.047	*		*		*		Nicotinamide N-methyltransferase
PPARD	*		*		3.49	0.00001	3.95	0.001	Peroxisome proliferative activated receptor, δ
PPARGC1A	*		6.80	0.015	5.83	0.001	6.03	0.007	Peroxisome proliferative activated receptor, γ, coactivator 1
PTGS1	*		11.14	0.013	6.91	0.001	6.15	0.007	Prostaglandin-endoperoxide synthase 1 (prostaglandin G/H synthase and cyclooxygenase)
RARA	1.79	0.023	*		*		*		Retinoic acid receptor, alpha
SULT1A1	1.78	0.022	*		*		*		Sulfotransferase family, cytosolic, 1A, phenol-preferring, member 1
SULT2A1	2.23	0.038	*		*		*		Sulfotransferase family, cytosolic, 2A, dehydroepiandrosterone (DHEA) preferring, member 1
SULT2B1	1.70	0.017	*		*		*		Sulfotransferase family, cytosolic, 2B, member 1
TBXAS1	-1.74	0.005	*		*		*		Thromboxane A synthase 1 (platelet, cytochrome P450, family 5, subfamily A)
TOP1	1.84	0.038	*		*		*		Topoisomerase (DNA) I
TPMT	-2.99	0.018	*		*		*		Thiopurine S-methyltransferase
XDH	*		3.53	0.001	*		*		Xanthine dehydrogenase

Three cultures for each TSC and control were analysed. Only genes analysed by SAM and found to be significant were listed.
TSC, tobacco smoke components.
*No significant change.

array data were normalized using global normalization. As a final assessment, the data were analysed using significance analysis of microarrays (SAM; Stanford University) analysis. SAM correlates gene expression data to a wide variety of parameters and uses data permutations to provide an estimate of false discovery rates for multiple testing. Changes in gene expression were expressed as a ratio (fold change). The lower cut-off point for identifying relevant genes was set at a ratio of 1.5 [18–20].

Quantitative reverse transcriptase-polymerase chain reaction

RNA ($n = 4$) prepared from PBS, nicotine, FA, ethyl carbamate and cadmium-treated ETM was converted to complementary DNA using QuantiTect reverse transcription kit (Qiagen). A small sample of genes ($n = 12$) highlighted by the SAM analysis were sampled to validate microarray results. Real-time PCR was performed on an MJ Research Opticon (BioRad, Hercules, California, USA) using the QuantiTect SYBR green PCR kit (Qiagen) under the following conditions: 1 cycle: 15 min 95°C; 40 cycles: 15 s 94°C, 30 s 55°C, 30 s 72°C. Ct values for the genes of interest were compared with the control samples to calculate fold change.

Results

When comparing gene expression in cadmium, FA and ethyl carbamate to PBS, 18 genes were upregulated by more than three-fold (Table 1). The greatest changes as noted were responses to DNA damage stimulus (CHK2 checkpoint homolog), cell stress (CTP synthase), chemokines [chemokine (C-X-C motif) ligand 10] and oxidoreductases [cytochrome P450, family 20, subfamily A, polypeptide 1, prostaglandin-endoperoxide synthase (PTGS)]. Nine genes were downregulated by more than three-fold (Table 1), with the most notable change observed in a gene involved in cell cycle [cyclin D1 (CCND1)]. In contrast, when comparing the gene expression of nicotine to PBS, fewer changes in mRNA expression were induced. Five genes were upregulated by more than 1.5-fold, with the largest change observed in sulphotransferases. Eleven genes were downregulated by more than 1.5-fold, with the greatest change in the oxidoreductases [cytochrome P450, family 7, subfamily A, polypeptide 1(CYP7A1)] and drug metabolism (TPMT; Table 1). Reverse transcriptase-PCR was carried out to validate the accuracy of the gene expression changes predicted by the microarray. RT-PCR confirmed 80% microarray gene expression changes (data not shown).

Further analysis placed the genes of interest into functional groups annotated by SuperArray. The functional groups of drug metabolism, transcription factors/regulators, stress response, cell growth/proliferation and differentiation and transporters were common for all
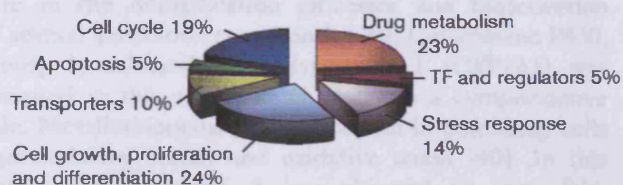
compounds. Moreover, nicotine also contained the DNA repair functional group (Fig. 1) and cadmium, ethyl carbamate and FA had genes in the apoptosis and cell cycle functional grouping (Figs 2–4).

Fig. 1
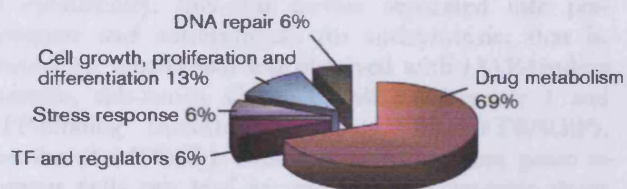
Functional classification of the significant genes from nicotine exposure of the EpiAirway tissue model. TF, transcription factors.

Fig. 2

Functional classification of the significant genes from cadmium exposure of the EpiAirway tissue model. TF, transcription factors.

Fig. 3

Functional classification of the significant genes from ethyl carbamate exposure of the EpiAirway tissue model. TF, transcription factors.

Fig. 4
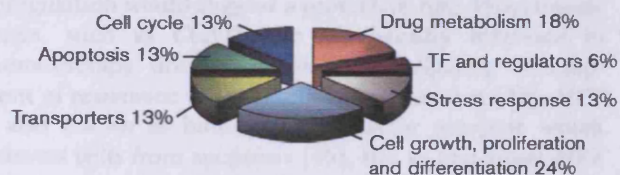

Functional classification of the significant genes from formaldehyde exposure of the EpiAirway tissue model. TF, transcription factors.
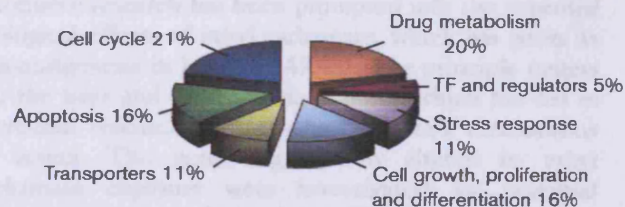
Discussion

A number of lung-related diseases associated with tobacco smoke [21] are observed. Studies in this field are complicated by the number of chemicals (about 4500; [22]) used in tobacco and individual smoking habits. An alternative approach is required to assess the biological responses and highlight potential biomarkers of harm for specific mechanisms of injury attributed to smoking. In this study, a subtoxic dose of nicotine, cadmium, ethyl carbamate and FA had significant effects on epithelial gene expression.

The effect of nicotine in the animal and cell system has been comprehensively researched [23,24]. Nicotine has been shown to elicit a variety of physiological effects (i.e. cardiac contractility, mobilization of blood sugars and increased free fatty acids), but for the purpose of this study only the thrombogenic and atherosclerotic mechanisms of nicotine were investigated. The majority of significantly altered genes from the nicotine exposure study were involved in drug metabolism. An additional functional group of DNA repair not present in other exposure studies was also identified. Further examination of the nicotine gene list found five of the 16 genes might be involved in atherosclerosis; these can be separated further into antiatherosclerosis and proatherosclerosis. The antiatherosclerosis genes *cytochrome P450, family 2, subfamily E, polypeptide 1, ELK1* – member of ETS oncogene family and *Hypoxia-inducible factor 1, α subunit* have different mechanisms of action; downregulation of *cytochrome P450, family 2, subfamily E, polypeptide 1* reduces reactive oxygen species (ROS) stabilizing the initiation of inflammation [25]. Decreased expression of *ELK1* – member of ETS oncogene family in smooth muscle cells leads to an increase in the expression of proteins required for the differentiated function of smooth muscle cells. A number of disease states are associated with a decrease of these muscle cell proteins [26]. Downregulation of *Hypoxia-inducible factor 1, α subunit* inhibits foam cell formation, and hence, atherosclerosis [27]. The proatherosclerosis genes are *CYP7A1* and haem oxygenase (*HMOX1*). *CYP7A1* encodes for a protein with a rate limiting enzyme activity for bile acid synthesis [28]. Downregulation of *CYP7A1* could result in a decrease of cholesterol absorption, and be classed as hypercholesterolemic with significant increases in the low-density lipoprotein fraction [29,30]. This is likely to result in an individual susceptibility to the development of atherosclerosis [30]. *HMOX1* is a cytoprotective gene that when induced, is one of the major defence mechanisms against oxidative stress [31]. This could indicate that reduced *HMOX1* may be involved in the mechanism of atherosclerosis because of the overproduction of ROS and increased inflammatory responses [32].

Many biological effects exerted by cadmium on membranes, mitochondrial structure and function, DNA and gene expression are present [33]. Oxidative stress is initiated by cadmium in many cell types; this has been determined by decreased activity of antioxidants [34,35]. The genes significantly altered by cadmium exposure were investigated for potential associations to cytotoxicity. Nine of a possible 20 genes were found to be related to cytotoxicity; this was further separated into pro-cytotoxic and anticytotoxic. An anticytotoxic, that is, protective, mechanism was observed with [ATP-binding cassette, sub-family C (CFTR/MRP), member 1 and ATP-binding cassette, sub-family C (CFTR/MRP), member 2 (*ABCC2*)]. Elevated levels of these genes in tumour cells can lead to resistance to cytotoxic drugs [36]. Another anticytotoxic mechanistic gene is B-cell leukemia/lymphoma 2-associated X protein (BAX), down-regulation of this gene could inhibit the initiation of mitochondrial dysfunction [37]. Mitochondrial dysfunction would lead to the release of cytochrome c, which activates DNA damaged initiated apoptotic pathways [38]. The xenobiotic-metabolizing enzymes play a crucial role in the detoxification processes and bioactivation of several xenobiotic compounds [39]. Cytochrome P450, family 1, subfamily A, polypeptide 1 (CYP1A1) was elevated in this study, which suggests a cytoprotective role. Metallothioneins play a vital role in defending cells against heavy metals and oxidative stress [40]. In this study metallothionein 3 was elevated by three-fold, similar to the results observed in a study with metallothionein 2A with a cadmium exposure to lens epithelial cells which resulted in a 20% protection against cadmium-induced oxidative stress [41]. Major vault protein is also known as lung resistance protein [42] and has a proposed role in drug resistance [43]; upregulation would suggest a protective role. Procytotoxic genes, such as *CCND1* are consistently inhibited in chemotherapy drug tests when investigating development of resistance to chemotherapy treatment [44]. *MVT* is also known as human growth factor receptor, which protects cells from apoptosis [45], but in this study *MVT* was downregulated indicating a decrease in protection against apoptosis. *XDH* is associated with the reductive activation of chemotherapeutic agents and elevation of this gene as observed in this study, would lead to a greater rate of formation of oxygen radicals and significantly increased cytotoxicity [46].

Extensive research has been prompted into the potential biological effects of ethyl carbamate, which has given its tumourigenesis in humans [47,48]. The principle targets are the liver and lung [49] in animals, which has led to increased research into ethyl carbamate's mechanisms of action. The genes significantly altered by ethyl carbamate exposure were investigated for potential associations to carcinogenicity. The ethyl carbamate exposure study found 10 of a possible 16 significantly altered genes associated with carcinogenicity. Further analysis differentiated genes into procarcinogenicity

and anticarcinogenicity. Anticarcinogenicity genes make up 90% of the significantly altered genes; this is demonstrated by *BAX*, also known as B-cell leukemia/lymphoma 2-associated X protein, that suppresses DNA repair [50]. This study found the genes to be down-regulated, increasing genetic stability and inhibiting DNA damage. Inhibition of caspase 10, apoptosis-related cysteine peptidase is associated with the pathogenesis of trophoblast tumourigenesis; [51] this study found an elevated level, which again demonstrates anticarcinogenicity. The *CCND1* gene is elevated in human breast cancers [52], which is opposed to the observations in this study that found *CCND1* to be inhibited. CHK2 checkpoint homolog has been reported as an important signal transducer of cellular responses to DNA damage and a candidate tumour surppressor [53]. Significantly elevated levels of this gene would suggest increased anticarcinogenicity. As observed in this study elevated expression of *Chemokine (C-X-C motif) ligand 10* has been shown to limit the cancerous process [54,55]. In addition, associations with increased epidermal growth factor receptor and pulmonary adenocarcinomas have been reported [56]. Downregulation was observed in this study, which could indicate an anticarcinogenicity mechanistic action. This downregulation was also observed with met proto-oncogene, also known as hepatocyte growth factor, with similar consequences of an anticarcinogenicity mechanistic role [57]. Only two procarcinogenicity genes that were significantly altered in this study are peroxisome proliferator-activated receptor δ (*PPARD*) and *CYP1A1*. *PPARD* is a nuclear receptor implicated in tumourigenesis by the activation of *PTGS2*, a rate limiting enzyme for prostaglandin synthesis and tumour growth [58]. Procarcinogens are substrates for *CYP1A1* and increased regulation observed in this study is thought to be associated to procarcinogenicity [59]. The low number of procarcinogenicity genes could be because of the bioavailability of the TSC, or possibly the lack of activation of specific metabolism mechanisms [60].

FA is mutagenic and genotoxic [2]. The mutagenic and genotoxic potential of FA is consistent with its ability to form cross linkages between protein and single stranded DNA (DNA-protein cross-links [61]). The genes significantly altered by FA exposure were investigated for potential associations to mutagenicity. The FA exposure study found six of a possible 19 significantly altered genes associated with mutagenicity. Further analysis differentiated genes into pro and antimutagenicity. As mentioned earlier *BAX* suppresses DNA repair [50], this study found this gene to be downregulated increasing genetic stability and inhibiting DNA damage and hence is antimutagenic. Investigation of cell cycle regulatory protein, *CCND1* suggested that it is found at elevated levels in tumour progression; the downregulation of this gene in this study implies an antimutagenic role. *Cytochrome P450, family 4, subfamily B, polypeptide 1* activates amines that can be carcinogenic [62]; downregulation of this gene would indicate an inhibition of amine activity. Elevated *E2F transcription factor 1* has been associated with increased sensitivity to apoptosis [63] indicating that downregulation of this gene would have an antimutagenic role. Two genes of significant change have been associated promutagenicity: *cyclin-dependent kinase inhibitor 2A* (*CDKN2A*) and *CYP1A1*. Inhibition of *CDKN2A* has been linked to specific activities that allow cells to evade differentiation processes, these properties are linked to malignancy [64]. In comparison with literature searches on ethyl carbamate and carcinogenicity, *CYP1A1* has been associated with the mediation of ROS, which in turn creates an environment favourable to DNA damage [65].

One gene [(*prostaglandin-endoperoxide synthase 1* (*PTGS1*)] was not associated to any of the specific mechanisms of toxicity investigated in this study, but was significantly induced in three out of the four compounds. *PTGS1* is thought to be responsible for the production of prostaglandins, which in turn are responsible for a host of physiological responses for example, inflammation and platelet aggregation [66].

This study has identified nine genes, which can be linked directly to the specific mechanisms of toxicity identified in this study (carcinogenic, cytotoxicity, mutagenic and thrombogenic). These genes (*CCND1, CDKN2A, CYP1A1, CYP7A1, HMOX1, MV1, PPARD, PTGS1 and XDH*) all have potential to act as genomic biomarkers for the onset and development of many respiratory diseases. Of these nine potential genomic biomarkers, three are of particular interests (*CYP7A1, HMOX1 and PTGS1*). Two genes are unique to a specific disease pathway whereas, the third is very highly upregulated across three of the compounds. These genes have also been used earlier in clinical research studies. *CYP7A1* has been documented as an adult liver cell marker [67] whereas *HMOX1*, the enzyme responsible for the synthesis of CO, is suppressed in lymphocytic bronchitis and airway luminal occlusion after transplantation [68]. Inhibition of *PTGS1* [also known as cyclooxygenase-1 (*COX1*)] is known to increase side effects of nonsteroidal anti-inflammatory drugs. Limited inhibition of *COX1* increases the drug tolerability [69], which indicates that *COX1* could play a vital role in future drug development.

Conclusion

The microarray analysis has provided transcriptional data on the exposure of human respiratory epithelium to TSC. The technique has been shown to be highly reproducible between replicates and this has been confirmed by RT-PCR. This study has identified nine genes with the potential as genomic biomarkers of specific disease mechanisms known to be associated with tobacco smoke, for example, cytotoxic. Another potential genomic

biomarker has been identified which has not been related earlier to tobacco smoke; PTGS1 is the key enzyme in prostaglandin biosynthesis and is inhibited by nonsteroidal anti-inflammatory drugs such as aspirin. This could result in a disruption of tissue homeostasis, which may lead to the onset of a number of diseases. As such this gene represents the most significant biomarker for TSC-related injury to the lung.

Acknowledgement

References

1 Overall evaluations of carcinogenicity: an updating of IARC Monographs volumes 1 to 42. *IARC Monogr Eval Carcinog Risks Hum Suppl* 1987; 7:1–440.

2 Formaldehyde, 2-butoxyethanol and 1-tert-butoxypropan-2-ol. *IARC Monogr Eval Carcinog Risks Hum* 2006; 88:1–478.

3 Meeting of the IARC working group on beryllium, cadmium, mercury and exposures in the glass manufacturing industry. *Scand J Work Environ Health* 1993; 19:360–363.

4 Pope CA 3rd, Burnett RT, Thun MJ, Calle EE, Krewski D, Ito K, *et al.* Lung cancer, cardiopulmonary mortality, long-term exposure to fine particulate air pollution. *J Am Med Assoc* 2002; 287:1132–1141.

5 Coggins CR. An updated review of inhalation studies with cigarette smoke in laboratory animals. *Int J Toxicol* 2007; 26:331–338.

6 MacNee W. Oxidative stress, lung inflammation in airways disease. *Eur J Pharmacol* 2001; 429:195–207.

7 Borgerding M, Klus H. Analysis of complex mixtures–cigarette smoke. *Exp Toxicol Pathol* 2005; 57 (Suppl 1):43–73.

8 ICCVAM (1993) Revitalization act of 1993 Plan for use of animals in research.

9 Europa (2001) Proposal for a directive of the European parliament and of the council amending Council Directive 86/609/EEC on the approximation of laws, regulations and administrative provisions of the Member States regarding the protection of animals used for experimental and other scientific purposes.

10 Russell W, Burch R. *The principles of humane experimental technique*. London: Methuen; 1959.

11 Agu R, Valiveti S, Paudel K, Klausner M, Hayden P, Stinchcomb A. Permeation of WIN 55 212-2, a potent cannabinoid receptor agonist, across human tracheo-bronchial tissue in vitro and rat nasal epithelium in vivo. *J Pharm Pharmacol* 2006; 58:1459–1465.

12 Berube K, Balharry D, Jones T, Moreno T, Hayden P, Sexton K, *et al.* Characterisation of airborne particulate matter, related mechanisms of toxicity: an experimental approach. In: Maynard R, editor. *Air pollution, health.* London: Imperial college press; 2006. pp. 69–110.

13 Chen SC, Eiting K, Cui K, Leonard AK, Morris D, Li CY, *et al.* Therapeutic utility of a novel tight junction modulating peptide for enhancing intranasal drug delivery. *J Pharm Sci* 2006; 95:1364–1371.

14 Ekwall B, Silano A, Paganuzzi-Stammati A, Zucco F. Toxicity tests with mammalian cell cultures. In: Bourdeau P, editor. *Short-term toxicity tests for nongenotoxic effects.* Hoboken, NJ, USA: Wiley; 1990. pp. 75–97.

15 Chilvers MA, O'Callaghan C. Local mucociliary defence mechanisms. *Paediatr Respir Rev* 2000; 1:27–34.

16 Godfrey RW. Human airway epithelial tight junctions. *Microsc Res Tech* 1997; 38:488–499.

17 Pampaloni F, Reynaud EG, Stelzer EH. The third dimension bridges the gap between cell culture, live tissue. *Nat Rev Mol Cell Biol* 2007; 8:839–845.

18 Balharry D, Sexton K, BéruBé K. An in vitro approach to assess the toxicity of inhaled tobacco smoke components: nicotine, cadmium, formaldehyde, urethane. *Toxicology* 2008; 244:66–76.

19 Treadwell J, Singh S. Microarray analysis of mouse brain gene expression following acute ethanol treatment. *Neurochem Res* 2004; 29:257–269.

20 DeVos S, Hofmann W, Grogan T, Krug U, Schrage M, Miller T, *et al.* Gene expression profile of serial samples of transformed B-cell lymphomas. *Lab Invest* 2003; 83:271–285.

21 Smith CJ, Perfetti TA, King JA. Perspectives on pulmonary inflammation, lung cancer risk in cigarette smokers. *Inhal Toxicol* 2006; 18:667–677.

22 Andreoli C, Gigante D, Nunziata A. A review of in vitro methods to assess the biological activity of tobacco smoke with the aim of reducing the toxicity of smoke. *Toxicol In vitro* 2003; 17:587–594.

23 Yildiz D. Nicotine, its metabolism, an overview of its biological effects. *Toxicon* 2004; 43:619–632.

24 Hukkanen J, Jacob P 3rd, Benowitz NL. Metabolism, disposition kinetics of nicotine. *Pharmacol Rev* 2005; 57:79–115.

25 Parke DV, Sapota A. Chemical toxicity, reactive oxygen species. *Int J Occup Med Environ Health* 1996; 9:331–340.

26 Zhou J, Hu G, Herring BP. Smooth muscle-specific genes are differentially sensitive to inhibition by Elk-1. *Mol Cell Biol* 2005; 25:9874–9885.

27 Jiang G, Li T, Qiu Y, Rui Y, Chen W, Lou Y. RNA interference for HIF-1alpha inhibits foam cells formation in vitro. *Eur J Pharmacol* 2007; 562:183–190.

28 Cohen JC, Cali JJ, Jelinek DF, Mehrabian M, Sparkes RS, Lusis AJ, *et al.* Cloning of the human cholesterol 7 alpha-hydroxylase gene (CYP7) and localization to chromosome 8q11–q12. *Genomics* 1992; 14:153–161.

29 Pullinger CR, Eng C, Salen G, Shefer S, Batta AK, Erickson SK, *et al.* Human cholesterol 7alpha-hydroxylase (CYP7A1) deficiency has a hypercholesterolemic phenotype. *J Clin Invest* 2002; 110:109–117.

30 Erickson SK, Lear SR, Deane S, Dubrac S, Huling SL, Nguyen L, *et al.* Hypercholesterolemia and changes in lipid and bile acid metabolism in male and female cyp7A1-deficient mice. *J Lipid Res* 2003; 44:1001–1009.

31 Brydun A, Watari Y, Yamamoto Y, Okuhara K, Teragawa H, Kono F, *et al.* Reduced expression of heme oxygenase-1 in patients with coronary atherosclerosis. *Hypertens Res* 2007; 30:341–348.

32 Griendling KK, FitzGerald GA. Oxidative stress and cardiovascular injury: Part I: basic mechanisms and in vivo monitoring of ROS. *Circulation* 2003; 108:1912–1916.

33 Pinot F, Kreps SE, Bachelet M, Hainaut P, Bakonyi M, Polla BS. Cadmium in the environment: sources, mechanisms of biotoxicity, and biomarkers. *Rev Environ Health* 2000; 15:299–323.

34 Yang CF, Shen HM, Shen Y, Zhuang ZX, Ong CN. Cadmium-induced oxidative cellular damage in human fetal lung fibroblasts (MRC-5 cells). *Environ Health Perspect* 1997; 105:712–716.

35 Cox LA Jr, Popken DA. Quantifying potential human health impacts of animal antibiotic use: enrofloxacin and macrolides in chickens. *Risk Anal* 2006; 26:135–146.

36 O'Connor R. The pharmacology of cancer resistance. *Anticancer Res* 2007; 27:1267–1272.

37 Wei MC, Zong WX, Cheng EH, Lindsten T, Panoutsakopoulou V, Ross AJ, *et al.* Proapoptotic BAX and BAK: a requisite gateway to mitochondrial dysfunction and death. *Science* 2001; 292:727–730.

38 Shiu LY, Chang LC, Liang CH, Huang YS, Sheu HM, Kuo KW. Solamargine induces apoptosis and sensitizes breast cancer cells to cisplatin. *Food Chem Toxicol* 2007; 45:2155–2164.

39 Lieber CS. Cytochrome P-4502E1: its physiological and pathological role. *Physiol Rev* 1997; 77:517–544.

40 Kagi JH, Schaffer A. Biochemistry of metallothionein. *Biochemistry* 1988; 27:8509–8515.

41 Hawse JR, Padgaonkar VA, Leverenz VR, Pelliccia SE, Kantorow M, Giblin FJ. The role of metallothionein IIa in defending lens epithelial cells against cadmium and TBHP induced oxidative stress. *Mol Vis* 2006; 12:342–349.

42 Scheffer GL, Wijngaard PL, Flens MJ, Izquierdo MA, Slovak ML, Pinedo HM, *et al.* The drug resistance-related protein LRP is the human major vault protein. *Nat Med* 1995; 1:578–582.

43 Kowalski MP, Dubouix-Bourandy A, Bajmoczi M, Golan DE, Zaidi T, Coutinho-Sledge YS, *et al.* Host resistance to lung infection mediated by major vault protein in epithelial cells. *Science* 2007; 317:130–132.

44 Hernandez-Vargas H, Rodriguez-Pinilla SM, Julian-Tendero M, Sanchez-Rovira P, Cuevas C, Anton A, *et al.* Gene expression profiling of breast cancer cells in response to gemcitabine: NF-kappaB pathway activation as a potential mechanism of resistance. *Breast Cancer Res Treat* 2007; 102:157–172.

45 Kakazu A, Chandrasekher G, Bazan HE. HGF protects corneal epithelial cells from apoptosis by the PI-3K/Akt-1/Bad- but not the ERK1/2-mediated signaling pathway. *Invest Ophthalmol Vis Sci* 2004; 45:3485–3492.

46 Yee SB, Pritsos CA. Reductive activation of doxorubicin by xanthine dehydrogenase from EMT6 mouse mammary carcinoma tumors. *Chem Biol Interact* 1997; 104:87–101.

47 Ritchie KJ, Henderson CJ, Wang XJ, Vassieva O, Carrie D, Farmer PB, *et al.* Glutathione transferase pi plays a critical role in the development of lung carcinogenesis following exposure to tobacco-related carcinogens and urethane. *Cancer Res* 2007; 67:9248–9257.

48 Stathopoulos GT, Sherrill TP, Cheng DS, Scoggins RM, Han W, Polosukhin VV, *et al.* Epithelial NF-kappaB activation promotes urethane-induced lung carcinogenesis. *Proc Natl Acad Sci U S A* 2007; 104:18514–18519.

49   Siemiatycki J, Richardson L, Straif K, Latreille B, Lakhani R, Campbell S,
     et al. Listing occupational carcinogens. Environ Health Perspect 2004;
     112:1447–1459.
50   Jin Z, May WS, Gao F, Flagg T, Deng X. Bcl2 suppresses DNA repair
     by enhancing c-Myc transcriptional activity. J Biol Chem 2006;
     281:14446–14456.
51   Fong PY, Xue WC, Ngan HY, Chiu PM, Chan KY, Tsao SW, et al. Caspase
     activity is downregulated in choriocarcinoma: a cDNA array differential
     expression study. J Clin Pathol 2006; 59:179–183.
52   Wang C, Pattabiraman N, Zhou JN, Fu M, Sakamaki T, Albanese C, et al.
     Cyclin D1 repression of peroxisome proliferator-activated receptor gamma
     expression and transactivation. Mol Cell Biol 2003; 23:6159–6173.
53   Nevanlinna H, Bartek J. The CHEK2 gene and inherited breast cancer
     susceptibility. Oncogene 2006; 25:5912–5919.
54   Palmer K, Hitt M, Emtage PC, Gyorffy S, Gauldie J. Combined CXC
     chemokine and interleukin-12 gene transfer enhances antitumor immunity.
     Gene Ther 2001; 8:282–290.
55   Ben-Baruch A. The multifaceted roles of chemokines in malignancy. Cancer
     Metastasis Rev 2006; 25:357–371.
56   Nakamura H, Kawasaki N, Taguchi M, Kato H. Epidermal growth factor
     receptor gene mutations in early pulmonary adenocarcinomas. Ann Thorac
     Cardiovasc Surg 2007; 13:87–92.
57   Shia S, Stamos J, Kirchhofer D, Fan B, Wu J, Corpuz RT, et al.
     Conformational liability in serine protease active sites: structures of
     hepatocyte growth factor activator (HGFA) alone and with the inhibitory
     domain from HGFA inhibitor-1B. J Mol Biol 2005; 346:1335–1349.
58   Xu L, Han C, Lim K, Wu T. Cross-talk between peroxisome proliferator-
     activated receptor delta and cytosolic phospholipase A(2)alpha/
     cyclooxygenase-2/prostaglandin E(2) signaling pathways in human
     hepatocellular carcinoma cells. Cancer Res 2006; 66:11859–11868.
59   Nebert DW, Dalton TP. The role of cytochrome P450 enzymes in
     endogenous signalling pathways and environmental carcinogenesis.
     Nat Rev Cancer 2006; 6:947–960.

60   Balharry D, Oreffo V, Richards R. Use of toxicogenomics for identifying
     genetic markers of pulmonary oedema. Toxicol Appl Pharmacol 2005;
     204:101–108.
61   Speit G, Schutz P, Hogel J, Schmid O. Characterization of the genotoxic
     potential of formaldehyde in V79 cells. Mutagenesis 2007; 22:387–394.
62   Imaoka S, Yoneda Y, Sugimoto T, Ikemoto S, Hiroi T, Yamamoto K, et al.
     Androgen regulation of CYP4B1 responsible for mutagenic activation of
     bladder carcinogens in the rat bladder: detection of CYP4B1 mRNA by
     competitive reverse transcription-polymerase chain reaction. Cancer Lett
     2001; 166:119–123.
63   Roos WP, Christmann M, Fraser ST, Kaina B. Mouse embryonic stem cells
     are hypersensitive to apoptosis triggered by the DNA damage O(6)-
     methylguanine due to high E2F1 regulated mismatch repair. Cell Death
     Differ 2007; 14:1422–1432.
64   Berman H, Zhang J, Crawford YG, Gauthier ML, Fordyce CA, McDermott
     KM, et al. Genetic and epigenetic changes in mammary epithelial cells
     identify a subpopulation of cells involved in early carcinogenesis. Cold
     Spring Harb Symp Quant Biol 2005; 70:317–327.
65   Hansen T, Seidel A, Borlak J. The environmental carcinogen 3-
     nitrobenzanthrone and its main metabolite 3-aminobenzanthrone enhance
     formation of reactive oxygen intermediates in human A549 lung epithelial
     cells. Toxicol Appl Pharmacol 2007; 221:222–234.
66   Park JY, Pillinger MH, Abramson SB. Prostaglandin E2 synthesis and
     secretion: the role of PGE2 synthases. Clin Immunol 2006;
     119:229–240.
67   Cai J, Zhao Y, Liu Y, Ye F, Song Z, Qin H, et al. Directed differentiation of
     human embryonic stem cells into functional hepatic cells. Hepatology 2007;
     45:1229–1239.
68   Minamoto K, Harada H, Lama VN, Fedarau MA, Pinsky DJ. Reciprocal
     regulation of airway rejection by the inducible gas-forming enzymes heme
     oxygenase and nitric oxide synthase. J Exp Med 2005; 202:283–294.
69   Asero R. Etoricoxib challenge in patients with chronic urticaria with NSAID
     intolerance. Clin Exp Dermatol 2007; 32:661–663.